Intergovernmental Oceanographic Commission
technical series

54

# Geological Processes on the Northeast Atlantic Margin

Preliminary results of geological and geophysical investigations
during the TTR-8 cruise of *R/V Professor Logachev*
June-August, 1998

Editors: N.H. Kenyon
M.K. Ivanov
A.M. Akhmetzhanov

UNESCO 1999

SC-99/WS/44

The designations employed and the presentation of the material in this publication do not imply the expression of any opinion whatever on the part of the Secretariats of UNESCO and IOC concerning the legal status of any country or territory, or its authorities, or concerning the delimitation of the frontiers of any country or territory.

**For bibliographic purposes, this document should be cited as follows:**
Geological Processes on the Northeast Atlantic Margin
*IOC Technical Series No. 54, UNESCO, 1999*
*(English)*

Printed in 1999
by the United Nations Educational,
Scientific and Cultural Organization
7, place de Fontenoy, 75352 Paris 07 SP

Printed in UNESCO's Workshops

© UNESCO 1999
*Printed in France*

# TABLE OF CONTENTS

Page

**ABSTRACT** ..... (iii)

**ACKNOWLEDGEMENTS** ..... (iv)

**INTRODUCTION** ..... 5

**METHODS OF INVESTIGATION** ..... 9

**I. PORTUGUESE MARGIN**

I.1. Introduction ..... 10
I.2. Seismic data ..... 11
I.3. OKEAN and OREtech side-scan sonar analysis: continental slope near Lisbon ..... 14
I.4. Bottom sampling ..... 20
I.5. Conclusions ..... 33

**II. PORCUPINE SEABIGHT: SHORT VISIT**

II.1. Introduction ..... 34
II.2. Preliminary Results ..... 38

**III. FAEROES MARGIN**

III.1. Introduction ..... 48

III.2. Eastern margin ..... 49
*III.2.1. Seismic and 3.5 kHz subbottom profiling* ..... 49
*III.2.2. Side-scan sonar data* ..... 55
*III.2.3. Bottom sampling* ..... 56

III.3. Northeastern margin ..... 62
*III.3.1. Seismic data* ..... 62
*III.3.2. Side-scan sonar data* ..... 64
*III.3.3. Bottom sampling* ..... 71

III.4. Results and preliminary conclusions ..... 76

**IV. NORWEGIAN MARGIN**

IV.1. Introduction..... 79

IV.2. Southern Vøring Plateau..... 81
*IV.2.1. Seismic profiling data*..... 81
*IV.2.2. Side-scan sonar data*..... 83
*IV.2.3. Bottom sampling*..... 90

IV.3. Eastern Vøring Plateau..... 107
*IV.3.1. Seismic profiling data*..... 107
*IV.3.2. Side-scan sonar data*..... 111
*IV.3.3. Bottom sampling*..... 113

IV.4. Bear Island Area..... 117
*IV.4.1. Seismic profiling data*..... 117
*IV.4.2. Side-scan sonar data*..... 120
*IV.4.3. Bottom sampling*..... 122

IV.5. Conclusions..... 136

**REFERENCES**..... 137

**ANNEX 1. LIST OF TTR-RELATED REPORTS**

# ABSTRACT

Geological processes at different locations along the European continental margin in the North Atlantic were studied on the TTR-8 Cruise (1998) with a wide range of equipment. They included: single-channel seismic reflection profiling carried out simultaneously with OKEAN 10 kHz long-range side-scan survey, high-resolution survey with the OREtech deep-towed instrument comprising 30 and 100 kHz side-scan sonar and 5 kHz subbottom profiler units. For more detailed studies, a bottom TV survey and different techniques of bottom sampling were employed.

The cruise data comprise more than 3000 km of seismic and long range side-scan sonar lines, 185 km of high resolution side-scan survey, about 20 km of bottom TV survey and 70 bottom samples.

On the Portuguese margin west of Lisbon, the broad network of canyons was successfully mapped with the OKEAN side-scan sonar. The data add to and fit well with the seismic and side-scan sonar datasets collected previously in the area by Portuguese scientists.

A study conducted in the Porcupine Seabight mud mounds areas was aimed at obtaining further bottom samples for geochemical and microbiological investigations. A more detailed survey was carried out with 100 kHz side-scan sonar on one of the mounds. A better understanding of the seabed processes observed during the TTR-7 cruise (1997) was achieved as a result of this second visit.

A slump affecting the upper part of the sedimentary section was mapped on the eastern Faeroes margin. Another large slide on the northern Faeroes margin was also visited and detailed studies showed the presence of a number of stages of slide development. The recognition of the latter can be crucial for the determination of potentially hazardous areas on the continental margins. The presence of a megaturbidite, whose formation is probably related to the giant Northern Faeroes Slide, was observed in cores taken downslope from the slide.

Investigations of the southeastern part of the Vøring Plateau adjacent to the Storegga Slide shed more light on this area known for its numerous fluid escape structures and possible gas hydrates presence. A bottom simulating reflector (BSR) was observed and in several places it was found to be pierced by diapiric structures disturbing the sedimentary cover and reaching the seafloor at some locations. Some of the pockmarks, well seen on the long range side-scan sonar data, were carefully studied with high-resolution acoustic tools and bottom TV. The latter revealed the presence of bottom biota activity possibly related to gas seepages, and direct observation of escaping fluids were made and videotaped. Many samples taken from the pockmarks contain gas-saturated sediments and concretions of carbonate minerals whose formation is very likely due to the methane oxidation.

The complex morphology of the seabed mounds located in the northwestern part of the Vøring plateau was observed on the OREtech sonograph.

The unique nature of the Haakon Mosby mud volcano located to the southwest of Bear Isle was confirmed by extensive seismic and OKEAN survey. No other mud volcanoes were found although several mud diapiric structures were recognised and sampled.

# ACKNOWLEDGEMENTS

The eighth Training-through-Research cruise would not have taken place without financial support from various sources, among which were: the Intergovernmental Oceanographic Commission (IOC) of UNESCO, the Geological Survey of Denmark and Greenland, the Graduate School and the Challenger Division of Southampton Oceanography Centre (UK), Instituto Geologico e Mineiro (Portugal), University College Cork (Ireland), Faroes GEM Network, STATOIL Exploration (Ireland) Ltd., University of Gent (Belgium), MAST Concerted action CORSAIRES (MAS3 CT 950045), the "Floating University" project of the Flemish Government (Belgium), the Ministry of Science and Technological Policy, the Polar Marine Geosurvey Expedition of the Ministry of Natural Resources and the Moscow State University (Russia). Logistic support was provided by the Netherlands Sea Research Institute (The Netherlands).

A number of people from different organizations supported the Training-through-Research Programme and were involved in the cruise preparation. The editors would like to express their gratitude for the contributions made by Prof. I. F. Glumov (Ministry of Natural Resources of the Russian Federation), Mr. V. Zhivago (Ministry of Science and Technological Policy of the Russian Federation), Dr. P. Bernal (Executive Secretary, IOC) and Dr. A. Suzyumov (UNESCO).

Credit also should be given to Mr. C. van Bergen Henegouw of the Netherlands Institute for Sea Research and Prof. Dr. V. T. Trofimov (Moscow State University) for administrative support.

Captains Pat Farnan, Harbour Master of Cork, and Jánsvein Lamhauge, Harbour Master of Tórshavn provided invaluable assistance in the organization of port calls in Cork and Tórshavn, respectively. University College Cork, and specifically Dr. N. Connolly from the College's Coastal Resources Centre, provided assistance in the organization of the port call in Cork. Support was also given by the Cork Chamber of Commerce.

Thanks are due to the administration and staff of the Polar Marine Geological Exploration Expedition (St. Petersburg) for their co-operation and assistance with the cruise organization. Captain A. Arutyunov and the crew of the R/V *Professor Logachev* are thanked for the successful carrying out of the operations at sea.

Mr. P. Shashkin from the UNESCO-MSU Marine Geosciences Centre was very instrumental in processing the acoustic data and the preparation of figures.

# INTRODUCTION

*M. Ivanov and N. Kenyon*

In 1998 RV *Professor Logachev,* owned by the Ministry of Natural Resources of the Russian Federation, was again chosen as a platform for the Training-through-Research Cruise (TTR-8) in the Northeastern Atlantic (Fig. 1). An international team of 68 scientists, postgraduate and undergraduate students, and technicians from 18 institutions of 11 countries (Belgium, Denmark, France, Ireland, Italy, The Netherlands, Poland, Portugal, Russia, Switzerland and the UK) participated in the three Legs of the cruise.

The objectives of the cruise were to study geological processes on continental slopes and to train students in marine geoscience research.

The cruise research programme was focused on the following major issues: (1) slope stability, (2) modern analogues of hydrocarbon reservoirs, (3) fluid venting, and (4) mud volcanism and related gas hydrate occurrences. The study areas and particular scientific targets for each of them were as follows:

*Area 1.* Study of the canyon system on the approaches to the Tagus Abyssal Plain, fed by the Lisbon Canyon. Another target was the scarp of a deep-seated fault on the Iberia Abyssal Plain. It was believed be the site of fluid seeps similar to those cored at ODP site 1068 in a similar situation (Krawczyk et al., 1996).

*Area 2.* Further investigation of carbonate mud mounds and related acoustic anomalies observed on the subbottom profiler records in the Porcupine Seabight.

*Areas 3 and 4.* Study of the East Faeroes margin, including the occurrence of small submarine slides as well as study of the giant slide known from north of the Faeroe Islands. It had previously been mapped by both GLORIA and TOBI side-scan sonars but high-resolution side-scan sonar survey and coring were required.

*Areas 5, 6 and 7.* Studies of gas seepage, possible gas hydrate occurrence and mud volcanoes on the Norwegian Sea margin. Several locations were visited including the Storegga Slide, the Vøring Plateau diapiric field and the spectacular Haakon Mosby mud volcano, recently discovered and studied by Norwegian, American, and Russian scientists (Vogt et al., 1997).

Area 1 was the focus of investigations during Leg 1 (13.06.98-24.06.98) which started in Lisbon (Portugal) and terminated in Cork (Ireland). During the first half of Leg 2 (25.06.98-8.07.98) research was carried out in the Porcupine Seabight and the second half of the Leg was taken up with study of the Faeroes margin. Leg 2 terminated in Thórshavn where the participants took part in a geological field trip over one of the islands. Leg 3 (10.07.98-1.08.98) was entirely devoted to investigations on the Norwegian continental margin after which the ship headed to St. Petersburg, where it docked on 1 August.

The present report refers to a considerable part of the data obtained during the cruise although the interpretation given is mainly preliminary and most of the analyses and advanced data processing will be done later.

Comprehensive reports from other TTR cruises are available within the series of UNESCO Reports in Marine Science (Nos. 56, 62, 64, 67 and 68) and IOC Technical Series (Nos. 48 and 52). Scientific results of the cruise are partially presented in abstract books of the post-cruise meetings published in UNESCO's *Marinf* series (Nos. 91, 94, 99, 100) and in IOC Workshop Report series (Nos. 129, 143) (Annex I). So far there have been about 40 TTR papers published in international journals including a special issue of *Marine Geology,* on Mediterranean mud volcanoes (Vol. 132, 1996), a special issue of *Geo-Marine Letters,* on TTR scientific studies in the Mediterranean Sea (Vol. 18, 1998) and an issue of *Geological Society Special Publications,* on gas hydrates (No 137, 1998).

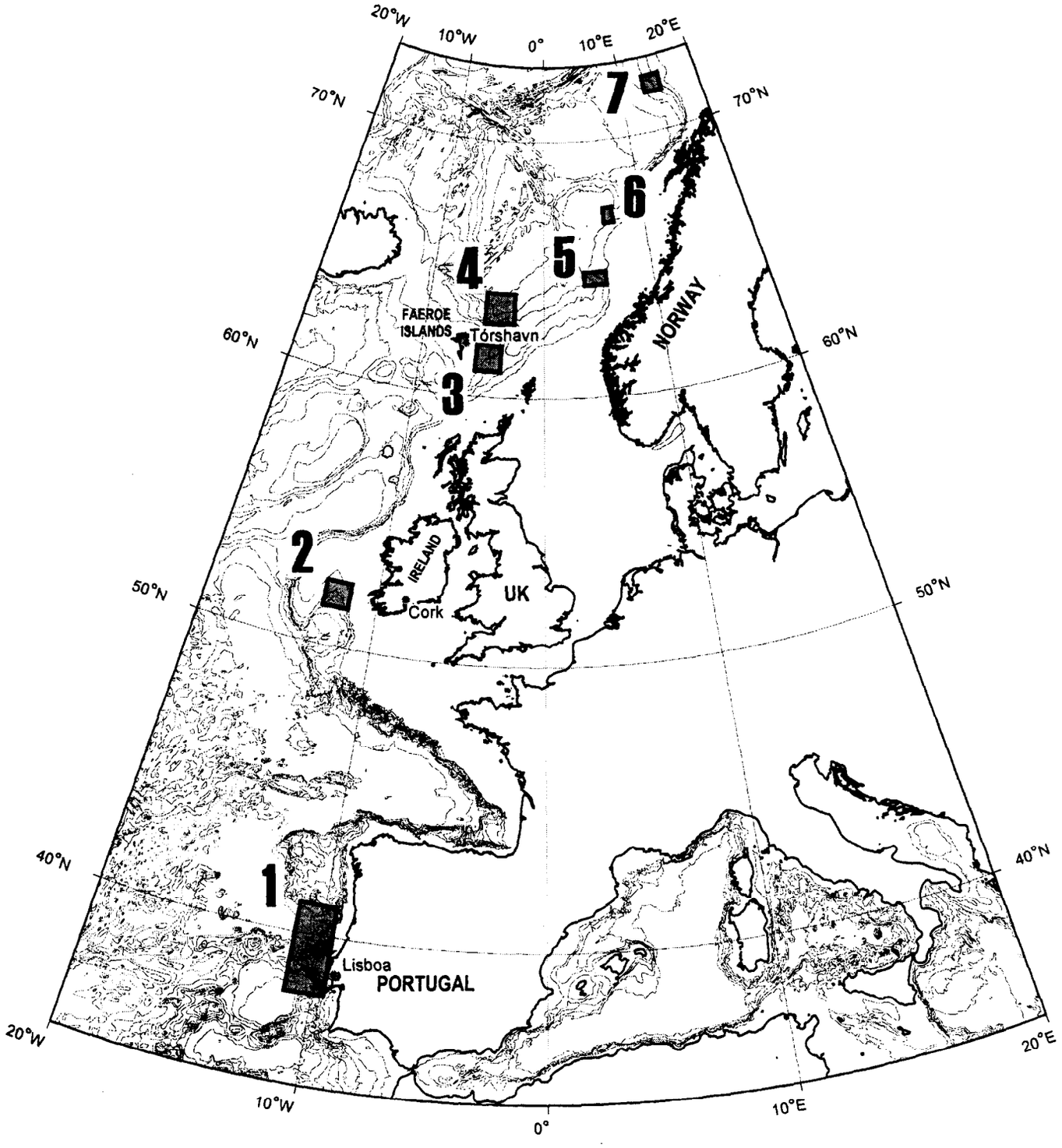


**1** - Portuguese margin
**2** - Porcupine Seabight
**3** - Eastern Faeroes margin
**4** - Northeastern Faeroes margin
**5** - Southern Vøring Plateau
**6** - Eastern Vøring Plateau
**7** - Southwestern Bear Island margin

Fig. 1. TTR-8 Cruise working areas

**List of the participants of the eighth Training-through-Research international cruise of the R/V *Professor Logachev* in the northeast Atlantic within the UNESCO/IOC "Floating University" Programme, 13 June-1 August, 1998**

| | | | Leg |
|---|---|---|---|
| **Belgium** | Ben De Mol | University of Gent | 1 2 3 |
| **Denmark** | Tove Nielsen* | Geological Survey of Denmark and Greenland, GEUS | 2 |
| | Antoon Kuijpers* | GEUS | 2 |
| | Malene Rank | GEUS | 2 |
| | Hilmar Simonsen | University of Aarhus | 2 |
| **France** | Ian Probert | University of Caen | 1 |
| | Giovanni Aloisi | Pierre et Marie Curie University of Paris | 3 |
| **Ireland** | Andy Wheeler* | University College, Cork, UCC | 3 |
| | Niamh Connolly | UCC | 3 |
| **Italy** | Adriano Mazzini | University of Genoa | 1 |
| | Raffaella Brambilla | University of Milan | 1 2 |
| **The Netherlands** | Henk de Haas | Netherlands Institute for Sea Research, NIOZ | 2 |
| **Poland** | Katarzyna Stachura | University of Gdansk | 2 |
| **Portugal** | Jose Monteiro* | Instituto Geologico e Mineiro, IGM | 1 |
| | Francisco Teixeira | IGM | 1 |
| | Mario Mil-Homens | IGM | 1 |
| **Russia** | Alexandr Arutyunov | Polar Marine Geological Exploration Expedition, PMGEE | 1 2 3 |
| | Boris Malin | PMGEE | 1 2 3 |
| | Alexandr Ashadze | PMGEE | 1 2 3 |
| | Alexandr Machulin | PMGEE | 1 2 3 |
| | Evgeny Samsonov | PMGEE | 1 2 3 |
| | Valery Babanov | PMGEE | 1 2 3 |
| | Gennady Antipov | PMGEE | 1 2 3 |
| | Irina Antipova | PMGEE | 1 2 3 |
| | Victor Sheremet | PMGEE | 1 2 3 |
| | Boris Smirnov | PMGEE | 1 2 3 |
| | Valentin Konfetkin | PMGEE | 1 2 3 |
| | Sergey Luybimov | PMGEE | 1 2 3 |
| | Alexandr Ivanov | PMGEE | 1 2 3 |
| | Alexandr Marakulin | PMGEE | 1 2 3 |
| | Nikolay Kisilev | PMGEE | 1 2 3 |
| | Mikhail Samovarov | PMGEE | 1 2 3 |
| | Anatoly Kuznetsov | PMGEE | 1 2 3 |
| | Alexandr Nescheretov | PMGEE | 1 2 3 |
| | Vasily Tokmenko | PMGEE | 1 2 3 |

| | | | |
|---|---|---|---|
| | Vyacheslav Gladush | PMGEE | 1 2 3 |
| | Vladislav Malin | PMGEE | 1 2 3 |
| | Michael Ivanov* | Moscow State University, MSU | 1 2 3 |
| | Grigorii Akhmanov | MSU | 1 2 3 |
| | Andrey Akhmetzhanov | MSU | 1 2 3 |
| | Elena Kozlova | MSU | 1 2 3 |
| | Sergey Buryak | MSU | 1 2 3 |
| | Anna Volkonskaya | MSU | 1 2 3 |
| | Alexander Morozov | MSU | 1 2 3 |
| | Roman Pevzner | MSU | 1 2 3 |
| | Anastasija Furkalo | MSU | 1 2 3 |
| | Michail Baturin | MSU | 1 2 3 |
| | Alexandr Tischenko | MSU | 1 2 3 |
| | Pavel Shashkin | MSU | 1 2 3 |
| | Alexey Almendinger | MSU | 1 2 3 |
| | Olga Savotina | MSU | 1 2 3 |
| | Evgeny Yakovlev | MSU | 1 2 3 |
| | Dmitry Isakov | MSU | 1 2 3 |
| | Alexander Sautkin | MSU | 1 2 3 |
| | Maxim Kozachenko | MSU | 1 2 3 |
| | Inna Mardanyan | MSU | 1 2 3 |
| | Alina Stadnitskaya | MSU | 1 2 3 |
| | Irina Belenkaya | MSU | 1 2 3 |
| | Svetlana Lubentsova | MSU | 1 2 3 |
| | Viktoria Krupskaya | MSU | 1 2 3 |
| **Switzerland** | Adrian Gilli | Zurich Technical University, ETH | 1 |
| | Laurent Sommer | University of Geneva | 2 |
| **UK** | Neil Kenyon* | Southampton Oceanography Centre, SOC | 1 |
| | Ellis Maginn | SOC | 1 |
| | Ruth Hale | SOC | 1 |
| | Adam Cook | SOC | 1 |
| | Joseph Lenham | SOC | 1 |
| | Silke Severmann | SOC | 1 |
| | Patrick Friend | SOC | 2 |
| | Justin Taylor | University of Aberystwyth | 2 |

* - co-chief scientists

# METHODS OF INVESTIGATION

Comprehensive description of the equipment available onboard R/V *Professor Logachev* and used during the cruise can be found in the report of the 7th cruise of the TTR programme (Kenyon et al., 1998). Since there were no significant changes only a brief listing of the methods used is given below.

The seismic system used during the cruise included two 1.5 litre "Tessey" air guns, a 420-metre hydrophone streamer and a PC-based digital recording system. The air guns were operated at a pressure of 120 atm, and were towed at a depth of 1-1.5 m. The shotpoint interval was 10 seconds. The received signals were amplified and filtered. The onboard processing included additional filtering and pre-stack deconvolution. Seismic profiling was carried out simultaneously with OKEAN 10 kHz long-range side scan sonar recording. At selected areas where higher resolution of the seabed features was considered necessary, an OREtech deep-towed side-scan sonar operating at 30 and 100 kHz frequencies and equipped with a 5 kHz subbottom penetrating echosounder was employed. Bottom samples were retrieved using a large diameter gravity corer, a box corer and a dredge. Positioning of the ship was carried out using GPS 4400. Deep towed equipment was positioned using a short baseline navigation system.

# I. PORTUGUESE MARGIN

## I.1. Introduction

*J. Monteiro, N. Kenyon*

*Objectives*

The main objective of leg 1 of TTR8 was to investigate the influence of downslope and along slope processes on the slope and rise off Lisbon and Nazaré. The limited time available and the short conducting cable for the deep towed sonar, several km of which were lost prior to our cruise, limited the main survey to the slope off Lisbon.

The second objective was to study possible seepage near the scarp of a deep-seated fault on the Iberia abyssal plain, SSE of the Vasco da Gama seamount and close to ODP site 901.

*Geological setting*

Southwest of Lisbon, the Tagus abyssal plain (TAP) forms a large basin well bounded to the NE by the Alentejo continental margin and the Estremadura Spur, which make an angle where the Cascais, Lisbon and Setubal canyons are located. The Estremadura Spur, which is almost joined with the Tore seamount, separates the Iberian abyssal plain from the TAP. Seaward of the Arrábida elevation there is a plateau (P. Afonso de Albuquerque ) bounded by the Lisbon and Setubal canyons. To the West the basin is limited by the Madeira-Tore Rise and to the south by the Gorringe Bank. On the continent side the area is bounded by the hills of the Lisbon region, the Arrábida and Grandola mountains and consists of the Tejo and Sado fault troughs in which the Tagus and Sado Estuaries are located.

The *shoreline* has two wide bays (Lisbon and Setubal) bounded by northern cliffed segments (Costa do Sol and Arrábida ) and crescent shaped southern beaches and dunes (Costa da Caparica and Costa da Galé).

The *shelf* is narrow and has intersecting faceted surfaces with alternation of flattened forms (upstream) and progradational forms (downstream). They are indented by a tight network of buried paleovalleys originally carved by upstream retreat of the canyon heads.

*The shelf edge, the continental slope and the submarine canyons* are either linear forms due to their tectonic origin or sinuous arrangements formed by fronts of progradation surfaces. The central part consists of the triple indentation of the Cascais, Lisbon and Setubal submarine canyons. The heads, although influenced by faults, were also possibly derived from headward erosion caused by mass movements and longshore currents at lower sea level stages. The slope is very steep ($7^{o}$) . Valleys and gullies disappear below 2000 m but slide blocks have been observed in seismic profiles indicating gravity mass transport at the base of the slope.

Present day sediment transport in the coastal zone off Portugal is from North to South due to the surface waves and current regime. The main sediment sources from modern rivers are also from the NW.

The canyons and their continuation as channels across the rise are the major terrigenous sediment pathways to Iberia, Tagus and Horseshoe abyssal plains. Shelf terrigenous sediment movements may have been favoured by low sea level and/or catastrophic slope failure, triggered by earthquakes or oversteepening.

The scarp on the Iberia abyssal plain (IAP), our second objective, is related to a deep-seated fault that has been seismically imaged to depth of over 12.5 km bsf. and is predicted to be the site of fluid seeps that may cause the growth of minerals, such as low temperature aragonite similar to the occurrences existing at ODP site 1068. The scarp is located at the outer limit of the extended continental crust off the Iberian Peninsula. Both the continental blocks and the transitional and oceanic crust are covered by turbidites, probably transported by the

numerous canyons, namely, the Nazaré, Aveiro and Porto canyons. Sediments also reach the IAP from the Biscay abyssal plain through the Theta Gap.

## I.2. Seismic data

*J. Monteiro, M. Mil-Homens, F. Teixeira, S. Buriak, A. Volkonskaya*

Seven lines were shot. PSAT34, PSAT 38, PSAT 39 run E-W and PSAT 35, PSAT 37, PSAT 40 run NW-SE, and PSAT36 is a short NE-SW connecting line (Fig. 2)

The seismic reflection data were collected simultaneously with OKEAN side-scan sonar records. Because they are in the same area as previous high-resolution seismic data from the EACM-AtlantisII and the STEAM94 cruises an attempt was made to compare this data with the PSAT data. STEAM94 data show a well stratified seismic record which consists of a stratified sedimentary cover overlying a basement of Middle Miocene age. The sedimentary cover is divided into two units. The lower unit is characterised by low amplitude continuous reflectors which are interpreted as an alternation of pelagic and turbiditic intervals deposited in a relatively tranquil pelagic environment. The reflectors of the upper unit are less continuous and have higher amplitude. Locally they show complex configurations interpreted as channels, channel fill and mass flows. The abrupt change of properties between the two units coincides with the base of a contourite sequence which is recognised on the slope further south between depths of 800 and 1600 m. This contourite drift is formed by the contour current flowing northward which originates from the Mediterranean outflow at Gibraltar Strait. This current is responsible for the high sediment input rates on the slope and for sediment drifts and contourites on both the southern and soouthwestern slope of Portugal (Gardner and Kidd, 1987).

A thick sediment accumulation reaching more than 2 s twt covers most of the area. The STEAM94 (lines L1,L2,L3,L4,L5,L12 and L13) were used for comparison. These lines intersect or are close to PSAT profiles and show a well defined seismic stratigraphy resting on an irregular diffractive acoustic basement cut by faults. In the lower unit a visible discontinuity separates the upper transparent unit from the unit below, with continuous reflectors of greater amplitude deformed at the emplacement of sub vertical fractures. Previous bottom coring and dredging of the places where the first unit outcrops suggests that the discontinuity marks the middle Miocene unconformity identified in the offshore wells of Algarve and related to the tectonic movements of the South Lisbon shelf and the Arrabida Miocene overthrust. This may also correspond to the time when the Neogene prograding sequences observed in several profiles off Portugal were deposited. In the upper unit several divisions can be made and at the base of the Lisbon and Setubal canyons slightly sinuous channels and levees have been identified (L2 and L3). Large slump structures and listric gravity faults are also visible in several seismic lines (L1,L3,L5).The underlying unit is recognised by strong reflectors over a transparent unit . Samples previously collected at the Principes de Aviz seamounts, where the reflectors seem to reach the bottom, revealed neritic limestone with abundant bioclasts dated as lower Miocene and Eocene-Oligocene. This sequence, being now at 500 to 3000 m shows the importance of subsidence of the margin since the Eocene. Below the above mentioned two units one can recognise tilted and rotated fault blocks (L5, L7) of acoustic basement and also the sediments filling the troughs between the horst structure. These structures can be seen in places were Miocene compression rejuvenated the rifted morphology resulting in uplift of the blocks.

After plotting the navigation files of both surveys (STEAM and Leg 1 of TTR8) we evaluated the consistency of seismic reflection data and despite the higher resolution of

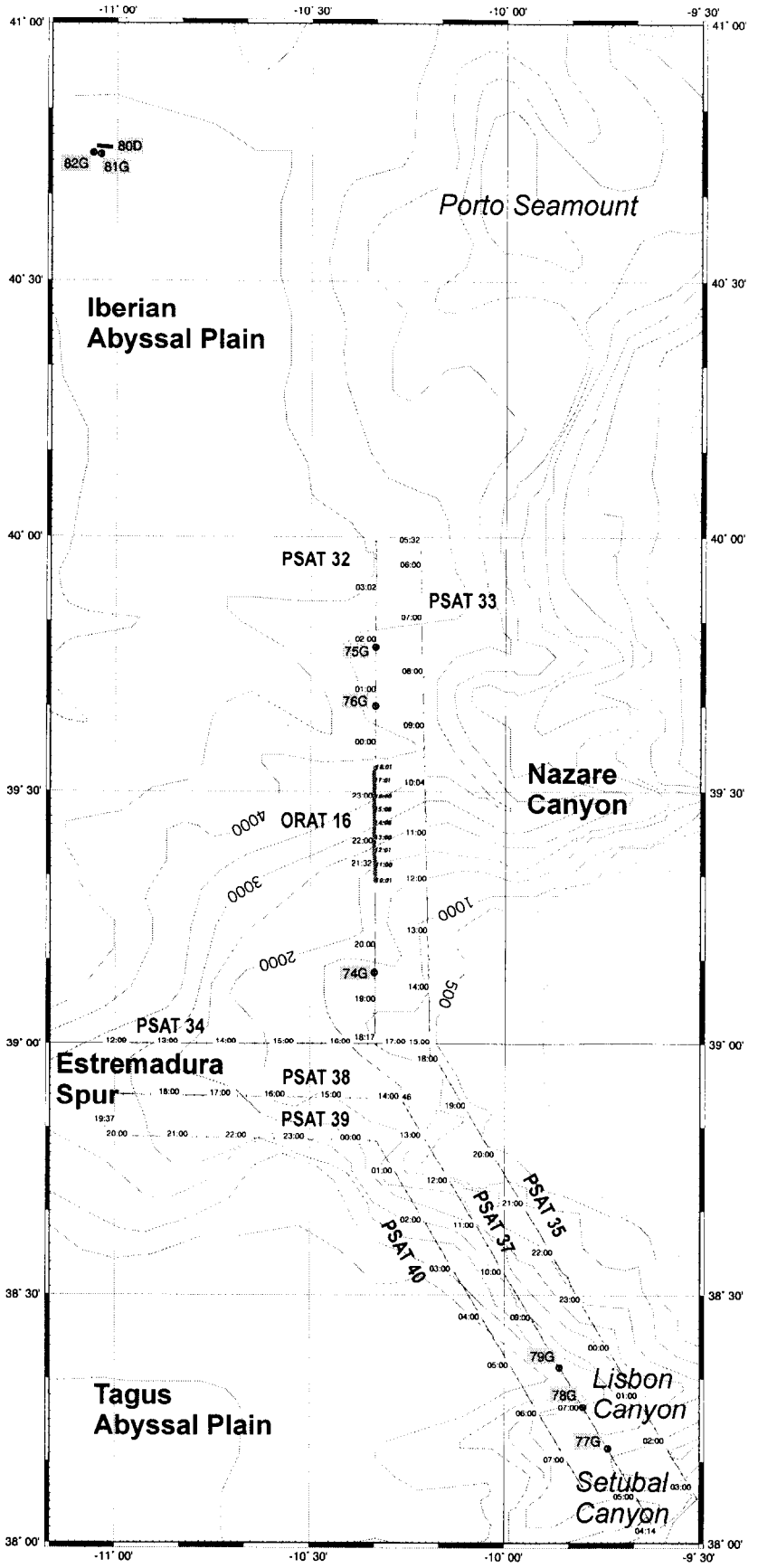


Fig 2. Location map of the Portuguese margin study area

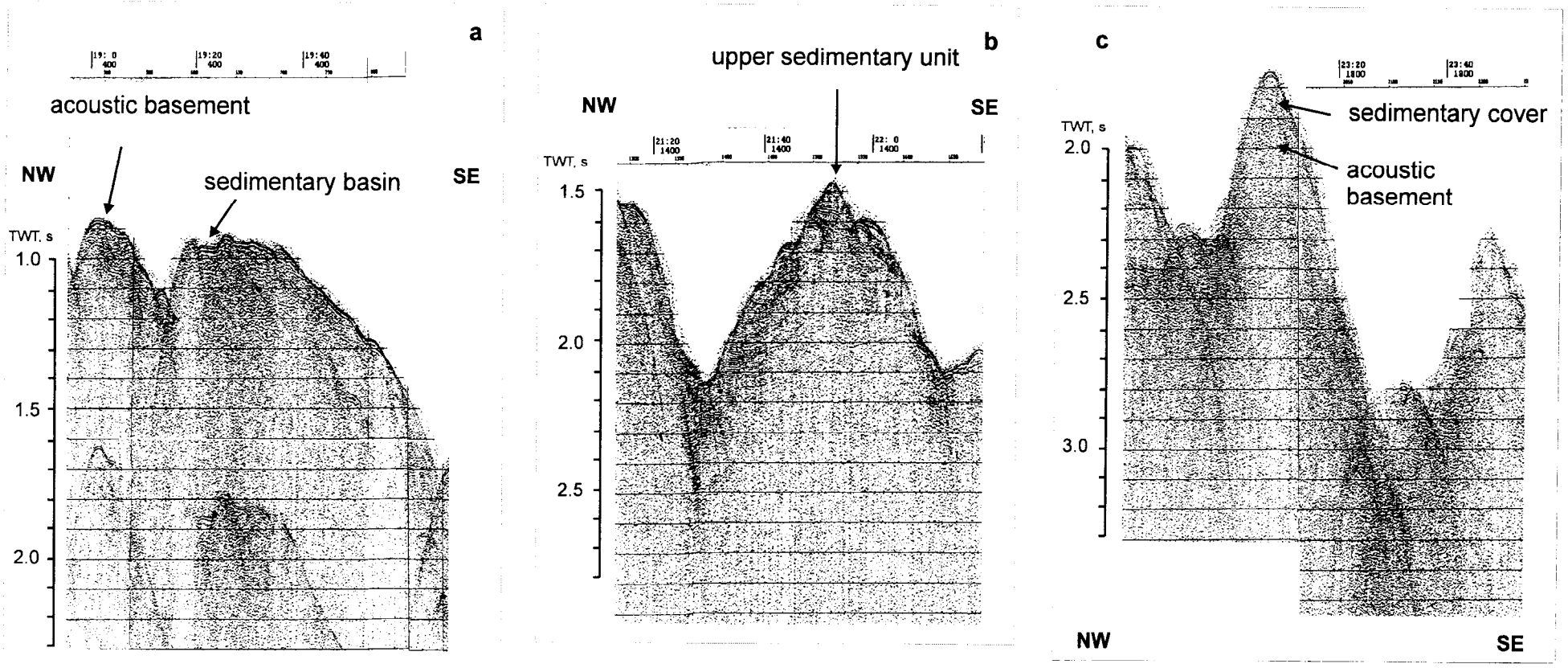


Fig. 3. Fragments of seismic line PSAT-35 showing: **a** - dislocated acoustic basement and local sedimentary basin; **b** - upper sedimentary unit; **c** - acoustic basement covered by thin cover of recent sediments.

STEAM multichannel data the PSAT lines are consistent and are useful to the interpretation of the side-scan sonographs.

Line PSAT 35 intersects at 19:22, 21:39 and 23:29 with the STEAM profiles 3, 1, and 5 at CDPs 4652, 2632 and 1516 respectively. At the crossing with line 3 the PSAT profile shows diffractive acoustic basement and a small deep with internal reflectors (Fig. 3a) compatible with the STEAM profile near the same location. On the crossing with line 1, the upper sediment unit is seen at the south flank of a canyon and also has internal reflectors (Fig. 3b). On the L1 profile several sub-vertical faults are seen affecting the lower sediment unit. Finally the southernmost crossing, with line 5, shows in both lines strong diffraction and a steep slope compatible with a thin veneer of sediments over an acoustic basement of harder rocks (Fig. 3c).

Line PSAT 37, which is deeper than the previous one, intersects the STEAM profiles 3, 1, and 5 at 12:04, 9:17 and 7:47 respectively at (CDPs 3836, 3724 and 2562). The crossing with profile 3 shows acoustic basement and possible strong side echoes. The intersection with line 1 is also marked by the strong diffractions produced by the acoustic basement in both profiles. The crossing with line 5 occurs in the bottom of the Lisbon Canyon which shows sediments on the north flank and acoustic basement on the south flank.

Line PSAT 40, the deepest line, intersects at 1:37, 4:34 and 5:44 with the STEAM profiles 3, 1, and 5 respectively (CDPs 2434, 4700 and 3312). The crossing with line 3 is over a ridge with strong diffraction probably related to older basement rocks. The crossing with line 1 is over the floor of the Lisbon Canyon, which at this level has the deepest axis (Fig. 4). The sediment filling of the canyon is clearly seen in the STEAM profile, but is also seen on the PSAT profile, where strong reflectors define the upper unit. Finally the intersection with line 5 is just on the flank of the Afonso de Albuquerque ridge that separates the Lisbon and Setubal canyons. On this STEAM profile two sedimentary units can be identified, lying in unconformity over the basement. The short NW-SE PSAT36 line south of the Setubal canyon shows the north extremity of a contourite unit on the slope of the Alentejo margin (Fig. 5), which is very well documented in the STEAM lines.

The N-S line EACM153 was parallel to the two lines PSAT 32 and 33 N of Lisbon which were run while testing the seismic and side-scan sonar equipment, and intersect the PSAT34, 38 and 39. The intersection reveals a compatible ocurrence of a relatively thick sediment accumulation on the south upper slope of the Estremadura spur. The E-W line EACM152 is also consistent with the PSAT NW-SE lines.

### I.3. OKEAN and OREtech Side-Scan Sonar Analysis: Continental Slope Near Lisbon

*N. Kenyon, J. Monteiro, A. Akhmetzhanov, J. Lenham, D. Isakov, F. Teixeira*

Two parallel lines of OKEAN side-scan sonar data (PSAT32 and PSAT33) were run north of the Estremadura Spur and down to the foot of the margin, near where the channel fed by the Nazaré canyon approaches the edge of the Iberia abyssal plain. They are more or less contiguous with three parallel east-west lines that were obtained, along the south side of the Estremadura Spur (PSAT34, PSAT38 and PSAT39) and three parallel southeast trending lines along the steep slope west of Lisbon. The data stretches along about 240 km of the Portuguese margin. The lines south of the Spur cover the slope from near the top to near the base. An interpretation of the OKEAN data is shown in Fig. 6. The only OREtech deep towed side-scan sonar line (ORAT-16) was part way along PSAT 32 which is part way down the north side of the Spur.

One artefact on the OREtech side-scan record, seen on the upper part of the line in water depths of about 1500-2000 m, is the well-known refraction effect. This produces a zigzag

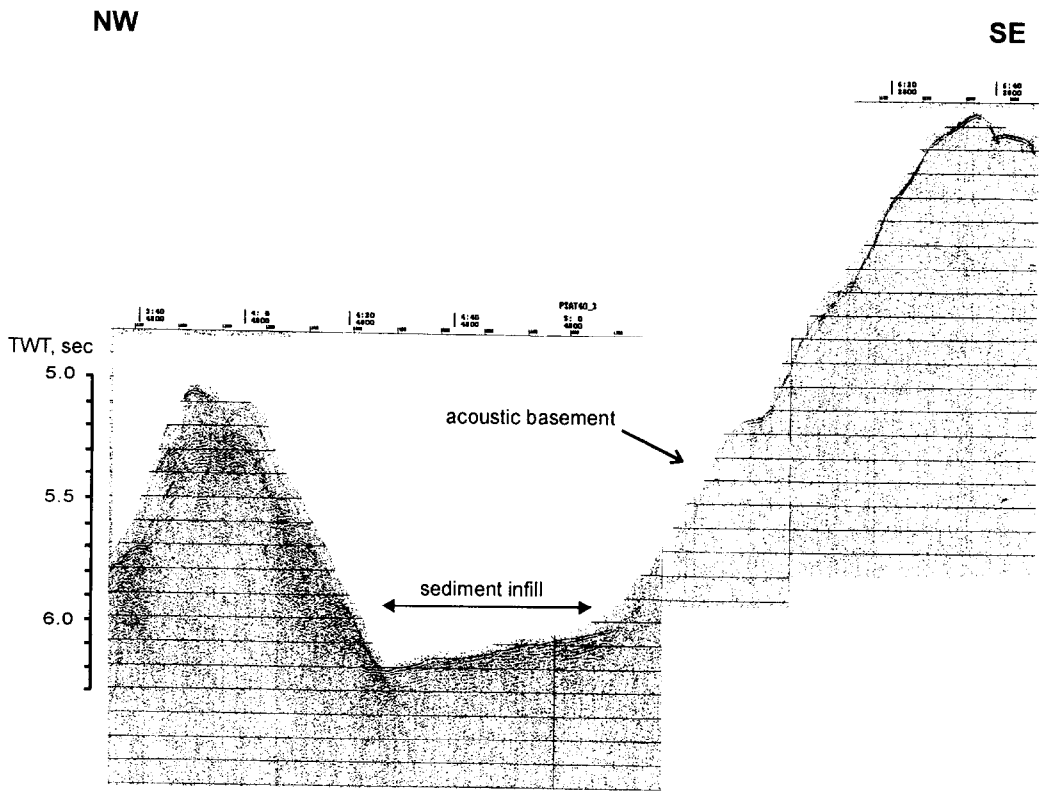


Fig. 4. Fragment of seismic line PSAT-40 showing thalweg of Lisbon Canyon filled in with bedded sediments.

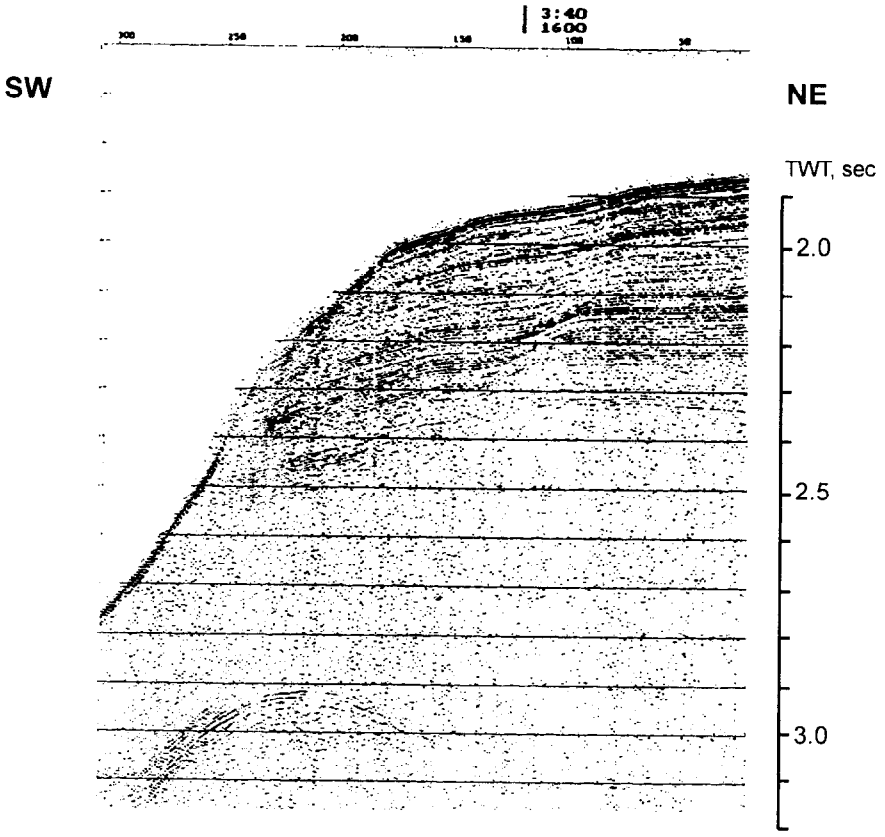


Fig. 5. Fragment of line PSAT36 line showing a contourite unit on the slope of the Alentejo margin.

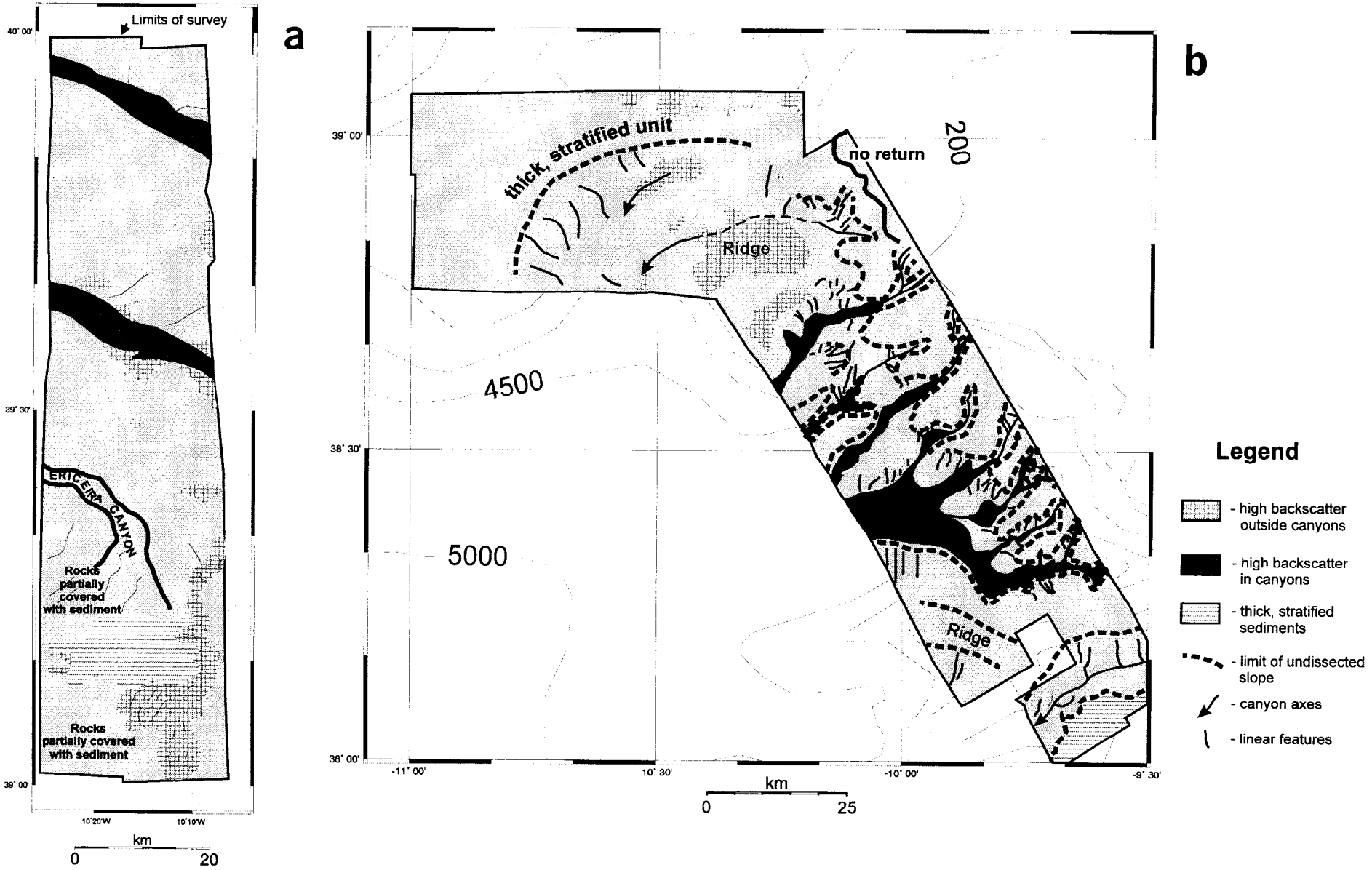


Fig. 6. Preliminary interpretation of the the OKEAN imageries of the area lying to the north of Estremadura Spur (a) and west of Lisbon (b).

pattern due to refraction of sound by internal waves along the boundary between two water masses.

The Estremadura Spur crest is at shelf depths at its eastern end and is at about 3000 m in the western end of our survey area. There are extensive patches of high backscatter near the top of the Spur and extending down both north and south. These look like rock outcrops and chalky rock was sampled at one site (AT 74G). The rocks are well seen on the OREtech line as a swirly pattern, familiar from outcrops of bedded sediments in shelf depths (Fig. 7). Within a slight deep at the top of the Spur there is a mappable area of low backscatter that appears to correspond to thicker superficial soft sediments. It is at a depth of about 1200 m, which is consistent with it being transported there by the Mediterranean water. A narrow canyon is crossed part way down the Spur offshore of Ericeira. The distal parts of the two major canyons running from the shelf to the Iberia abyssal plain are also crossed. The Nazaré canyon has a weak backscattering floor and gullies down the channel walls. The Leiria canyon has a stronger backscattering floor and no obvious gullies on the walls. As the floors were not sampled it is not possible to say why the channels should be different in their acoustic characteristics.

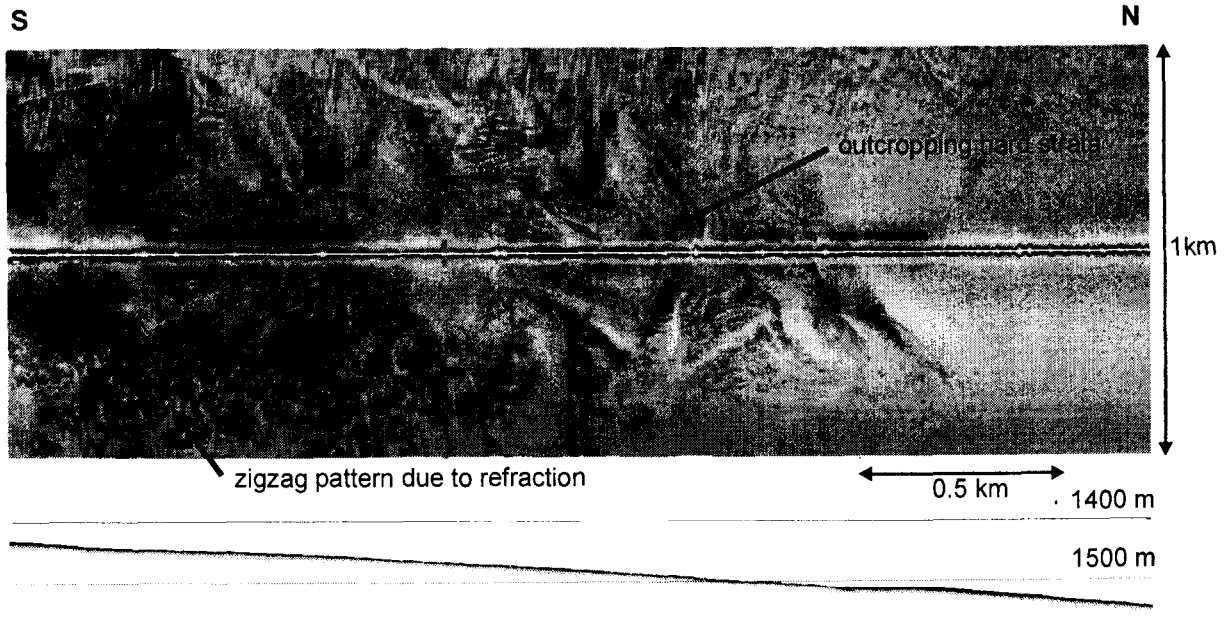


Fig. 7. Fragment of ORAT-16 sonograph and subbottom profiler record showing rock outcrop at the Estremadura Spur crest.

A broad bight in the contours of the lower slope is located south of the Estremadura Spur at a latitude of about 10°40'W. The overall backscatter levels of the south side of the Spur are uniformly low but are interrupted in places by patches of strong, speckled looking backscatter (Fig. 8). The low backscatter levels are related to the cover by a thick, stratified upper unit, attributed, at least in part, to deposition under the influence of contour currents and hemipelagic sedimentation processes. Some of these strong backscattering patches are along the crest of the Spur, shallower than 1800 m, and correspond on the seismic profiles to outcrops of basement rocks that are perhaps swept clear of superficial sediment by currents. Others are within an area below about 2200 m where the unit of well bedded sediments is partly eroded. The strong backscatter patches here also correspond to places where the underlying basement is revealed. The relief patterns in the erosional area within the upper

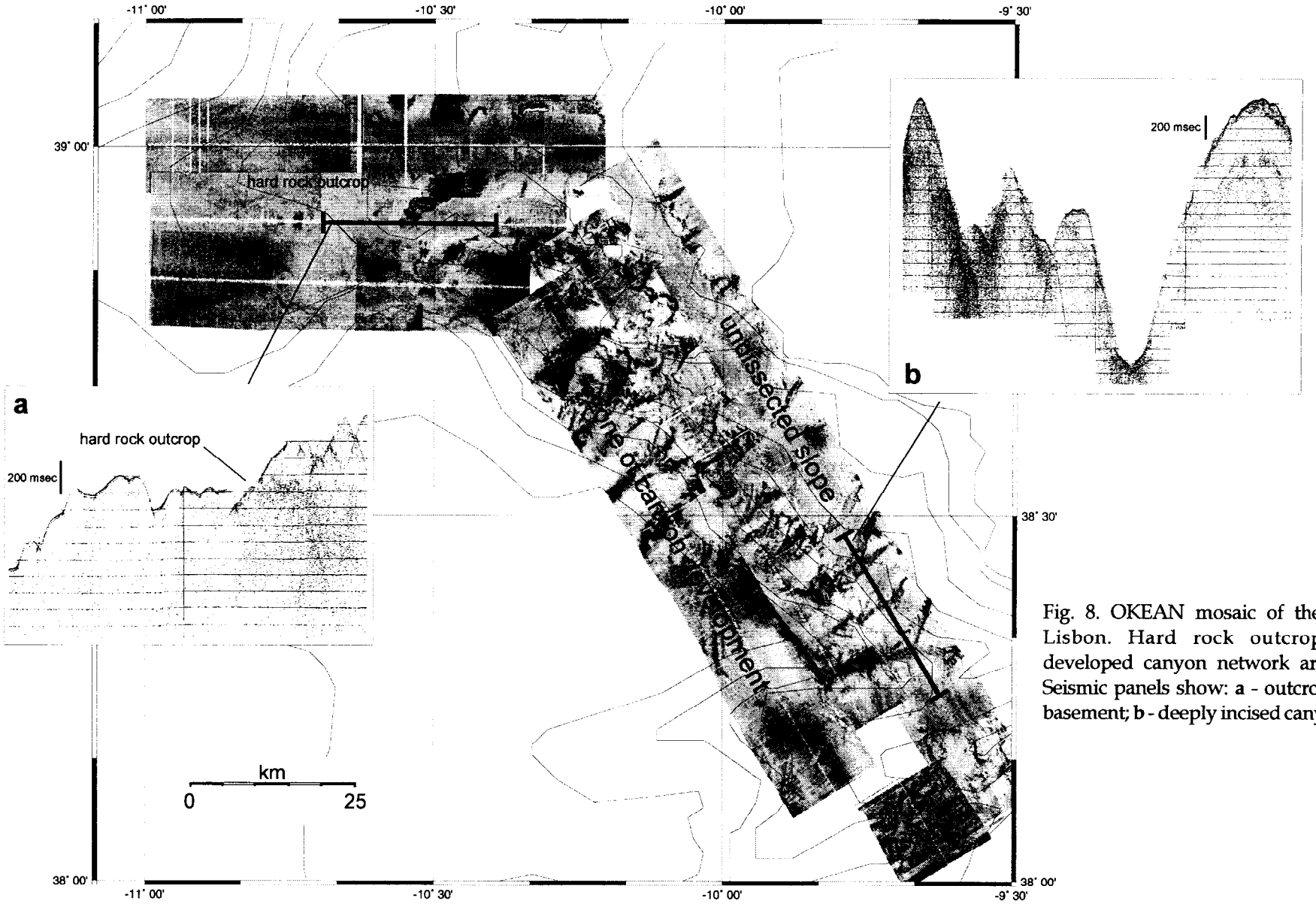


Fig. 8. OKEAN mosaic of the area west of Lisbon. Hard rock outcrops and well-developed canyon network are clearly seen. Seismic panels show: **a** - outcropping acoustic basement; **b** - deeply incised canyons.

bedded unit are not mappable from the side-scan data. Presumably this is because the sediment is fine grained, uniform in composition and unlithified and hence does not reflect much sound. The erosion is presumed to be by an episode of either gullying of the slope by frequent small turbidity currents or by infrequent slumping events. Most of the upper stratified unit was laid down before the erosional episode.

The axis of one canyon system appears to run northwest along the slope and to reach the bight in the foot of the Estremadura Spur by making its way north of a prominent ridge. There are extensive areas of basement outcrop on this ridge, mapped as high backscatter levels. Thus the ridge is formed of particularly resistant rocks.

The slope offshore from the shelf south of Lisbon is particularly steep (greater than 1 in 10). It is extensively canyoned with canyons that tend to increase in depth to the south. The southernmost canyon is the Setubal Canyon, which is broad and deep and is the only one in this region which cuts back across the shelf to head close to the shore. It is isolated from the others by a broad ridge, that trends approximately east-west. The other canyons are all tributaries of the Lisbon canyon system and feed into the north side of the broad canyon running along the foot of the ridge.

The Setubal canyon is only imaged in its mid reaches, where it is about 15 km wide and 1500 m deep. There are gullies down the sides and a rim is mappable in places but there is no obvious thalweg seen on the OKEAN data.

The Lisbon canyon tributaries are relatively narrow in their upper reaches and are separated from each other by undissected slope. These undissected spurs have low backscatter levels and some fine scale ornamentation on OKEAN records (Fig. 8) that could be small slump scars or contour current formed mud waves. The spurs are broad as far down as an identifiable line at about 2200 m depth. Below that they are knife edged or arête-like ridges separating gullies or canyons. At this level the canyons become wider and the whole slope is eroded. In contrast to the canyons of the Biscay Margin (Kenyon et al., 1978) there are few obvious tributary gullies (apart from one amphitheatre shaped, leaf like pattern). Rather there are irregular shaped, or concave downslope relief features associated with canyon floors, that are probably related to differential erosion of bedding and to fault patterns. Concave downslope outcrops of resistant rocks within a canyon indicate that there are bedding planes, striking along slope but with a low dip. The axes of many of the canyons are marked by a belt of stronger backscatter (Fig. 8) (but not the Setubal Canyon). A similar pattern was seen west of Corsica and Sardinia (Limonov et al., 1995). Here it was found, from sampling and high resolution side-scan sonar data, that the backscatter was due to bare rock in the canyon thalweg or to sheets of well sorted, rippled pebbles or coarse gravels. A similar origin is expected here and the two samples from areas of strong backscattering bands (AT 77G and AT 78G) bear this out as they contain rock or a small quantity of hemipelagic ooze. If this does represent scoured floor then the height of the boundary between the high backscattering bands and the low backscattering upper walls of the canyon may provide enough information to calculate the cross section of the eroding flows at several points down the canyons.

The deepest canyon of the Lisbon canyon system along our uppermost line is the southernmost one. However where seen on our middle line this canyon has virtually disappeared as a relief feature although its course can clearly be followed as a high backscattering band. Turbidity currents passing down the canyon meet the highly resistant east west ridge and are forced sharply to the right.

There are a number of places where the canyon and gully trends seem to be influenced by structure and also places where geological structures of some kind are mapped. The commonest linear trends are N-S or NNE-SSW. This is consistent with the fault trends on the nearby land (Carta Geológica de Portugal, 1992).

## I.4. Bottom sampling

*G. Akhmanov, A. Mazzini, S. Severmann, B. De Mol, A. Akhmetzhanov, A. Stadnitskaya, A. Sautkin, I. Belenkaya, E. Kozlova, A. Gili, R. Brambilla, I. Mardanyan, R. Hale, M. Kozachenko, V. Krupskaya, S. Lubentsova, I. Probert, A. Cook, E. Maginn*

A total of 9 stations in 3 study areas were sampled, using a gravity corer or a dredge (Fig. 2). Area 1 and 2 are both potentially high-energy settings characterised by along-slope and down-slope currents. Three cores were collected from the first area lying to the north of Estremadura Spur in order to sample a high backscattering area (core AT-74G) and a gently dipping slope northward of the Nazaré Canyon (AT-75G and AT-76G). Area 2 is located in the area of the Lisbon canyon system (cores AT-77G, AT-78G and AT-79G). In area 3 we sampled the sediments near the north-south trending scarp of a very deep seated fault that has been investigated previously during ODP leg 149, site 901A (Sawyer et al., 1993). One dredge profile perpendicular to the fault was carried out (AT-80D) and two gravity cores recovered (AT-81G and AT-82G) from the sediments covering the scarp.

The main sampling site parameters and the sedimentological, acoustic and geological characteristics are summarised in tables 1 and 2.

| Station No | Date | Time (GMT) | Latitude | Longitude | Depth, m | Recovery |
|---|---|---|---|---|---|---|
| TTR8-AT-74G | 15-06-98 | 20:32 | 39°06.888 | 10°20.039 | 1066 | 17 cm |
| TTR8-AT-75G | 16-06-98 | 23:55 | 39°46.931 | 10°21.676 | 3638 | 32.2 cm |
| TTR8-AT-76G | 17-06-98 | 02:55 | 39°40.134 | 10°20.528 | 3900 | 373.5 cm |
| TTR8-AT-77G | 19-06-98 | 10:17 | 38°11.587 | 09°44.033 | 1605 | 168 cm |
| TTR8-AT-78G | 19-06-98 | 12:14 | 38°16.698 | 09°47.934 | 3420 | 10 cm |
| TTR8-AT-79G | 19-06-98 | 14:32 | 38°21.666 | 09°51.810 | 4090 | CC |
| TTR8-AT-80D | 20-06-98 | 11:14<br>12:04 | 40°45.157<br>40°44.997 | 11°03.581<br>11°02.883 | 4635<br>4564 | 0,3 $m^3$ |
| TTR8-AT-81G | 20-06-98 | 14:47 | 40°45.007 | 11°03.488 | 4530 | 425 cm |
| TTR8-AT-82G | 20-06-98 | 18:10 | 40°44.996 | 11°03.359 | 4488 | 378 cm |

**Table 1.** General information on the sampling stations on the Portuguese margin.

*Area lying to the north of Estremadura Spur (Fig. 9)*

Core TTR8-AT-74G

Only a very short core was recovered (17 cm). The upper section consisted of fragments of carbonate crust, a well preserved polyp of *Desmophyllum sp.*, several coral branches and one echinoderm spine intermixed with a soupy marl rich in foraminifera. The second interval consists of structure-less white and partially lithified coccolith ooze with a very low amount of terrigenous admixture.

Core TTR8-AT-75G (Fig. 10)

The core can be divided into two main sedimentary facies, which are separated by a sharp redox-boundary as evident from the abrupt colour change. The upper oxidised layer consists of brownish marl rich in foraminifera, which becomes more consolidated with depth.

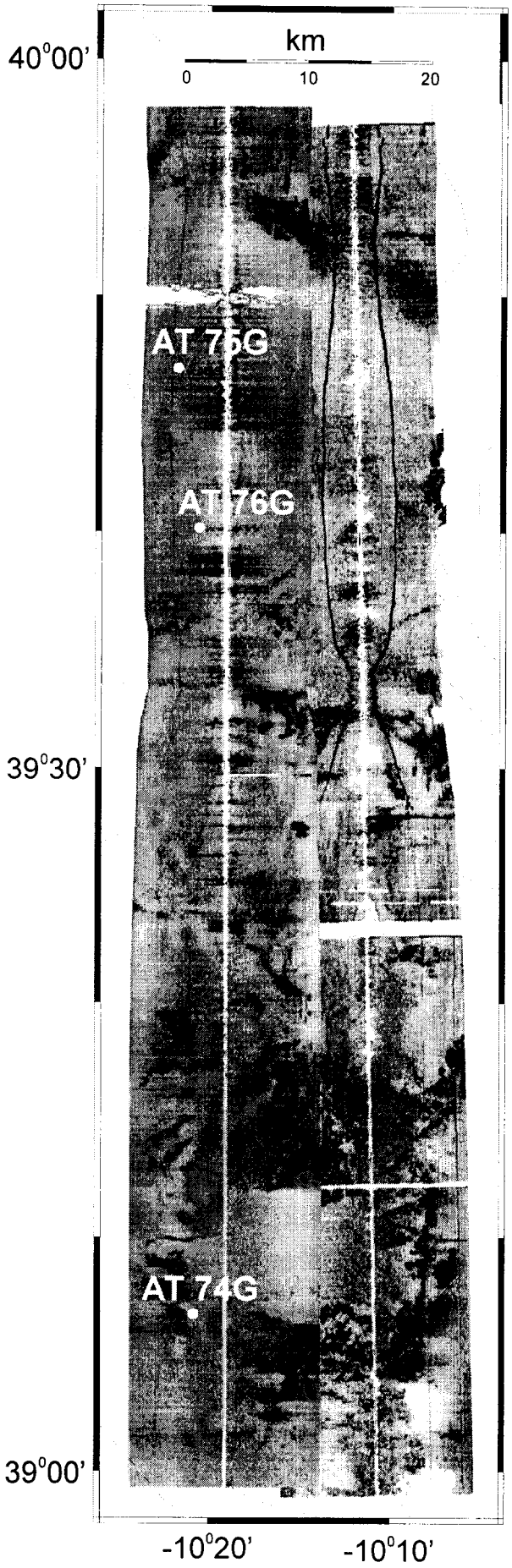


Fig. 9. OKEAN mosaic of the area north of the Estremadura Spur. Sampling sites are shown.

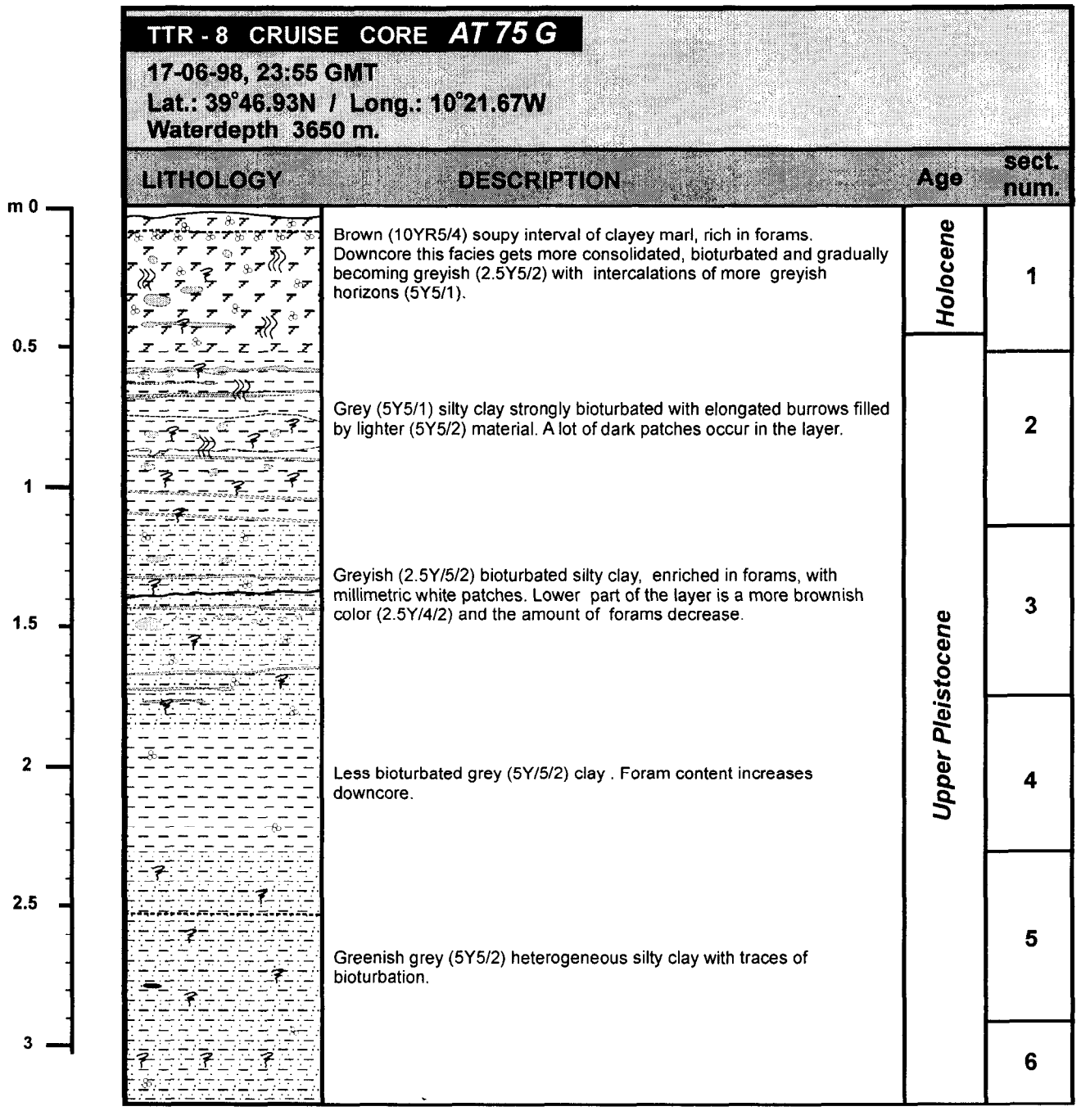


Fig. 10. Core log AT75G.

The colour is gradually changing from brown to grey, and the composition is changing from marl to silty clay toward the redox-boundary. The entire core is thoroughly bioturbated and the colour in the lower section is gradually changing from grey to greenish grey to olive grey. Large burrows and small white patches, a few mm in diameter (carbonate infilled), occur between 135 and 175 cm depth.

| Station No. | Geographical Setting | Sedimentary Summary | Instrumentation | Acoustic characteristics |
|---|---|---|---|---|
| TTR8-AT-74G | In a depression on the top of a small hill in the north-eastern slope of Estremadura Spur. | Mixture of foraminiferal ooze, carbonate crust, polyps of dead *Desmophyllum sp.*,. and coral branches in the upper part, and coccolith ooze in the lower part. | OKEAN side-scan sonar, echo sounder profile | Medium to high backscattering area on OKEAN line 32 |
| TTR8-AT-75G | Higher part of a gently dipping slope, north side of the Nazaré Canyon | A layer of oxidized marl at the surface which is gradually becoming silty clay and strongly bioturbated towards the bottom | OKEAN side-scan sonar, echo sounder profile | Very low backscatter on a flat area on OKEAN line 32 |
| TTR8-AT-76G | Lower part of a gently dipping slope, north outflow of the Nazaré Canyon, about 14 km south of AT-75G | Same as AT-75G but with evidence of slumping in the lower half of the core. | OKEAN side-scan sonar, echo sounder profile | Very low backscatter on a flat area on OKEAN line 32 |
| TTR8-AT-77G | Flat shelf on top of a ridge between Lisbon and Setubal canyons crossing the continental margin south of Lisbon (PSAT 37, 5:53) | A layer of oxidized marl at the surface which is gradually becoming silty clay and strongly bioturbated towards the bottom | OREtech side-scan sonar, single channel high resolution seismics | Medium backscatter on OKEAN line 37 |
| TTR8-AT-78G | Southern slope of Lisbon canyon (PSAT 37, 6:58) | Grey silty clay sediment on the top, massive lithified mudstone on the lower part. | OKEAN side-scan sonar | High backscatter on OKEAN line 37 |
| TTR8-AT-79G | Bottom of Lisbon canyon (PSAT 37, 7:50) | Small amount of brownish marl with millimetric rock fragments. | OKEAN side-scan sonar, single channel high resolution seismics | High backscatter on OKEAN line 37 |
| TTR8-AT-80D | Across fault scar in the southeastern part of the Iberia Abyssal Plain | Foraminifera-rich clay, few echinoderms, no hard substrate. | Bathymetric map, echosounder profile | No data |
| TTR8-AT-81G | Steep lower part of the slope of fault scar (near AT-80D) | Oxidized marl in the upper part and intercalations of clayey and silty clayey layers in the lower part, indication of slumping | Bathymetric map, echosounder profile | No data |
| TTR8-AT-82G | Highest part of the fault scar (near AT-80D) | Same as AT-81G but without slumping. | Bathymetric map, echosounder profile | No data |

**Table 2.** Sedimentological, acoustic and geological characteristic of sampling stations on the Portuguese margin.

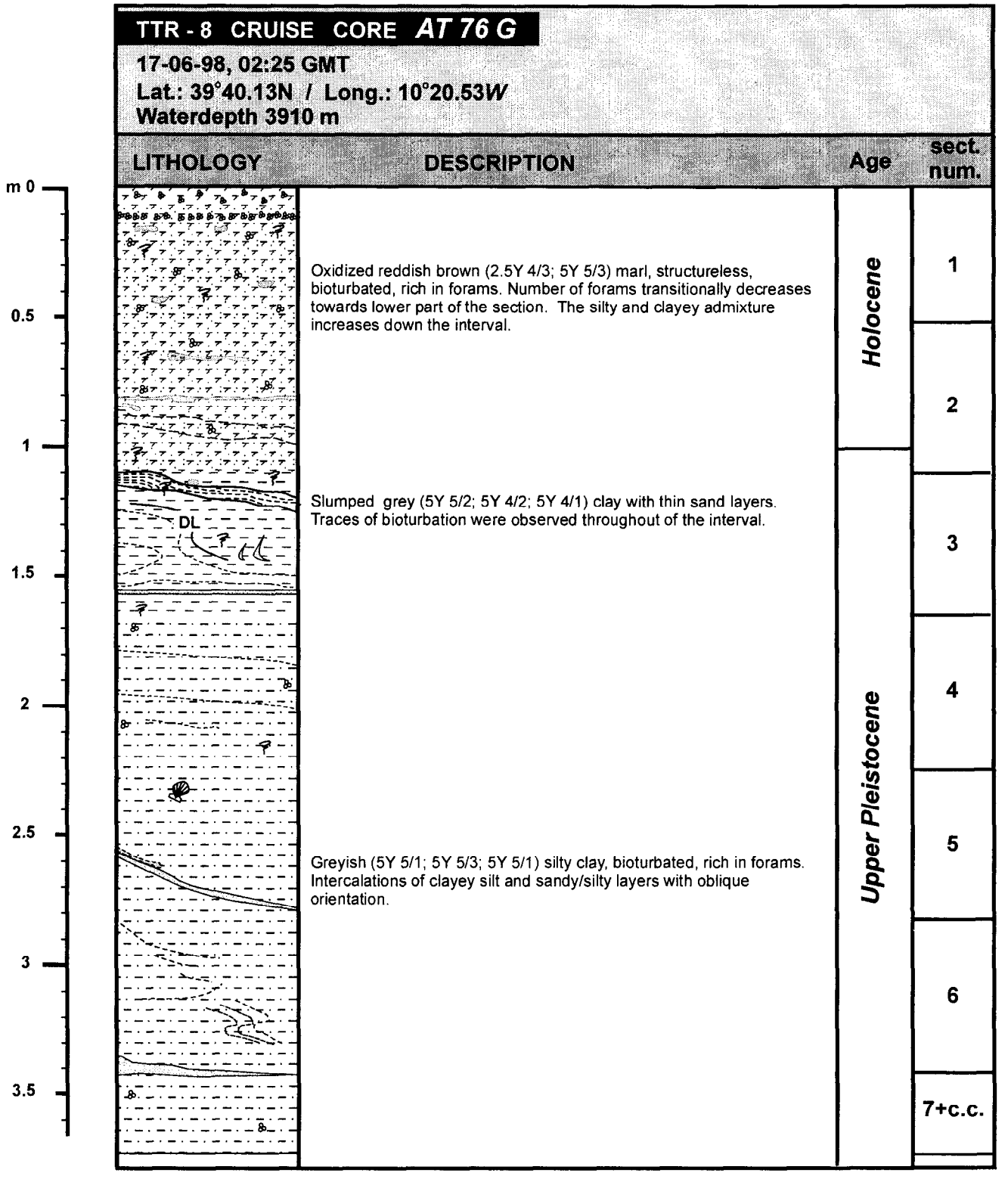


**Total length: 373.5 cm**

Fig. 11. Core log AT76G.

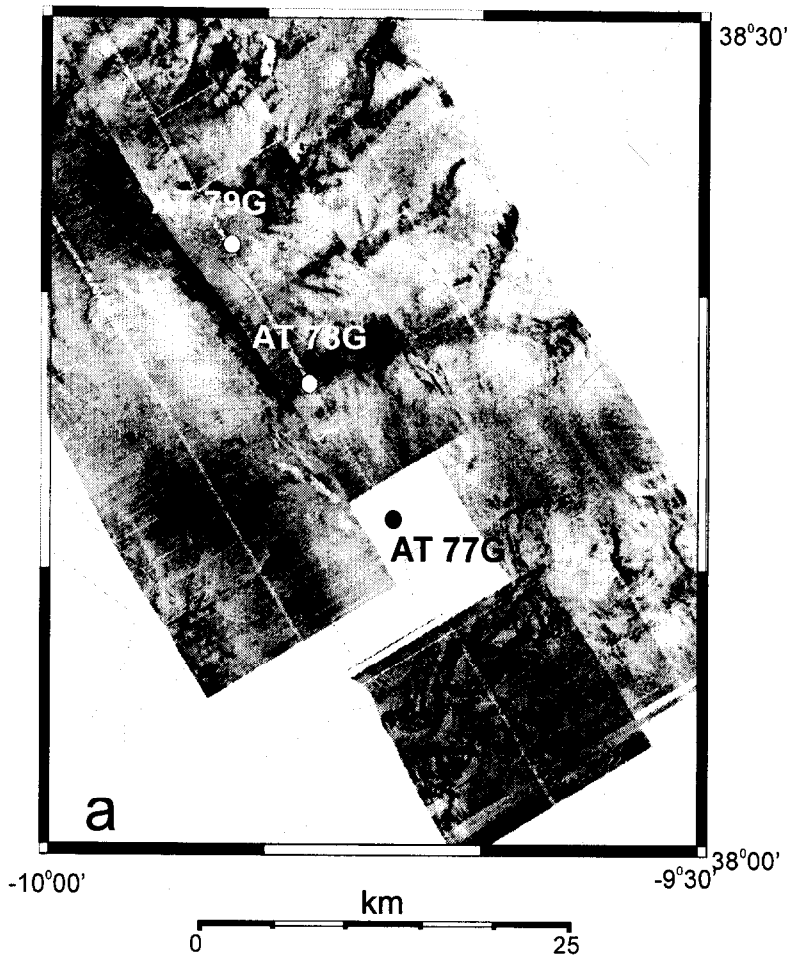


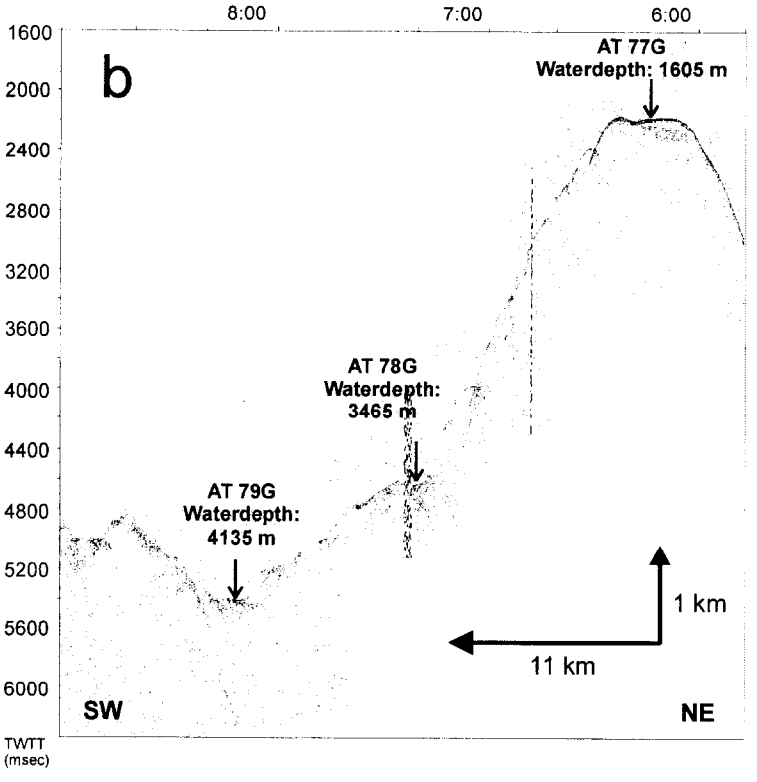


Fig. 12. Location of sampling sites on the OKEAN mosaic(a) and along seismic line PSAT-37 (b) in the area lying to the west of Lisbon

Core TTR8-AT-76G (Fig. 11)

It is very similar to core AT-75G with an upper oxidised layer of red-brown marl. The lower section is composed of well bioturbated, grey silty clay. In contrast to the previous core this section shows evidence of two slumps. The lower boundary of the upper slump is intercepted by a horizontal layer of fine sand, and a second oblique layer of fine sand was found further downcore.

*Area of the Lisbon canyon system (Fig. 12)*

Core TTR8-AT-77G (Fig. 13)

The uppermost interval (0-11 cm) of the core consists of marl, greyish brown due to oxidization, rich in forams, becoming more consolidated towards the lower part where the sediment turns to a greyish colour. The rest consists of grey silty clay with intervals enriched in forams and terrigenous silty admixture. The lowermost recovered interval shows lamination of grey and pale grey clayey layers. Some intervals contain a number of burrows, where the sediment has a higher amount of forams and is more silty/sandy. A few oblique layers imply a slump activity moving material from the uppermost part of the sampled ridge.

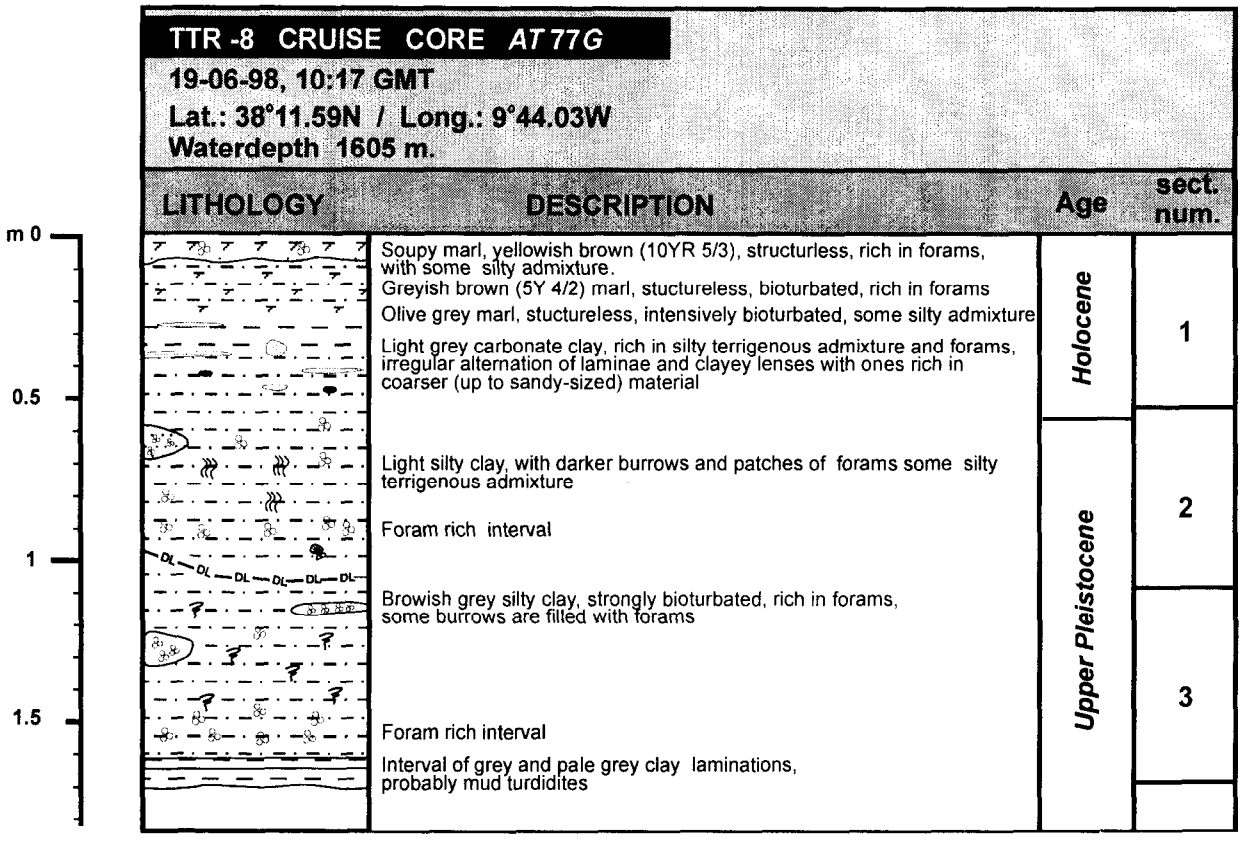


Fig. 13. Core log TTR8-AT77G

Core TTR8-AT-78G

The recovered sediments consisted of a 6 cm thick dark grey, lithified, massive mudstone, with small-scale, elongate bioturbation structures and overlain by 4 cm of brownish grey silty clay containing foraminifera.

Core TTR8-AT-79G

A small volume (< 20 $cm^3$) of brownish soupy marl, containing few foraminifera, bioclasts and a modest proportion of angular rock fragments, up to 3 mm in diameter was recovered from a canyon at the foot of the same slope sampled at the two previous stations. The presence of rock fragments in this sample suggests that the basement was close below the sediment surface and prevented further penetration of the corer.

*Scarp of a deep-seated fault on the Iberian abyssal plain (Fig. 14)*

Dredge TTR8-AT-80D

Approximately 0.3 $m^3$ of yellowish brown, structure-less soupy marl was recovered. The foraminifera rich sediment also contained a few living worms and two echinoderms: one well preserved *Ophiurida* and one fragment of a sea urchin.

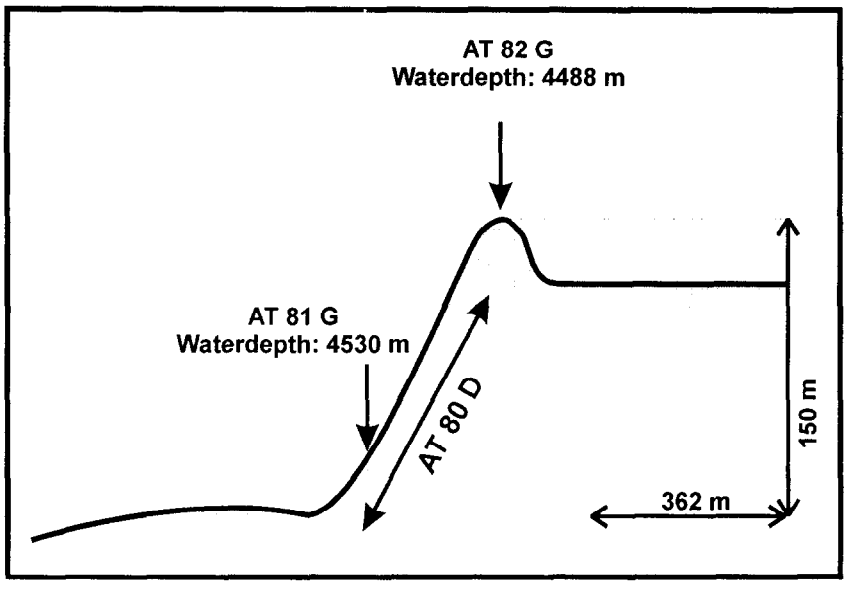


Fig. 14. Echosounder bathymetry profile and sampling sites in the area of the fault scarp in the Iberia abyssal plain.

Core TTR8-AT-81G (Fig. 15)

The sediment recovered showed an upper part (0-16.5 cm) of structureless reddish brown marl rich in foraminifera, with intercalation of oblique layers of Fe/Mn-oxide crusts (?). The unoxidised part of this core consists of two main lithologies: lighter foraminifera-rich carbonate clay and darker bands of silty clay with higher terrigenous admixture are clearly distinguishable. The entire core is strongly affected by bioturbation and distortion of the oblique boundaries. The burrows are infilled with three different types of sediments. The majority contains a finely grained, greenish material. Few burrows are filled with dark grey, soupy, pelitic sediment without any foraminifera or terrigenous admixture, whereas others contain dark grey silty sandy material. The orientation of the layers suggests recent slumping that effected the first 164 cm of the core.

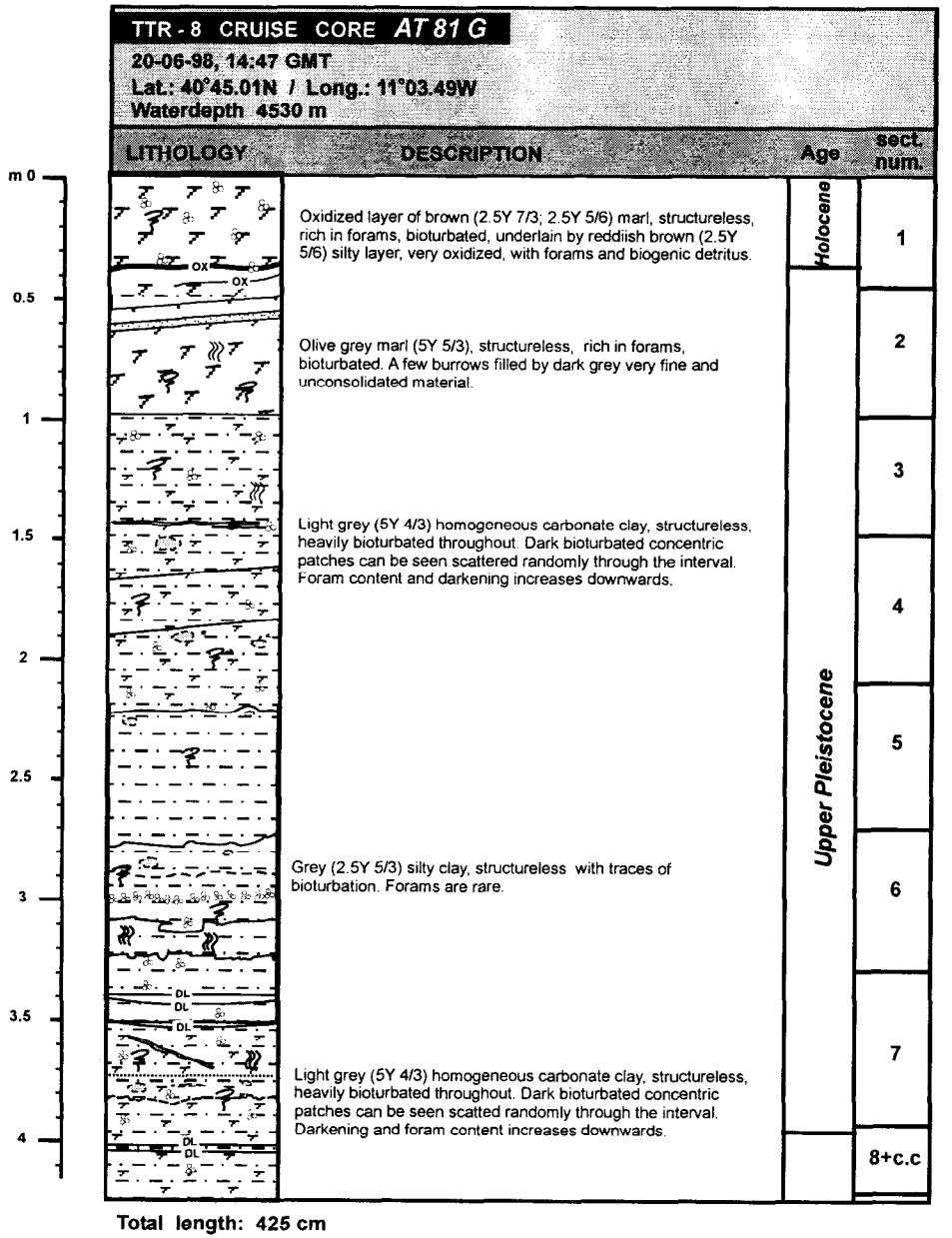


Fig. 15. Core log AT81G.

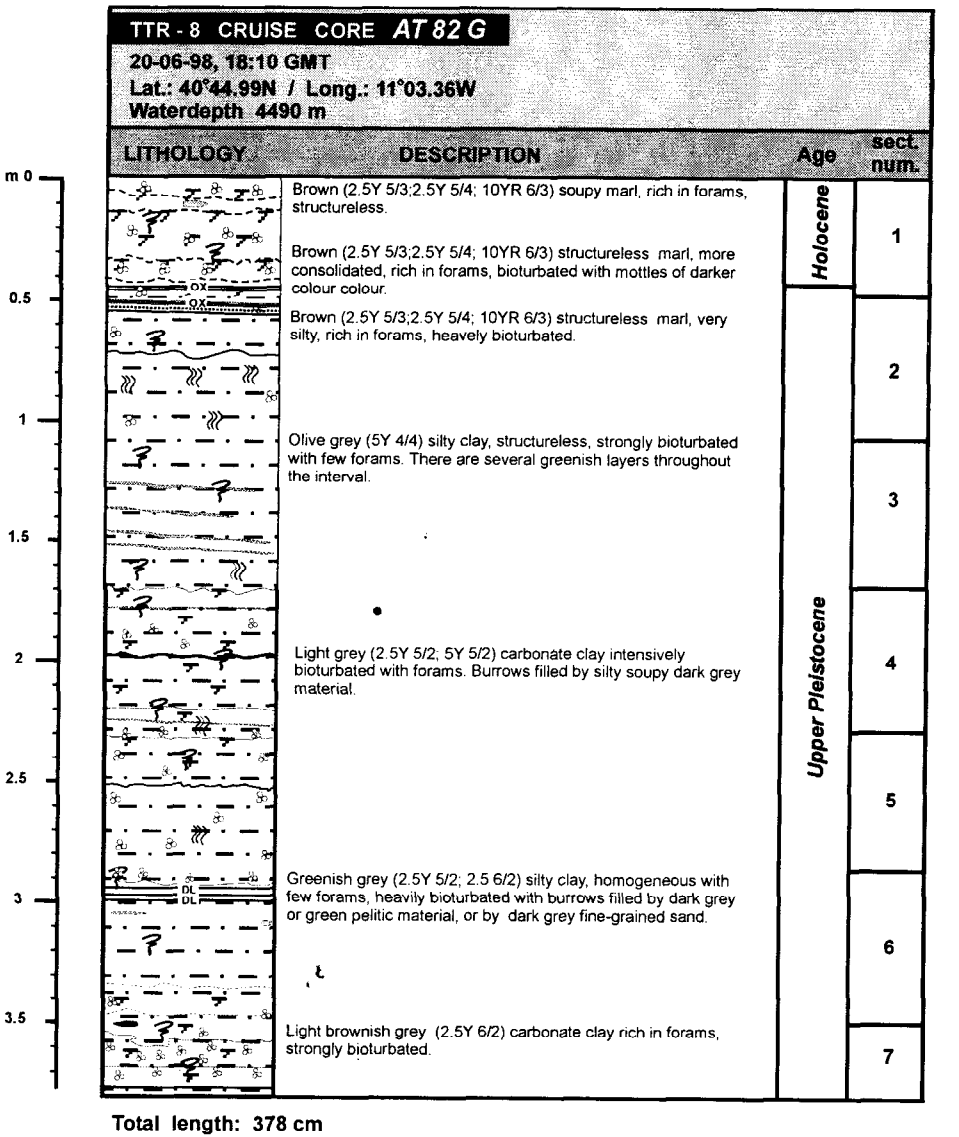


Fig. 16. Core log AT82G.

Core TTR8-AT-82G (Fig. 16)

The sequence recovered shows characteristics very similar to the previous core. It also consists of reddish-brown oxidised, structureless marl, rich in foraminifera. Light grey carbonate clay layers rich in foraminifera alternate with grey silty clay layers, and both are intensively bioturbated. The same three types of sediment infill as in the previous core were recognised inside the burrows. Most of the layers throughout the core have an oblique orientation, implying slumping.

*Micropalaeontological investigation*

The aim of the micropalaeontological investigations was to date the cores using planktonic and benthic foraminifera and coccoliths and to provide some palaeoceanographic interpretations. Samples were taken from the different lithologies seen in cores AT75G, AT75G, AT77G, AT81G and AT82G. One sample was taken from each of cores AT74G and AT78G as only a small amount of sediment was recovered. Foraminiferal residues and smear slides were prepared for identification of species, and dating of the cores was carried out.

The Holocene foraminiferal assemblages in cores AT75G, AT76G, AT77G, AT81G and AT82G are dominated by typical warm-water planktonic species (*Globigerinoides ruber, Orbulina universa, Hastigerina siphonifera, Globigerina rubescens, Globigerinoides tenellus*). Some pink coloration is seen in *G. ruber* and *G. rubescens* which is typical of warmer water conditions. The presence of the cosmopolitan species *Globigerina bulloides* in all of the sections is characteristic of upwelling. There is also an increased number of benthic species including some agglutinated types. The presence of some cold-water benthic species such as *Epistominella exigua* in the Holocene section of AT75G may suggest the presence of colder bottom water currents.

The Pleistocene assemblages are dominated by cold-water planktonic species (*Neogloboquadrina pachyderma, Globorotalia inflata, Globigerina quinqueloba, Globorotalia scitula*). There are fewer benthic forms in these sections and the abundance of foraminifera is generally lower. This is due to reduced circulation and productivity in the colder intervals.

The Holocene and Pleistocene sections were dated using the presence of the planktonic species *Globorotalia truncatulinoides* and *Globorotalia crassaformis* as they are only found in these periods. The presence of *G.tenellus* is also a good indicator of Holocene - Pleistocene sediment.

For the identification of coccoliths, the system presented by Perch-Nielsen (Bolli et al., 1985), was used. The taxa identified are predominantly the following: *Emiliania huxleyi* (most common species in Upper Pleistocene-Holocene sediment) and *Gephyrocapsa* (common genera in Pleistocene- Holocene sediments). All *Gephyrocapsa* were subdivided into the four main groups: *G. muellerae, G. oceanica, G. caribbeanica* and 'small' *Gephyrocapsa* (includes all *Gephyrocapsa* less than 2 μm). In almost all the samples *Coccolithus pelagicus* (cool-water species very abundant in the North Atlantic), *Calcidiscus leptoporus* (transitonal species) and subtropical species *Helicosphaera carteri, Syracoshaera pulchra* and *Rhabdosphaera claviger* were found. In many samples *Umbilicosphaera sibogae* and *Pontosphaera sp.* were observed. Species that were rare in the sediments are *Scapholithus fossilis, Braarudosphaera bigelowi* and *Scyphosphaera sp.*. Some reworked calcareous nannofossils such as *Micula cf. decussata, Discoaster sp, Neochiastozygus sp, Chiasmolithus sp.* were detected in small amounts (up to 5%) in the sediments.

There are differences between the Glacial and Interglacial assemblages of coccoliths. In glacial sediments, the total quantity of coccoliths is relatively small and the assemblage consists of *E. huxleyi,* some *Gephyrocapsa sp., C. pelagicus* and *C. leptoporus,* and subtropical and tropical species become rare or very rare. In the Holocene and interglacial sediments, the total quantity and diversity of coccoliths is very high. The assemblage consists of *E. huxleyi,*

numerous *Gephyrocapsa sp, H. carteri, C. Pelagicus, C. leptoporus, S. pulchra, R. claviger* and others.

For stratigraphical subdivision of the sediments, the stratigraphical scale of nannoplankton zonation (Gartner, 1977) was used. The Pleistocene-Holocene was subdivided into four nannoplanktonic zones: *Pseudoemiliania lacunosa* zone (LO (last occurrence) of *Discoaster brouweri* to LO *P. lacunosa*), *Gephyrocapsa oceanica* zone (LO of *P. lacunosa* to FO (first occurrence) of *E. huxleyi*), *Emiliania huxleyi* zone (interval of dominance of *Gephyrocapsa* in the assemblage) and *Emiliania huxleyi* ACME zone (interval of dominance of *E. huxleyi* in the assemblage). Stratigraphical subdivision and correlation of the cores is shown in figure 17.

Core AT74G contained an interesting assemblage of foraminifera including the planktonic form *Hantkenina* spp. This particular type of foraminifera is only found in the Mid-Late Eocene. In the coccolith assemblage *D. elegans, D. saipanensis, D. wemmelnsis, D. cf. tanii, Chiasmolithus cf. oamaruensis* were found. This species is characteristic of Mid-Late Eocene

Another interesting assemblage was found in core AT78G which contained the planktonic foraminifera *Morozovella formosa formosa,* which is the type species of a mid Early Eocene foraminiferal zone. In the assemblage of coccoliths *C. pelagicus, Pontosphaera sp., Rhabdosphaera sp., Micula cf. decussta* were found. Preservation of coccoliths is very poor. The presence of numerous *M. cf. decussta* confirmed that the sample was of Eocene age.

The foraminiferal assemblages in core AT81G indicate that there were a number of climatic fluctuations during the Pleistocene period in this area. At the base of the core the foraminiferal assemblage is characterised by warm-water planktonic species and high benthic diversity suggesting that productivity is high. This is characteristic of inter-glacial conditions. Warm-water conditions continue upcore until section 6 where there is an increase in cold-water planktonic forms. This is accompanied by a decrease in the abundance of benthic species suggesting a change to glacial conditions. Glacial conditions persist until there is a change in the foraminiferal assemblage in section 4 to one dominated by warm-water planktonics and an increase in benthic productivity indicating a shift to inter-glacial conditions. At this point the foraminifera present indicate that this is a warm temperature optima. Warm temperatures continue upcore until there is another change in foraminifera at the base of section 2 to an assemblage containing only cold-water species. There are no benthic foraminifera at this level, which suggests that a return to glacial conditions has occurred. The foraminifera in the samples from this section indicate that temperatures were colder than during the previous glacial interval. Cold-water conditions persist upcore until warm-water planktonic foraminifera again become dominant in section 1. In this section the foraminifera are typical warm-water Holocene forms and benthic species diversity and productivity is again high.

The coccolith assemblages in the cores AT81G, AT82G, indicate climatic changes from glacial to interglacial periods. In the lowest part of core AT81G redeposited discoasters were observed. Trends similar to those seen in the foraminifera results were observed in the coccolith assemblages. The relatively warm assemblage in the lower part (sections 7-6) becomes colder towards the top of the core. In this interval there are shifts between coccolith and foraminiferal assemblages. The coccolith assemblage indicates warmer conditions than the foraminiferal one (section 6) The warm coccolith assemblage is replaced by a cold one (sections 6-5). The next intervals (sections 4-3) are characterised by the warmest assemblages for both foraminifera and coccoliths. Afterwards the assemblages become colder and the coldest ones were found in sections (2-1). In the upper part of the core warm-water Holocene assemblages are present (Fig. 17). Similar changes in the foraminiferal and coccolith assemblages can be observed in core AT82G (Fig. 17).

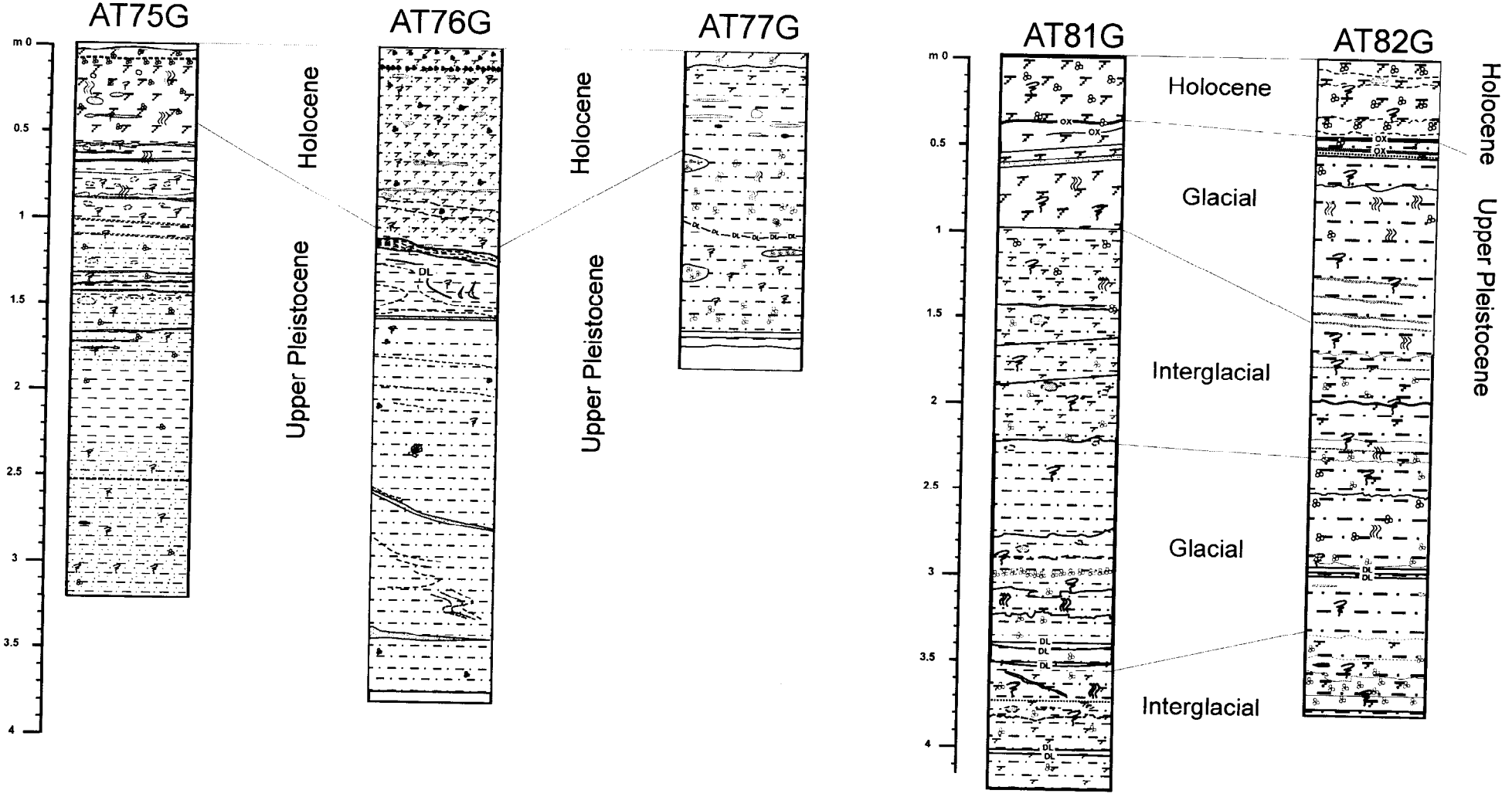


Fig. 17. Correlation of cores taken on the Portuguese margin.

*Discussion*

The three cores recovered in the area north of Estremadura Spur show two different trends. The first core (AT-74G) was recovered from an area which was interpreted from the OKEAN profile as a topographic high covered with a hard substrate. This interpretation was confirmed by the occurrence of the lithified coccolith ooze in the lower part of the core. It was dated as upper Eocene and indicates pelagic conditions of open warm sea with very low, if not absent, input of terrigenous material. The upper layer, which contains fragments of cold water corals (*Desmophyllum sp.*) and crust fragments admixed with Holocene sediments, could be interpreted as debris from the very top of the sampled hill and might imply propitious conditions for the growth of the coral colony. Deep-water corals require hard substrate in regions with low sedimentation rates and strong bottom currents. The other two cores from this area were taken from the topmost and middle part of a gently dipping slope north of the Nazaré canyon (AT-75G and AT76G respectively). Both show Holocene - Upper Pleistocene hemipelagic sequences with an oxidised surface layer, and a lower section that gradually appears darker towards the bottom with a continuously increasing silt content. In the lower half of the core slump deposits are intercalated with undisturbed intervals, implying repeated slumping and re-sedimentation.

The three cores taken in the area west of Lisbon were intended to form a transect from the very top of a spur to the canyon floor, where current activity is evident from the OKEAN profile. The intricate morphology of this sector is mirrored in the complexity of the sediment, which clearly show the different sedimentary processes typical of canyons and ridges. Very little sediment was recovered at station AT-79G, possibly indicating the presence of in-penetrable material at the base of the canyon. Similarly, core AT-78G recovered a sample of lithified mudstone covered by a thin layer of silty clay, suggesting periodic scouring by turbidity currents. The lithology of core AT-77G from the top of the ridge show similarities with the hemipelagic cores taken from the level area north of the Estremadura Spur, thus reflecting similar conditions of hemipelagic sedimentation, which is probably characteristic for the region.

No hard substrate was recovered during the dredging of the fault scarp on the Iberian Abyssal Plain, suggesting that the basement high, if not the entire scarp, is covered by a sedimentary layer of significant thickness. That was confirmed by two long gravity cores taken from the middle and uppermost parts of the scarp. In the lower section of both cores, glacial-interglacial cyclicity is evident from the distinct changes in composition and colour. This was further confirmed by the paleontological analyses that led us to distinguish four intervals corresponding to climatic fluctuations of warmer and colder periods. Interglacial periods are characterised by finer carbonate sediments rich in foraminifera, whilst increased terrestrial runoff during glacial periods leads to increased surface productivity and higher terrigenous input.

Generally sedimentation processes are ongoing on flatter areas and topographic highs, including the tops and slopes of ridges separated by canyons. Holocene-Upper Pleistocene sediments are mainly represented by clayey marl and silty clay reflecting hemipelagic conditions of a passive continental margin. Lithological and paleontological records of climatic fluctuation during Holocene-Upper Pleistocene were recorded in the sediments. Oxidation of the recent uppermost sediment is widespread in the area. Bioturbation strongly affects the whole Holocene-Pleistocene hemipelagic sedimentary succession.

The canyons show evidence of periodical erosional current activity that caused outcrop of the basement hard rocks.

## I.5. Conclusions

*J. Monteiro, N. Kenyon, M. Ivanov*

On the Portuguese margin a seismic and OKEAN side-scan sonar survey aimed at extending the existing data set, comprising EACM-AtlantisII and the STEAM94 cruises seismic lines and a GLORIA mosaic.

The new acoustic images of the seafloor allowed successful mapping of a broad network of bifurcating downslope trending canyons. Sonographs clearly showed the development of numerous gullies on the canyon walls. Most of the canyons, including Nazaré and Lisbon were found to be active at the present time and their floors are characterised by dominant erosion.

Unfortunately the shortage of towing cable did not allow a high-resolution side-scan survey of the scarp of a deep-seated fault on the Iberia Abyssal Plain. Cores taken from its top and base showed the presence of thick Holocene-Late Pleistocene hemipelagic veneer and no indications of escaping fluids were recognised.

# II. PORCUPINE SEABIGHT: SHORT VISIT

*B. De Mol, P. Friend, A. Akhmetzhanov, M. Ivanov, H. de Haas, I. Belenkaya, A. Stadnitskaya*

## II.1. Introduction

*Aims of survey*

Processes occurring at the mud mound sediment-water interface have important implications for the flux of chemical components between the water column and deposited sediments. Of particular interest is the direct or indirect precipitation of calcium carbonate by benthic organisms. The role played by the microbiota in these processes is poorly understood and little researched. Furthermore, while the importance of the micro-organism effect on the stability of sediment at such an interface has been realised for sometime, it is only recently that improved measuring techniques have made quantification of the micro-organism effect on sediment transport possible. Therefore, it was one of the aims of the sampling programme to collect undisturbed samples from the sediment-water interface of cold carbonate mud mounds to observe the sedimentary microstructure, and to quantify the Extracellular Polymeric Substances (EPS) content that has been shown in related studies (e.g. Meadows et al., 1994) to correlate with sediment stability.

A further aim of the geochemical sampling programme was to re-examine two areas described previously (e.g. Hovland et al., 1994; Cruise Report Belgica, 1997; Kenyon et al., 1998) where coral reef mounds are known to exist. Sampling was intended to build on work undertaken during previous research cruises, and to test some of the emergent hypotheses following the 1998 TTR7 Post-Cruise meeting. Such themes included the different growth mechanisms responsible for mound formation, and the effects of the relatively strong thermohaline circulation and internal tidal waves on mound stability. Microbiological tests, geochemical analyses such as XRF, ICP-MS and stable isotope analyses and petrographic techniques (SEM, light microscopy and XRD) will be conducted. Where possible, living coral specimens were collected for use in studies of coral attachment mechanisms, and dead coral specimens for use in decay and diagenesis studies. Of particular interest is a plume-like acoustic anomaly observed on a subbottom profiler record (OREtech line ORAT-5) during TTR7 Leg1; an additional OREtech line was run perpendicular to ORAT-5, and a box core was taken to examine whether this anomaly is likely to be attributable to gas bubbles or fish in the water column.

A seabed sampling survey was carried out in a square shaped area with sides of 2.5km in the northern Porcupine Basin. A total of 8 box-cores, 3 gravity cores and 2 video profiles were taken along the diagonals of the square (Fig. 18). All box-cores were logged and subsampled for biological, geochemical, physical and engineering studies. The subsamples will be analysed to produce a detailed local biogeochemical study and reliable sensitivity indices in a potential operations area for the petroleum industry. The scale and detail are chosen to be commensurate with local benthic processes.

*Procedures*

At the "Belgica-Logachev", and "Hovland" areas (in the eastern and northern Porcupine Basin respectively), a total of 7 cores were taken (Table 3). 2 gravity and 2 box cores were taken from the "Belgica-Logachev" area; 2 gravity and 1 box core was taken from the "Hovland" area. Interesting coral samples (retrieved by box core) were air-dried for later

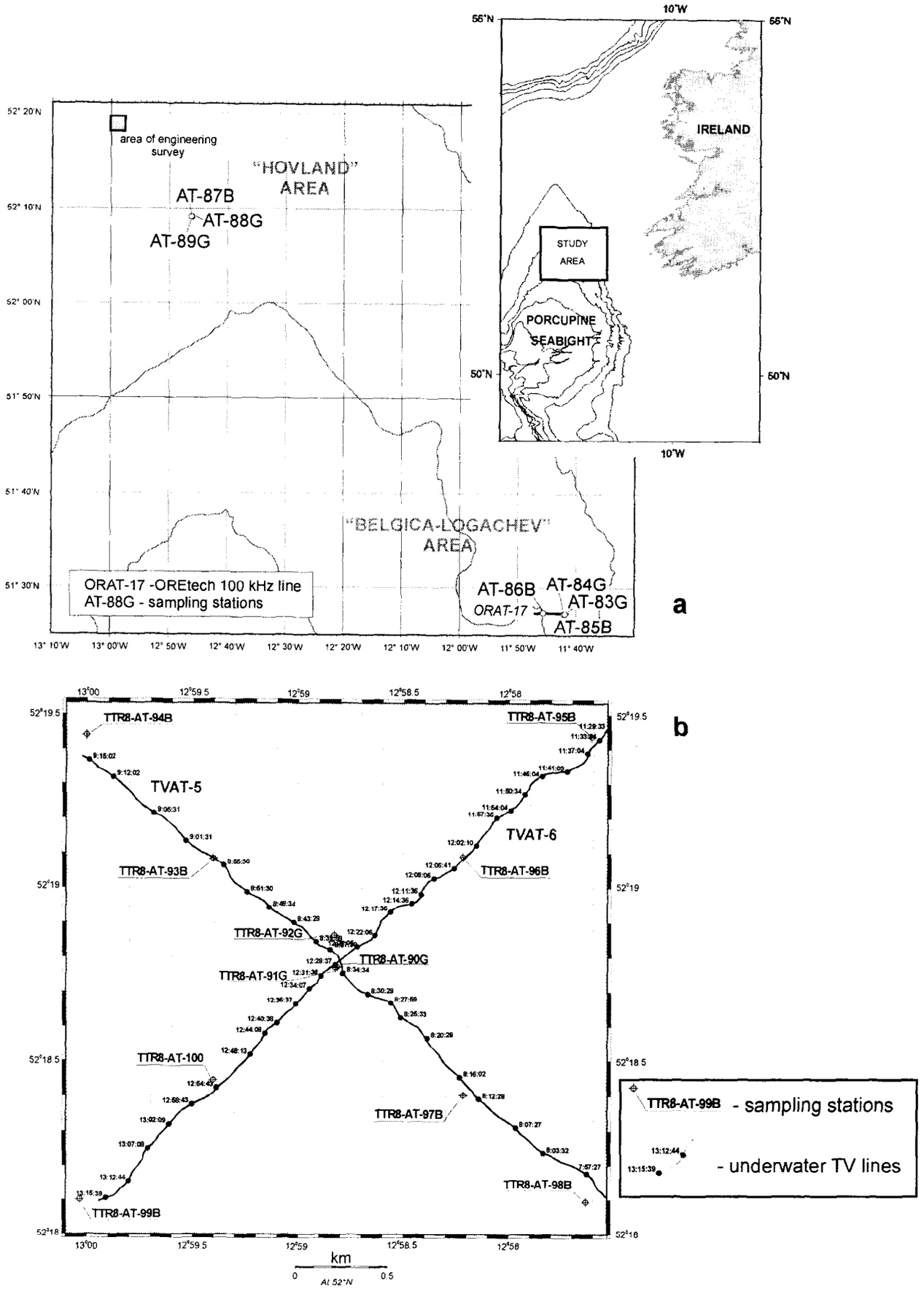


Fig. 18. Location map of the Porcupine Seabight study area (a) and detailed view of the area of engineering survey (b).

analysis. Subsampling of the box cores for sediment fabric studies and copolymer content was undertaken as described below. One gravity core from each site was retained in its core-liner, cut into sections and numbered from the bottom to the top (bottom section is section 1). The unsplit sections were sealed using greaseproof paper and wax, and stored at 4°C. Detailed descriptions of the lithologies of the remaining gravity cores, as well as the box cores, were made (See Table 4).

8 box cores and 3 gravity cores were collected for detailed biogeochemical study from a potential future operations area ("Magellan" mounds area) of the petroleum industry. Here, sample sites were arranged in a grid pattern to facilitate later statistical analysis. 1 gravity core was opened and described, the other 2 cores were retained in their liners, cut into sections, numbered and sealed as described above. Subsampling of the box cores for sediment fabric studies and copolymer content was undertaken as described below.

| Station No | Date | Time (GMT) | Latitude | Longitude | Depth, m | Recovery, cm |
|---|---|---|---|---|---|---|
| TTR8-AT-83G | 26.06.98 | 08:35 | 51°27.285 | 11°41.925 | 715 | 322.5 |
| TTR8-AT-84G | 26.06.98 | 09:41 | 51°27.291 | 11°42.120 | 716 | 300 |
| TTR8-AT-85B | 26.06.98 | 11:00 | 51°27.308 | 11°41.921 | 707 | 26 |
| TTR8-AT-86B | 26.06.98 | 18:45 | 51°27.368 | 11°45.647 | 930 | 22 |
| TTR8-AT-87B | 27.06.98 | 01:33 | 52°09.076 | 12°46.033 | 755 | 23 |
| TTR8-AT-88G | 27.06.98 | 02:33 | 52°09.093 | 12°46.094 | 700 | 333 |
| TTR8-AT-89G | 27.06.98 | 03:46 | 52°09.125 | 12°46.221 | 706 | 200 |
| TTR8-AT-90G | 27.06.98 | 14:57 | 52°18.772 | 12°58.817 | 650 | 351 |
| TTR8-AT-91G | 27.06.98 | 15:44 | 52°18.770 | 12°58.826 | 655 | 361 |
| TTR8-AT-92G | 27.06.98 | 16:40 | 52°18.865 | 12°58.829 | 655 | 310 |
| TTR8-AT-93B | 27.06.98 | 19:09 | 52°19.084 | 12°59.405 | 645 | 33 |
| TTR8-AT-94B | 27.06.98 | 19:50 | 52°19.439 | 13°00.004 | 645 | 35 |
| TTR8-AT-95B | 27.06.98 | 21:13 | 52°19.437 | 12°57.610 | 645 | 36 |
| TTR8-AT-96B | 27.06.98 | 22.06 | 52°19.089 | 12°58.219 | 657 | 35 |
| TTR8-AT-97B | 27.06.98 | 22.46 | 52°18.402 | 12°58.218 | 655 | 33 |
| TTR8-AT-98B | 27.06.98 | 23:59 | 52°18.095 | 12°57.634 | 656 | 33 |
| TTR8-AT-99B | 28.06.98 | 00:51 | 52°18.101 | 13°00.032 | 659 | 36 |
| TTR8-AT-100B | 28.06.98 | 01:30 | 52°18.445 | 12°59.404 | 650 | 34 |

**Table 3.** General information on the sampling stations in the Porcupine Seabight

*Subsampling*

Sub-sampling, using the (liquid nitrogen) cryo-technique (Wiltshire et al., 1997), was carried out on all the box cores. Care was taken to ensure that the sediment surface was sufficiently chilled by liquid nitrogen vapour, prior to the direct application of liquid nitrogen for the purposes of 'freezing' a 'biscuit' sized sediment sample (approximately 5 cm diameter, 1 cm thick). For LTSEM analysis box core sampling was used as this was the best available method to ensure high preservation potential of the undisturbed sediment-water interface. After 'freezing' samples were immediately stored at -15°C for later analysis of the microfabric by LTSEM. In addition, a short core (approximately 8 cm length, 6 cm diameter) was taken from each of the box cores, and stored at -15°C for later sectioning and colloidal carbohydrate analysis (using a standard acid-assay method).

Subsampling procedures for biological, geochemical, physical and engineering purposes were carried out on each of the box cores from the "Magellan" area. These are now briefly described:

Engineering sampling

Each box core was sampled with a U4 steel tube for engineering purposes. The steel tube was first inserted in the box core, then gently pushed down in one movement. Sealing of the U4 tube was carried out using greaseproof paper, a layer of wax, and filling with expandable polystyrene and caps. Samples are labelled with the core number and an E indicating an Engineering sample.

| Station No. | Geographical Setting | Sedimentary Summary | Instrumentation | Acoustic characteristics |
|---|---|---|---|---|
| TTR8-AT-83G | Upper slope, flank of the carbonate mound. Close to AT-23GR, TTR-7 | Succession of dark greyish brown silty sandy carbonate clay, heavily bioturbated, with foraminifera and rare shell fragments, overlain by thin olive brown interval of poorly sorted sand with a few pebbles. Several upstanding worm tubes stick out from the surface | OREtech sidescan sonar | Moderate backscatter on the OREtech line ORAT-5 |
| TTR8-AT-84G | Top of the carbonate mound. Close to AT-23GR, TTR-7, to the east of AT-83 | Not opened on board | OREtech sidescan sonar | Same at AT- 83 on the OREtech line ORAT-5 |
| TTR8-AT-85B | The same as AT-84 | Dark greyish brown silty sandy carbonate clay, heavily bioturbated, overlain by sandy interval with a few pebbles. Echinoderms, bryozoa, octocorals, brachiopoda, bivalvia, gastropoda, hydrozoan, shell and coral fragments, dropstones are at the surface | OREtech sidescan sonar | Same at AT- 83 on the OREtech line ORAT-5 |
| TTR8-AT-86B | Plume-like acoustic anomaly on the profiler record, flank of topographic high | Living corals and associated fauna at the surface. Brownish grey silty sandy carbonate clay, bioturbated, underlain by interval composed by coral debris in marly matrix | OREtech sidescan sonar | Plume-like acoustic anomaly on the subbottom profiler record, OREtech line ORAT-17 (15:25) |
| TTR8-AT-87B | Flank of the carbonate mound. | Dropstones, coral branches, bivalvia shells at the surface. Grey carbonate clay with abundant coral debris and silty sandy admixture. Uppermost part is oxidized | OREtech sidescan sonar (21:24), TV profile (04:34) | Moderate backscatter on the OREtech line ORAT-1 |
| TTR8-AT-88G | Top of the carbonate mound. Close to AT-87B | Intercalation of light grey and olive grey layers of silty marl rich in foraminifera and coral debris. Uppermost part is oxidized | OREtech sidescan sonar (21:24), TV profile (04:34) | Moderate backscatter on the OREtech line ORAT-1 |
| TTR8-AT-89G | The same as AT-88 | Not opened on board | OREtech sidescan sonar (21:24), TV profile (04:34) | Moderate backscatter on the OREtech line ORAT-1 |
| TTR8-AT-90G | Engineering survey area | Succession of olive grey silty carbonate clays. Some intervals are enriched in foraminifera and with shell fragments. Bioturbation occurs throughout whole succession . | TV-profile 5, 6 | Heavily bioturbated seafloor surface with numerous burrows |
| TTR8-AT-91G | Engineering survey area | Not opened on board | TV-profile 5, 6 | Heavily bioturbated seafloor surface with numerous burrows |
| TTR8-AT-92G | Engineering survey area | Not opened on board | TV-profile 5, 6 | Heavily bioturbated seafloor surface with numerous burrows |
| TTR8-AT-93B | Engineering survey area | Olive grey silty clay with foraminifera, heavily bioturbated, with burrows filled by sandy material. Upper 3 cm is oxidized. Surface is perforated by numerous burrows, up to 5 cm in diameter. | TV-profile 5 | Heavily bioturbated seafloor surface with numerous burrows |
| TTR8-AT-94B | Engineering survey area | Olive grey silty clay with foraminifera, heavily bioturbated, with burrows filled by sandy material. Surface is perforated by numerous burrows, up to 5 cm in diameter. | TV-profile 5 | Heavily bioturbated seafloor surface with numerous burrows |

**Table 4.** Sedimentological, acoustic and geological characteristic of sampling stations in the Porcupine Seabight.

| | | | | |
|---|---|---|---|---|
| TTR8-AT-95B | Engineering survey area | Olive grey silty clay with foraminifera, heavily bioturbated, with burrows filled by sandy material. Upper 1 cm is oxidized. Surface is perforated by numerous burrows, up to 5 cm in diameter. | TV-profile 6 | Heavily bioturbated seafloor surface with numerous burrows |
| TTR8-AT-96B | Engineering survey area | Olive grey silty clay with foraminifera, heavily bioturbated, with burrows filled by sandy material. Upper 3 cm is oxidized. Surface is perforated by numerous burrows, up to 5 cm in diameter. | TV-profile 6 | Heavily bioturbated seafloor surface with numerous burrows |
| TTR8-AT-97B | Engineering survey area | Olive grey silty clay with foraminifera, heavily bioturbated, with burrows filled by sandy material. Surface is perforated by numerous burrows, up to 5 cm in diameter. | TV-profile 5 | Heavily bioturbated seafloor surface with numerous burrows |
| TTR8-AT-98B | Engineering survey area | Olive grey silty clay with foraminifera, heavily bioturbated, with burrows filled by sandy material. Upper 1 cm is oxidized. Surface is perforated by numerous burrows, up to 5 cm in diameter. | TV-profile 5 | Heavily bioturbated seafloor surface with numerous burrows |
| TTR8-AT-99B | Engineering survey area | Olive grey silty clay with foraminifera, heavily bioturbated, with burrows filled by sandy material. Surface is perforated by numerous burrows, up to 5 cm in diameter. | TV-profile 6 | Heavily bioturbated seafloor surface with numerous burrows |
| TTR8-AT-100B | Engineering survey area | Olive grey silty clay with foraminifera, heavily bioturbated, with burrows filled by sandy material. Upper 2 cm is oxidized. Surface is perforated by numerous burrows, up to 5 cm in diameter. | TV-profile 6 | Heavily bioturbated seafloor surface with numerous burrows |

**Table 4.** *(Continuation)*

Biological sampling

Three perspex tubes were gently inserted into the box-core and filled to the same level. The tube contents were placed in a labelled sample bag together with formaldehyde. Samples were labelled with a B and a number with reference to the location. All visible living organisms were collected in a cup and placed in formaldehyde.

Geochemical sampling

Approximately 250 g sediment sample was collected from the upper 2 cm, placed in a sampling bag and frozen at -10°C. Samples are labelled with the box-core number and a G.

Physical sampling

Samples were collected in the same way as the geochemical samples, but stored at +4°C. On the label they are indicated with a P.

## II.2. Preliminary Results

*Bottom sampling: Gravity cores*

TTR8 AT83G (Fig. 19)

This core has a total length of 322.5 cm. The top (0-3 cm) of core AT83G consists of coarse sand and gravel interpreted as a lag deposit. From 3 cm to the base of the core, olive grey to olive brownish (carbonate rich) sandy silty clay is present. In the lower part of the core (230 cm-base of core), the sandy fraction consists of terrigenous sand grains, foraminifera and biogenic carbonate debris. The very base of the core contains some dropstones with a diameter of about 1 cm. Bioturbation structures are present throughout the core. pH and Eh measurements show normal progress for Atlantic sediments. The lower boundary of the oxidation zone is approximately at 20cm.

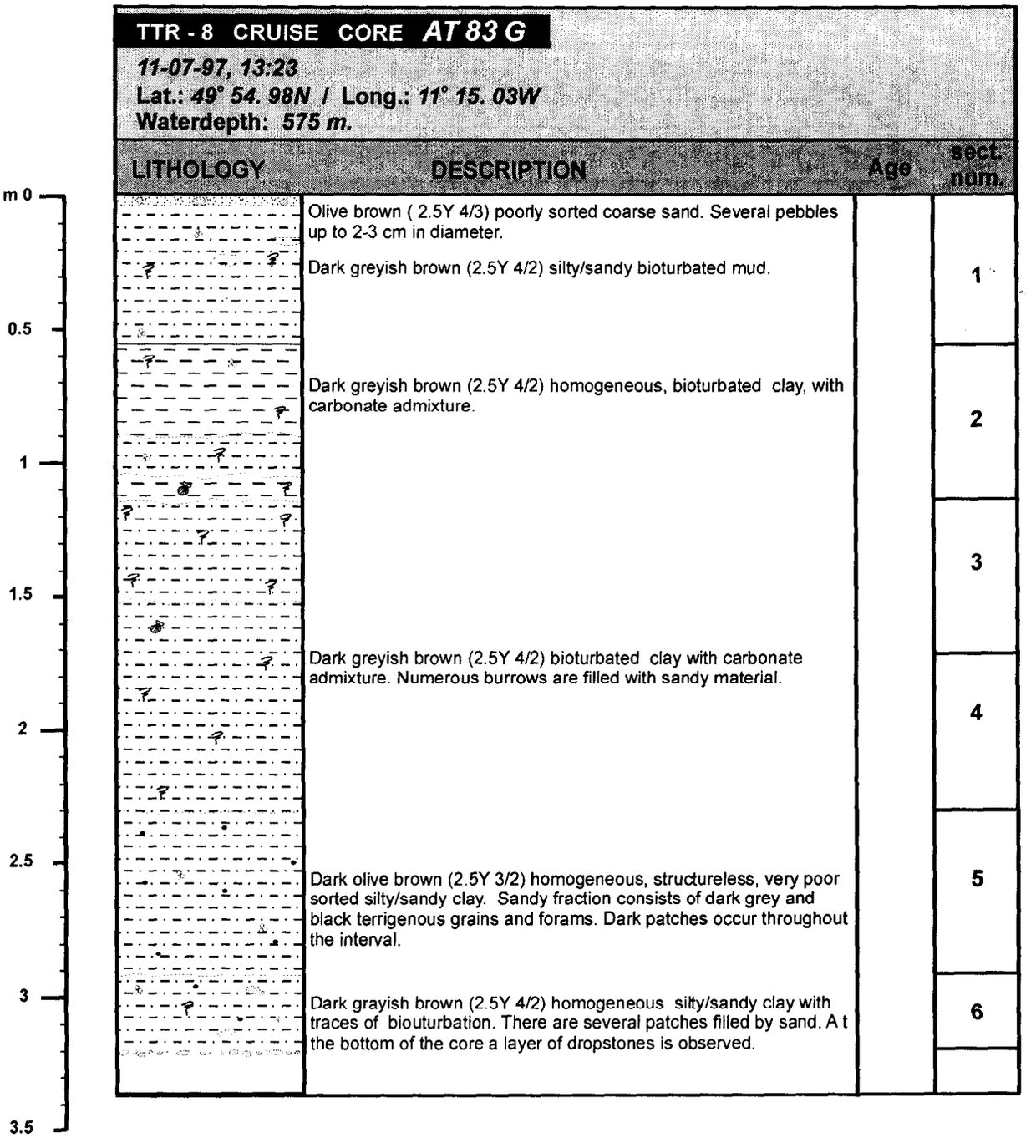


Fig. 19. Core log AT-83G

The magnetic susceptibility of this core does not show any large variability (Fig. 20). It shows a small gradual decrease from the base to the top. This could result from a possible upward decrease in bulk density resulting from compaction of the sediment column (although no bulk density measurements were performed). Only at the base of the core and at 235 cm core depth, small peaks in magnetic susceptibility are observed. The peak at the

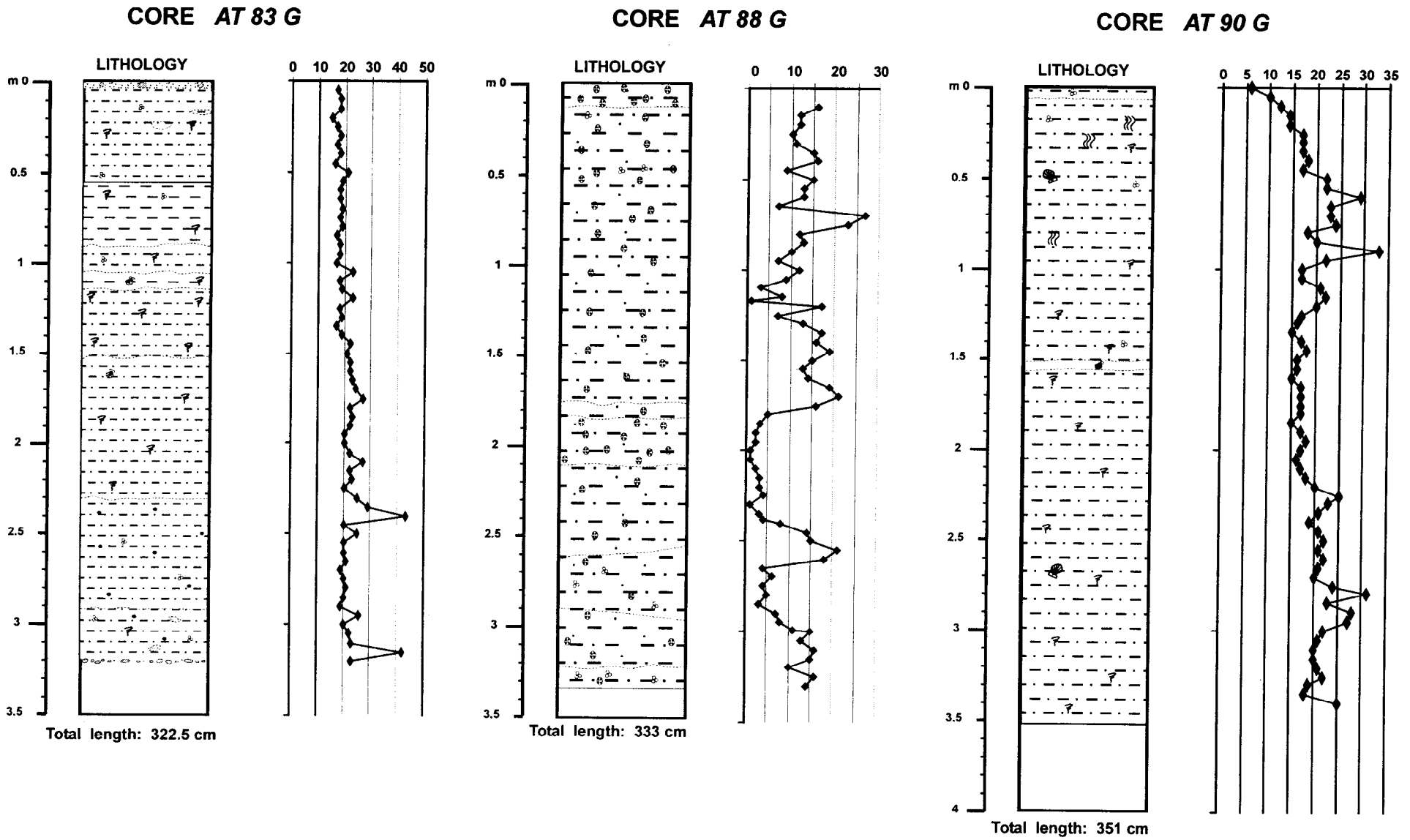


Fig. 20. Magnetic susceptibility pattern of the cores collected in the Porcupine Seabight

base could result from a higher input of terrigenous sediments when the dropstone layer was formed. The cause of the peak at 235 cm is unknown.

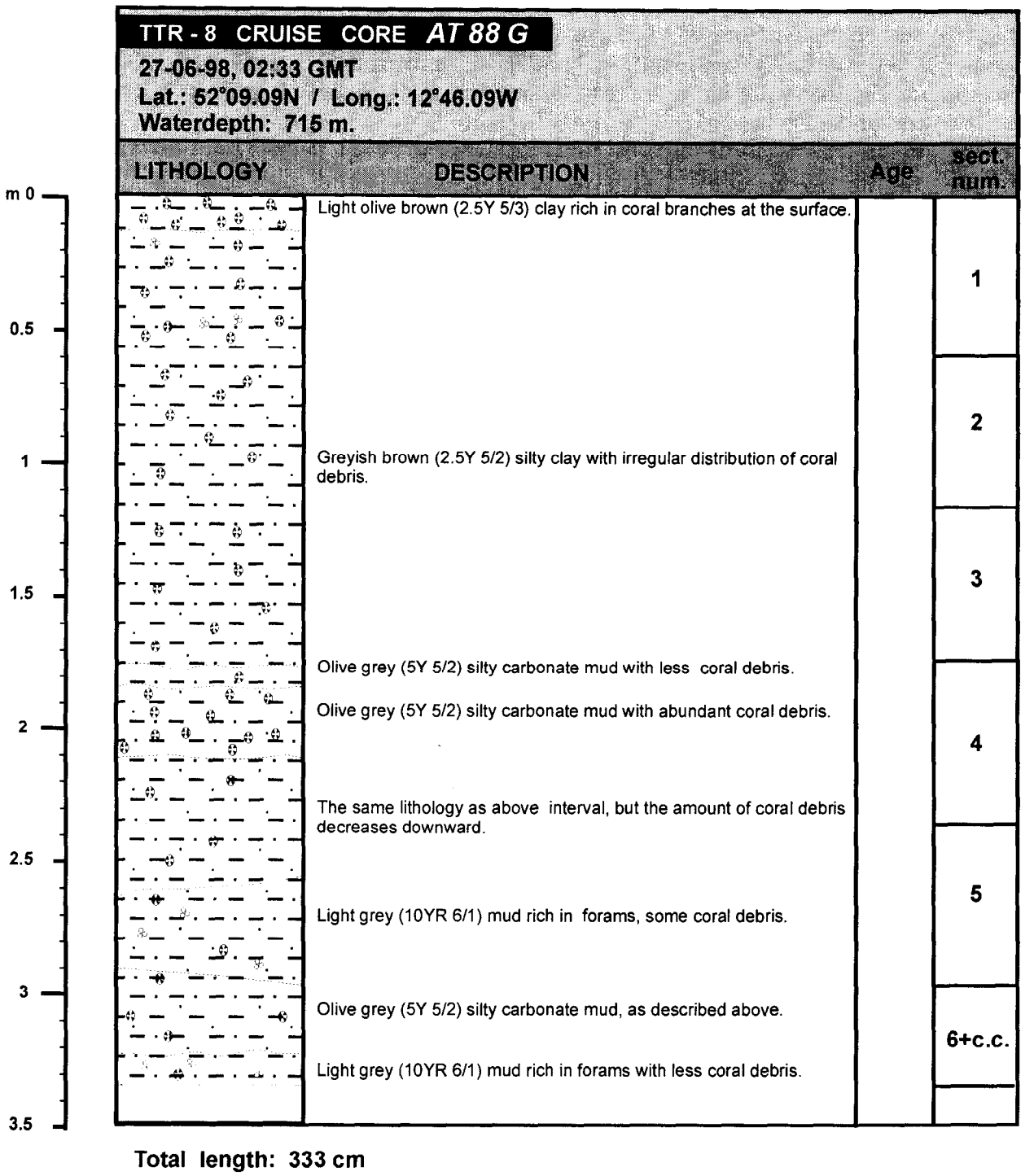


Fig. 21. Core log AT-88G

TTR8 AT88G (Fig. 21)

This core has a length of 333 cm. Core AT88G consists of a succession of relatively dark and light (olive green and brown) silty marl containing irregularly distributed lumps of coral debris with a maximum size of 6 cm. The oxidized top of the core (0-13 cm) has a light olive

brown colour.

The magnetic susceptibility of this core shows distinct intervals of low and high values, which can be correlated fairly well to the light and dark sediment colour intervals. From the top of the core to a depth of 70 cm, the magnetic susceptibility shows moderate, fluctuating, values (Fig. 20). This section is interpreted as the Holocene part of the core. The peak in magnetic susceptibility, from 70 to 85 cm depth, followed by the interval with decreasing values to a depth of 120 cm are interpreted as deposits formed during the Younger Dryas and the Allerod. The interval with high (120-175 cm), low (175-240 cm), high (240-265 cm), low (265-295) and high (295-base of core) magnetic susceptibility are interpreted as isotope stages 2-6 respectively.

TTR8 AT90G (Fig. 22)

The total length of this core is 351 cm. Core AT90G consists of a homogeneous succession of olive gray silty clay containing forams and some biogenic carbonate debris. Burrows are found throughout this core. The upper 6 cm of this core consist of oxidized slightly sandy silty clay. The sandy fraction consists largely of foraminifera.

The magnetic susceptibility, as measured in this core, can be divided into two main intervals. The magnetic susceptibility of the upper interval (0-45 cm) gradually increases towards the lower half, where it becomes stable. This is most likely the result of an increase in water contents of the sediments from base to top (Fig. 20).

The lowermost interval of this core can be divided into three sections. The upper (45-135 cm) and lower (270 cm to base of core) sections show slightly increased magnetic susceptibilities. The middle section (135-270 cm) shows magnetic susceptibility values comparable to the lower part of the upper interval. There do not appear to be significant differences in the magnetic susceptibility between the three sections. However, the irregular pattern in the upper and lower section, and the smooth magnetic susceptibility curve of the middle section (which looks like the lower part of the uppermost interval) suggest that deposition occurred:

a) in the upper interval during the Holocene; which is confirmed by the foraminifera biostratigraphy

b) in the upper section of the lower interval, during isotopic stage 2;

c) in the middle section during stage 3;

and d) in the lower section during stage 4.

It should be noted that this is a preliminary interpretation requiring confirmation by palaeontological study.

*Bottom sampling: Box cores*

TTR8-AT-85B

The core generally comprised a dark brown, silty/sandy, heavily bioturbated marl. The top few cm was composed of a foram-rich silty sand. This layer also contained a few pebbles, on some of which were attached living and dead *Bryozoans*. Also recovered were living and dead specimens of *L. pertusa* and *M.oculata*. On one pebble, *Bryozoa* were attached to both the upper and lower surfaces.

TTR8-AT-86B

The core contained a remarkable number of specimens of living and dead *L. pertusa* and *M. oculata*. Worthy of note was the growth of new *Lophelia* on dead *Madrepora* branches, and vice versa. Also of interest were the large numbers of *Bryozoa, Hydrozoa,* and sponges, as well as octocorals attached to *Lophelia* and *Madrepora*. Also present were *Eunicidea* and *Polychaeta,*

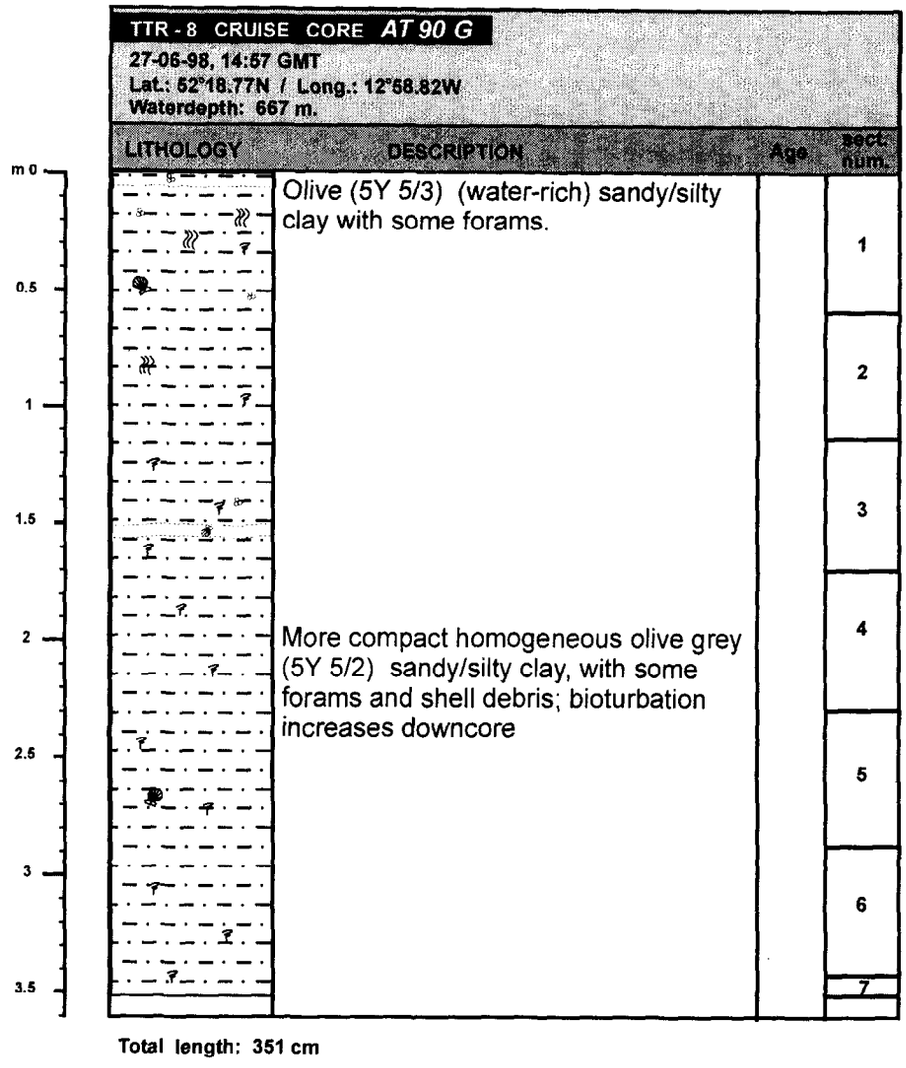


Fig. 22. Core log AT-90G.

*Cirripedia, Cidaroidea, Munidea* and *Gastropoda*. The living and dead assemblages were underlain by a significant layer of coral debris in a marly matrix. Some of the living species were air-dried, others preserved in formaldehyde.

TTR8-AT-87B

At the core surface, there were coral branches, pebbles (upto 5 cm diameter of sedimentary and metamorphic origins) and *Bivalvia*. Underlying these was a grey, silty/sandy, foram-rich marl, containing much coral debris. On one of the dropstones there was a solitary coral polyp of *L. pertusa*. In contrast to the previous core, there were few living species in general. At 50 cm depth, there was a concentration of coral debris.

TTR8-AT-93B to TTR8-AT-100B

All the cores were heavily bioturbated, with two distinct sizes of circular holes in the sediment surface. The larger holes were up to 5 cm diameter, the smaller ones, approximately 1-2 cm diameter. In general, the core sediments were olive grey silty clay with foraminifera.

*Bottom TV profiles*

Two underwater tracks were made across the Magellan mound area in order to provide an overview of the bottom relief features, sediment characteristics, and to elucidate biological communities existing in this area. Total recording time of TVAT-5 and TVAT-6 constituted three hours starting at 07:55 and 11:20 respectively. The water depth in the area covered by both TV-profiles remained approximately 650 m.

The bottom sediments are represented by homogeneous, yellowish brown mud with an unconsolidated, water-saturated thin oxidised upper layer, which was easily resuspended by the video camera approach.

Commonly, relief appears to be smoothed and the sediment surface is punctuated throughout with hummocks and holes of differing morphologies on a surface of low relief. Relatively large holes are arranged in irregular lines and in some places surrounded by a number of smaller holes. The large holes have a diameter of up to 3 cm. Sometimes they are filled with living worms, protruding vertically to the surface.

Poor biological diversity is characterised by a small number of fish, colourless small clams, worms, and rare Actinia, which occasionally occur on the sea floor.

Generally, the two video lines do not appear any different in the characteristics of their relief, sediments, benthic and neritic biota.

*Side-scan sonar and subbottom profiler record - ORAT-17*

A two-hour survey with OREtech side-scan sonar operating with a frequency of 100 kHz was conducted on the eastern Porcupine margin. The line was aimed to check plume-like features observed on the 30 kHz side-scan sonar data and subbottom profiler record obtained during the TTR-7 cruise. The line runs in a W-E direction and is normal to the 30 kHz mosaic. This gives better resolution to some of the previously observed features.

Several acoustic facies can be recognised (Fig. 23). The western half of the line is characterised by highly variable acoustic backscatter, although the average level is relatively low. Abundant wave-like patterns, occasionally interspersed with smooth areas, can be clearly seen and are likely to be caused by the presence of sand wave fields. Except in the extreme western part of the line, the waves tend to become organised into trains which trend in a south-north direction. Sometimes wave patterns decorate the slopes of the seabed mounds seen on the recent profiler record, as well as on the TTR-7 data (Kenyon et al., 1998). In general, the wave crests are orientated in an west-east direction, sometimes following the contours of local mounds. The waves are larger at the western end of the line where their wavelength is about 20-25 m. To the east, wave height decreases (as derived from the wave crest shadows on the sonograph). Here, the average wavelength is also less, and is about 10-15 m.

From the subbottom profiler record, the wave fields correspond to the uppermost unit composed of numerous overlapping lens-like bodies. For this layer, a maximum thickness of 11 m was found at the western end of the line. Underneath this unit an acoustically transparent layer, described below, was recognised.

At the western part of the line, elongate zones of higher and uniform acoustic backscatter disturb a sand wave field. Further to the east, they prevail over the wavy pattern and are normally localised between the mounds. In the middle part of the line (and also to the east) such uniform backscatter is complicated by weaker backscattering streaks. These streaks are normally S-N orientated and only at the very eastern end their direction changes to SW-NE.

The subbottom profiler recorded a sedimentary sequence down to 30 m below the seafloor. It shows a well-stratified succession with a distinct transparent layer in the upperpart unconformably overlying lower strata. Its thickness is about 10 m. At some places

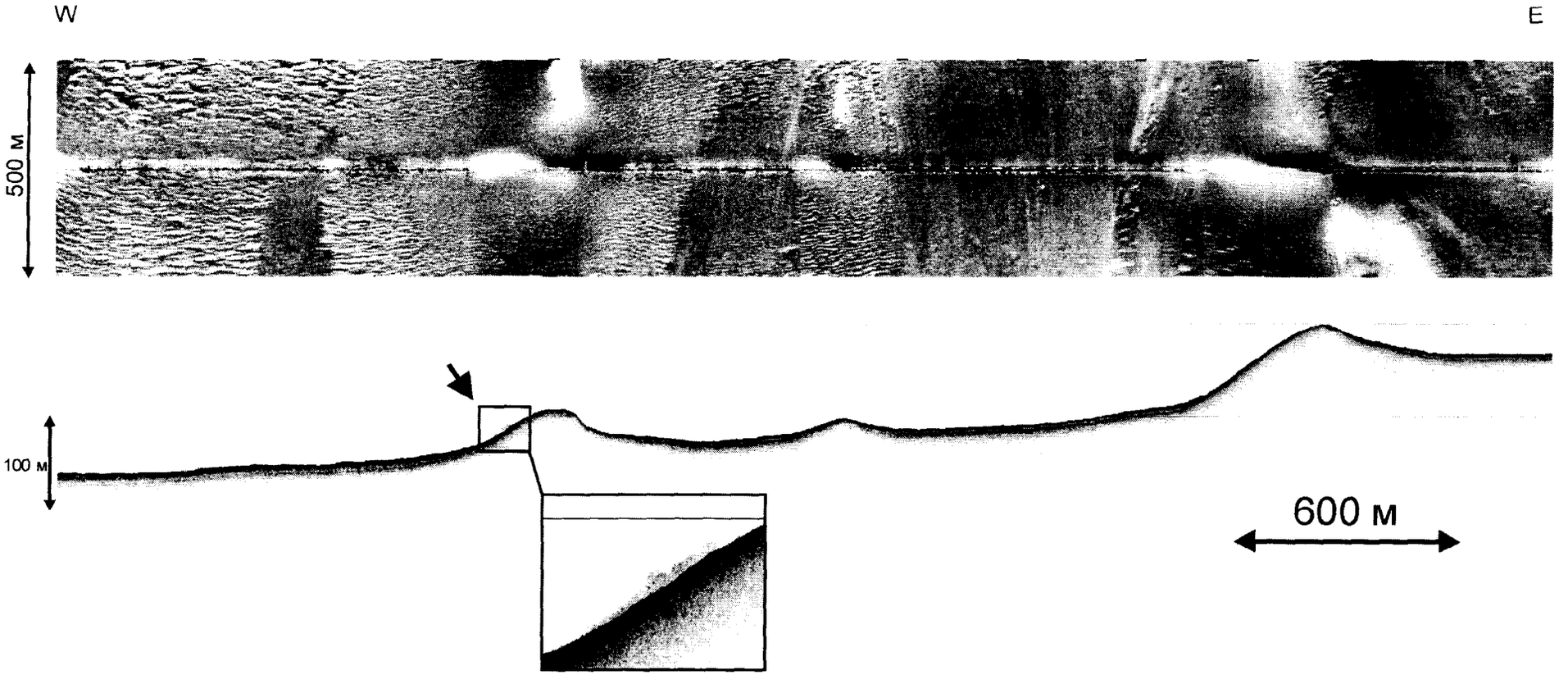


Fig. 23. Sonograph and subbotom profiler record along line ORAT-17 (100 kHz mode). Well-developed fields of sand waves are clearly seen. An arrow indicates an acoustic anomaly on the subbottom profiler record interpreted as fish shoals.

(14:38, 15:02), the sonograph shows isometric features which, from their backscatter pattern, are believed to be obstacles of unknown nature on the seabed. To the north of these, trains of waves are observed.

Mounds observed on the subbottom profiler record may reach heights of up to 190 m. (e.g. at 14:30). They correspond to the areas of uniform moderate backscatter on the sonograph; rather often their slopes are covered with waves. No penetration was seen on the sediment profiler record.

Higher resolution, 100 kHz mode, revealed that bands of weak backscatter seen on 30 kHz imageries from the TTR-7 cruise are trains of waves, thus confirming the presence of sheets of sand transporting material northward. Sand was found to be swept over those mounds (where heights do not exceed 30-50 m) as indicted by the mound surface coverage with wave fields. To conclude it can be said that both the 100 kHz and the 30 kHz data sets show a good correlation. Data obtained entirely support last year's findings.

The observed acoustic backscatter pattern on the sonograph suggests the presence of active hydrodynamic conditions in the studied area on the eastern Porcupine margin. Bedform assemblages are thought to be formed due to strong bottom current activity; the presence of different acoustic facies indicates variations in the flow regime. Wave trains, observed beyond obstacles, indicate that the current is directed to the north. These obstacles, together with mud mounds in the path of the current, create additional turbulence that slows down the current, leading to deposition of sandy material and formation of the wave fields.

These observations fit with the descriptions by Pingree and Le Cann (1989, 1990) of a mean northward current near the seabed following the local topography (Rice et al., 1991) on the eastern flank of the Porcupine Seabight. The observations can be confirmed by the OREtech side-scan sonar images of TTR7, which show seabed structures that indicate a northern current following the local topography of the mounds in the "Hovland" and "Belgica-Logachev" area. This results in moat forming around the mounds, a feature also observed on seismic profiles (Belgica 97, Kenyon et al., 1998, Belgica 98).

Smoothed areas on ORAT 17, with uniform or streaked backscatter, are interpreted as zones of higher current speed, where sedimentation is severely restricted. In these areas, however, currents are of insufficient velocity to create significant erosion.

Wave fields indicate recent sediment transport in those regions where current velocity is sufficiently great. Both the presence of waves and the low level of the backscatter suggest that the main material transported by currents is fine, well-sorted sand.

The hydrodynamic regime can explain the absence of thick carpets of phytodetritus which have been encountered at depths below 1300 m (Rice et al., 1991) in the gravity cores. It is believed that generally higher than average near-bottom currents velocities at these shallower depths keep the phytodetritus in suspension, preventing it from settling and thus generating bottom nepheloid layers. The occurrence of bottom nepheloid layers in the Porcupine Basin was first reported on the Porcupine Bank by Dickson & McCave (1986). They found intermediate nepheloid layers in the Porcupine Seabight at depths of 700-800 m and, on some occasions at least, these can be traced back to bottom nepheloid layers on the Porcupine Bank.

On ORAT 17 it is clear that, on the upper part of the slope, there are stronger currents than in the lower part. This can be interpreted as a transition zone between two oceanographic states. The most possible transition will be between the Eastern North Atlantic Water (ENAW) which is found to a depth of about 750 m and Mediterranean Water (MW) (Hargreaves, 1984; Lee & Ellett, 1965; Harvey, 1988; Vangriesheim, 1985; Ellet et al., 1986; Rice et al., 1991).

From the perspective of the benthic fauna, the residual flow direction is of importance for the dispersion of species and possibly for the transport downstream over relatively long distances of suspended material. The instantaneous current speed, on the other hand, would seem to be more significant for the biota, since it will determine factors such as the ability of

seem to be more significant for the biota, since it will determine factors such as the ability of sessile fauna to remain attached to the seabed, the area over which food sources may be present, and the degree of resuspension of food material. Presumably such resuspension causes an increase in the food supply to suspension feeders, but a decrease in the availability of the same material to deposit feeders. Enhanced current velocity on the Eastern margin of the Porcupine Basin indicates the region of the mounds which are covered by scleractinian corals and other suspension feeders. A similar connection to areas with enhanced internal tidal currents has been noted by Frederiksen et al. (1992) around the Faroe islands.

A box core retrieved from such a mound was found to contain large numbers of cold-water corals, sponges, bryozoa and other associated fauna, showing a high abundance of benthic life on mound slopes. Fish shoals grazing in the vicinity of such places may cause the observed acoustic anomalies on the sonographs (ORAT-5 and ORAT-17).

It is obvious that the suspension feeders living on the mounds take advantage of the enhanced current velocity, which provides them with nutrients and prevents suffocation by sediments. The sediment succession of the cores shows coral-rich debris layers alternating with coral-poor layers in a marly matrix. This may indicate changes in oceanographic conditions during interglacial and glacial times.

*Conclusions*

- The presence and orientation of bedforms indicate that there are strong, but locally variable, north flowing currents in both the «Hovland» and «Belgica-Logachev» areas. These currents follow the contours of the local topography.
- Differences in acoustic facies indicate that there is a transition zone between two oceanographic states which occurs between water depths of 750 - 900 m.
- There are alternating bands of different coral density in the uppermost seabed sediments. These can be attributed to changes in physio-oceanographic states, which are linked to glacial/interglacial cycles.
- In the «Magellan» mound area, there is intense bioturbation of the surficial sediment, indicative of normal North Atlantic benthic faunal activity.
- A high concentration of suspension feeders (e.g. on the west slope of a «Belgica-Logachev» mound) will attract fish shoals, which can cause plume-like acoustic anomalies on the subbottom profiler record.

# III. FAEROES MARGIN

## III.1. INTRODUCTION

*T. Nielsen, A. Kuijpers*

*Geological setting*

The Faeroe Platform was formed at the initiation of the opening of the North Atlantic about 60 million years ago. The Platform is characterised by the presence of a thick, lower Tertiary volcanic strata, which mainly consist of subaerial extruded basalt (Waagstein, 1988 ). During the Eocene to Miocene the Platform was affected by at least three compressional tectonic phases (Boldreel & Andersen, 1993), which formed several compressional ridges, e.g. the Munkagrunnar Ridge at the southern end and the Fugloy Ridge at the north-eastern end of the Faroe Platform.

Towards the east, the Faeroe Platform is separated from the NW European continent by a NE-SW striking deep water area, the Faeroe-Shetland Channel. The channel deepens in a northward direction, and reaches a water depth of 1500 m, before entering the Norwegian Sea. Towards the south, the channel narrows and the water depth decreases to approximately 500 m. Continuation of the channel southwards is blocked by the compressional Wywille-Thomson Ridge.

The eastern margin of the Faroe Platform bordering the Faeroe-Shetland Channel is formed by a sedimentary sequence overlying the volcanic series, which is up to 2000 metres thick (Boldreel and Andersen, 1994). , At least 2 regional unconformities developed during deposition of the sediment succession, related to the compressional tectonics and formation of the ridges mentioned above; these are a late Oligocene Unconformity and a late Neogene Unconformity. A third unconformity was formed during the glaciation of the northern hemisphere, the Glacial Unconformity. Additionally, a number of local unconformities are seen within the sedimentary succession of the eastern Faeroes margin.

The northern sector of the Faeroe Platform forms a continental margin bordering the Norwegian Basin, which developed during the opening of the North Atlantic. The basement underlying this basin consists of oceanic crust. Recent investigations (Nielsen et al., 1998; Van Weering et al., 1998; Taylor et al., submitted) have shown that this part of the Faeroes margin is characterised by large-scale slope instability, as shown by sleevegun seismic studies and side-scan sonar (TOBI and GLORIA) profiling. This large-scale slumping and sliding of the middle and lower slope has affected sediments of presumed Miocene to Quaternary age.

During Quaternary glaciation of the Faeroe Platform, the Faeroes ice sheet probably reached at least the 400 m depth contour to the south-east of the Faeroe Islands (Waagstein and Rasmussen, 1975; Hedebol Nielsen et al., 1979). The former authors suggest that the majority of the basaltic erratics on the shelf and slope were probably derived from the south-east central part of the Faeroe Islands, suggesting the presence of a local ice stream here. In addition, the authors report the presence of two troughs on this part of the shelf, which they conclude to have a glacial origin.

*(Paleo) Oceanography*

The hydrography of the Faeroes waters is characterised by the presence of relatively 'warm' and saline surface waters advected by the North Atlantic Current. North-eastward transport of these waters into the Norwegian Sea is strongest along the eastern slope of the Faeroe-Shetland Channel. Immediately west of the Faeroe Islands the North Atlantic Current system has a branch, which is found to continue over the shelf north of the Faeroe Islands.

In contrast, cold bottom water masses from the Greenland and Norwegian Sea flow southward via the Faeroe-Shetland Channel and Faeroe Bank Channel into the Iceland Basin. These currents are strongly concentrated along the western and northern slope of these channels, respectively. Due to turbulent mixing, the temperature of these 'Norwegian Sea Overflow Waters' (NSOW), which at the northern entrance of the Faeroe-Shetland Channel initially is below zero degrees (C), gradually increases to +2 or +3 degrees (C) west of the Faeroe Bank Channel outlet. Associated with NSOW flow, a bottom current speed of 100 cm/s, or occasionally even more, has been measured in the Faeroe Bank Channel (Anonymous, Nordic WOCE). The Wyville-Thomson Ridge principally forms a major barrier for the overflow waters, although occasional overflow of this ridge has been reported.

Recent studies performed near the northern entrance of the Faeroe-Shetland Channel (Rasmussen et al., 1996 & 1998) and at the outlet of the Faeroe Bank Channel (Kuijpers et al., 1998) have shown major changes of the current system outlined above, occurring in relation with Late Quaternary climate change. A typical feature of cold or glacial climate stages is a weakening or cessation of the NSOW flow, together with an increased deposition of fine-grained, clay-sized sediments in the channels, replacing the silty and (fine) sandy deposits typical of warmer climate conditions.

*Objectives*

The main objective of TTR8 Leg2, Area 4, has been to collect further information on slope instability of the Faeroes margins. This applies not only to the northern sector of the margin, where in recent years several surveys were performed within the framework of the European 'ENAM' (European North Atlantic Margin) project (Nielsen et al., 1998; Van Weering et al., 1998), but also the south-eastern margin of the Faeroe Platform, where hydrocarbon exploration activities have significantly increased recently, has been selected as a target area.

Thus, important issues defined for the work of this study area were to investigate the timing of the (last) major instability event(s), and the nature and origin of various slope instability features observed on the seabed during previous studies. For this purpose we selected a variety of techniques, including airgun seismic, subbottom profiling, OKEAN long-range and OREtech high-resolution side-scan sonar, as well as sediment coring.

In order to trace sediment flow pathways and to determine the character of deep-water sedimentary processes associated with slope instability on the northern Faeroes margin, a further target area was selected in the adjacent Norwegian basin. The selection of the latter area was based on a GLORIA side-scan sonar survey collected as part of the European ENAM II project (Dowdeswell, 1996; Taylor et al., submitted).

## III.2. EASTERN MARGIN

### III.2.1. Seismic and 3.5 kHz subbottom profiling data

*T. Nielsen, A. Kuijpers, J. Taylor, M. Rank, H. Simonsen, L. Sommer*

SEISMIC PROFILING

A total of ca. 400 km in 9 lines were collected using the single channel airgun system, with OKEAN side-scan sonar and the hull-mounted 6 kHz subbottom profiler collected simultaneously. Average survey speed was 6 knots. The survey grid consists of 2 slope parallel lines, lines PSAT 41 and 43, running NE-SW, located at the top and base of the slope

respectively. Perpendicular to the slope parallel lines, four down slope lines run NE-SW (PSAT 44, 45, 47, 49). These are connected by shorter NW-SE oriented lines (PSAT 46 and 48) (Fig. 24).

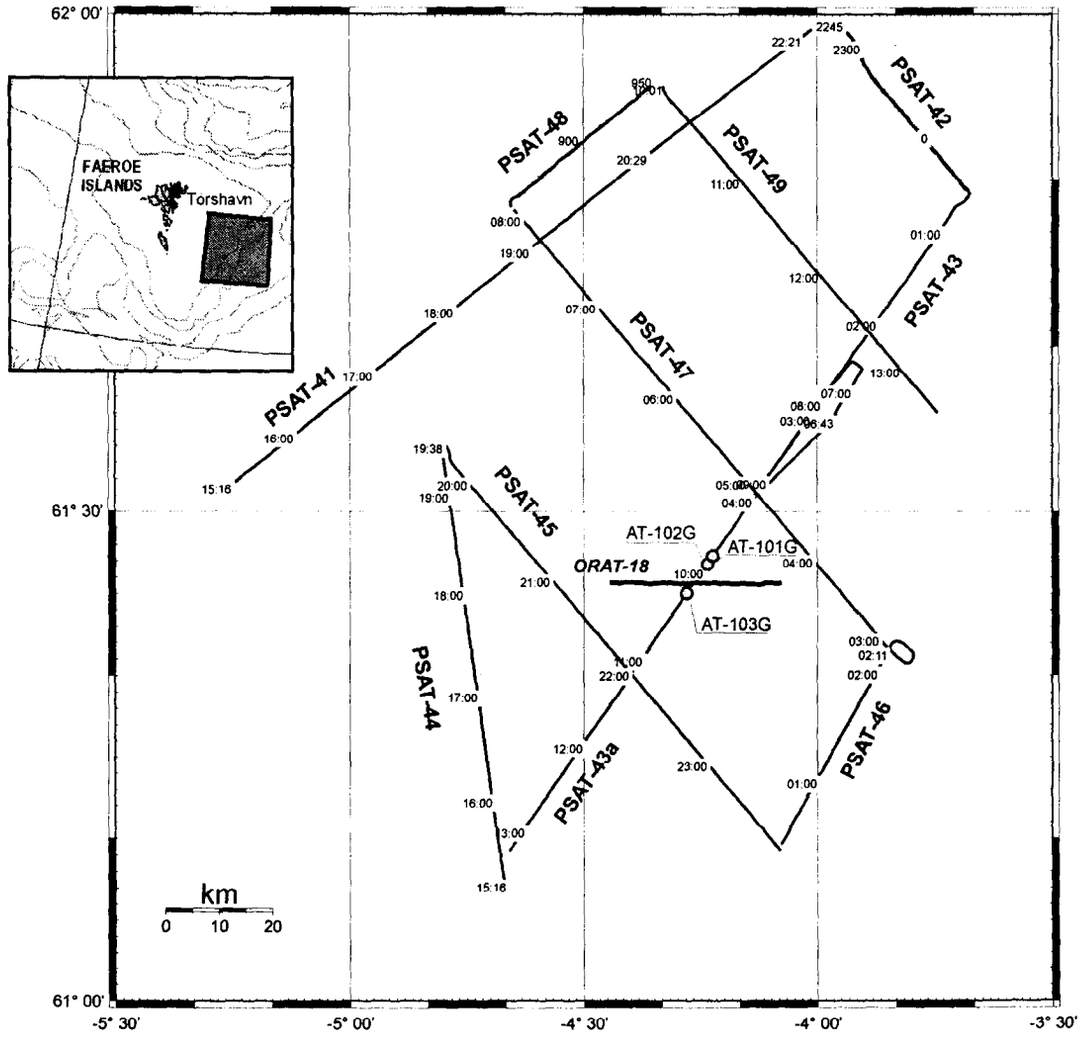


Fig. 24. Location map of the southeastern Faeroes margin.

*Seismic description*

In general, the quality of the seismic data is good, especially in the lower slope and channel regions. Penetration is up to 650 ms TWT and allows six seismic units to be identified, labelled unit 1 to 6 from below.

**Unit 1** forms the acoustic basement. It is found only in the northeast of the survey region and is defined by an upper reflector which is discontinuous and medium to strong in amplitude. On those seismic lines oriented SW-NE (43, 46, 48) the upper reflector is undulating. The internal reflection pattern is chaotic when visible, which is rarely and only seen just below this upper reflector. The unit dips eastwards from 950 to 2100 ms TWT.

**Unit 2** is not easily picked in the western part of the area. Overall it forms basins and highs. The highest part is the north and west part of the survey area in the shelf region at 650 ms TWT, with a secondary local high at 1500 ms TWT at the base of the slope. The major basin is elongate, with a NE-SW axis along the base of the slope and is seen at roughly 2100

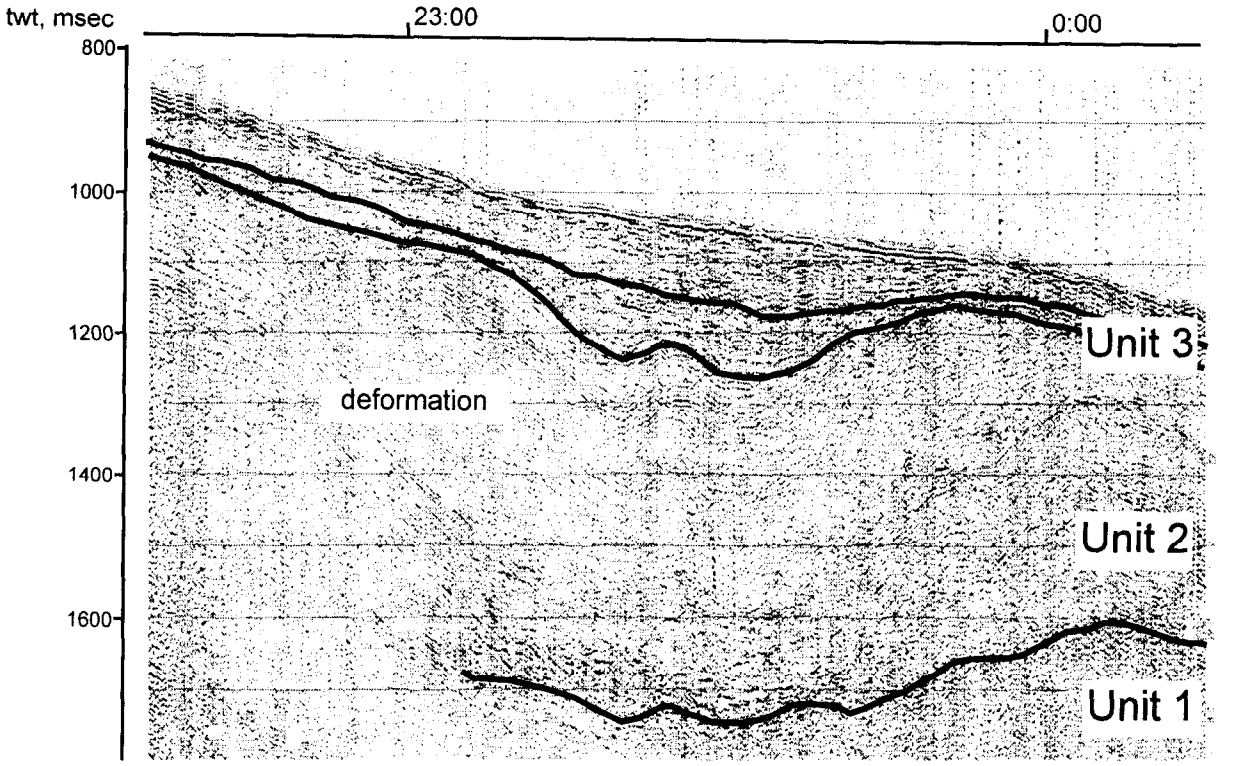


Fig. 25. Section from seismic profile PSAT 42 showing the deformation within unit 2 and the top bounding erosive unconformity. Also visible are the draping parallel reflectors of unit 3, topped by another unconformity.

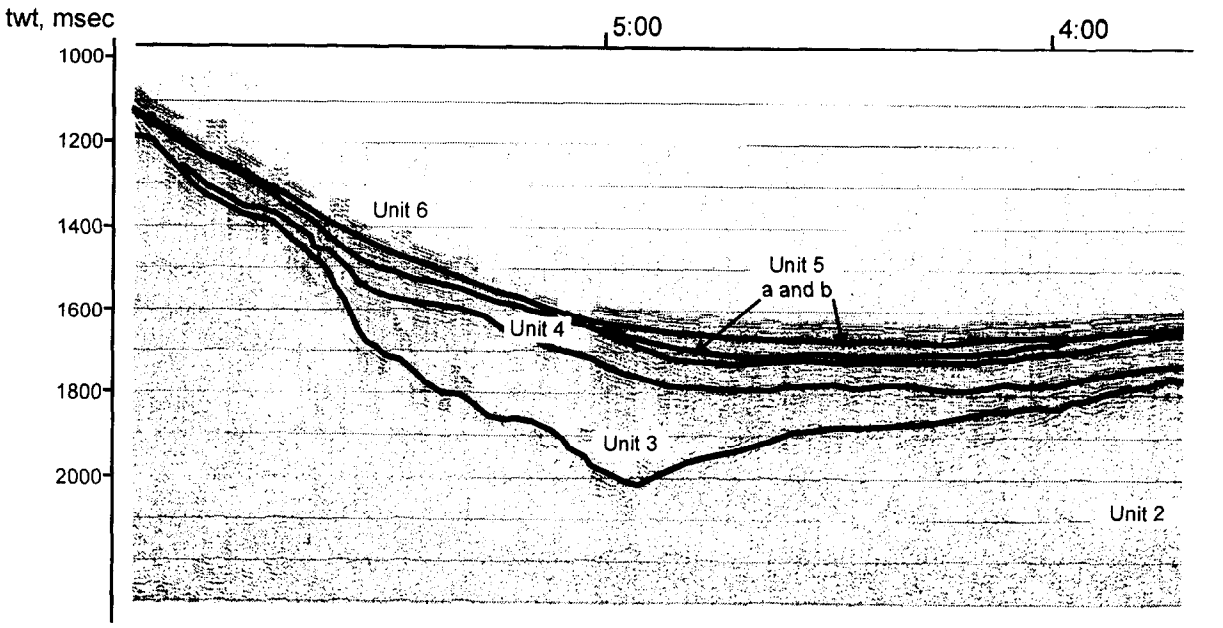


Fig. 26. Section from seismic profile PSAT 47 showing the parallel reflectors of facies 1 of unit 4 onlapping unit 3 and unit 2, which form the highs around the main basin. The two subunits of unit 5 (subunit a and b) can also be seen, subunit a characterized by parallel continuous reflectors onlapping underlying unit 4. The internal reflector pattern of the lense shaped subunit b is chaotic.

ms TWT. Other small basins are found in the north (PSAT 49, 1600 ms TWT) and far south (PSAT 43, approx. 2000 ms TWT). The slope between the shelf high and the slope basin is quite steep. The surface reflector is continuous, varying from very strong to almost locally absent. It forms an erosive unconformity in the north. Internal reflectors are extensive, continuous, parallel and generally overlying unit one where it is visible. The unit shows deformation or disturbance in the form of folding, especially in the far north (Fig. 25). Thickness can only be described for the NE of the area and is approximately 500 ms TWT at its thickest, thinning towards the north-west and south-east.

**Unit 3** is clearly picked across the area where it is present and forms a partial fill for unit 2. The topography of the top reflector is slightly undulating and relatively smooth. The reflector is mostly continuous and of medium to high amplitude. Internal reflectors fill and smooth the topography of unit two, and unit three is absent over the highs in the survey area. The internal reflection pattern in the lower part of unit three shows deformation structures which are parallel to those in unit two. The unit is bound at the top by an unconformity (Fig. 25). The unit is thickest in the north (350 ms TWT) and in the large basin in the south (250 ms TWT). On the shelf it is 50 ms TWT thick.

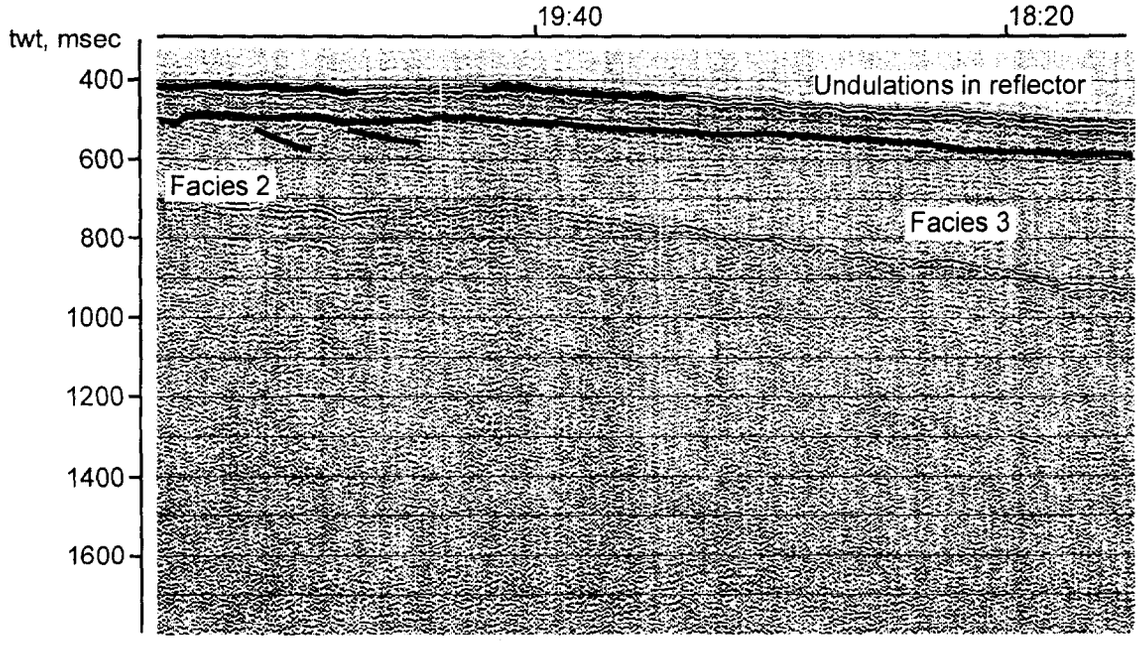


Fig. 27. Section from seismic profile PSAT 41 showing two of the three facies of unit 4 (facies 2 and 3). Facies 2 is characterized by a sigmoidal reflection pattern with an erosional truncation surface. Undulation of surface reflectors in unit 6 can also be seen.

**Unit 4** also fills the basins and drapes the remaining area. It is inferred to be present across the whole survey area and is close to the surface in many places; it is sometimes lost in the seafloor reflector. The top reflector is medium to sometimes strong and generally smooth. In the north and on the shelf it is occasionally undulating. The internal structure can be divided into 3 different seismic facies. Facies 1 is present in the large basin (Fig. 26) and is characterized by stratified parallel reflectors which are locally broken. These reflectors onlap the highs to the SE and NW. Seismic facies 2 (Fig. 27) is present in the far west, and is characterized by sigmoidal reflectors, which show erosional truncation at the top. In the rest of the areas seismic facies 3 is present (Fig. 27), characterized by a lack of internal reflectors. The unit is thickest on the shelf (>200 ms TWT) and in the basin (100-150 ms TWT); on the slopes it averages 50 ms TWT thick, and is absent on the local high in the south.

**Unit 5** is only traceable in the southern part of the survey area, i.e.the large basin area and the local high in the SE. Otherwise it may be hidden in the seabed reflector. It is possible to trace the unit on to the shelf on PSAT 44, but only with low confidence. The top reflector is of medium strength and continuous, and shows erosion in the SE (PSAT 47). The thickness of the unit is greatest in the large basin, up to 200 ms TWT. The unit may be divided into two subunits based on the internal reflection pattern (Fig. 26); a lower (5a) and an upper subunit (5b). The lower subunit is characterized by generally continuous and parallel internal reflectors, which onlap on to unit 4. The thickness of the subunit is generally less than 100 ms TWT. The upper subunit is lense shaped and characterized by a chaotic internal reflection pattern. It has a maximum thickness of 125 ms TWT. The separation of the two subunits is based on termination of the internal reflectors within the lower subunit.

The uppermost unit, **Unit 6**, is present in the whole of the study area. On the shelf, down to 750 ms TWT, the unit is bounded at the top by a very strong, discontinuous and undulating seabed reflector. Below this TWT depth the unit is bounded at the top by a very strong continuous reflector (Fig. 27). On PSAT 45 between SP 800 and 1100 this reflector is weakly undulating. The unit is thickest in the basin (100 ms TWT) and on the shelf (150 ms TWT); elsewhere it thins and is often hidden in the seabed reflector. On the shelf the internal reflectors are chaotic. Elsewhere the unit is characterized by a parallel internal reflection pattern which shows onlap towards NW (PSAT 45). Occasionally there can be seen small lenses with a more chaotic pattern (PSAT 45 between SP 800 and 1100).

*Seismic interpretation*

Unit 1 forms the acoustic basement and is thought to be of Eocene age, due to the fact that the basalt, which is regional in extent and known to underlie the survey area, was deposited during the late Paleocene and early Eocene. Because unit 1 is not visible across the whole survey, it is not possible to say anything further about it. Unit two is thought to be formed during the tectonic deformational phases of the Oligocene (Boldreel and Andersen 1993) and is topped by an erosive unconformity, which is also thought to be of late Oligocene age (Damuth and Olson 1993, Stoker 1995). The basins and highs which this unit forms control all subsequent sedimentation within the study area. The deformation structures seen in the lower part of unit 3 are interpreted as the result of a second phase of compression in the survey area. According to Boldreel and Andersen (1993), this second phase occurred during the Miocene. The unit is topped by a second erosional unconformity, therefore suggested to be mid Miocene, and to be coincident with the widespread unconformity seen to the south and east of the survey area (Stoker, 1995). Unit 4 forms a basin fill at the base of the slope, a prograding wedge on the shelf high, with a structureless unit in between. This may represent a form of downslope transport of sediment, but the resolution of the data in not adequate to comment further on the transitional facies. The unit is thought to be late Miocene to early to middle Pliocene, and is topped by an unconformity, perhaps related to the onset of glacial conditions during this period. Unit 5a is interpreted as being a basin fill, above which is a large erosive slump, in the southern area (unit 5b). It is not possible to locate the source of the slumping, but slumping post-dates the deposition of unit 5a, and is thus attributed to the late Pliocene. The erosion seen towards the high in the Faeroe-Shetland Channel may be a result of enhanced deep water currents, established at this time (Burton et al., 1997). Unit 6 therefore is thought to be the Pleistocene/Holocene unit; at the shelf, undulations of the seafloor reflector down to 750 ms TWT are interpreted as iceberg ploughmarks. Glaciation and/or iceberg ploughing may have homogenised the sediments on the shelf, giving rise to the lack of structure here. Parallel reflectors within the basin and onlapping onto the slope may be contourite deposits, associated with deep water movement through the channel. The chaotic

lens found between these two areas is considered as slump or downslope transport deposits, thought to have occurred throughout the Pleistocene.

## 3.5 kHz SUBBOTTOM PROFILING

According to the (hull-mounted) subbottom profiler records from the slope of the Faeroe-Shetland Channel, a marked change of seabed acoustic properties occurs at mid-slope depth at water depths of 450-550 m. Above that level a markedly hummocky seabed topography prevails with generally little or no acoustic penetration. Below that level the seafloor gradually flattens, whereas acoustic penetration increases. This is particularly evident downslope of a small plateau (e.g. PSAT-44, 17:10 hrs) found on the slope in the southern part of the area. The same feature had previously been recorded on lines run by the R.V. *Dana* (Kuijpers et al., 1997) immediately south of the present study area.

The channel floor deposits found north of ca 61.30 N generally display well-defined, regularly parallel acoustic lamination. The seafloor shows little relief, and maximum acoustic penetration is about 30 ms.

Further south, the acoustically laminated channel floor deposits are locally overlain by deposits with a transparent acoustic character and positive relief. On line PSAT43 this occurs in the profile section run between 09:17 and 09:48 hrs, and, on a larger scale, between 10:05 and 12:00 (Fig. 28). In the former section the underlying acoustically laminated sediment section is still clearly visible below the superficial transparent unit, which has a thickness not in excess of ca 20 ms. In the latter section, however, the laminated unit gradually disappears below the transparent upper unit. At the same time the seafloor rises 30 to 40 m, while displaying a more undulating relief. Further to the south-west (after 11:50, PSAT43) acoustic lamination reappears, while penetration increases to 15-20 ms. This layering is, however, less fine and more diffuse than was found more to the north. Moreover, a gradual flattening of the seabed occurs at the same time. A small and thin (ca 6 ms) lens of acoustically transparent sediment overlies these more diffusely layered sediments at 12:38 hrs (PSAT43).

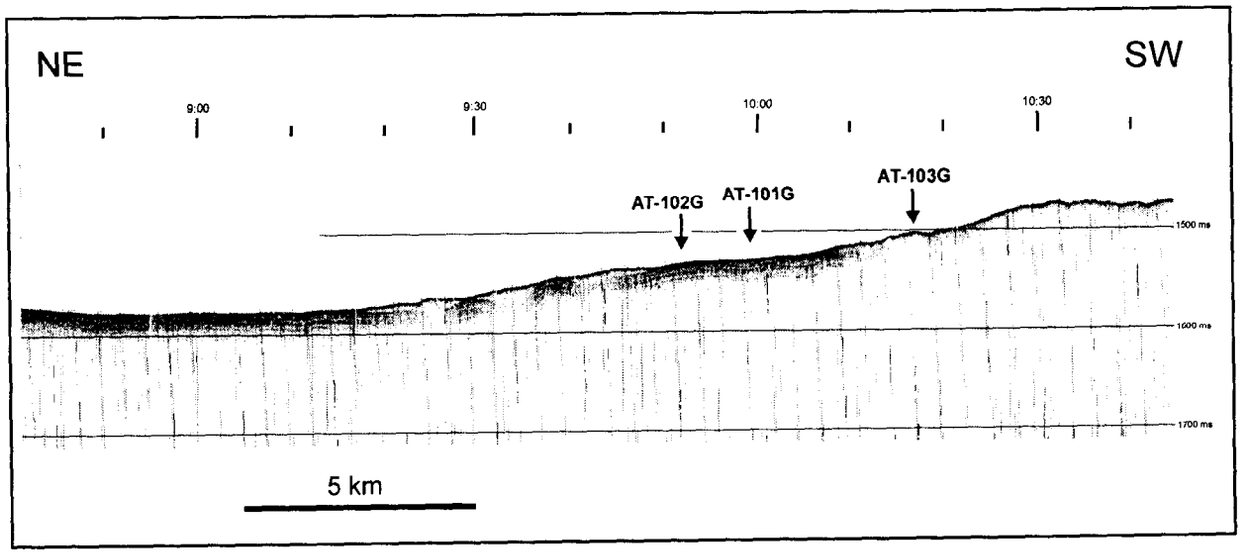


Fig. 28. 3.5 kHz profiler record showing muddy slump deposits. Positions of sampling stations are also indicated.

After coring at locations AT101G, 102G, and 103G, it could be confirmed that the transparent surface unit, with its undulating seafloor topography, represents muddy slump

deposits. From previous coring in the channel, we know that the acoustically laminated channel deposits consist of an alternation of (thicker) glacial silty clays, and thin interglacial/interstadial silty sediments with fine sand.

A change from acoustic fine lamination characterising seafloor deposits north (-east) of the slump to more diffuse acoustic layering was observed south of the slump. This may be the effect of the (Holocene) southerly NSOW currents having transported slump material to areas to the south.

In addition, the OREtech deep towed subbottom profiler clearly shows that on the lower part of the slope the slump is covered by up to ca 1.5m of presumably Holocene contourite deposits. From this, and from the fact that the slump, in turn, covers the 'normal' channel floor deposits we may conclude that the last major slumping event most likely occurred in late glacial times. It should be noted, however, that the profiler record from the more upslope part of the deep towed line yields additional evidence for more than one late Pleistocene slumping event.

The hummocky relief at water depths of less than 450-550 m can be ascribed to glacial reworking of sediments. The small plateau at approximately the same water depth might be related to slumping. It may, however, also originate from strong contour current activity, since this water depth (ca 500-600 m) represents the depth stratum of the current axis of strong southerly NSOW flow. The side-scan records collected during the RV *Dana* 1997-cruise show, in fact, that current lineations and sand streamers are a typical feature for this part of the slope.

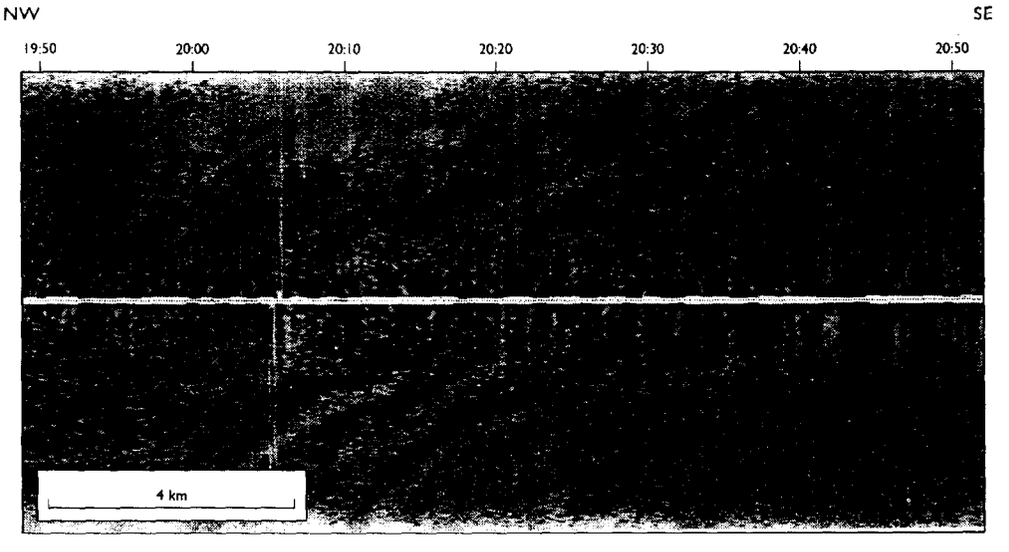


Fig. 29. Example of "OKEAN" side scan sonar record (line PSAT-45) showing features presumably related to downslope mass flow at a water depth of around 1250 ms.

### III.2.2. Side-Scan Sonar Data

*A. Kuijpers, A. Akhmetzhanov, M.Ivanov, and A. Wheeler*

The OKEAN sonographs show only a few features. This may be ascribed to shallow water depth on the shelf, and possibly to a relatively uniform backscatter pattern in the deeper parts of the Faeroe-Shetland Channel. The records from the shelf and uppermost part of the slope show an ill-defined imagery of seabed structures related to glacial reworking. Features presumably related to downslope mass wasting were recorded at water depths between 900

and 1000 m (Fig.29, PSAT45 21:00-21:30 hrs), somewhat upslope of the slump described above. A minor channel associated with these features may be interpreted as a turbidite channel (see also below).

In contrast, the OREtech deep towed side-scan record of an E-W line, ORAT-18 run over the distal part of the slump, reveals a variety of details of the slump (Fig. 30 a,b). The seafloor imagery of the channel floor outside the slump (Fig. 30a, 01:30-02:30 hrs) is characterised by uniform moderately strong backscattering, whereas Holocene sediments covering the slump upslope (Fig. 30b, 04:00-04:30 hrs) display much weaker backscatter.

In addition, the sonographs from the channel floor outside the slump show the presence of isolated ice-rafted boulders outcropping from the (Holocene) surface sediments.

In between the two areas with uniform backscattering, an area characterised by marked differences in back-scattering showing a lobate and wavy pattern can be observed. This is the area where subbottom profiling demonstrated the presence of the acoustically transparent superficial sediment unit with its undulating seafloor topography, i.e. the area of the major slump deposit. In addition to the lobate structures of the slump, a larger (filled) channel is observed more upslope on the slump (Fig.30b). Other linear features, likewise downslope trending, are also seen in the other parts of the slump. Lobate structures of different backscatter character in the most distal part of the slump (ca 02:30 hrs) may yield evidence for repeated slumping. The presence of a turbidite channel system present on top of the slump may also be evident from the (hull-mounted) subbottom profiler record from coring site AT103G. This core was collected from the margin of a shallow (ca 6 ms), buried channel, of which the sediment in-fill showed a markedly weaker acoustic reflectivity than the surrounding slump deposits.

### III.2.3. Bottom sampling

*G. Akhmanov, A. Stadnitskaya, E. Kozlova, A. Akhmetjanov, P. Friend, H. De Haas, A. Sautkin, R. Brambilla, I. Belenkaya, S. Lubentsova, M. Kozachenko, I. Mardanyan*

*Introduction*

The aim of the sediment sampling program on the southeastern Faeroes margin was to investigate features revealed by seismic and side-scan surveys of the slide area with a view to dating the slump events and to studying in detail processes which accompany slumping.

Sampling locations were chosen from subbottom profiles, side-scan sonographs, and seismic lines. For locations see tables 5, 6 and Figs. 24 and 28.

Core TTR8-AT-101G (Fig.31)

A 389 cm long core was recovered, presenting Holocene-Upper Pleistocene hemipelagic sediments interbedded by intervals of slump - debris flow deposits. The former are mainly represented by silty clay, varying in colour from light olive grey to very dark grey, and probably reflect changes in carbonate content resulting from short range climatic fluctuations in the Upper Pleistocene. These hemipelagic deposits are mostly heavily bioturbated and contain abundant foraminifera. Subangular fragments of more consolidated clay, up to 0.3 mm in diameter, are often observed to be randomly spread throughout the intervals. These clay fragments, together with a few sandy lenses and several dropstones, suggest a large contribution from ice-rafted material. The slump - debris flow intervals consist of basically the same lithologies, reworked during resedimentation processes and giving a characteristic structural pattern to the sediments. Four such intervals were described, varying in thickness from 30 to 70 cm. They are composed of subrounded, differently shaped fragments of clay,

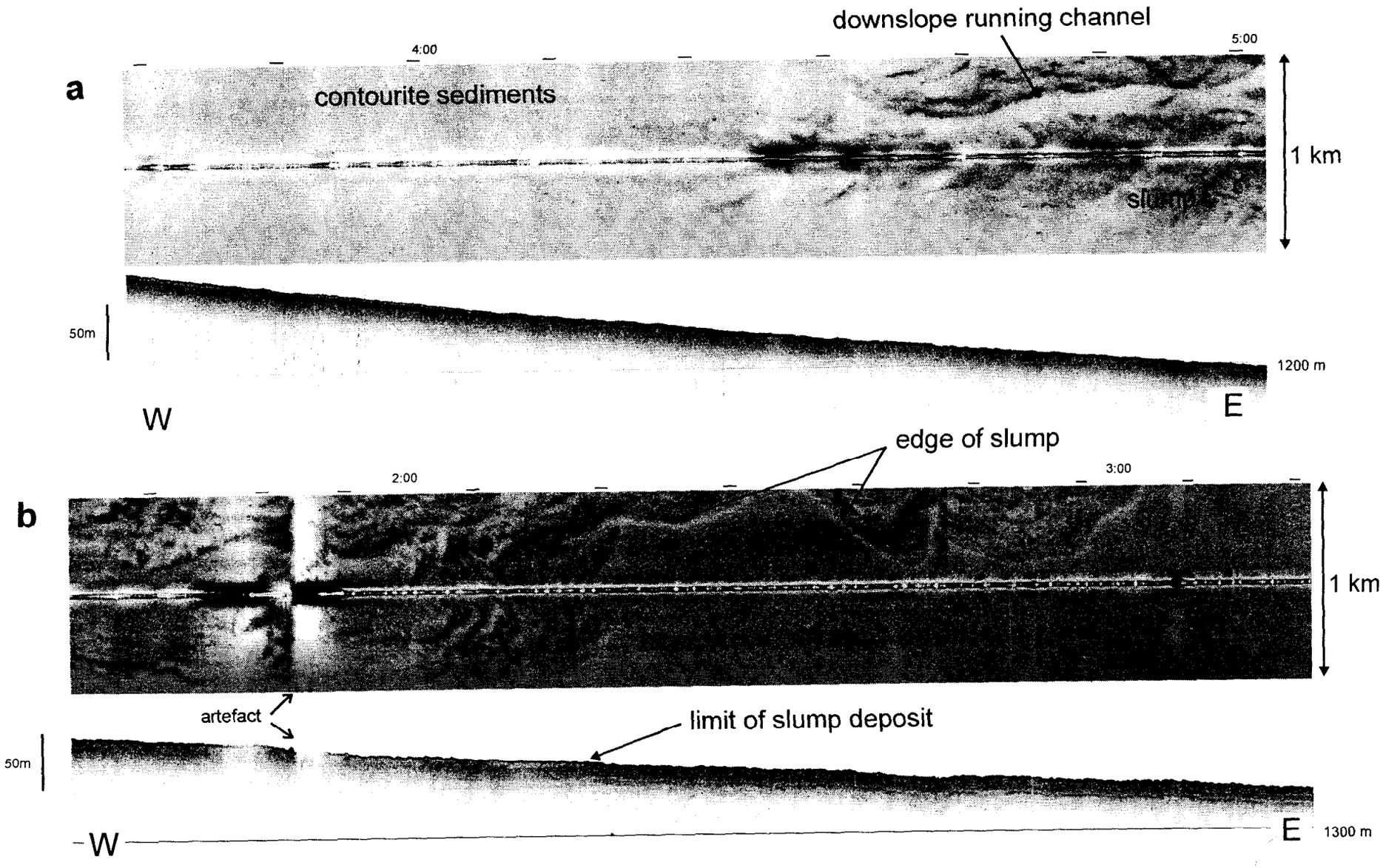


Fig. 30. Fragments of ORAT-18 100 kHz sonograph and 5 kHz subbottom profiler record across a slump on the eastern Faeroe margin: **a** - *upper slope part covered with contourite sediments;* **b** - *lower boundary of slump.*

| Station No | Date | Time (GMT) | Latitude | Longitude | Depth, m | Recovery, cm |
|---|---|---|---|---|---|---|
| TTR8-AT-101G | 02.07.98 | 16:54 | 61°26.820' | 04°14.102' | 1157 | 389 |
| TTR8-AT-102G | 02.07.98 | 18:06 | 61°27.312' | 04°13.401' | 1164 | 395 |
| TTR8-AT-103G | 02.07.98 | 19:44 | 61°25.018' | 04°16.797' | 1138 | 264 |
| TTR8-AT-104G | 04.07.98 | 10:07 | 62°59.048' | 03°40.545' | 1978 | 372 |
| TTR8-AT-105G | 04.07.98 | 11:43 | 62°54.459' | 03°37.509' | 1456 | 341 |
| TTR8-AT-106G | 04.07.98 | 13:13 | 62°54.362' | 03°37.653' | 1440 | 356 |
| TTR8-AT-107G | 04.07.98 | 14:21 | 62°54.421' | 03°41.422' | 1468 | 302 |
| TTR8-AT-108G | 07.07.98 | 07:55 | 63°34.134' | 03°31.349' | 3054 | 472 |
| TTR8-AT-109G | 07.07.98 | 11:37 | 63°39.877' | 03°15.394' | 3028 | 502 |
| TTR8-AT-110G | 07.07.98 | 13:13 | 63°40.092' | 03°15.724' | 3035 | 350 |

**Table 5.** General information on the cores sampled on the Faeroes margins and the Norwegian basin study areas.

| Station No. | Geographical Setting | Sedimentary Summary | Instrumentation | Acoustic characteristics |
|---|---|---|---|---|
| TTR8-AT-101G | Flat surface close to recent slump body | Holocene-Upper Pleistocene hemipelagic silty clays interbedded with intervals of slump-debris flow deposits. Uppermost interval is represented by structureless sandy layer, olive grey, oxidised at the very top | Seismic and OKEAN sidescan sonar profiles, subbottom profiler, PSAT-43(B), 9:56 | Layered sequence on the subbottom profiler PSAT-43(B) |
| TTR8-AT-102G | Flat surface close to recent slump body | Holocene-Upper Pleistocene hemipelagic succession of dark grey and grey silty clays, heavily bioturbated. Uppermost interval is represented by structureless sandy layer, olive grey, oxidised at the very top | Seismic and OKEAN sidescan sonar profiles, subbottom profiler, PSAT-43(B), 9:50 | Layered sequence on the subbottom profiler PSAT-43(B) |
| TTR8-AT-103G | Small depression filled by sediments on the rough surface of the recent slump body | Stiff sandy, silty clay of slump body covered in depression by interval of debrites, hemipelagic sediments and contourites | Seismic and OKEAN sidescan sonar profiles, subbottom profiler, PSAT-43(B), 10:17 | Transparent layer on the subbottom profiler PSAT-43(B) |
| TTR8-AT-104G | Small shelf on the lower slope of the Northern Faeroes Margin (large slump area) | Slump, debrite interval covered by hemipelagic clayey succession with tephra layer at the base and three sandy layers of contourites | Subbottom profiler, PRAT-04, 5:06,5 | Layered sequence on the subbottom profile PRAT-04 |
| TTR8-AT-105G | Top of small scarp in upper slope area of large slump | Undisturbed hemipelagic succession of light olive grey and dark grey silty clays varying in foraminifera and silty admixture contents. Three graded silty layers with fining up - possible interbasinal turbidite deposits. Brown tephra layer | OREtech sidescan sonar, subbottom profiler, (ORAT-19, 21:16) | Transparent layer on the OREtech sidescan record ORAT-19 |
| TTR8-AT-106G | Top of small scarp in upper slope area of large slump | Hemipelagic succession of grey and dark grey bioturbated clays, slightly affected by small scale faulting in the lower part. Several graded silty layers with fining up – possible turbidites. Black tephra layer | OREtech sidescan sonar, subbottom profiler, (ORAT-19, 21:14), | Transparent layer on the OREtech sidescan record ORAT-19 |
| TTR8-AT-107G | Local depression within slumped sediment area covered by recent undisturbed deposits (upper slope of the large slump) | Hemipelagic succession of grey and dark grey bioturbated clays varying in silty sized terrigenous admixture and foraminifera content Several graded silty layers with fining up - possible turbidites. Brown tephra layer | OREtech sidescan sonar, subbottom profiler, (ORAT-19, 22:29), | Transparent layer on the OREtech sidescan record ORAT-19 |
| TTR8-AT-108G | Norwegian Basin. Deepest part of the elongate depression cutting the basin | Very thick interval of olive grey, very homogeneous, well sorted, very fine-grained clay overlain by intercalations of light olive brown clay with thin graded silty and sandy layers. Hemipelagic olive brown clay at the top | Seismic and OKEAN sidescan sonar, subbottom profiler, (PSAT-51, 20:08) | Layered sequence on the subbottom profiler PSAT-51 |

**Table 6.** Sedimentological, acoustic and geological characteristic of sampling stations on the Faeroes margins and the Norwegian basin study areas.

| | | | | |
|---|---|---|---|---|
| TTR8-AT-109G | Norwegian Basin. Deepest part of the elongate depression cutting the basin | Very thick interval of olive grey, very homogeneous, well sorted, very fine-grained clay overlain by intercallation of light olive brown clay with thin graded silty and sandy layers. Hemipelagic olive brown clay at the top | Seismic and OKEAN sidescan sonar lines, subbottom profiler, (PSAT-56, 08:39) | Layered sequence on the subbottom profiler PSAT-56 |
| TTR8-AT-110G | Norwegian Basin. Deepest part of the elongate depression cutting the basin | Not opened on board | Seismic and OKEAN sidescan sonar lines, subbottom profiler, (PSAT-56, 08:42) | Layered sequence on the subbottom profiler PSAT-56 |

**Table 6.** ***(Continuation)***

silty clay, and clayey silt of different size, which were plastically deformed and redeposited within clayey matrix. No visible evidence of bioturbation was found within these intervals, but bioturbation occurred at the upper and lower interval boundaries. This implies very rapid, one-act deposition of the whole interval as a debrite or slump deposit.

The uppermost 14 cm of the core are represented by grey, fine-grained sand with a certain silty clayey fraction, oxidized on the very top. The interval is structureless and can initially be interpreted as recent bottom current deposits.

Core TTR8-AT-102G (Fig. 32)

The 395 cm recovered mainly show an alternation of silty clay layers, varying in colour from light olive grey to very dark grey, and probably reflecting different carbonate material input in the Upper Pleistocene due to climatic fluctuations. Bioturbation heavily affects the whole sequence, except the lower 36 cm of dark greyish brown, silty structureless clay. Lack of significant compositional variations throughout the core implies a predominant hemipelagic sedimentation constant throughout the time of deposition. A few dropstones observed suggest the input of ice-rafted material.

The uppermost 10 cm of the core are represented by grey fine-grained sand with silty clayey fraction, oxidized on the very top and structureless, implying deposition by recent bottom currents.

Most of intervals of this core can be correlated with the hemipelagic intervals of the core TTR8-AT-101G.

Core TTR8-AT-103G (Fig. 33)

The recovery of 264 cm consists of two main intervals. The lower part of this succession is represented by very stiff silty clay, very dark grey in colour, structureless, and enriched in a sandy admixture. There were also a large amount of pebbles of different composition, shape, sphericity, and size. Although the origin of this very chaotic mixture is still not clear, apparently it presents the lithology of the slump body expressed on the profiler line. The upper succession overlies the lower slump body formation boundary. This upper succession started with deposition of dark olive grey silty sandy clay, with a considerable gravel and pebble fraction; this can be interpreted as a debris flow deposit. This inter-slump debrite is covered by a 70 cm thick hemipelagic clay, grey in colour, and heavily bioturbated throughout the whole interval. The uppermost part of the core consists of a thick, structureless silty layer, water-saturated at the very top and more consolidated below. This interval seems to be deposited by bottom currents and should correlate with upper intervals of the cores AT-101G and AT-102G, reflecting high recent bottom current activity in the area.

Despite the fact that only a few cores were taken at the South-Eastern Faeroes margin, an impression was gained of the variety of recent sedimentary processes ongoing in this area. Upper Pleistocene hemipelagic sedimentation, with deposition of clay and ice-rafted material, has been disturbed by large slump formation. Slope mass instability has led to the creation of several debris flows that have redeposited material in front of the large slump.

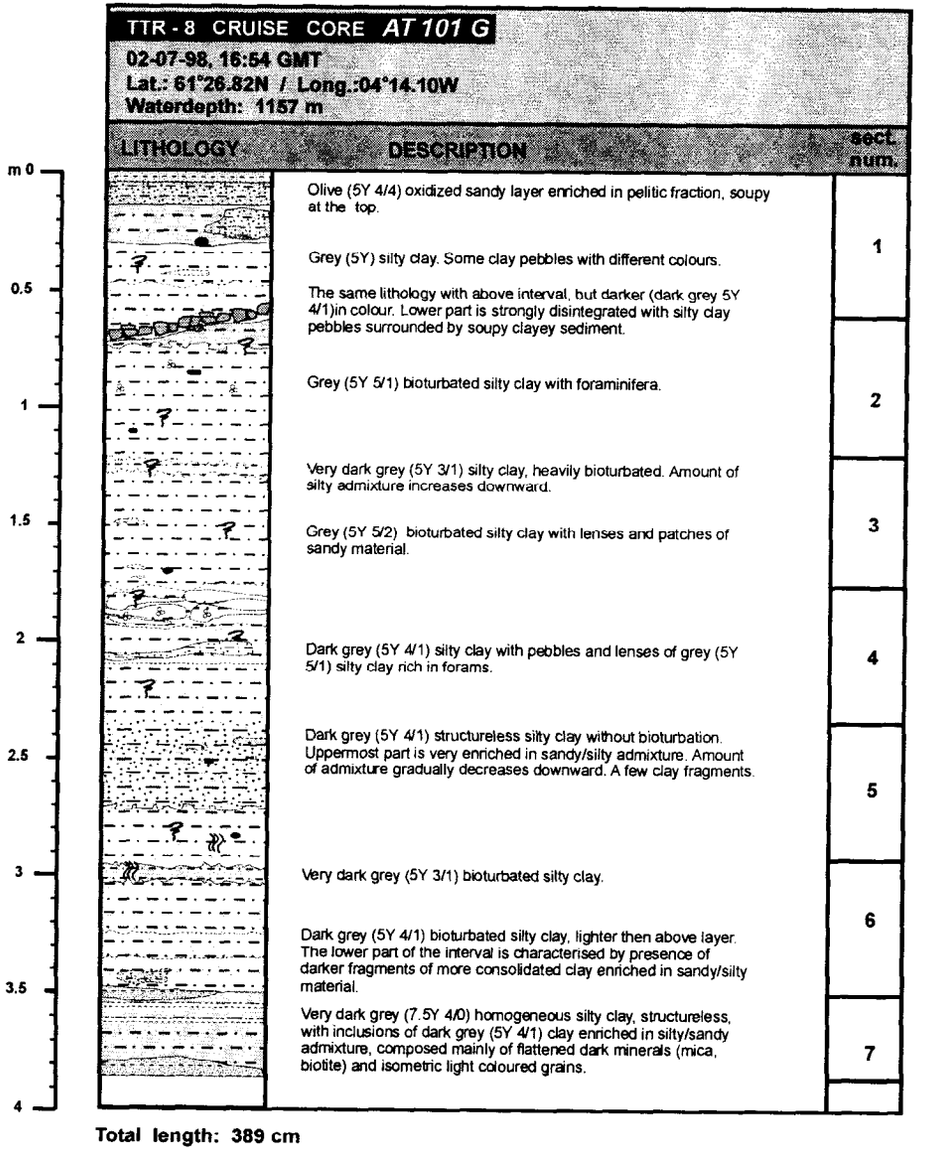


Fig. 31. Core log AT-101G.

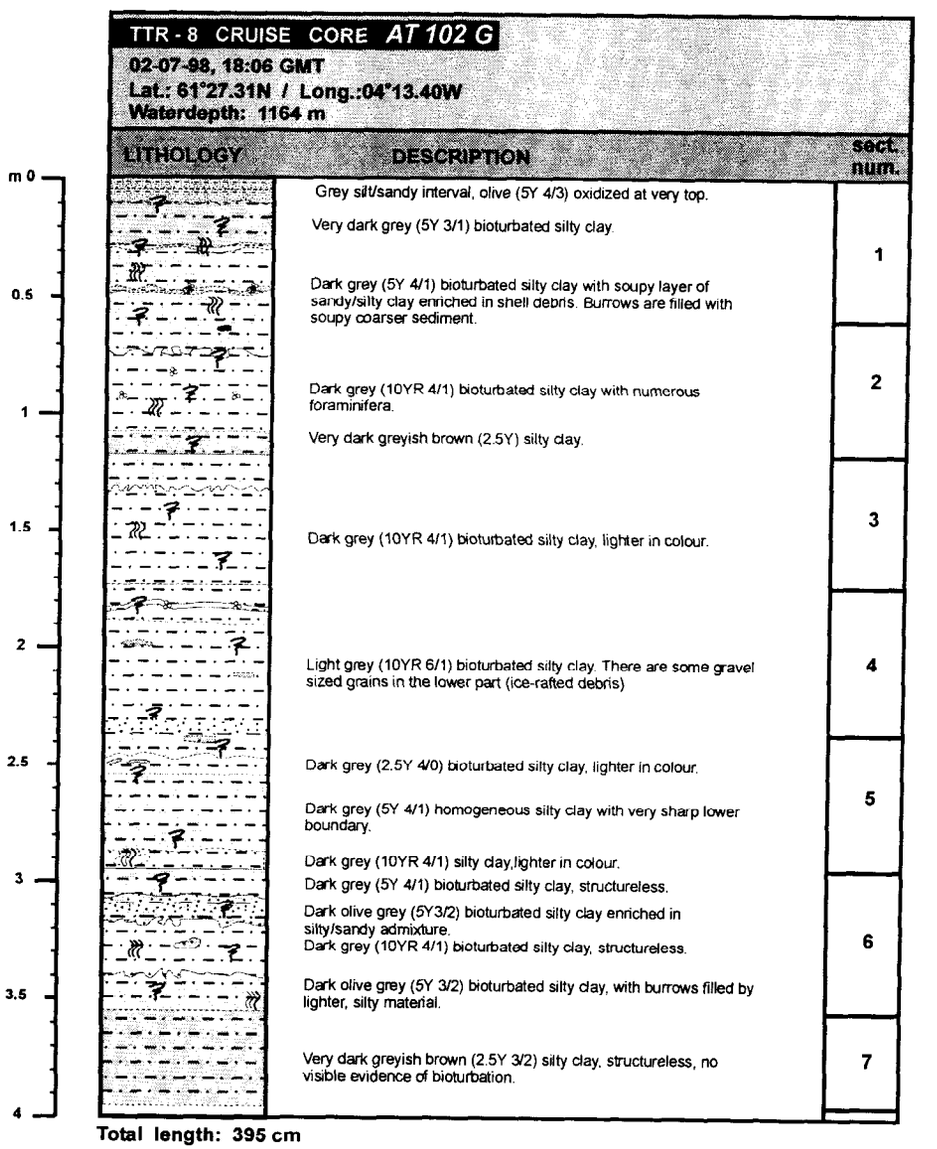


Fig. 32. Core log AT-102G.

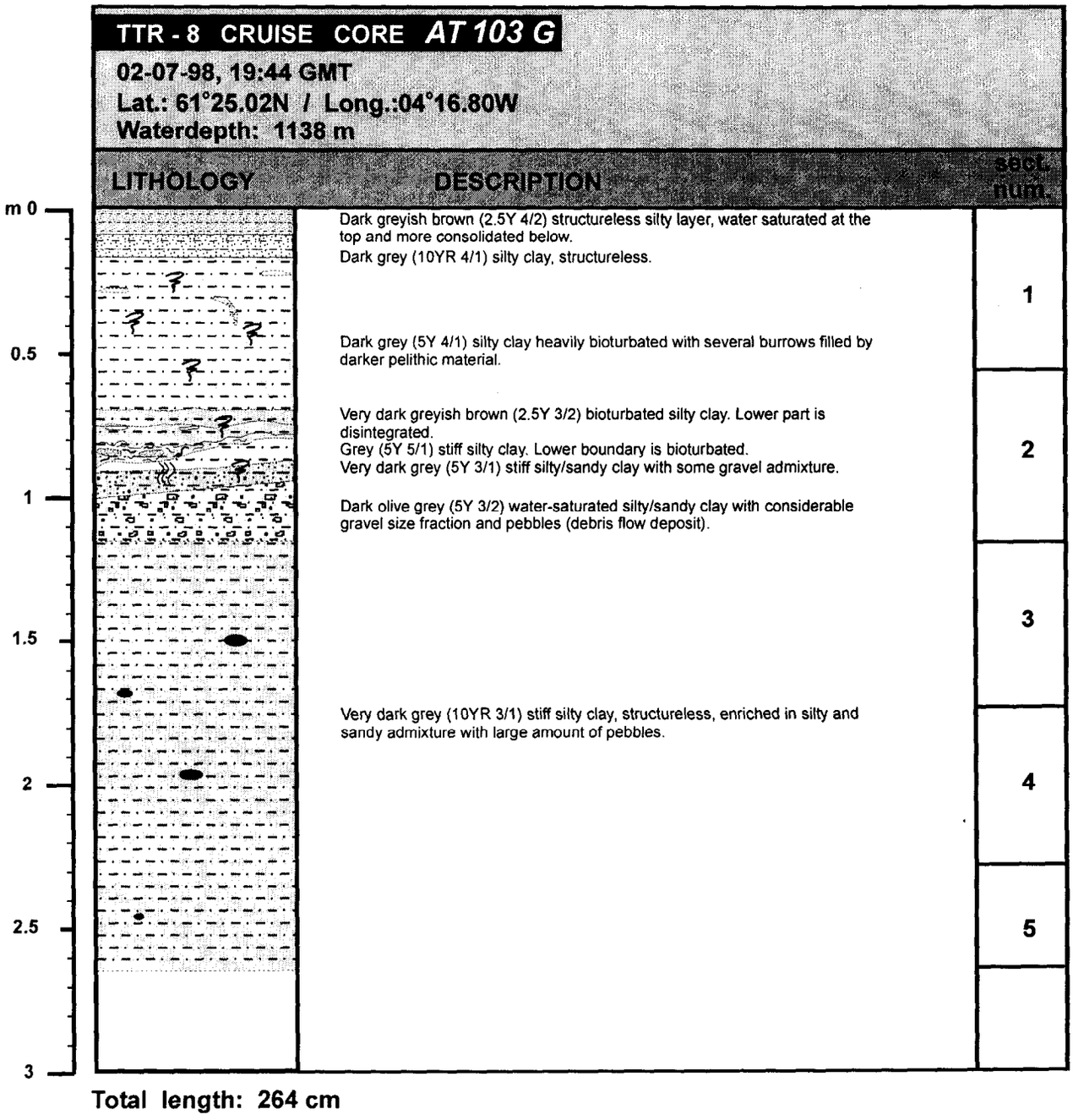


Fig. 33. Core log AT-103G

The age of slump formation is not clear from the available data, but apparently should also be considered as Upper Pleistocene. The Holocene sedimentation has been strongly affected by bottom currents that have supplied and deposited sandy material in front of the slump body and over it. A relatively large thickness of contourites in the core AT-103G can imply the presence of certain channel systems over the slump body. This is in contrast with the area in front of the slump, where contourites are widely distributed and do not form a thick cover.

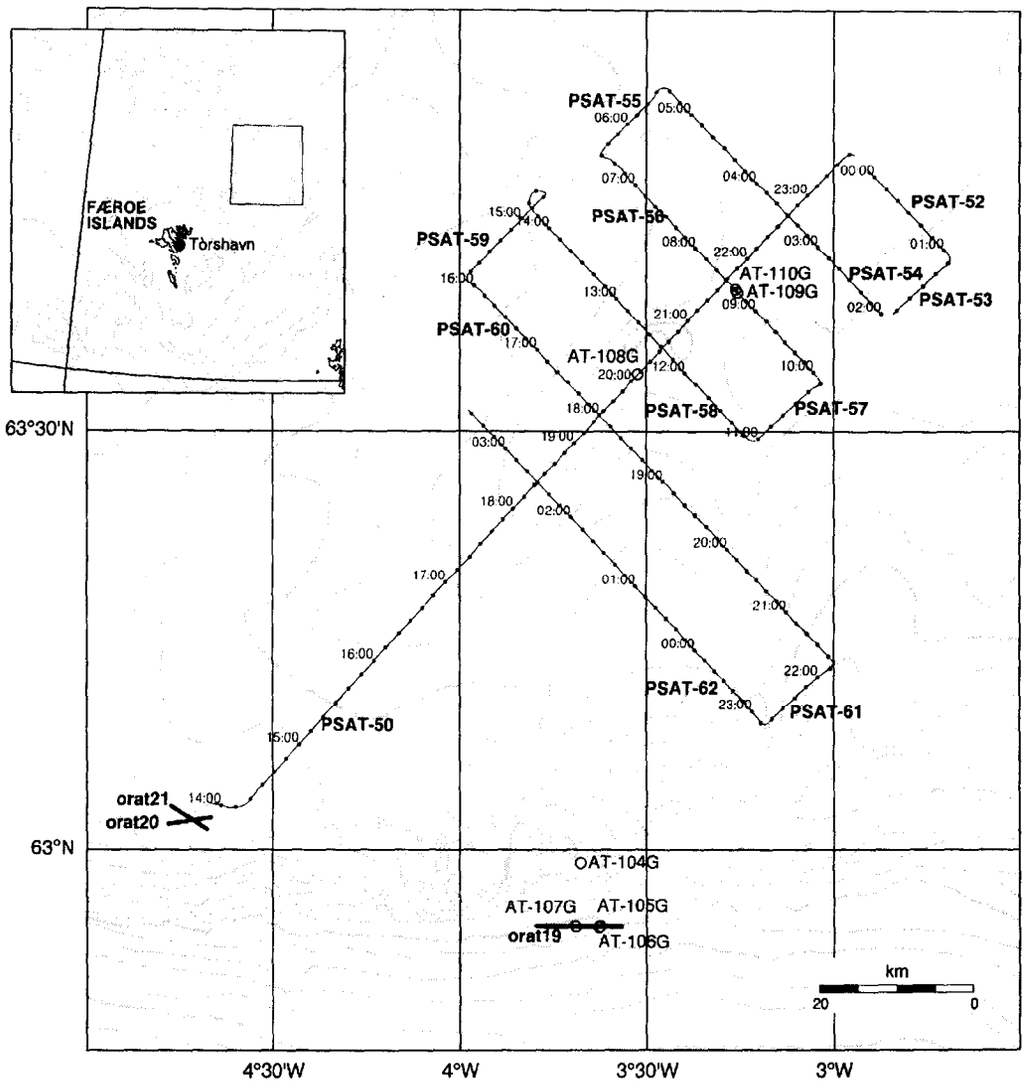


Fig. 34. Location map of the northeastern Faeroes margin

## III.3.NORTHEASTERN MARGIN

### III.3.1. Seismic data

*T. Nielsen, M. Baturin, J. Taylor, E.Yakovlev, O. Savotina, N. Furkalo, S. Tischenko*

The investigated lines, to the north of the Faeroese Platform, are located to examine distal sediment transport pathways associated with upslope instability on the North Faeroes margin. The main research target for this area was a depression on the seafloor of the Norwegian basin of unknown genesis, first recognised on GLORIA and contemporaneously collected 3.5 kHz subbottom profiler records and on a revised bathymetry covering the entire North Faeroese margin (Taylor et al., submitted).

The survey grid consists of twelve lines with a total length of 430 km. The longest line, PSAT 51, is oriented SW-NE, along the axis of the depression. Lines PSAT 52, 54, 56, 58, 60, and 62 were shot perpendicular to PSAT 51 and are connected to each other by five shorter lines (PSAT 53, 55, 57, 59 and 60) (Fig. 34). Water depths in the study area vary between 2500 and 3000 m. Seismic penetration was up to 1200 ms TWT and 6 seismic units were identified (Fig. 35)

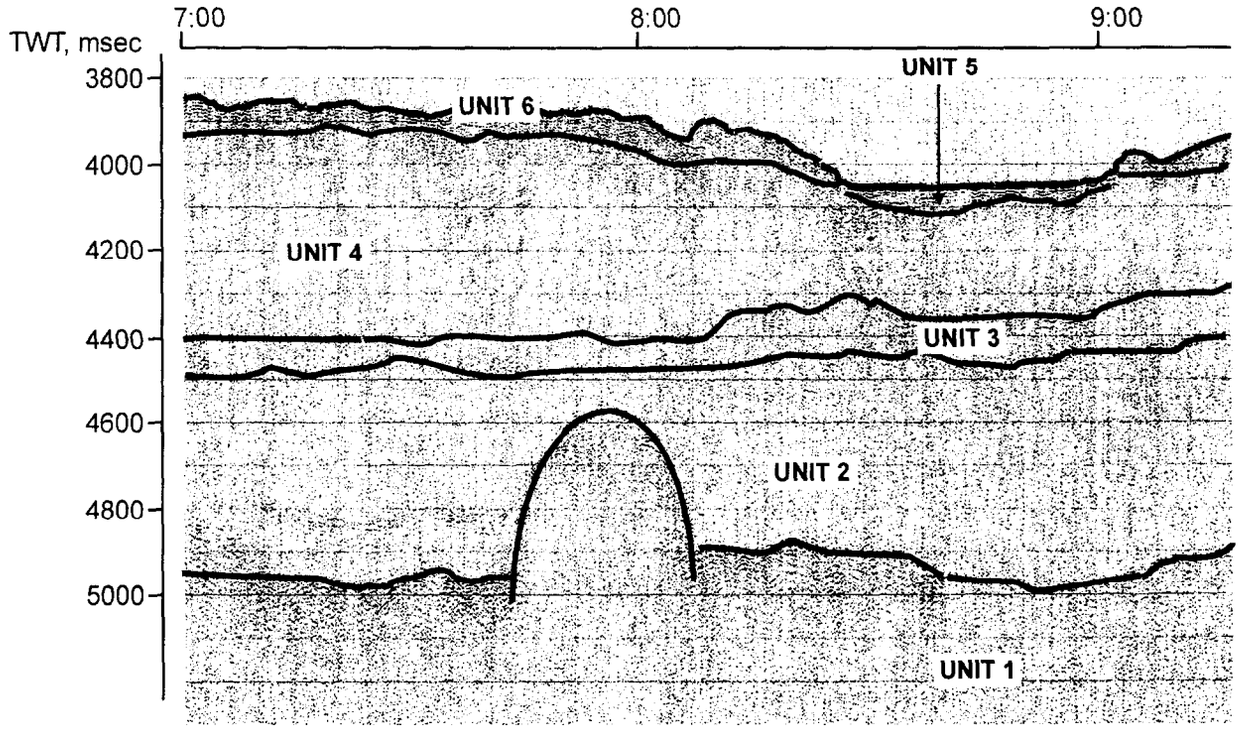


Fig. 35. Fragment of the line PSAT-56 showing main seismic units. Note a dome-like feature at the top of the Unit 1 interpreted as an intrusion.

*Seismic description*

Unit 1 represents acoustic basement in the survey region, and can be traced throughout the area, sloping from 4000 ms TWT in the north-east to 6000 ms TWT in the south-west. The top of the unit is formed by a high-amplitude reflector with an irregular morphology of intermittent, upstanding hyperbolae. The elevations of vertices reach depths of 3800-4400 ms TWT and the overall morphology of the topbounding reflector is that of a depression. Evidence for faulting is occasionally visible.

Unit 2 conformably overlies Unit 1, and has a thickness of 200-700 ms TWT. The surface of the unit is found at a more level depth of 4100-4300 ms TWT, and is characterised as an undulating medium strength reflector. Internal reflectors are infrequent.

Unit 3 is observed on all lines, except PSAT-57 and PSAT-59. Its upper surface is characterised by a medium amplitude reflector with a relatively smooth morphology, found at a depth of 3300-4100 ms TWT. The thickness of the unit is about 200 ms TWT, increasing slightly to the south-east.

Unit 4 also is found through most of the area and its upper reflector is prominent and of high amplitude. The unit has a minimal thickness in the south-east, and thickens towards the north-west, where it reaches a maximum thickness approaching 500 ms TWT. Internal reflectors are infrequent.

Unit 5 is confined to the deepest section of the channel system identified in available bathymetries and as such can be seen only on lines PSAT-51, 56, 60 and 62 (Fig. 34). On these lines, the unit appears as an infill sequence, with a flat surface reflector forming the seabed, and an internal structure of continuous parallel reflectors. The thickness of the unit is about 50 ms TWT.

The uppermost unit, Unit 6, is found across the whole survey region outside of the occurrences of Unit 5 in the bathymetric lows, lying directly on Unit 4. Its upper surface, forming the sea floor, has a variable character; in the southeastern part of the grid the upper (sea floor) reflector has a relatively flat morphology. Elsewhere, the reflector appears as hummocky or irregular, principally to the north of the bathymetric lows forming Unit 5. Internal reflectors of the unit are discontinuous and chaotic. The thickness of the unit varies from 50 to 200 ms TWT.

*Seismic interpretation*

Unit 1, the acoustic basement, is interpreted as the regional basaltic basment, and as such is determined to be of Late Paleocene to Early Eocene age (Nielsen and van Weering, 1998). The dome-like features on its upper surface are interpreted as instrusions. The overlying units therefore represent the Eocene to present sedimentary cover. It is tempting to fit Units 2 to 4 to the sequences proposed by Nielsen and van Weering (1998) and Nielsen et al. (1998) further upslope of the survey region. However, this is difficult without further analysis using the ties obtained, because there is no obvious link between the two sets of facies identified. For example, the lower unit identified here, Unit 2, may fit well with either Unit 1 or Sequence 1 identified in earlier work upslope. The seismic grid presented here does indicate clearly that the east-west trending ridge to the west of the bathymetric lows is indeed sedimentary in origin, and Taylor et al. (submitted) suggest that it probably consists of failed deposits derived from the Faeroese shelf. The massive thickness of Unit 4 in the region of this region may be related to its origin. Unit 6 is consistent with a slump or gravitational failure deposit, accentuating the morphology of the acoustic basement and overlying sedimentary sequence. The irregular surface of the deposits and chaotic internal structure result in attenuation of the acoustic signal. This significantly degrades the resolution of the underlying units and makes the relationship between Units 4, 5, and 6 difficult to ascertain. Unit 5 forms a channel fill sequence within the depression formed by the other units. The stratified nature of the reflectors may be related to hemipelagic deposition, or, more likely given the channels' location downslope of the instabilities recognised previously, is derived from repeated sediment input from multiple phases of failure on the slope. Units 5 and 6 are therefore most likely to be Quaternary in age.

### III.3.2. Side-Scan Sonar Data

*A. Akhmetzhanov, J. Taylor, R. Pevzner, M.Ivanov, A. Kuijpers and A. Wheeler*

*ORAT 19: Description and interpretation*

The 100 kHz OREtech line ORAT-19 was run across one of the shallow slides imaged during the 1995 TOBI survey, carried out as a contribution to ENAM I (van Weering et al., 1998). The higher resolution provided by the 100 kHz system was required to obtain a more

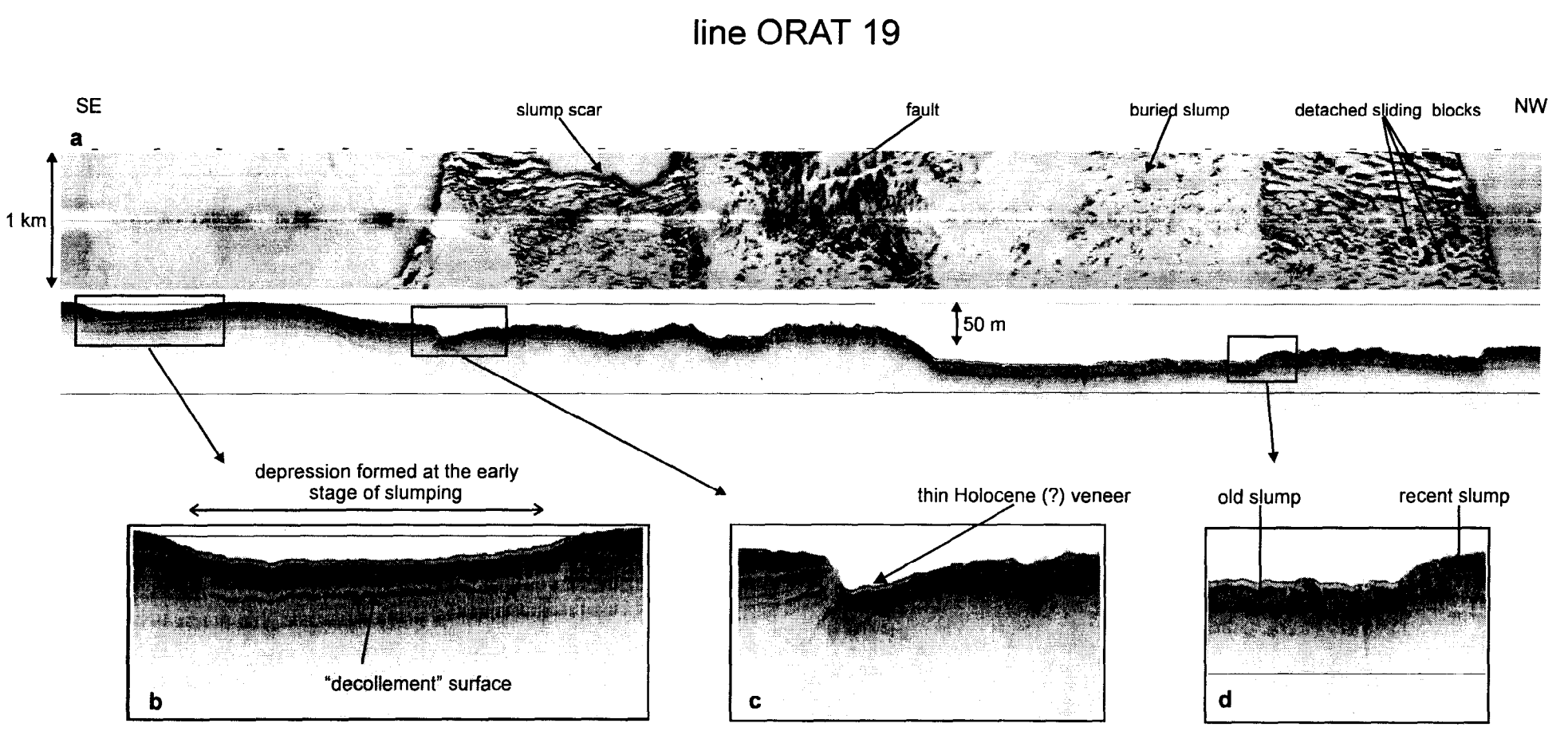


Fig. 36. ORAT-19 100 kHz sonograph and subbottom profiler record across a shallow slide on the norther Faeroes margin. Insets show different morphological features generated due to intensive sliding of the upper sedimentary cover (see description in the text).

detailed picture of slope instability processes. Five zones are defined from the imagery and associated profiler records.

The eastern end of the line, from the beginning to 21:12, is characterised by a low level of acoustic backscatter. The profiler records show about 30 m of well-stratified sediments (Fig. 36a). Between 20:18 and 20:37, a broad depression, 1 km wide and 10 m deep, was imaged and corresponds to a band of lower backscatter with a broadly north-south axis. The depression is also infilled with a well-stratified sedimentary succession although an unusually thick and well defined acoustically transparent layer delimits the lower boundary of the sediment infill (Fig. 36b).

From 21:10 to 22:30, the backscatter pattern changes significantly. The sonograph is characterised by the presence of a highly variable field of dominantly high backscatter. The field has a sharp, uneven outline and is bounded to the east and south by seafloor characterised by a featureless, low backscatter. Within this field, there are numerous elongate features oriented parallel to the southern boundary. The subbottom profiler reveals the boundary between the two different areas as a 15 m high escarpment (Fig. 36c). Westwards of the escarpment, and coincident with the change in appearance on the 100 kHz imagery, the seafloor topography is rougher, and acoustic penetration decreases to 20 m on profiler records. A strong, relatively flat reflector can be traced beneath the area of rough topography, defining an acoustically semi-transparent unit with a chaotic internal reflection pattern. The lower unit consists of well-stratified sediments. The chaotic unit is about 15 m thick. Between 21:55 and 22:05, a shallow 500 m wide depression is imaged, coincident with two strong reflectors visible on the profiler record. The upper reflector is correlated with the lower boundary of the principal chaotic unit, overlain by a thin veneer of acoustically transparent material. This upper reflector is underlain by an acoustically transparent unit, defined by the second strong, basal, reflector. The sonograph displays a series of faint north-south (downslope) oriented bands of weak backscatter. Westwards of this depression, the irregular topography and cracked appearance on the OREtech data are re-established, although this time the background backscatter level is slightly higher. Also, on the port side record, a 1 km long linear, very low backscattering feature is observed between 22:05 and 22:25. There are also some discontinuous but strongly reflective features, suggestive of bedding, within the upper chaotic unit.

The chaotic unit is interpreted as a slide body, and the slope-parallel elongate features are interpreted as regions of tension cracks within this body, where the upper sedimentary section is strongly disturbed, due to downslope-oriented lateral tension within the sediment column, associated with the early stages of movement.The strong reflector separating the unit from the well-stratified material beneath is believed therefore to be a glide plane. Transport direction is indicated as being directly downslope (south to north), both from the orientation of the tension cracks, and also the north-south orientation of the draped depressions within the slide body. The 1 km linear feature on the OREtech imagery in the western slide section is interpreted as a fault line. Where local depressions occur within the surface topography of the slide unit, a thin (ca. 2 m) veneer of presumably Holocene fine-grained hemipelagic deposits is found. This interpretation is supported by the observation of areas of low backscatter between the slide scars.

Between 22:30 and 23:20 the sonograph shows a relatively smooth area with a generally low acoustic signature, although from 22:50 the pattern changes slightly as numerous high backscattering spots and speckles become apparent (Fig. 36a). These latter appear occasionally to be arranged into a semicircular pattern or resemble sinuous channel-like features (e.g. at 22:52). The subbottom profiler shows a broad depression over 2 km wide and about 30 m deep, with the uppermost sediment represented by an acoustically transparent veneer up to 5 m thick. The veneer thins where small notches of the unit beneath outcrop, corresponding to the high backscatter features outlined above on the OREtech imagery.

Below this veneer, there is a 10 m thick lens-shaped unit with a chaotic inner structure. The upper surface of the unit is rough, with strong reflectors visible at the base of the unit, below which there is no penetration.

Further west (23:20-23:50) the backscatter pattern changes again, closely resembling the the tension crack field described at the east of this line. The zone is 1.5 km wide and is delimited to the west by an escarpment, seen clearly on both the sonograph and the profiler records. At about 23:40, on the starboard side of the sonograph, three features are visible, which have an irregular shape with extremely uneven edges and an average diameter of about 15-20 m (Fig. 36a). These are probably detached and/or displaced blocks of sediment which have slid downslope. To the west of the escarpment, normal undisturbed sedimentary cover is imaged on both the sonograph and the profiler record.

This line is thus fundamentally important in understanding the evolution of this shallow slide, the whole of which was probably initiated as a result of retrogressive failure back from the main slide headwall, as the upslope sediment column became unsupported. The depression observed at the eastern end of the line is interpreted as originating at the very beginning of the slide formation, when ductile deformation took place. This resulted in thinning of the sedimentary pile without a disturbance of seafloor integrity. At the base of such a thinned sequence, a décollement surface has been formed and is seen on the profiler record as a thin transparent layer. This appearance on the profiler is suggestive of the presence of disintegrated sediments which are probably water saturated. Subsequently, the fields of tension cracks were developed. Therefore, the formation of such fields of tension cracks is suggested to occur at an early stage of the development of the shallow slide, resulting in large fragments of sedimentary cover being transported downslope. During further slide development, the pattern of tension cracks disappears as the transported sediments disintegrated and became more uniform, forming a debris flow. The most deeply incised depression (22:30-23:20) was probably formed by an older event, since it is covered by hemipelagic sediments and is also overlapped by another chaotic sedimentary body corresponding to one of the crack fields (Fig. 36d).

*ORAT 20 and 21: Description and interpretation*

Two lines, of 2 hours each, were collected from the north Faeroes margin. The aim was to investigate in detail the unusual swarms of trails possibly caused by the downslope movement of sediment blocks, which had been imaged in this area by the 1995 TOBI survey (van Weering et al., 1998).

ORAT-20 runs from the east to the west and ORAT-21 from the south-west to the north-east, intersecting in the middle of both. Overall levels of acoustic backscatter on the OREtech imagery are low to medium on both lines, and both lines also show similar patterns of north-east-south-west oriented low backscattering lineations (Fig. 37a); these lineations are imaged most clearly on the ORAT-21 sonograph. The lineations have very low backscatter axes and are bound by high backscatter edges. Widths vary from 30 to 50 m, with maximum observed lengths of about 2 km, although the TOBI data indicate that the trails are far more extensive than this. Some lineations are straight whilst others display a low sinuosity. The widths of the most of the lineations do not vary considerably, although periodically the lineation width can decrease from 50 to 25 m within a distance of 50-70 m, and then increase again, forming a bead-like pattern. Occasionally, the linear features have elongate objects at their terminations (Fig. 37c). The longer axes of these objects appear to be transverse to the orientation of the lineations and the objects can reach a width of 30-50 m, which correlates well with the dimensions of the lineations. The average height of the objects is 18-20 m,

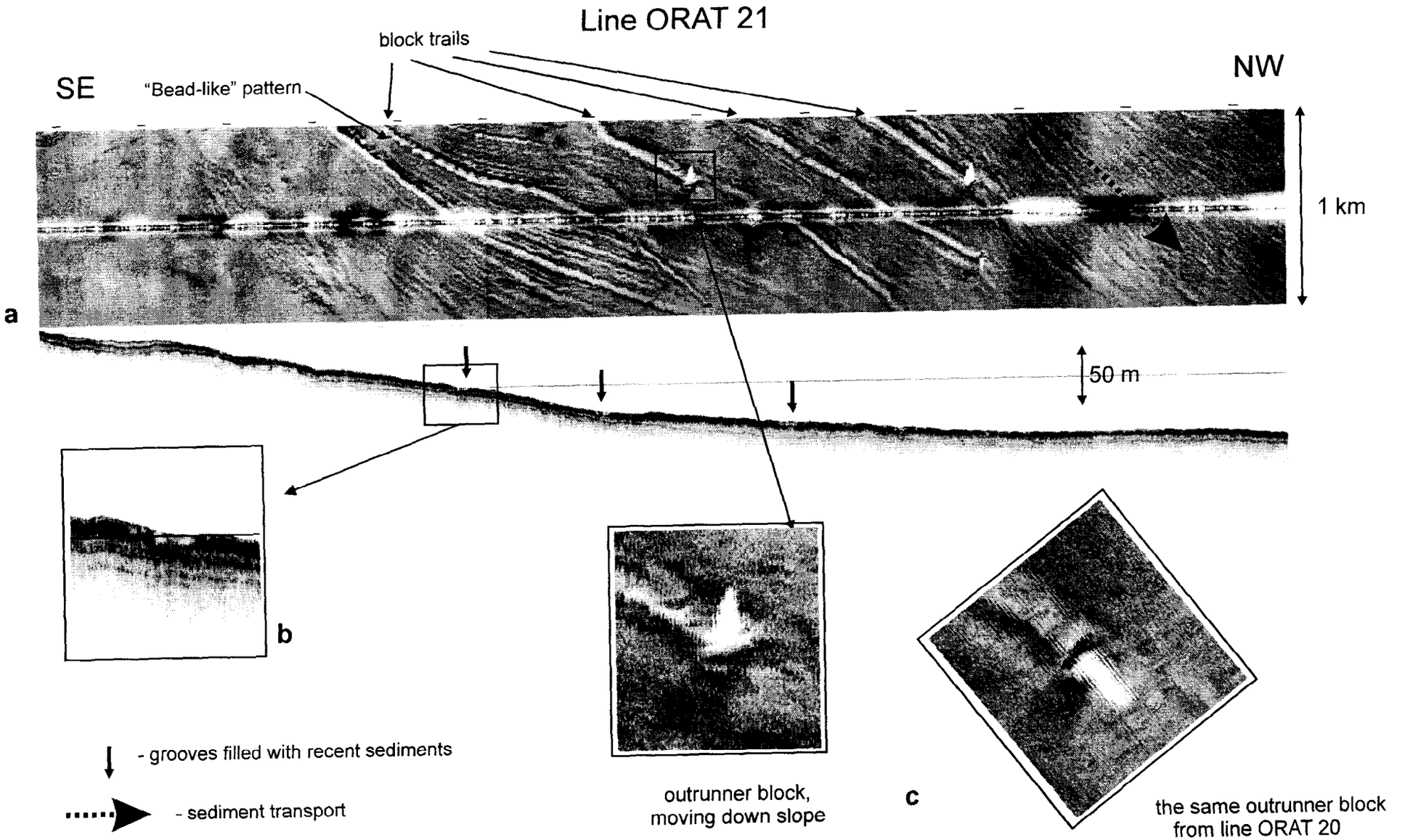


Fig. 37. ORAT-21 100 kHz sonograph and subbottom profiler record across a zone of block trails on the northern Faeroes margin (see description in the text).

calculated from the lengths of their clearly defined shadows. The sonographs also show the lineations to be clearly cross-cutting. As well as these principal lineations, another type of the seabed striation was observed on the northwestern end of ORAT-21. These striations are formed by closely spaced, low backscatter streaks oriented approximately north-south. The striations occur also between 5:50 and 6:30 on the ORAT-21, where they are overprinted by lineations associated with block trails. The width of these striations is about 10-15 m.

The subbottom profiler record along ORAT-20 line reveals a broad depression about 3.3 km wide and 25 m deep. This depression is well expressed because it appears to lie almost perpendicular to the orientation of the line. The subbottom profiler record has a penetration of about 30 m and displays well-stratified sediments, composed of several units. The lowermost unit is represented by gently undulating parallel beds. On the eastern flank of the depression, the lower unit is overlaid by a complex succession composed of stratified and transparent intervals. To the west, the upper unit pinches out at about 21:25, with the lower unit lying very close to the seafloor within the depression. Basins formed by the undulating upper surface of the lower units are filled with acoustically transparent lens-like bodies. The surface layer imaged on the subbottom profiler is 5-7 m thick. At the locations where the lineations of weak backscatter intersect with the profiler line, grooves are seen to cut into the upper veneer (Fig. 37b). Depths range from 2 to 4 metres. The subbottom profiler record shows that most of them are infilled with later sediments, which are probably responsible for the low backscatter signature of these features.

It has been suggested in previous studies (van Weering et al., 1998) that these lineations are the trails of outrunner blocks moving downslope. From the shapes of the trails, their regional context, and the presence of objects at their terminations, it is possible to speculate on the type of the downslope motion responsible for these features. The sinuosity of some of the trails and the apparent transverse orientations of the objects found at their termini suggest that the pattern has been created by the rolling downslope large blocks of relatively soft sediments. This rolling action is also probably responsible for remoulding the blocks into their present elongate form. The bead-like pattern of some parts of the trails may be a result of blocks bouncing along the seafloor, as momentum builds and velocity is acquired. Alternatively the blocks may have simply slid down the slope, with no rolling action at all. The absence of any obvious build-up at the downslope face of blocks that would be associated with such ploughing of material through the upper part of the sediment column would argue against this. However, the trails are clearly erosive in nature, apparent from the recessed and infilled trails on the profiler records, explicable either by a ploughing motion, or accretion onto the block as it rolls. It is likely that both types of motion were involved at various stages in block transport, similar to the motion of large blocks of snow through snowfields. The occurrence of the trails is confined to the broad depression, which serves as a conduit for downslope transport of blocks. Striations seen at the north-western end of ORAT-21 are probably evidence of fabrics in debris flows, which are derived from the liquidised part of the North Faeroes slide complex, or turbidity currents deposited subsequently. In either respect, deposition of the blocks and their trails postdates this emplacement, evidenced by their erosion into the surface unit, and their subsequent imprint upon the flow fabric pattern.

*OKEAN side-scan sonar mosaic from the Norwegian Basin*

The OKEAN survey was carried out simultaneously with the seismic profiling described above, and the mosaic covers completely the location of two linear depressions in the floor of the Norwegian Basin, downslope of the previously surveyed North Faeroes slide complex. Generally the imagery is of a good quality, despite numerous dropouts in the coverage due to marginal weather conditions, and displays many interesting features (Fig. 38). The

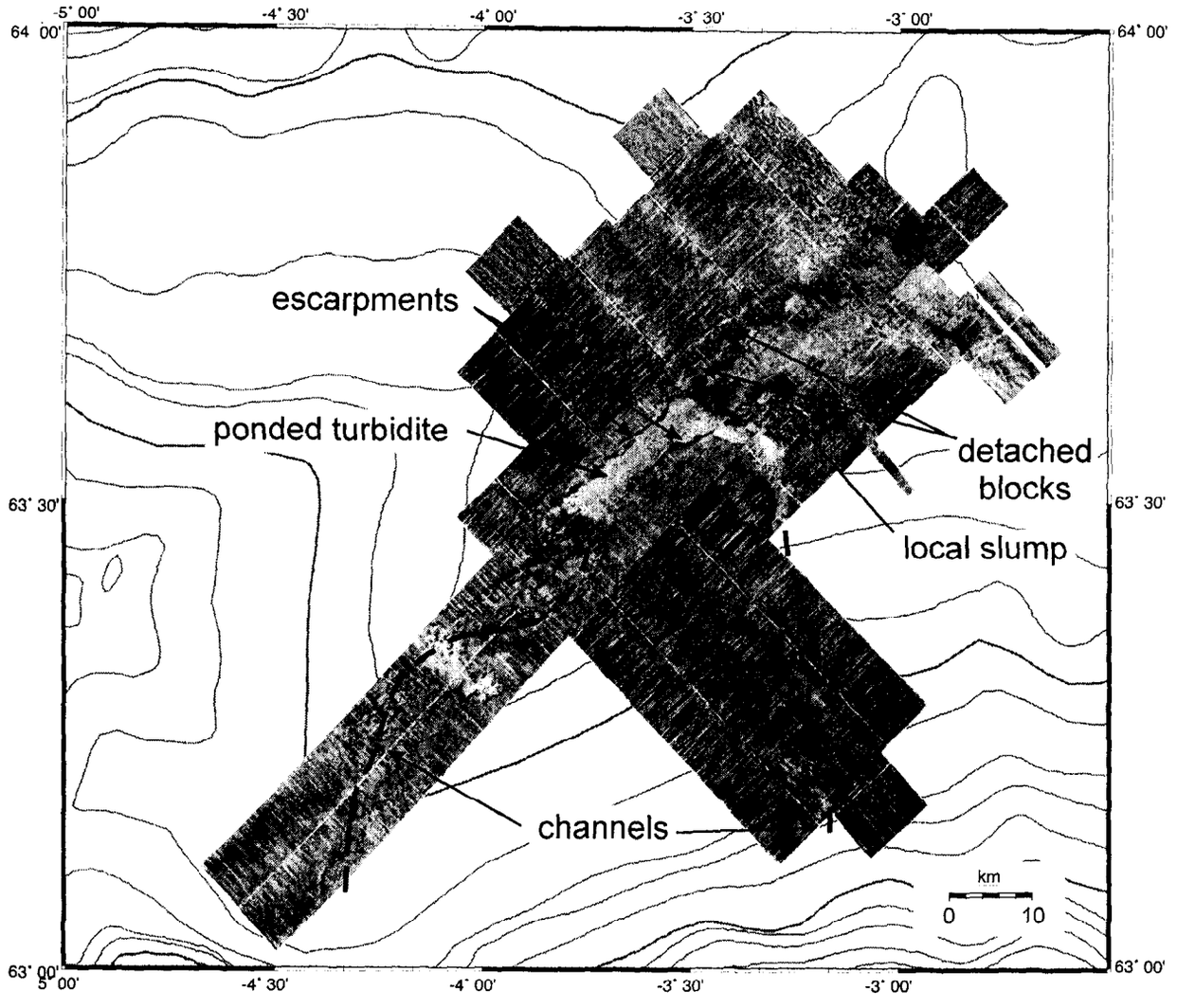


Fig. 38. OKEAN mosaic of the area of large elongate seabed depression in Norwegian Basin.

strongest feature, running through the centre of the mosaic, is an elongate, featureless south-west to north-east oriented area of very low backscatter, about 20 km in length and 5 km in width. A second, smaller elongate zone of weakly backscattering character is found further downslope, oriented similarly. This second area is 10-15 km long and 5 km wide, although there is no well defined basinward termination to enclose the depression. Both low backscatter regions are located in the deepest parts of the bathymetric feature and separated by a high, which is expressed as a narrow zone of higher, blocky backscatter on the OKEAN imagery. The elongate depressions are bound on their longest sides by narrow bands of very high backscatter, leading to regional bathymetric highs to the north-west and south-east. These highs are medium-to-high backscattering areas with an intermittently and poorly resolved rough texture, suggestive of subdued blockiness. Large oblong blocks on these surfaces, up to 1.5 km in width and 10 km in length, are often separated from the main bodies by further multiple narrow bands of high backscatter, in addition to the principal headwalls. The far north-east of the mosaic is characterised by a low-gradient area of blocky deposits, 50 - 1000 m in size (median approximately 250 m), each block being clearly defined by strongly backscattering, facing surfaces.

Immediately upslope of the two depressions, the survey region is characterised by a similar south-west to north-east orientation in bathymetry, although the OKEAN imagery is

blocky, describing a broad, curved, rough textured, high backscatter feature up to 6 km in width. Strong extensive headwalls are limited, due to the much shallower gradient of the bathymetry of the bounding areas in this region. The northeastern terminus of this blocky feature is into the southwestern end of the larger and more clearly defined low backscatter basin described above. The second channel, defined from the bathymetry, is visible clearly, up to 50 km to the east as a SSE-NNW oriented blocky linear feature, with low backscattering lateral bounding walls. The expression of this channel is much weaker than the principal channel further west. This channel also terminates in the larger low backscatter basin, although in the downslope northeastern end, just before the separating high between the two basins.

Cores taken from the southern, principal basin sampled a thick homogeneous soupy clay. Together with the low backscatter, featureless surface and level surface topography, the basin fill is interpreted as a muddy turbidite, which has become ponded within the basins. The basins may have at one point been linked, but are now separated by a high of blocky backscatter, probably a slump deposit from the regional high to the south-east. This has led to a diversion of the turbidites derived from the eastern-most channel westwards, and making this a regionally important depocentre. The margins of the channels show extensive signs of instability, with large blocks sliding and slumping from the steep lateral bounding walls. The channels themselves, outside of the two linear depressions, contain little depositional material other than large quantities of blocks, which may be derived from either the instabilities upslope, which are also the source of the turbidites, or from the channel walls. However, the low gradient of the walls in these more upslope areas suggests that the blocks are derived ultimately from further upslope. The blocky deposits at the northeastern end of the mosaic are more difficult to interpret, and may be related to either debris flow deposits from the margin of the North Sea Fan to the east, rafted material from the turbdites and instabilities upslope, or derived from the ridge to the south (Taylor et al., submitted). The lack of blocks within the depressions further upslope would tend to rule out any association with the North Faeroes slide complex, however.

### III.3.3. Bottom sampling

*G. Akhmanov, A. Stadnitskaya, E. Kozlova, A. Akhmetzhanov, P. Friend, H. De Haas, A. Sautkin, R. Brambilla, I. Belenkaya, S. Lubentsova, M. Kozachenko, I. Mardanyan*

*North Faeroes Margin*

Core TTR8-AT-104G (Fig. 39)

The 372 cm thick recovered sequence can be subdivided into two parts. The lower interval is represented by 2 m of slump-debris flow deposits, composed of numerous fragments of different shaped and sized sediments within a silty clayey, more plastic matrix. Significantly, the upper part of this interval shows a predominance of plastic deformation (the fragments can not be distinguished always easily from the matrix) and slump structures, whereas the lower part resembles a typical debrite.

The slumped interval is covered by heavily bioturbated silty clays, alternately varying in colour from olive grey to dark greyish brown, and rich in foraminifera. These reflect background hemipelagic sedimentation in the area. A tephra interval, greyish brown in colour, is observed as well. Three fine-medium grained sandy layers, up to 10 cm thick, were found, showing upward-coarsening and good sorting. They were preliminarily interpreted as contourites and imply bottom current activity affecting Upper Pleistocene sedimentation even in the headwall area of the slide scar.

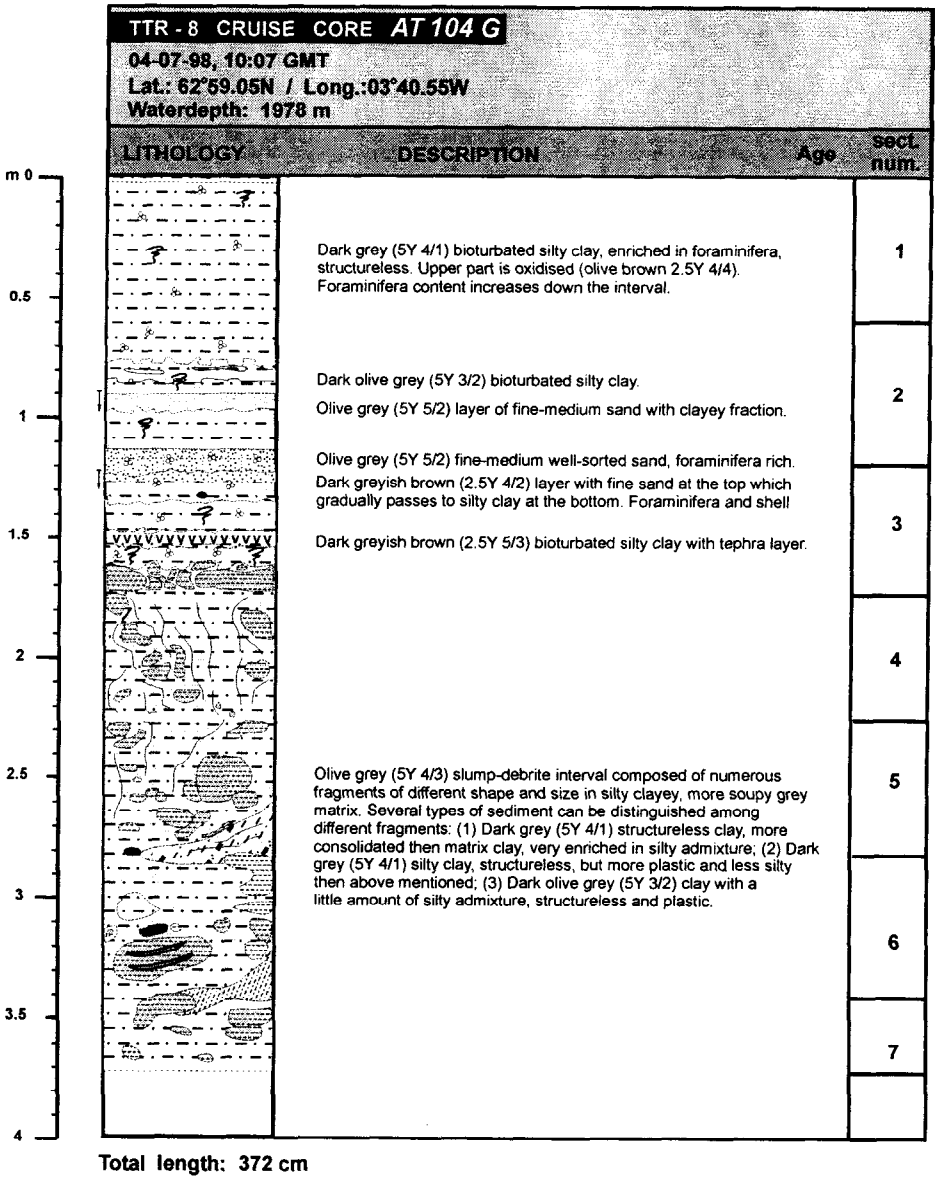


Fig. 39. Core log AT-104G.

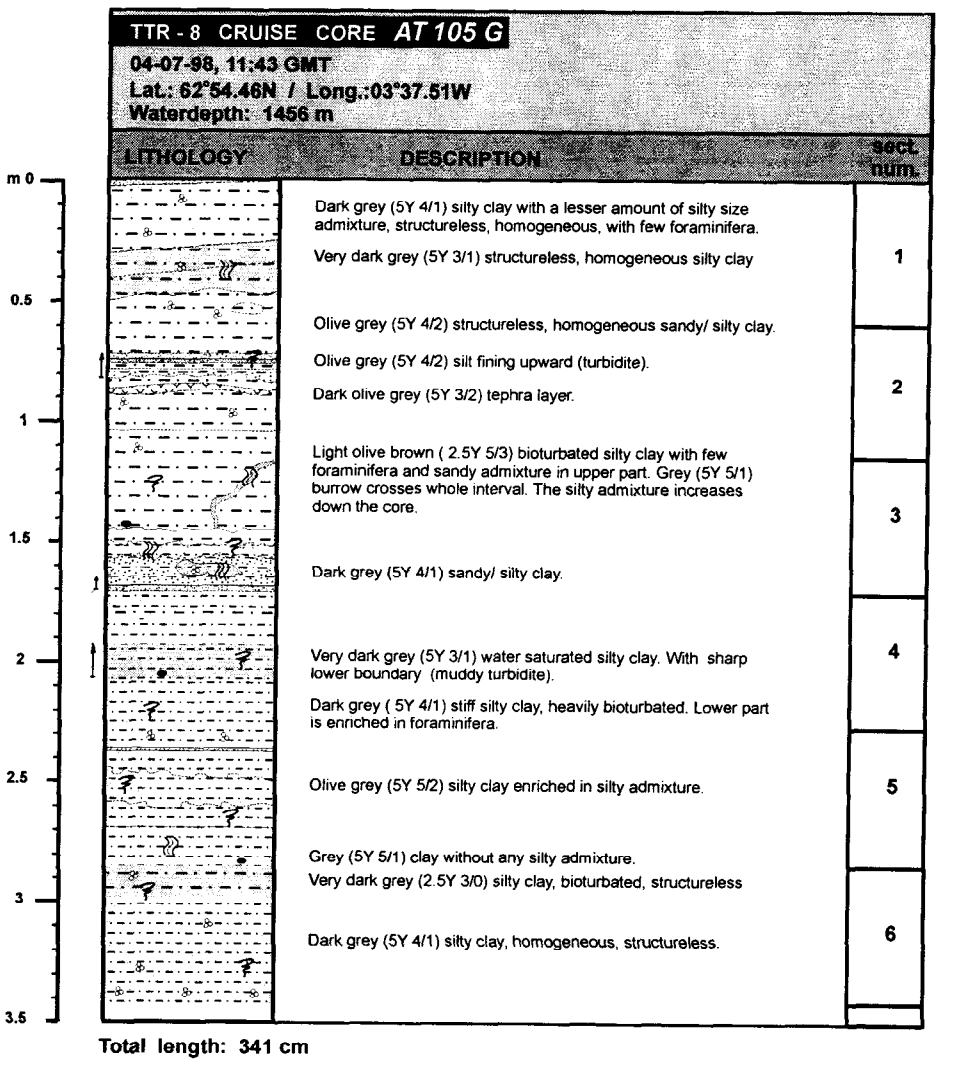


Fig. 40. Core log AT-105G.

Core TTR8-AT-105G (Fig. 40)

The core AT-105G recovered an undisturbed 341 cm succession, composed mainly of alternating bioturbated light olive grey and dark grey silty clays, together with ice-rafted material. The silty clays vary in their content of foraminfera and silty admixtures, are structureless and heavily bioturbated, and are thought to reflect background hemipelagic sedimentation during the Upper Pleistocene and Holocene. Three graded silty layers, with upwards fining, were observed in the core and are likely to be related to contour current activity in the area. A dark olive grey tephra layer was also found, within the upper part of the succession.

Core TTR8-AT-106G (Fig. 41)

The recovered 356 cm core showed basically the same lithological alternation as core AT-105G. It contained mostly bioturbated grey and dark grey silty clays, varying in foraminifera content and carbonate mineral admixture. These reflect predominant hemipelagic sedimentation in the area with rather low velocity gravity settling of material from the water column. The hemipelagic sequence is interbedded by several thin fining-upwards silty/sandy layers, suggesting periodic contour current activity. A black tephra layer, composed of well-sorted, fine, silty-sized ash, was observed at 250 cm depth and differs from that described in AT-105G.

Core TTR8-AT-107G (Fig. 42)

The core recovered a 302 cm thick alternation of grey and dark grey clays, varying in silty sized terrigenous admixture and foraminifera content. The recovery mainly reflects hemipelagic sedimentation with widespread bioturbation and a rather high input of ice-rafted material. Several possible contourite layers, composed of silty sized grains with fining-up, were described as well. Additionally, the core contained a few thin silty layers with coarsening upwards and one layer negative to positive grading. A brown tephra layer, similar to that found in core AT-105G, was observed.

Summarising the results of the bottom sampling on the North Faeroes Margin, the following conclusions can be made. The Upper Pleistocene-Holocene sequence was recovered in all four cores, implying a predominance of recent hemipelagic sedimentation strongly affected by bioturbation and supply of ice-rafted material. No evidence of recently ongoing mass-wasting processes was found in the cores, suggesting that slumping is not active presently in the area or is present only locally. A relatively thick hemipelagic cover (up to 1.5 m) has been formed after the main phase of slumping in the principal scar, and any instability in the sampled upslope area (cores AT 105G, AT 106G, and AT 107G) has not resulted in any mixing or deformation within the sediment column. Regionally important tephra layers provide a poentially useful chronological control in assessing the time-scale of events on this part of the margin. Recent hemipelagic sedimentation of silty clay has occurred with intermittent contourite deposition.

*Norwegian Basin*

Core TTR8-AT-108G (Fig. 43)

This core was taken from an elongate, linear depression, which is well-expressed on the OKEAN mosaic and seismic records, with a well-layered infill (Fig. 44). A 472 cm long recovered sedimentary sequence can be subdivided into two parts. The upper interval

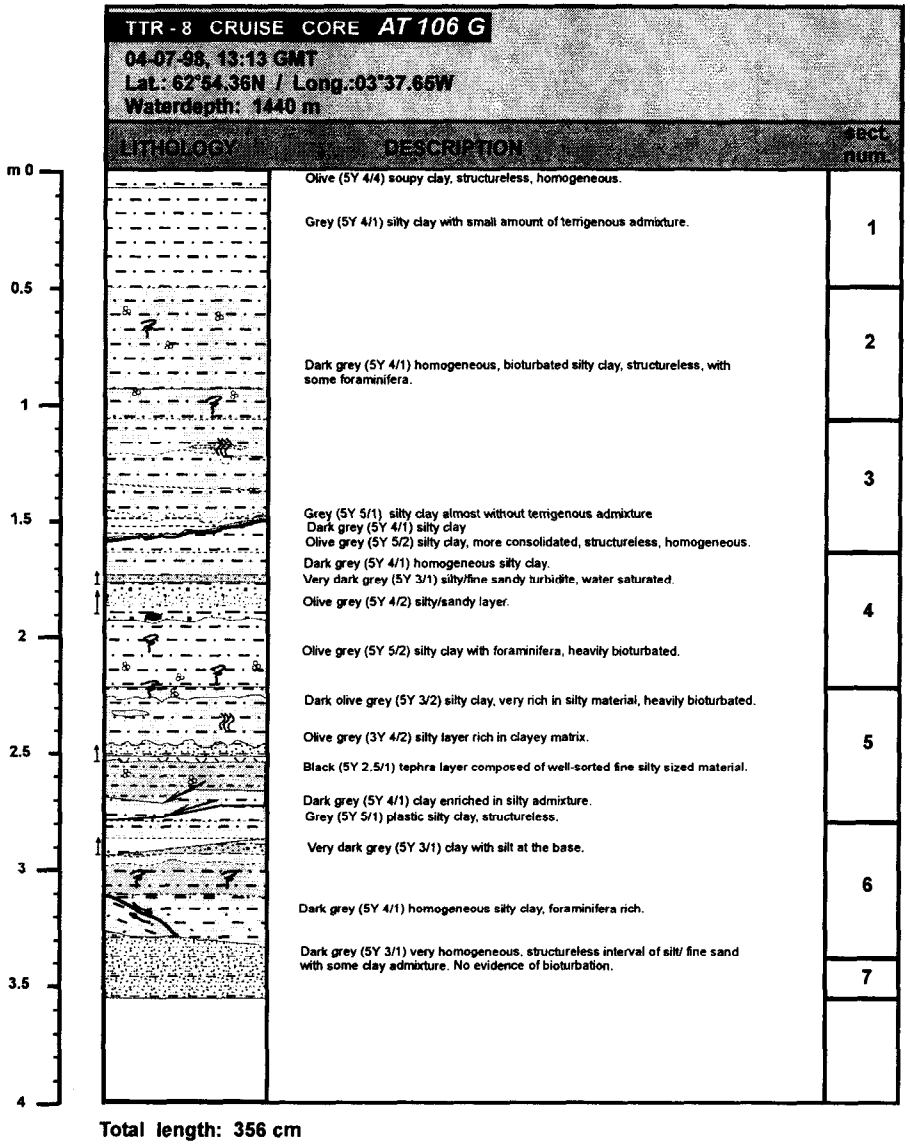


Fig. 41. Core log AT-106G.

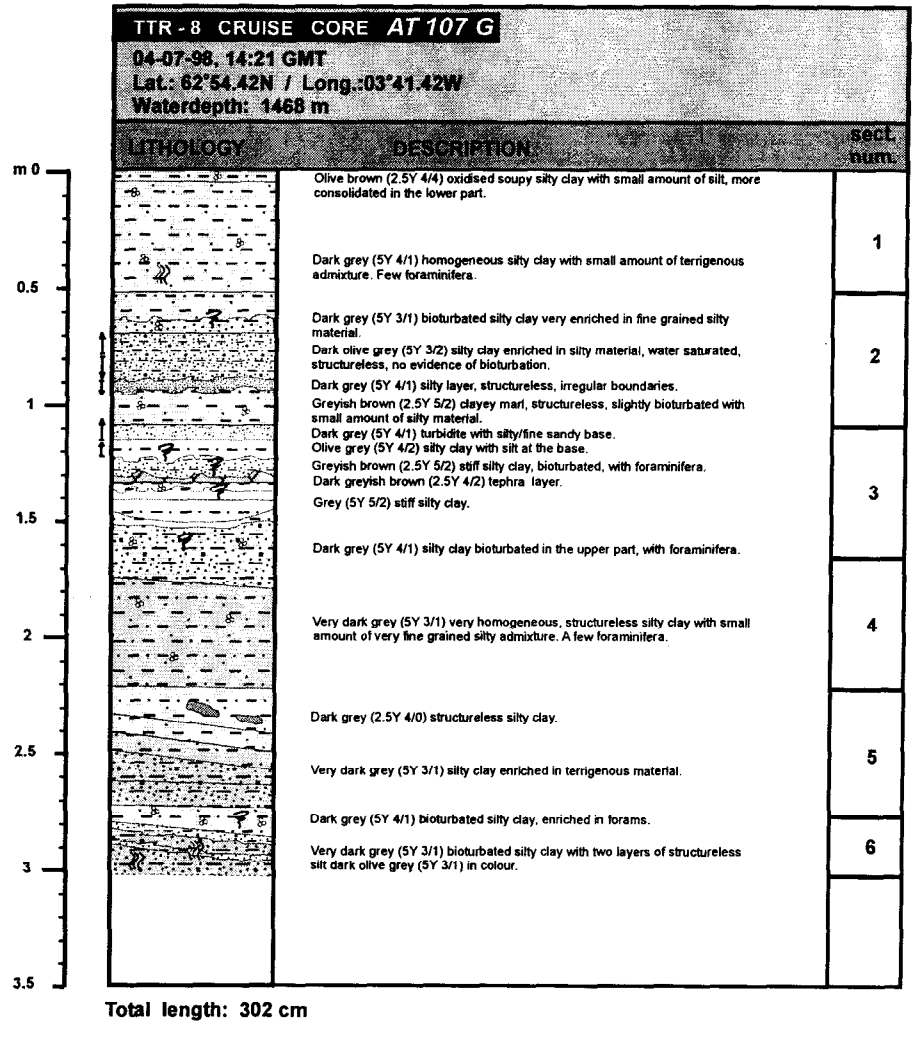


Fig. 42. Core log AT-107G.

consists of light olive brown homogeneous clay with intercalations of graded thin silty and sandy layers, implying a turbiditic genesis of the interval. The number of coarser grained turbidites increases gradually toward the top, whereas the lower part consists mainly of homogeneous and thin laminated clay, also of possible turbiditic origin. Overall, the sequence can be interpreted as a relative progradation of a turbiditic system through the Upper Pleistocene.

A 3.5 m thick interval of olive grey, very homogeneous, structureless, soupy, very fine, very well sorted clay composed the lower part of the core. The clay did not contain any coarser admixture and no bioturbation was observed throughout the interval. The homogeneous nature of this interval clearly indicates that the formation was in response to a single event. Although the lower boundary of this interval was not penetrated, and thus any genetic interpretation is purely conjecture, we are inclined to consider its deposition as an interbasinal megaturbidite deposited in the Upper Pleistocene.

Core TTR8-AT-109G (Fig. 45)

A 502 cm long core was recovered. The recovery was very similar to core AT-108G. The Upper Pleistocene succession of clayey and silty layers of turbiditic origin was underlain by a 3.5 m thick interval of very homogeneous, very well sorted, olive grey structureless clay, without evidence of bioturbation, which has been also interpreted as a megaturbidite deposit. All intervals of the core can be correlated perfectly with the sequences of core AT-108G. The only difference is that in core AT-109G, the Holocene succession, composed of light brown bioturbated clay enriched in foraminifera, is significantly thicker than in core AT-108G, suggesting sedimentation rates as high as 8 cm/ky.

Core TTR8-AT-110G

The core AT-110 was taken as a duplicate to the previous core. The core was kept in its liner, without opening and splitting, for later analyses.

The bottom sampling carred out allows characterisation of the sedimentary processes occurring within the channel sequence and elongate depressions found on the North Faeroes margin. All cores are taken in relatively close vicinity to each other and reflect a very similar sedimentation pattern and channel fill evolution.

The composition and lithology of the several metres thick homogeneous clay layer recovered in the cores probably resulted from settling of very fine-grained sediment from autosuspension. The unusual thickness of the layer (much greater than 3 m) and the consequently large volume of redeposited sediments implied (approximately 1.5 $km^3$ for the 62 $km^2$ and 15 ms TWT thick upper unit in the upslope basin alone) imply massive remobilsation of basin wall and floor sediments. Analogies from the literature suggest one of two likely origins for the deposits; the Eastern Mediterranean "homogenite" is most probably derived from sediments resuspended by a tsumani created during the Santorini eruption and caldera collapse (Kastens and Cita, 1981, Cita et al., 1996). A similar tsunami, triggered by the catastrophic slumping upslope, may have resuspended the hemipelagic material of the Norwegian Basin. However, several uninterrupted palaeoceanographic records in the region covering at least the last 120,000 years (Kellogg, 1980, Rasmussen et al., 1996a, b, c,) argue against such an interpretation. A second analogy is provided by massive homogenites described by Rothwell and Weaver (1994); here, massive homogenites are thought to have formed by the ponding of low-concentration turbidity currents in confined basins, where the incoming tails of turbidity currents increase in concentration to change to a muddy debris flow, which then freezes. Alternatively, the sequence may just represent the upper section of a massive turbidite associated with massive liquification of sediments derived from the North Faeroes slide complex, located directly upslope.

All cores are covered by an Upper Pleistocene, finely laminated turbiditic sequence. This is replaced by prevalent hemipelagic settling during the Holocene, reflecting the onset of a period of relative stability higher on the margin.

## III. 4. RESULTS AND PRELIMINARY CONCLUSIONS

*T. Nielsen, A. Kuijpers, M. Ivanov*

*Eastern Faeroes Margin*

The extent of a major slump complex is determined on the basis of mapping from airgun seismic data. It is concluded that these slump deposits originate from the (upper) Faeroes slope of the Faeroe-Shetland Channel. Seismo-stratigraphic analysis of the seismic sections from the channel and the presence of a large trough cut into a presumably Pliocene sedimentary sequence, observed in the seismic records on the nearby shelf, suggest a Late Pliocene or, more likely, Quaternary age for the slump complex. In addition, evidence has been found for repeated slumping having occurred also in the latest part of the Quaternary. The extent and morphology of the latter slump deposits are determined by high-resolution (100 kHz) side-scan sonar and subbottom profiling; the nature of the slump deposits is determined by sediment coring.

Both the subbottom profiler records and the sediment cores indicate a late glacial age for the last slumping event. Since the beginning of the Holocene, increasing NSOW contour current activity at mid-slope depth (500-600 m) has resulted in the deposition of an up to 1.5 m thick contourite covering the slump deposits downslope. These Holocene contourites thin towards the basin floor, where slump deposits are near or at the seabed.

*North Faeroes Margin*

Two targets were examined using deep towed high-resolution (100 kHz) side-scan sonar. The first target area lies upslope of the main slide headwall, and the second target area lies basinward of the main slide headwall and deposits. On TOBI side-scan sonar records, the upslope area shows a wavy backscatter pattern. The downslope target is characterised on TOBI imagery by the presence of extremely numerous basinward-trending trails, with the occasional presence of a small block at the end of a trail.

Based on results from our present study, we can conclude that the wavy backscatter pattern seen on TOBI side-scan sonar records can be attributed to disruption of superficial sediment layers by shallow sliding. This is confirmed by subbottom profiling data showing regularly parallel laminated sediments outside the deformation area, and acoustic evidence of slumping within the area. The entire sequence of failure, from initial ductile deformation through to debris flow development, is imaged in the single line.

Sediment cores, taken from within this upslope slide-slump area and downslope of the major headwall, indicate widespread failure activity during the Late Weichselian. Hemipelagic and contourite deposition are seen to prevail since the beginning of the Holocene.

The high-resolution sonographs of the area downslope of the main headwall demonstrate the presence of a swarm of erosive trails, some of them with a block at the end. The records clearly show that most trails are concentrated within a shallow depression. The trails originally eroded to a depth of several meters below the surrounding seabed, but these

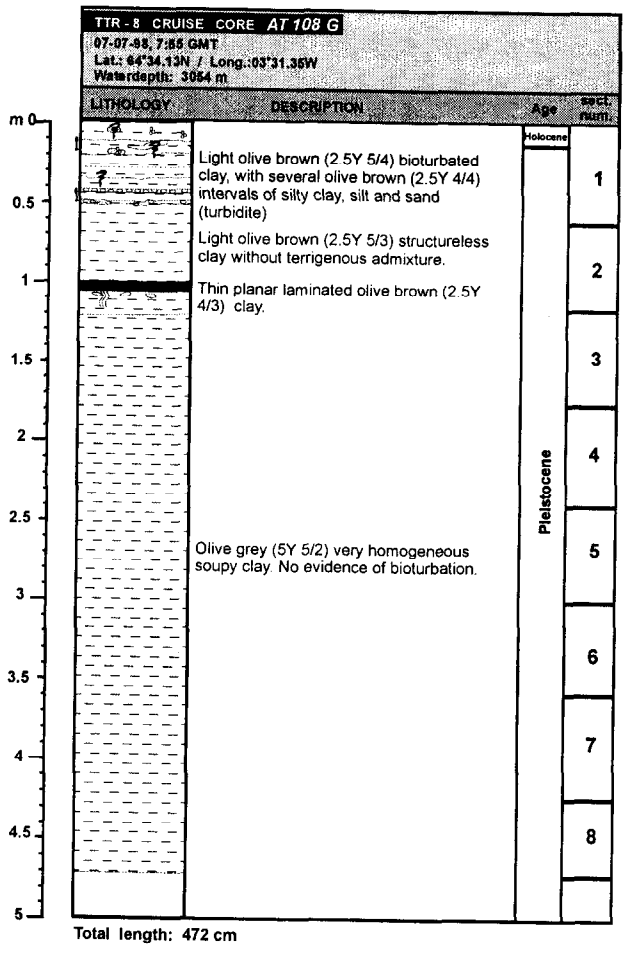


Fig. 43. Core log AT-108G

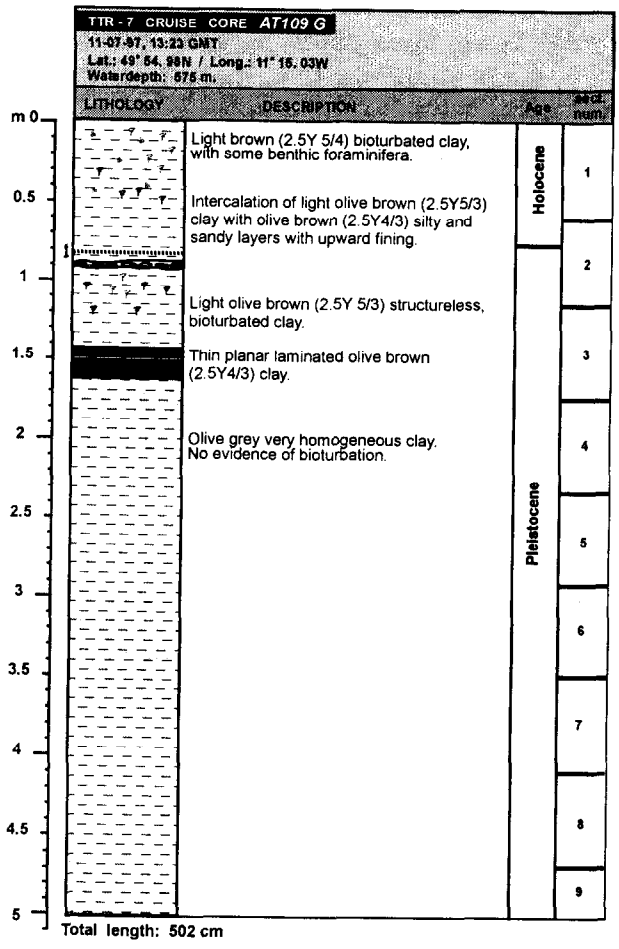


Fig. 45. Core log AT-109G.

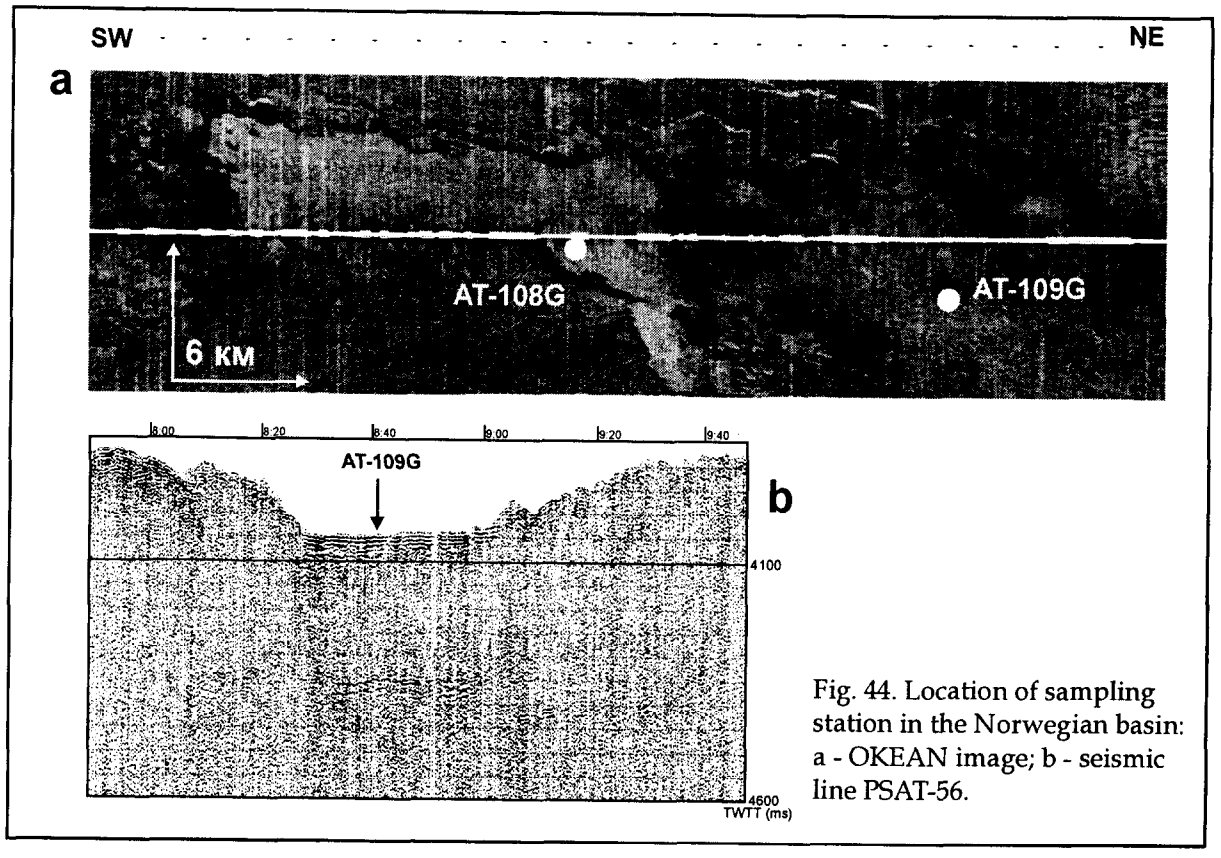


Fig. 44. Location of sampling station in the Norwegian basin: a - OKEAN image; b - seismic line PSAT-56.

grooves have been partly filled subsequently with sediments of presumably Holocene age. Blocks are apparently elongate, oriented across the principal axis of the trail, and 30 to 50 m in length. Blocks have a height of 18 to 20 m. The orientation of the blocks, the extensive runout distances, their erosive nature, and the absence of any sediment build-up before the blocks argue for an accretionary, rolling action, athough an element of sliding can not be excluded. The block trails represent the final stage of sedimentation processes associated with the North Faeroes slide complex, evidenced from their postdating the debris flow and turbidite material beneath.

*Norwegian Basin*

The Norwegian Basin, downslope of the North Faeroes slide complex, is dominated by a channel complex, clearly expressed in bathymetry, seismic records, and OKEAN side-scan sonar imagery. The downslope expression of the channel consists of a sequence of acoustically transparent and low backscattering muddy turbidites held within two principal basins, derived from two relatively poorly defined channels filled with blocky deposits. The margins of the basins are characterised by sliding instabilities of the bounding regional highs, themselves relatively highly backscattering areas of subdued blockiness. Seismic data suggest that the morphology of the basins and channels are tectonically controlled, and the bounding highs are themselves interpreted as slump deposits.

Thus the most recent episodes of deposition in this area are related largely to repeated episodes of large-scale failure and its associated deposits; the basin-fill turbidite sequence is the most recent deposit, derived from channels associated with the more recent elements of the North Faeroes slide complex. These turbidites have variously interacted with local instabilities generated within the basins. The last turbiditic emplacement predates a regionally extensive tephra layer, probably that described by Rasmussen et al. (1996a, b, c), fixing deposition at Late Weichselian. The bounding highs, forming the basins, are themselves earlier large-scale slump deposits, which appear to accentuate an underlying, tectonically controlled depositional sequence, itself at least partly composed of tectonically-driven margin instability deposits. The most downslope blocky deposits in the mosaic are probably interacting turbidites and debris flow material, derived from the North Sea Fan to the east.

# IV. NORWEGIAN MARGIN

## IV.1. INTRODUCTION

There are a number of papers on the Vøring Plateau geology and on the Storegga Slide in particular (e.g. Bugge et al., 1987, Evans et al., 1996, Mienert et al., 1998). The length of the slide is more than 800 km and the total volume of the early Tertiary-Quaternary sediments involved in sliding is about 6000 km$^3$. The slide is estimated to have been active on several occasions, with the latest occurring 7000 years ago (Dawson et al., 1988). The causes of sliding include decomposition of gas hydrate layers. The presence of gas hydrates is suspected from seismic records, which show a bottom simulating reflector (BSR) in the vicinity of the main scarp of the Storegga Slide (Bugge et al., 1987, Mienert et al., 1998). Beside BSR's there are many other evidences of increased fluid activity in the area. Evans et al. (1996) described fields of pockmarks on the southern edge of Vøring Plateau adjacent to the Storegga Slide. The area was also recognised by the presence of mud diapirs and possibly mud volcanoes (Mienert et al., 1998). One of the main tasks of the third leg of the TTR-8 cruise in this area was to conduct detailed investigations of these structures with different side-scan sonar tools, an underwater video recording system, and to obtain bottom samples from the places of potential fluid escape. Analysis of gas composition from such samples would show what gases were involved.

On the northeastern part of the Vøring Plateau, in the Vema Dome area, previous workers had described several fields of diapir-like structures expressed in the seabed topography (Hjelstuen et al., 1997, Hovland et al., 1998). These structures are normally found above structural highs composed mainly of Cretaceous rocks. The highs are covered by a thick cover of Tertiary and Quaternary, the accumulation of which was affected by the increased input of terrigenous material during glacial/interglacial stages in the Late Pliocene-Pleistocene. In the upper part of the sedimentary cover seismic studies revealed the presence of lens-like acoustically transparent bodies. They were either buried or exposed at the surface, forming the above mentioned fields. DSDP borehole 339/340 recovered from one such diapir a sequence of redeposited, Eocene highly ductile siliceous oozes (Talwani et al., 1976). It is believed that these oozes were squeezed out by the pressure of the overlying thick sedimentary package, along faults formed by movements of uplifted blocks of the basement. Detailed study of these diapir fields with side-scan sonars would allow better understanding of their morphology and also could localise the places of fluid escape that are often associated with mud diapirism (Ivanov et al., 1996, Limonov et al., 1997).

Investigations with side-scan sonar equipment, conducted in the area of the Bear Island Trough by the Naval Research Laboratory (USA) in 1989, mapped two circular features which were interpreted as mud diapirs. Expeditions by R/V *Haakon Mosby* in 1995 and by R/V *Professor Logachev* in 1996 discovered that one of the features is a mud volcano with an associated field of gas hydrates and increased heat flow. The mud volcano was named Haakon Mosby (Vogt et al., 1997). It is a circular structure up to 1.5 km in diameter and with a height above the seafloor of 7-15 m. The crater of the mud volcano is a flat area about 200 m in diameter. Mud flows running out from the crater can be traced for more than 3 km. The crater is also characterised by an increase in the temperature of the sediments (up to 15°C).

The mud volcano is located in front of the Bear Island Trough within the continent-ocean transitional zone of the continental margin. The oceanic crust in the area is of Miocene-Pliocene age. The thickness of the sedimentary sequence varies from 4 to 6 km and its age ranges from Eocene to Recent. The pre-glacial Eocene-Pliocene part of the sequence is composed mainly of clastic deposits derived from the adjacent elevated volcanic provinces.

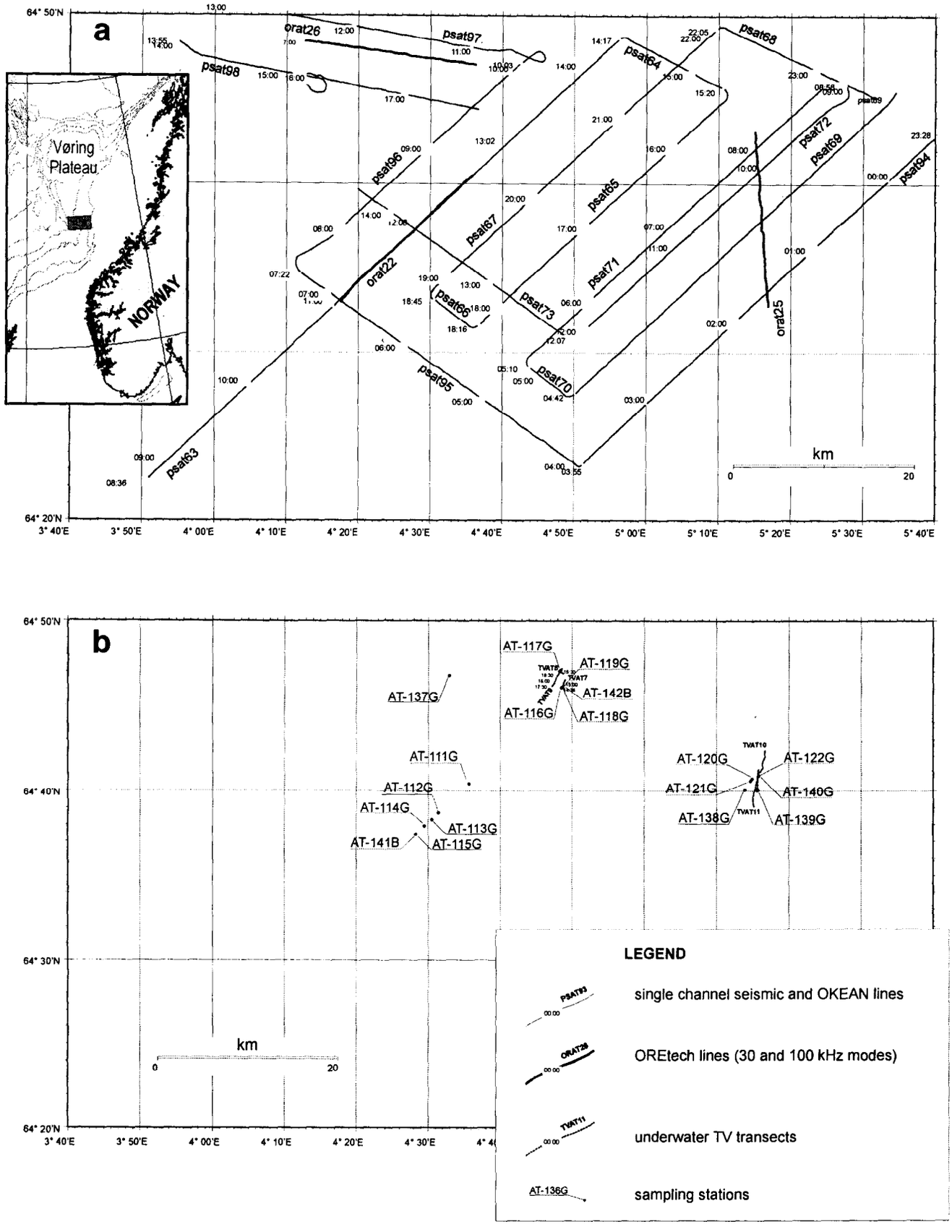


Fig. 46. Location map of the southern Vøring Plateau

The Pliocene-Pleistocene glacial terrigenous sequence can be divided into glacial and glaciofluvial units. The latter have been deposited within the last 2.3 millions years and comprises about 50 -70% of the whole sedimentary succession. The Haakon Mosby mud volcano (HMMV) is located in the area where the thickness of the sedimentary cover is about 3-4 km.

During the third leg it was planned to conduct additional seismic and acoustic investigations in the area of HMMV in order to find and map similar structures and places of possible fluid escape.

## IV.2. SOUTHERN VØRING PLATEAU

### IV.2.1. Seismic profiling data

*S. Bouriak, B. De Mol, M. Baturin and E. Yakovlev*

The aim of the seismic and OKEAN side-scan sonar survey was to map gas related features near the Storegga Slide.

The survey grid consists of sixteen lines with a total length about 430 km (Fig. 46). The lines were run in a SW-NE direction, along the continental slope (PSAT 63, 65, 67, 69, 71, 72, 94, 96) and are connected by four shorter lines (PSAT 64, 66, 68, and 70) and one long line (PSAT 95). Two long lines were run transverse to the main trend. Line PSAT 73 crosses lines PSAT 63, 65, 67, and 70 and line PSAT 95 crosses PSAT 63. Two other lines (PSAT 97 and 98) begin from PSAT 96 and have an orientation to WNW. The water depths in the study area vary between 600 and 2000 meters (PSAT 63). The acoustic penetration achieved was up to 1000 ms TWT.

Seven seismic units can be distinguished on the profiles (Fig. 47). Along the main scarp of the Storegga slide units 3-6 are truncated and are overlaid by unit 7. All units are dipping to the SSE, generally parallel with the surface slope.

Unit 1 forms the acoustic basement with a chaotic internal structure. The top of the unit is a smooth reflector with medium amplitude, which is found all over the study area except in the places where it lies below the penetration depth.

Unit 2 also has a broad distribution and shows a chaotic pattern of internal reflectors, although in some places few continuous reflectors are seen. It has a smooth top in the Vøring Plateau area and is uneven and discrete within the Storegga Slide. In the north-east the unit lies below the penetration depth. The observed thickness of the unit is 150-200 msec.

Unit 3 is composed of a set of continuous parallel reflectors of low amplitude. In some places a significantly increased amplitude of the signal is observed, forming "bright spot" acoustic anomalies. This suggests the presence of free gas in sediments (McQuillin et al., 1984). In the vicinity of the Vøring Plateau edge, the "bright spots" are truncated by a reflector with inverse polarity, which roughly follows the seabed topography and intersects the internal reflectors of the unit (BSR). This reflector was interpreted as a possible lower boundary of a gas hydrate layer. In the northern part of the studied area the unit is disturbed by the presence of acoustically transparent narrow vertical zones crossing the whole sedimentary succession and interpreted as clay diapirs. One such structure is observed on the line PSAT-72, where it crops out and appears as a dome-like feature (Fig. 48).

These transparent zones still can be traced within unit 2 but below that the limit of acoustic penetration prevents observations of where they are rooted.

Unit 4 also displays moderate amplitude, parallel, continuous reflectors with minor internal discontinuities. A prominent high-amplitude reflector traced over the whole study area represents the top of the unit. In the northern part of the area the unit contains 'bright

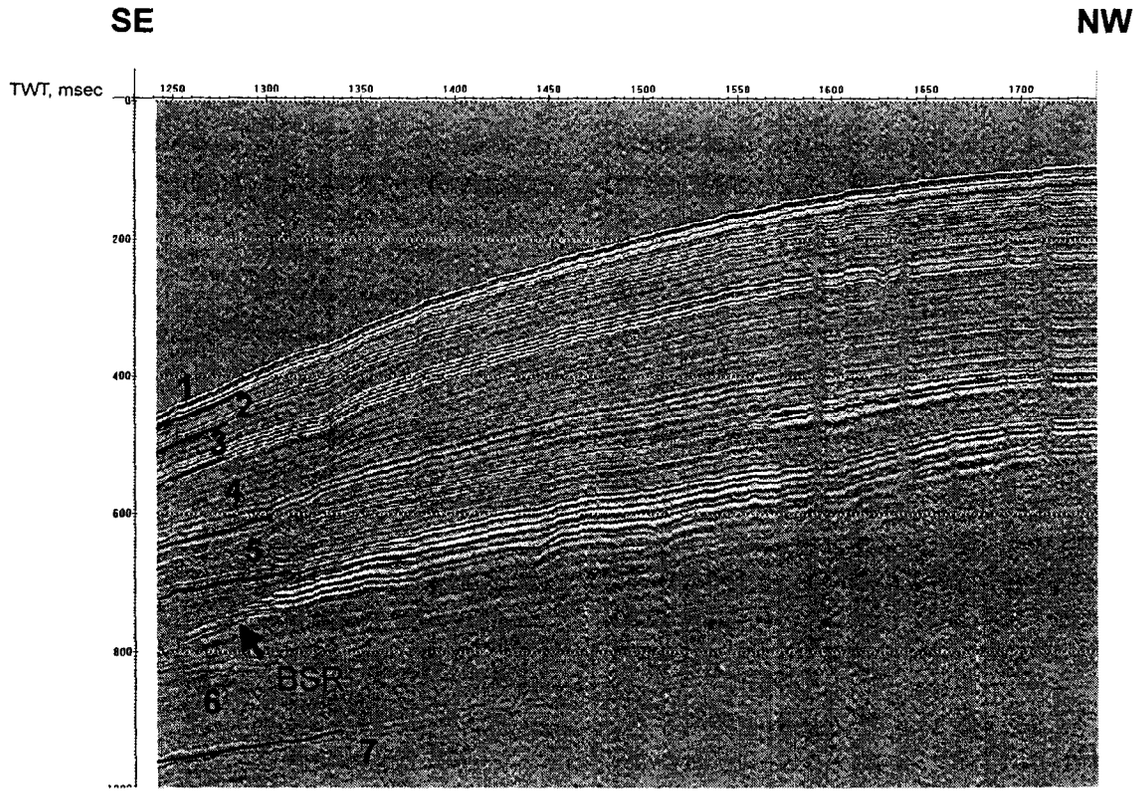


Fig. 47. Fragment of seismic line PSAT-63 with the main seismic units (1-7) indicated.

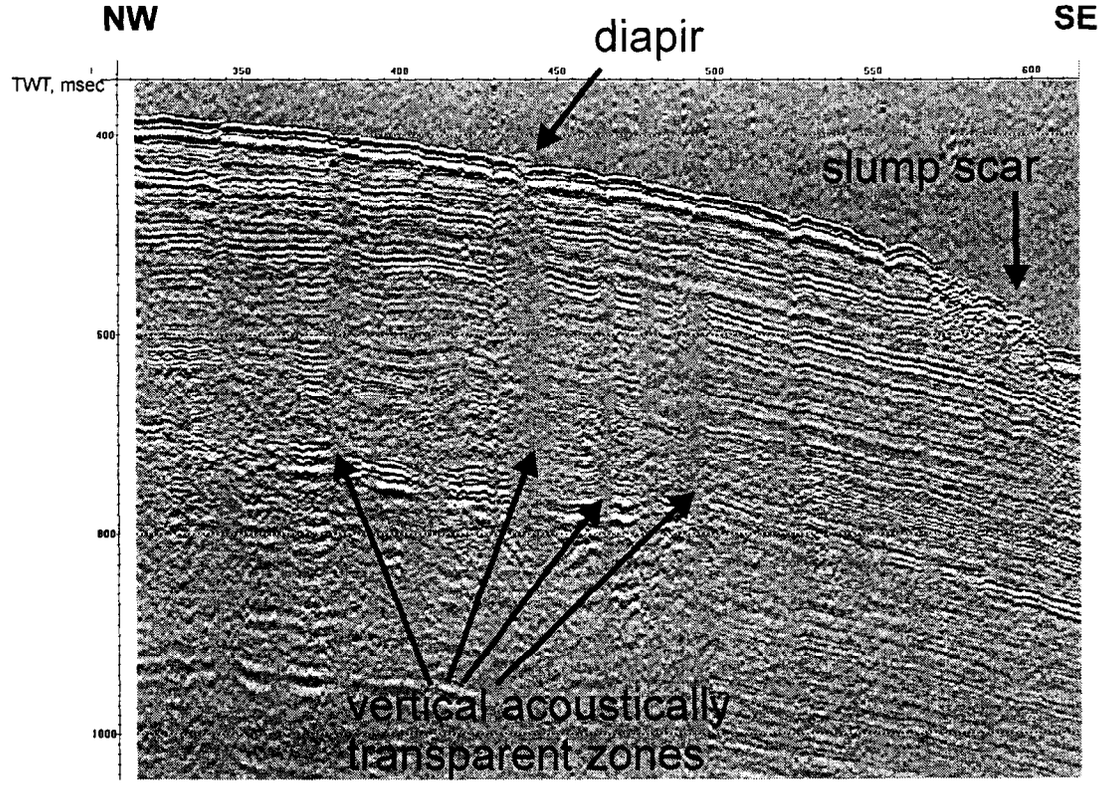


Fig. 48. Fragment of seismic line PSAT-72 showing a group of closely spaced clay diapirs, one of which crops out at the surface.

spot' acoustic anomalies, probably related with free gas and the presence of gas hydrates is also suspected within the overlying unit.

Units 5 and 6 have a similar appearance and display a well-layered pattern of numerous parallel events of moderate to high amplitude. The units are separated by a strong reflector traced over the whole study area.

Unit 7 is found only within the Storegga Slide and is an acoustically transparent package up to 150 msec thick.

### IV.2.2. Side-Scan Sonar Data

*A.Wheeler, A. Akhmetzhanov, B.De Mol, M. Ivanov*

*Description of OKEAN long-range 10kHz side-scan sonograph mosaic from the Storegga Slide area*

The OKEAN long-range side-scan sonograph mosaic from the Storegga Slide area (Fig. 49) has two acoustic facies. One is of uniform low backscatter and the other is of patterned high backscatter separated by a curvilinear boundary.

The area of the uniform low backscatter acoustic facies occupies the northerly portion of the mosaic and is relatively featureless. The character of the subbottom profiler image implies an area of thin hemipelagic sedimentation of probable contouritic origin. This uniform cover does, however, contain clusters of small areas of high backscatter. These have an average diameter of 200m, are elongate and usually ovate in form. The subbottom profile shows these to be shallow depressions above locally disturbed sediment. They have been interpreted as pockmarks, a hypothesis supported by bottom sampling, deep-towed video, and seismic data. Three clusters of possible pockmarks are seen, two of which occur on the northern-most portion of the sonograph mosaic. One defines a broad area, trending approximately east-west, in which 27 individual pockmarks have been identified (Area 1). The other area (Area 2) has a greater density of pockmarks with some 29 or so identified pockmarks. To the southeast from these areas there is another group (Area 3) which is the smallest one. Two gravity cores were taken on these features, which clearly show evidence of gas saturated sediments. On the subbottom profiler record and seismic line PSAT-71 it seems likely that the southernmost feature of this area (64° 40'N, 5° 14'E) can be interpreted as a mud volcano.

Other features that are evident in the area of the uniform low backscatter acoustic facies are two lineations of high backscatter. Both of these occur near to the boundary of the two acoustic facies with the longest of them cutting this boundary. On the subbottom profiler record, these lineations are identified as small scarps with topographic relief and represent the limit of minor slides which may potentially generate into major slide events. The shortest of these lineations (64° 35'N / 4° 42'E to 64° 34'N / 4° 45'E) trends NW-SE parallel to the boundary between the two acoustic facies and has a curvilinear form. The larger of these lineations trends E-W, is again curvilinear and runs from 64° 36'N / 4° 32'E to 64° 33'N / 4° 56'E, cutting the boundary at 64° 33'N / 4° 43'E. South of the largest of these lineations, and east of where the lineation cuts the boundary, is an area of very low backscatter. This is interpreted as a probable partially collapsed terrace block.

The boundary between the two acoustic facies can be traced from 64° 39'N / 4° 25'E to 64° 37'N / 5° 17'E. The boundary initially trends NW-SE from 64° 39'N / 4° 25'E before turning more than 90 ° to the NE at 64° 32'N / 4° 55'E. This north-easterly trend becomes an E-W trend at 64° 38'N / 5° 04'E. The boundary has a curvilinear form, becoming sinuous in the area with an E-W trend. The subbottom profiler records shows this is the top of a major slump scarp, with sediments up-slope (low backscatter facies) being undisturbed and sediments down-slope (high backscatter facies) being slumped deposits. The curvilinear

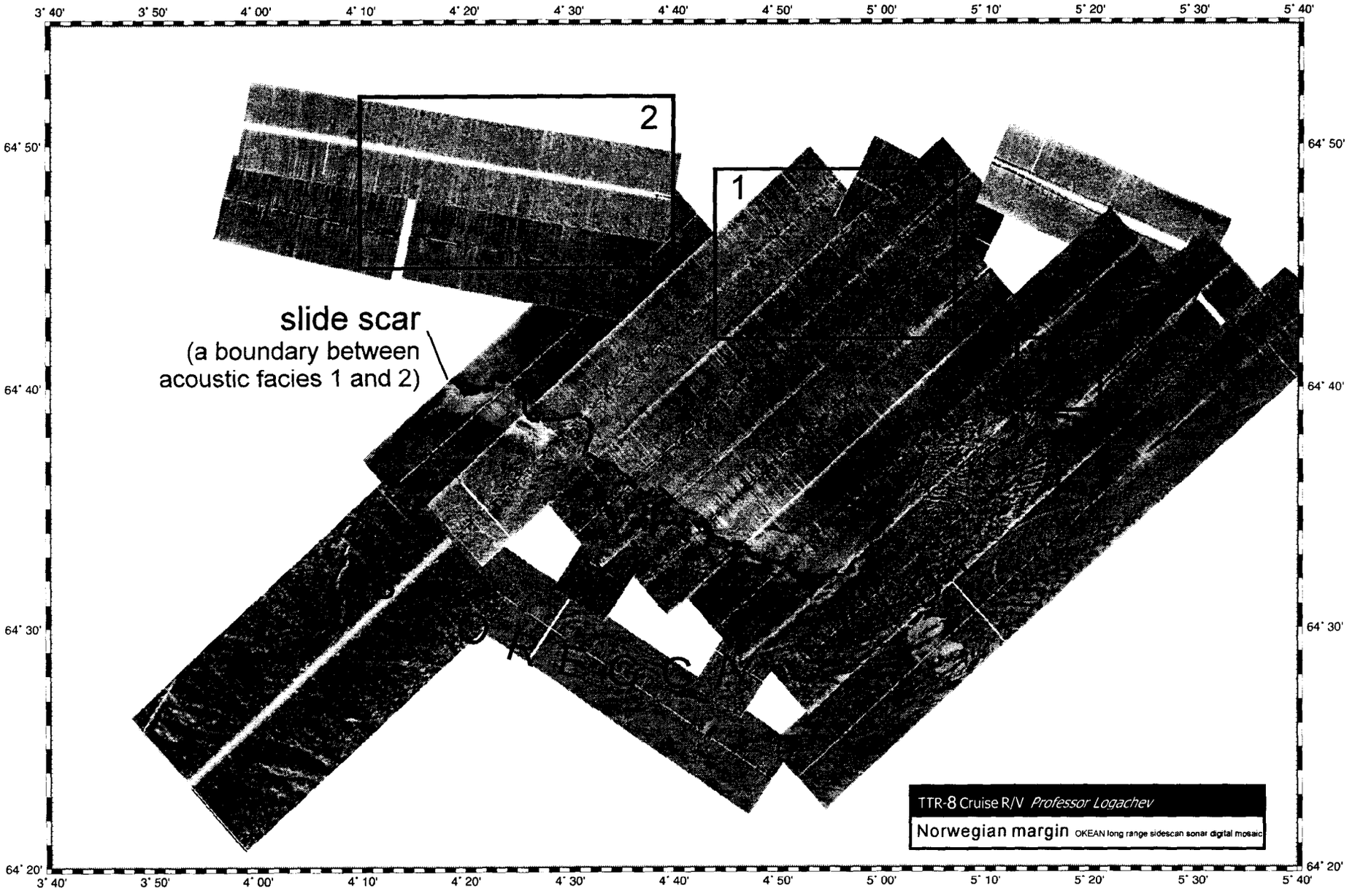


Fig. 49. OKEAN mosaic of the southern Voring Plateau in the vicinity of the Storegga Slide. Rectangles show main areas of pockmark/diapir occurrence discussed in the text.

nature of the boundary is probably due to indentations made by individual slides. The change in trend of the boundary, from NW-SE to SW-NE, indicates a major retreat of the slide scarp and possibly a more recent failure. This interpretation is supported by an increase in sinuosity at the head of this inferred retreated portion of the scarp and by the more clear pattern of the slump deposits.

The southern portion of the mosaic has a patterned high backscatter acoustic facies best seen in the area of inferred recent failure (64° 34'N to 64° 39'N and 5° 02'E to 5° 17'E), where it has alterating curvilinear and coalescing hands of high and low backscatter generating a "zebra-like" pattern. These have been interpreted as tension-cracking in the upper part of the slide, running perpendicular to the slump direction. An analysis of boundaries between sets of patterns shows three main slump bodies whose origins are also expressed as a marked indentation in the major slump scarp. The eastern-most slump body initially slides to the south and then gently changes trajectory to the south-west. The western slump initially moved to the west and joins another slump which is sliding north-west. The amalgamated western slumps also join the eastern slump further downslope. A relic of a former slide is preserved between the two sides. Further downslope, beyond where the two slides have joined, the surface topography of the slides becomes gradationally less distinct, probably due to a poorer expression of tension cracks. Along the major slump scarp, lineations of high backscatter, sub-parallel to the major scarp, are evident. These are interpreted as minor scarps and confirmed as topographic features on the subbottom profiler record. The tops of these scarps often exhibit low backscatter and are interpreted as slumped blocks.

The southwestern portion of the high backscatter acoustic facies has a chaotic pattern, probably due to a high degree of surface roughness on the inferred older slumped surfaces. On the south-westernmost portion of the mosaic a different irregular pattern of high backscatter is expressed, suggesting the presence of approximately east-west trending ridges of larger dimensions than previously discussed, being approximately 2 km between ridge crests. These are best expressed at the start of the line between 64° 23'N to 64° 27'N and 3° 48'E to 4° 12'E, where they have sub-parallel and curvilinear forms. The lineations have been interpreted as push-up ridges associated with slumping. A different lineation of high backscatter is also evident between 64° 34'N / 4° 09'E and 64° 28'N to 4° 17'E and is tongue-shaped, pointing downslope to the southwest. The subbottom profiler record suggests that this is a minor scarp.

*ORAT-22*

OREtech line 22 was intended to investigate in detail a depression located on the edge of the Storegga Slide. The image shows a sub-circular feature about 2.5 km in diameter, infilled with collapsed sediments. According to one of our initial interpretations the presence of a mud volcano was suspected within this structure.

5.5 hours of survey, with the instrument operating at frequency of 100 kHz, were carried out along a line oriented SW-NE across the depression (Fig. 50). Generally, the sonograph and subbottom profiler record show two types of acoustic backscatter pattern, one of which is characteristic of undisturbed hemipelagic sediments and the other one indicative of the presence of sediment failure deposits. The latter are more common.

From 1:10 to 2:40 the average backscatter level is medium to high and the backscatter variations are due to the very irregular topography. At the start of the line (1:10-1:30) high backscatter seabed is found. The seafloor is generally flat although it has some small-scale roughness. From 1:30 the backscatter level becomes weaker but a tongue-shaped pattern of high backscatter ridges is seen. The ridges are about 100 m wide and they are 5-8 m high with gentle slopes. They are interpreted as pressure ridges occurring at the edge of a debris

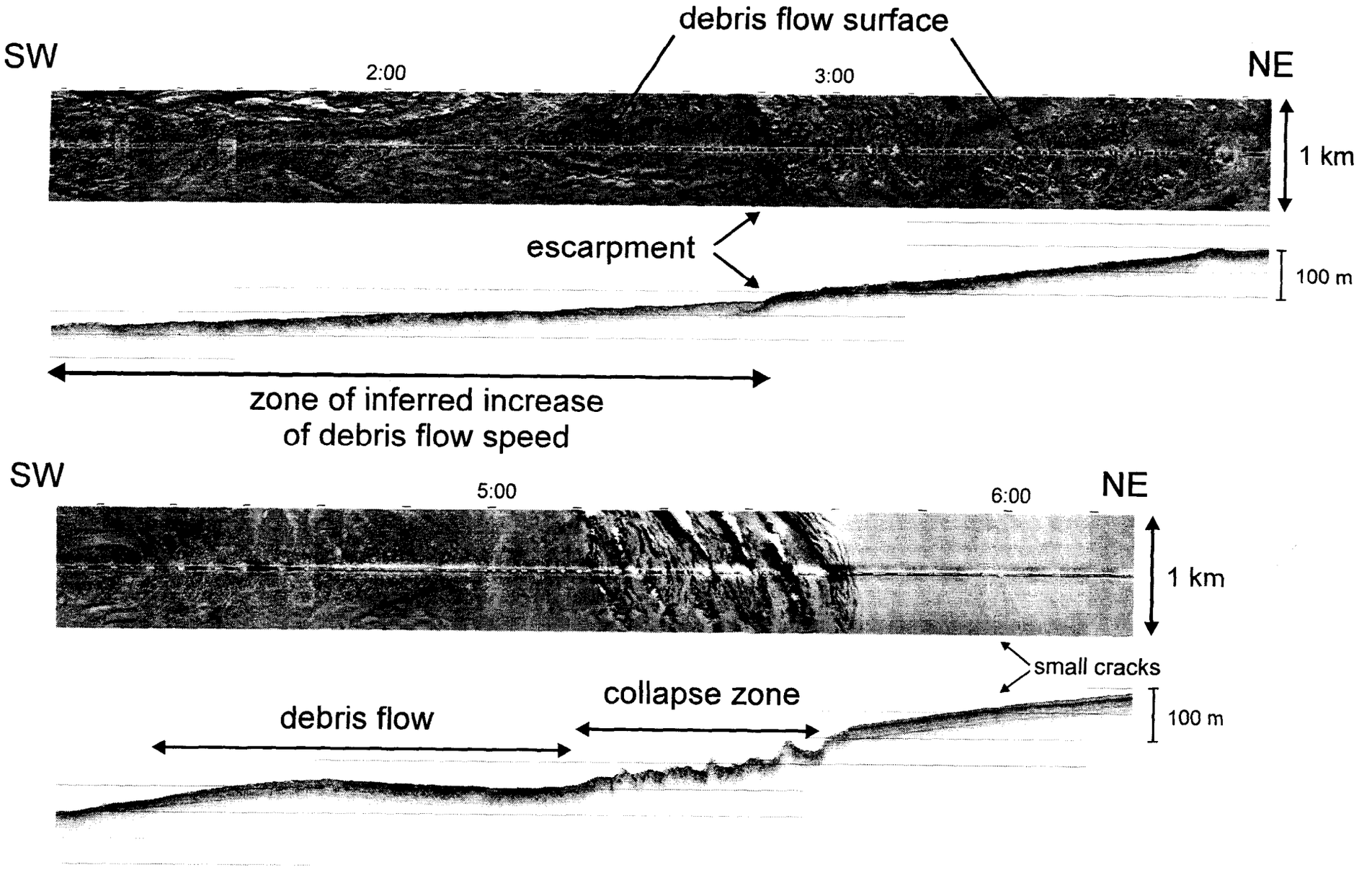


Fig. 50. Fragments of ORAT-22 sonograph and subbottom profiler record across a collapse structure at the edge of the Storegga Slide.

flow. The flow surface is also decorated with a pattern of lineations, probably resulting from lateral shear stress, which emphasises the flow structure. The sonograph also shows several rafted blocks, which are carried by the flow. From 2:40, just above a 10 m high escarpment seen on the profiler record, the backscatter pattern changes as the tongue-shaped pattern disappears. The moderate backscattering seabed is relatively flat but there are several irregularly shaped areas of high backscatter where particularly rough topography is inferred. These areas are interpreted as accumulations of rafted blocks transported by the debris flow. They can be up to 250 in diameter and have a thickness of 5-10 m. The subbottom profiler shows that there is a chaotic unit in the uppermost part of the sedimentary section, which overlies well-stratified sediments below without significant erosion. This unit thins upslope and pinches out at approximately 4:15. The change in the character of the upper surface of the debris flow is believed to be due to the presence of the increased slope gradient, which might have caused the flow's acceleration when the later was passing over the escarpment seen at 2:40. From 4:20 till 5:10 the seafloor is again smooth and has a slightly weaker backscatter level. Numerous small low backscatter spots and patches are seen on the sonograph throughout this part of the record. This pattern corresponds to a chaotic, lens-shaped uppermost unit imaged by the subbottom profiler. This unit overlies well-stratified sediments and thickens to the northeast. It is likely that another debris flow is imaged in this part of the line. The underlying stratified sediments form a gentle anticline with its crest seen at 4:40 where it is disturbed by small-scale grabens. The bedded sequence then dips down to the northeast. From 5:10 to 5:40 ORAT-22 crosses the collapse depression which is imaged on the sonograph as a serious of well-expressed, highly backscattering slide scars. The subbottom profiler record shows that this zone has a very rough topography and is formed by several tilted and displaced blocks resulting from the failure of the upslope stratified sediments. Most of the blocks have undisturbed internal structure. This collapse depression is thought to be a source of the debris flow found immediately to the southwest from the base of the depression. The debris flow can be traced for at least 3. 5 km. The northeastern edge of the collapse depression is characterised by the presence of a zone of crown cracks about 200 m wide and from them, till the end of the line (5:40-6:40) a smooth, weakly backscattering seafloor is imaged. The subbottom profiler record shows a well-stratified succession with a prominent, highly reflective event lying approximately 7.5 m below the seafloor. Only at 6:00 it is disturbed by cracks arranged into a graben-like structure, which is also imaged on the sonograph as faint lineations parallel to the scars. These cracks can be either contemporary to the collapse event or younger, therefore indicating farther development of the slope failure processes.

Subbottom profiler data suggest that the displacement resulting from the past failure is about 150 m.

*Description of ORAT 25*

A 100kHz OREtech high resolution side-scan survey with 6.5kHz subbottom profiler was run north south with a 1km swath width (Fig. 51). This sonograph is coincident with OKEAN long-range side-scan sonographs PSAT71, PSAT 73, PSAT69 and PSAT94, deep-tow TV line TVAT10 and over gravity core site AT120-22, AT138-140 and box-core AT141.

The line was run to generate a detailed coverage of this area which shows both well-expressed recent slide deposits and a concentration of pockmarks and mud diapirs. The OKEAN sonograph and single-channel seismic surveys reveal this area is a crucial area of interest, where both gas related and slide-related features are coincident.

Two main acoustic facies were recognised on the sonograph. The northern end of the sonograph shows an area of low backscatter on a smooth gently dipping slope, the southern area and more dominant facies, is characterised by higher and more varied backscatter and a

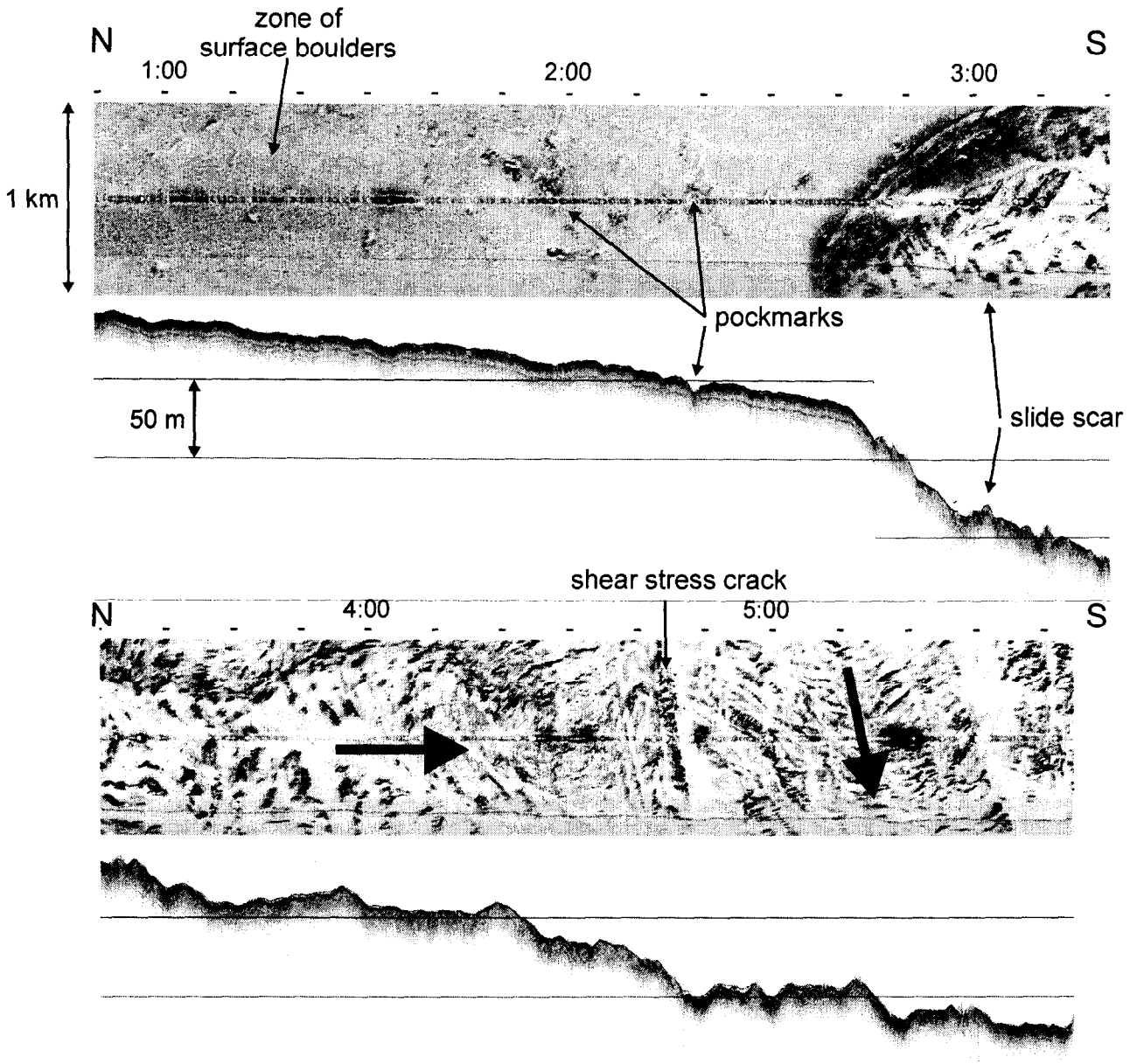


Fig. 51. Sonograph and subbotom profiler record ORAT-25 showing a cluster of pockmarks in the vicinity of the Storegga Slide scar. Large arrows indicate directions of mass movement.

more irregular topography.

The northern end of the sonograph can further be divided into two main background facies. The most northern facies, from 00.50 to 01.50, reveals a stippled patternation of high backscattering spots against low backscatter. The spots are positive topographic features possessing acoustic shadows and are revealed on the subbottom profiler as surface roughness. The subbottom profiler shows a well-stratified sediment sequence parallel to the seabed to a depth of 15m. One strong reflector can be traced underlying the entire northern acoustic facies. The high backscatter spots are interpreted as surface boulders. The northern most facies also shows larger 20-30m diameter spots, and lineations of low backscatter with high backscatter on their far sides, suggesting that these are depressions. Some of these

features are visible on the subbottom profile as small depressions. Deep-tow TV and cores suggest that these may be gas-related. The remainder of the northern facies is similar but reveals an area of uniform background acoustic backscatter. The subbottom profiler shows clearly a drape of hemipelagic sediments which smooths any surface irregularity. This area also reveals larger features of low backscatter (30-40 m diameter). Some of these features are crossed by the subbottom profiler and are expressed as steep-walled depressions. An absence of statified layers under the depressions suggests that these may be associated with fluid seepage. There is also an absence of a surface hemipelagic drape overlying these features.

The boundary between the main low and high backscatter facies is a sharp curved line of high backscatter marking the edge of a steep escarpment, which was also recognised on the OKEAN sonograph. This has been interpreted as a recent slump scarp.

The facies to the south of the slump scarp shows a pattern of high backscatter lineations indicating topographic highs, as confirmed on the subbottom profiler. The facies represents slump deposits with well expressed push-ridges. Adjacent and east of the slump scarp, three clear terraces can be traced, below these the lineations become less coherent. No clear orientation to the ridge can be inferred due to the shadowing effect of the topographic highs. The eastern part of this area of the sonograph shows more coherence in ridge morphology, which may suggest less disturbance in comparison with the western side of the sonograph.

The subbottom profiler for the main southern acoustic facies shows a lack of sub-surface stratification. The local topographic lows in the profile are covered by a sedimentary drape which is absent close to the scarp and on the highest push-ridges. The subbottom profiler also reveals a minor scarp at 04.45, also apparent on the OKEAN sonograph. South of this minor scarp, the sediments are at a lower elevation but possess the same topographic characteristics as the more northerly slumped area. These are also interpreted as slumped deposits with well expressed push-ridges and are also covered by a patchy sediment drape.

The sonograph for this most southern facies shows a difference in patternation, characterised by NE-SW trending ridge crests with smaller scale ridges trending N-S in the intervening troughs.

*ORAT-26*

The east-west trending line ORAT-26 was run in the northwestern part of the study area in order to investigate in detail fields of pockmarks seen on the large-scale OKEAN acoustic seafloor image (Area 2, Fig. 49). The high-resolution 100 kHz sonograph that was obtained for the most part shows a flat seafloor characterised by low acoustic backscatter. On the subbottom profiler record a well-layered sedimentary sequence is seen. There is one prominent and continuous high-amplitude reflector at about 20 m below the seabed. Pockmarks are crossed by the line at 7:55, 10:15, 11:40, 12:20 and 13:00 and are seen on the sonograph as patches of high backscatter 100-250 m in diameter (Fig. 52). Their numbers increase at the northeastern edge of the line, where several types of pockmark morphology can be distinguished. At 11:15 there is one of the simple pockmarks representing just a shallow depression. Small patches of low backscatter may be local areas of the overlying sedimentary veneer. At 11:40 the sonograph shows a seafloor elevation of about 70 m. The top of the elevation is disturbed by a centripetal system of cracks. A pockmark observed at 13:00 has a similar appearance to that at 11:15, but is surrounded by a field of numerous small pockmarks whose diameter does not exceed 20 m.

On the subbottom profiler record pockmarks are seen only if they are crossed directly by the vehicle line, and then a narrow vertical acoustic void is observed with pushed up sedimentary strata along the rim.

The observed types of pockmark morphology probably represent different stages of their development. Thus, the pockmark at 11:40 may correspond to the early stage of formation when the relicts of the upper sedimentary veneer still can be recognised. The one at 13:00 is

believed to be quite active and is associated with intensive fluid flow responsible for the formation of smaller satellite pockmarks surrounding the main one. If the fluid activity gets weaker these smaller pockmarks would be covered by sediments with only the main one still maintaining an expression at the seabed. The pockmark observed at 11:15 may represent this stage.

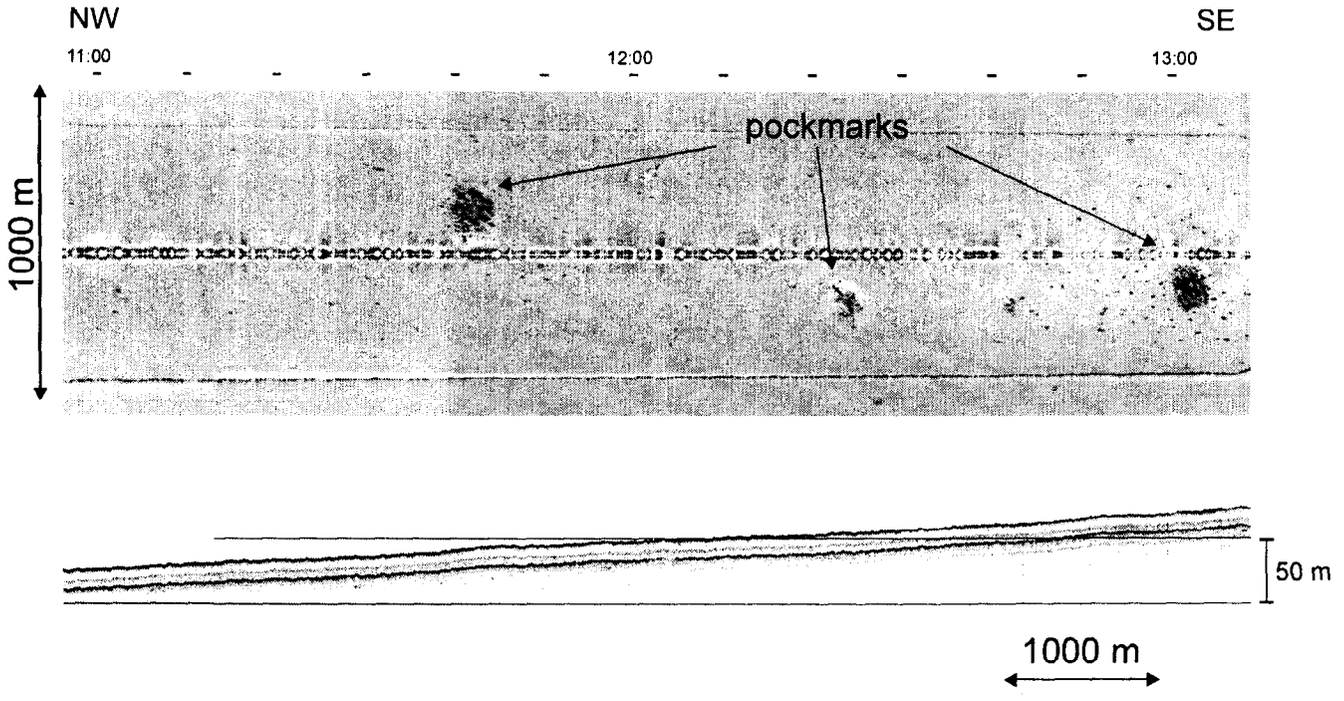


Fig. 52. Fragment of ORAT-26 sonograph and subbottom profiler record showing several large pockmarks surrounded by fields of smaller ones.

### IV.2.3. Bottom Sampling

*G. Aloisi, G. Akhmanov, A. Akhmetzhanov, E. Kozlova, A. Wheeler, B. De Mol, A. Stadnitskaya, I. Belenkaya, V. Krupskaya, M. Kozachenko, I. Mardanyan*

*Introduction*

Several sectors of the slope area connecting the Vøring Plateau to the upper portion of the Storegga Slide were chosen as preferred locations for the study of seabed features connected to gas seeping and mud intrusion/expulsion processes. A selection of the most interesting areas was made on the basis of available TOBI side-scan sonar. A number of seabed features appeared as sub-circular, high backscatter patches of variable diameter (from 100 to 350m). Some of these structures where thought to be bioherms possibly connected to gas seepage on the basis of side-scan sonar data only, but were never cored. Lack of detailed bathymetric data made it impossible to determine if they where positive or negative features.

The geophysical survey evidenced two sectors of particular interest for the study of gas seepage and mud intrusion/expulsion related features. A total of sixteen gravity cores and three box cores where taken from these areas (Fig. 46 for location map) (see table 7 for a summary of the coring data in this area).

| Station No | Date | Time (GMT) | Latitude | Longitude | Depth, m | Recovery, cm |
|---|---|---|---|---|---|---|
| TTR8-AT-111G | 12.07.98 | 16:49 | 64°40.419N | 4°35.640E | 1056 | 389 |
| TTR8-AT-112G | 12.07.98 | 18:10 | 64°38.703N | 4°31.392E | 1197 | 317 |
| TTR8-AT-113G | 12.07.98 | 19:10 | 64°38.298N | 4°30.508E | 1254 | 419 |
| TTR8-AT-114G | 12.07.98 | 19:56 | 64°37.912N | 4°29.474E | 1296 | 364 |
| TTR8-AT-115G | 12.07.98 | 21:18 | 64°37.417N | 4°28.293E | 1291 | 387 |
| TTR8-AT-116G | 13.07.98 | 12:33 | 64°46.060N | 4°48.485E | 815 | 381 |
| TTR8-AT-117G | 13.07.98 | 20:30 | 64°47.080N | 4°48.379E | 802 | 457 |
| TTR8-AT-118G | 13.07.98 | 22:24 | 64°46.105N | 4°48.659E | 805 | 531 |
| TTR8-AT-119G | 14.07.98 | 00:03 | 64°46.090N | 4°48.641E | 806 | 407 |
| TTR8-AT-120G | 14.07.98 | 02:59 | 64°40.875N | 5°15.815E | 734 | 223 |
| TTR8-AT-121G | 14.07.98 | 04:26 | 64°40.586N | 5°14.717E | 730 | 317 |
| TTR8-AT-122G | 14.07.98 | 05:29 | 64°40.878N | 5°15.808E | 734 | 142 |

**Table 7.** General information on the sampling stations on the southern Vøring Plateau

| Station No. | Geographical Setting | Instrumentation | Acoustic characteristics |
|---|---|---|---|
| TTR8-AT-111G | Upper part of the slope on the isometric slump scar on the edge of Storegga Slide | Seismic, OKEAN side scan sonar and onboard profiler profiles PSAT-63, 12:30 | Moderate backscatter on the OKEAN image, bedded sedimentary sequence on the onboard profiler record |
| TTR8-AT-112G | Very steep part of the middle slope on the slump scar on the edge of Storegga Slide | Seismic, OKEAN side scan sonar and onboard profiler profiles PSAT-63, 12:09 | High backscatter on the OKEAN image, chaotic reflector on the onboard profiler |
| TTR8-AT-113G | Slump body of the slump scar on the edge of Storegga Slide | Seismic, OKEAN side scan sonar and onboard profiler profiles PSAT-63, 12:03 | Moderate backscatter on the OKEAN image, bedded sedimentary sequence on the onboard profiler record |
| TTR8-AT-114G | Flat bottom between small hill and steep scar of the slump scar on the edge of Storegga Slide | Seismic, OKEAN side scan sonar and onboard profiler profiles PSAT-63, 11:58 | Moderate backscatter on the OKEAN image, bedded sedimentary sequence on the onboard profiler record |
| TTR8-AT-115G | Top of the small hill in front of the slump body on the slump scar on the edge of Storegga Slide | Seismic, OKEAN side scan sonar and onboard profiler profiles PSAT-63, 11:52 | Moderate backscatter on the OKEAN image, bedded sedimentary sequence on the onboard profiler record |
| TTR8-AT-116G | Small depression on the flat surface in the central part of the edge of Storegga Slide | OKEAN side scan sonar and onboard profiler profiles PSAT-64 | High backscatter on the OKEAN image |
| TTR8-AT-117G | Mud diapir on the flat surface in the central part of the edge of Storegga Slide | OKEAN side scan sonar and onboard profiler profiles PSAT-64 | High backscatter on the OKEAN image |
| TTR8-AT-118G | Small depression on the flat surface in the central part of the edge of Storegga Slide | OKEAN side scan sonar and onboard profiler profiles PSAT-64; TV-profile TVAT-8, onboard profiler 18:28 | Fragment with chaotic acoustic character on the subbottom profiler record |
| TTR8-AT-119G | Small depression on the flat surface in the central part of the edge of Storegga Slide | OKEAN side scan sonar and onboard profiler profiles PSAT-64 | Fragment with chaotic acoustic character on the subbottom profiler record |
| TTR8-AT-120G | Mud diapir on the flat surface in the northeastern part of the edge of Storegga Slide. | Seismic, OKEAN side scan sonar and onboard profiler profiles PSAT-72; onboard profiler, echosounder profile PRAT-8 | High backscatter on the OKEAN image, fragment with chaotic acoustic character on the subbottom profiler record |
| TTR8-AT-121G | Small depression on the flat surface in the northeastern part of the edge of Storegga Slide | Seismic, OKEAN side scan sonar and onboard profiler profiles PSAT-72; onboard profiler, echosounder profile, PRAT-9 | High backscatter on the OKEAN image, fragment with chaotic acoustic character on the subbottom profiler record |
| TTR8-AT-122G | The same as AT-120G. | Seismic, OKEAN side scan sonar and onboard profiler profiles PSAT-72; onboard profiler, echosounder profile, PRAT-8 | High backscatter on the OKEAN image, fragment with chaotic acoustic character on the subbottom profiler record |

**Table 8.** Geological and acoustic characteristics of sampling stations.

*Orat 22 groundtruthing: cores 111G-115G*

A set of five cores was taken across a large collapse structure seen on the ORAT-22 sonograph and subbottom profiler (Fig. 53).

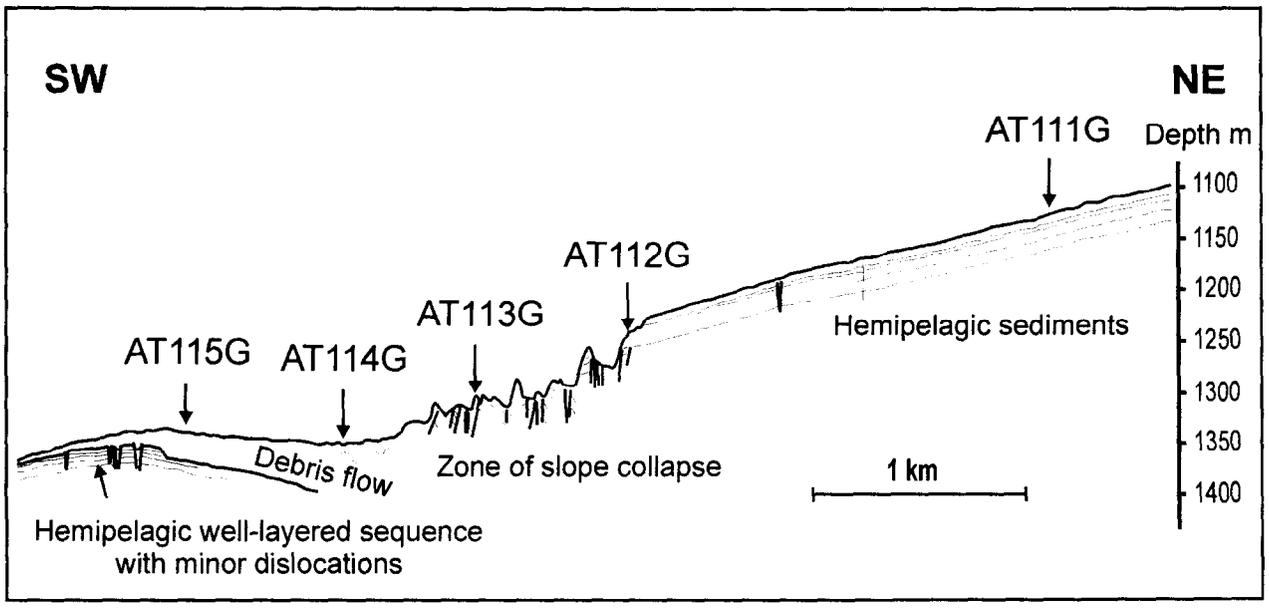


Fig. 53. Interpretation of ORAT-22 subbottom profiler record. Sampling stations are indicated.

Core AT-111G (Fig. 54) was collected from the place where the sediment profiler recorded a well-stratified upper sedimentary sequence. The core recovered undisturbed Holocene-Upper Pleistocene hemipelagic silty clays.

Core AT-112G (Fig. 55) aimed to sample an edge of the collapse structure and also showed no significant disturbance of the sedimentary cover apart from some inclination of strata. According to the micropaleontological data the Late Pleistocene sequence is considerably reduced, comprising 0.5 m compared to about 4 m in the Core AT-111G. Turbidites observed in the lower part of the core probably also belong to an older glacial sequence.

Core AT-113G (Fig. 56) was taken from the area of blocky relief in the central part of the collapse structure. The core also recovered relatively undisturbed hemipelagic clayey sediments and only some curvature observed for a few layers can be attributed to the slumping activity. An Upper Pleistocene interval was noticed in this core.

Core AT-114G (Fig. 57) was taken from the base of the collapsed structure, immediately down slope from the area of blocky relief. The subbottom profiler recorded a flattened seafloor with absence of acoustic penetration. The recovered sequence comprised several sedimentary units of two types. One type represented relatively undisturbed clusters of hemipelagic sediments, the other bore features of intensive slumping with numerous microfolds and faults. In the upper part of the core, underneath the Holocene upper veneer, the distinguishing structureless diatomite layer, 30-cm thick, was observed. Fragments of similar layers were found among the underlying slumped sediments also.

Core AT-115G (Fig. 58) was collected further downslope from the area where the sediment profiler recorded an acoustically transparent lens overlaying well-stratified sediments. The recovered sequence showed minor evidences of disturbance represented by mainly tilted strata, unconformably overlain by horizontal upper sediments. The diatomite layer was also found in this core although it was interbedded within the tilted interval of hemipelagic silty clay. The layer had a complex inner structure and was composed of different facies of diatomites, probably indicating the presence of several cycles.

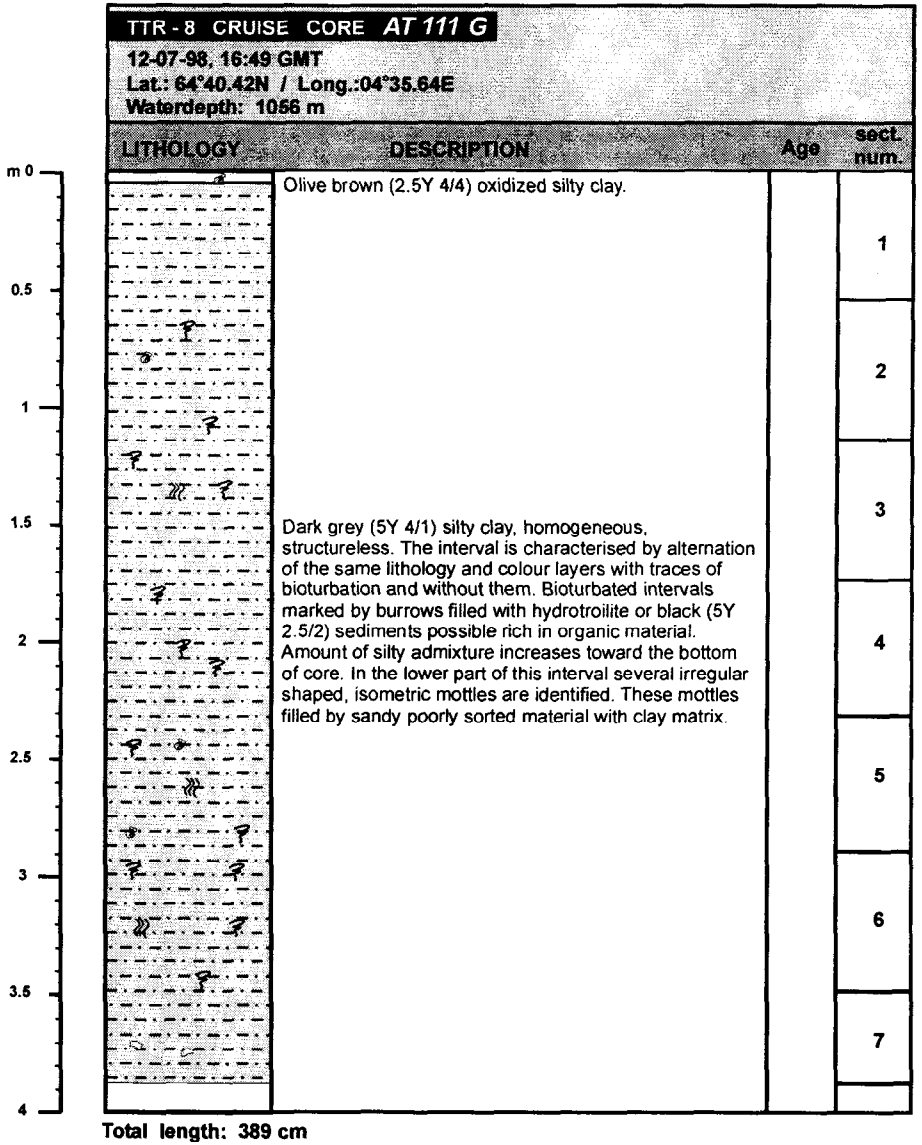


Fig. 54. Core log AT-111G.

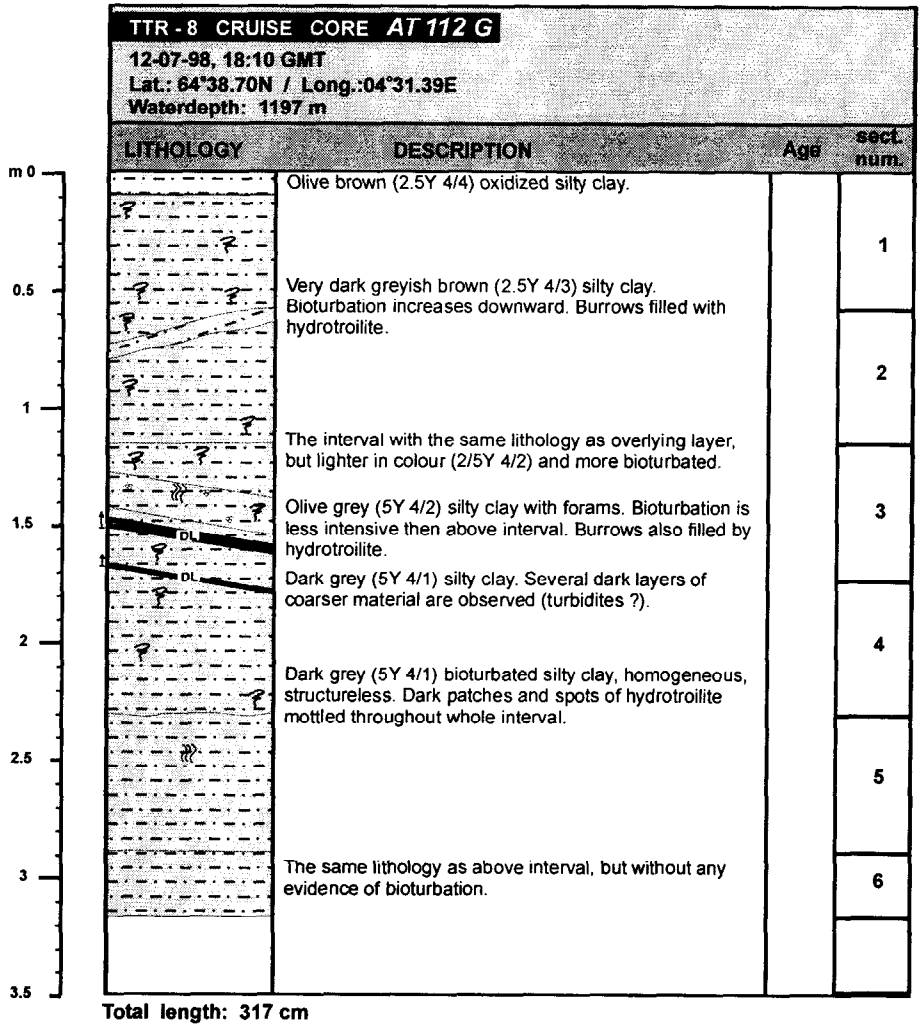


Fig. 55. Core log AT-112G.

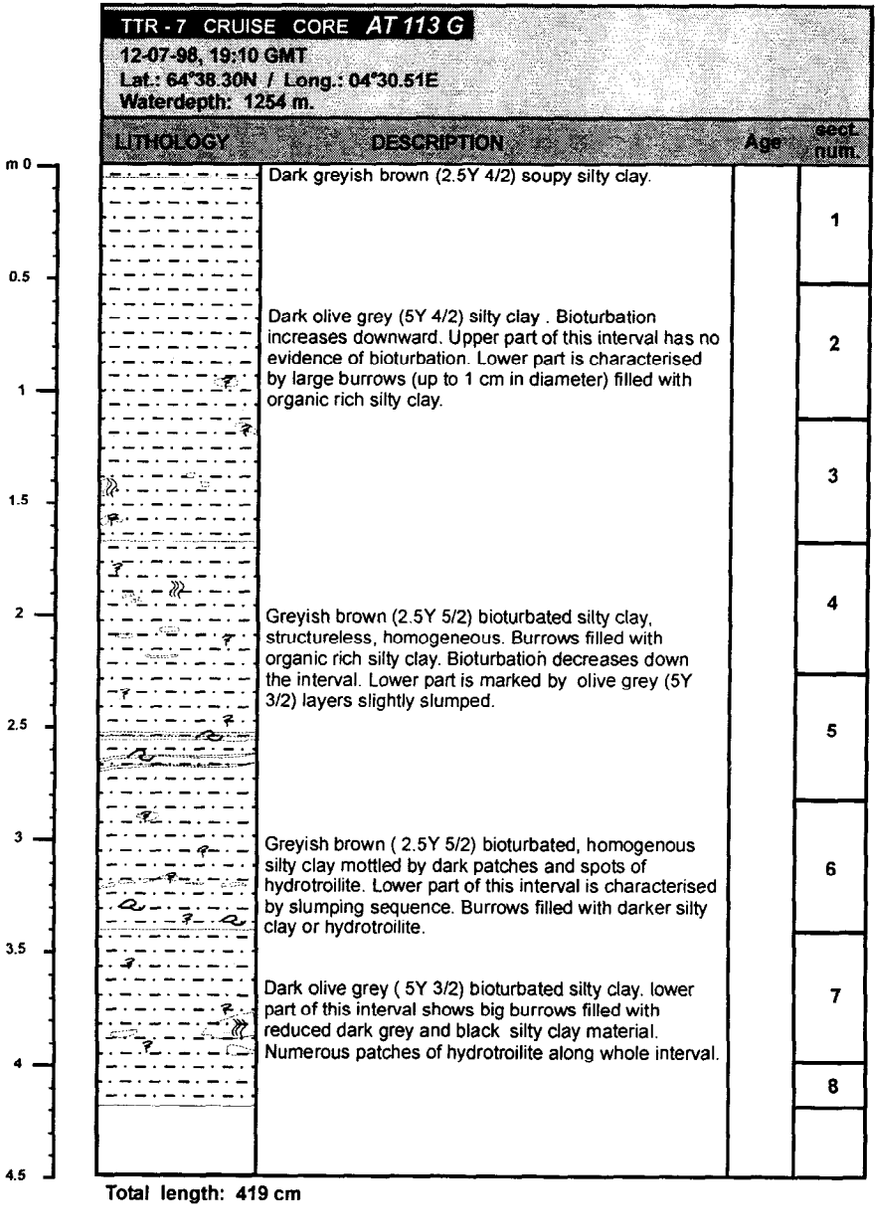


Fig. 56. Core log AT-113G.

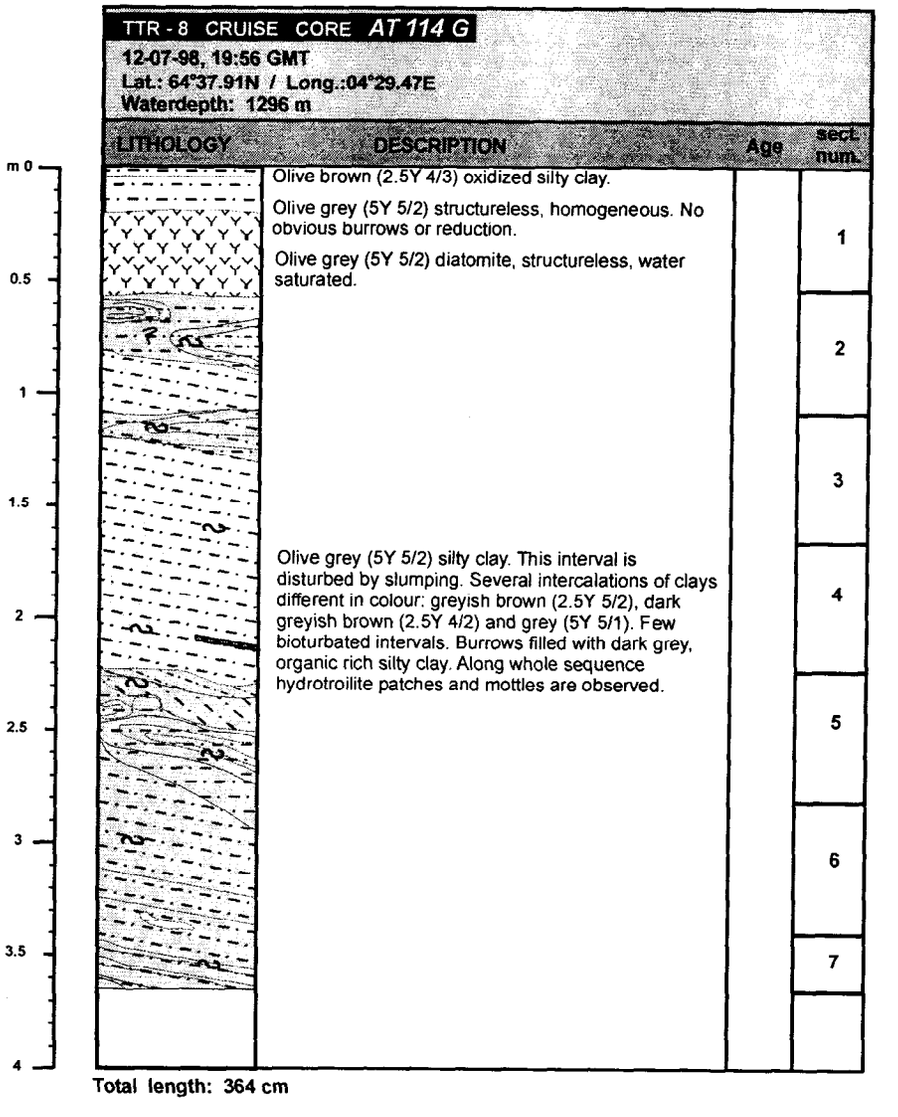


Fig. 57. Core log AT-114G.

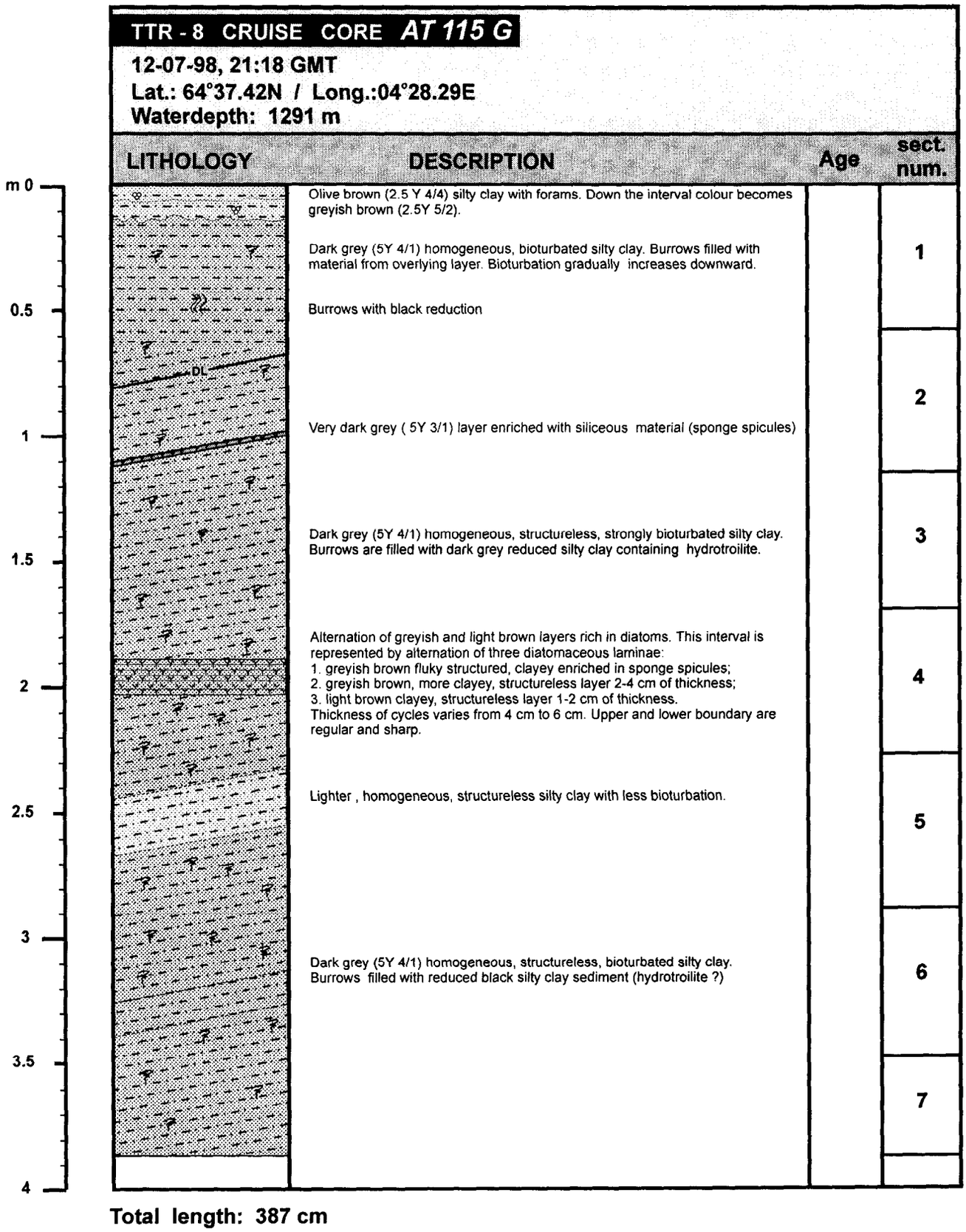


Fig. 58. Core log AT-115G

Interpretation

The described sedimentary sections are thought to be characteristic for processes of sliding and slumping which had taken place in this part of the margin. Thus, cores AT-112G and AT-113G show that within the collapse structure the sedimentary succession was emplaced mainly by sliding and large clusters of sediments still have an undisturbed inner structure or were only faulted. The collapse event initiated a debris flow which can be observed on the subbottom profiler record as an acoustically transparent body. Core AT-114G taken from the debris flow shows that it is composed of undisturbed blocks of hemipelagic silty clays separated by slumped intervals, resulting probably from the movements of the blocks relatively to each other. The size of these block can be quite large and exceeds 2-3 m, as demonstrated by the relative integrity of Core AT-115G which probably hit one of these blocks.

Other conclusions can be made from the presence of the diatomite layers found in the cores from the lower part of the surveyed slope and which are absent in the upper part. This may be an indication of alongslope sediment transport, probably by a bottom current which can bring such northern siliceous facies to this area. Some side-scan sonar images also show evidence of alongslope sediment transport.

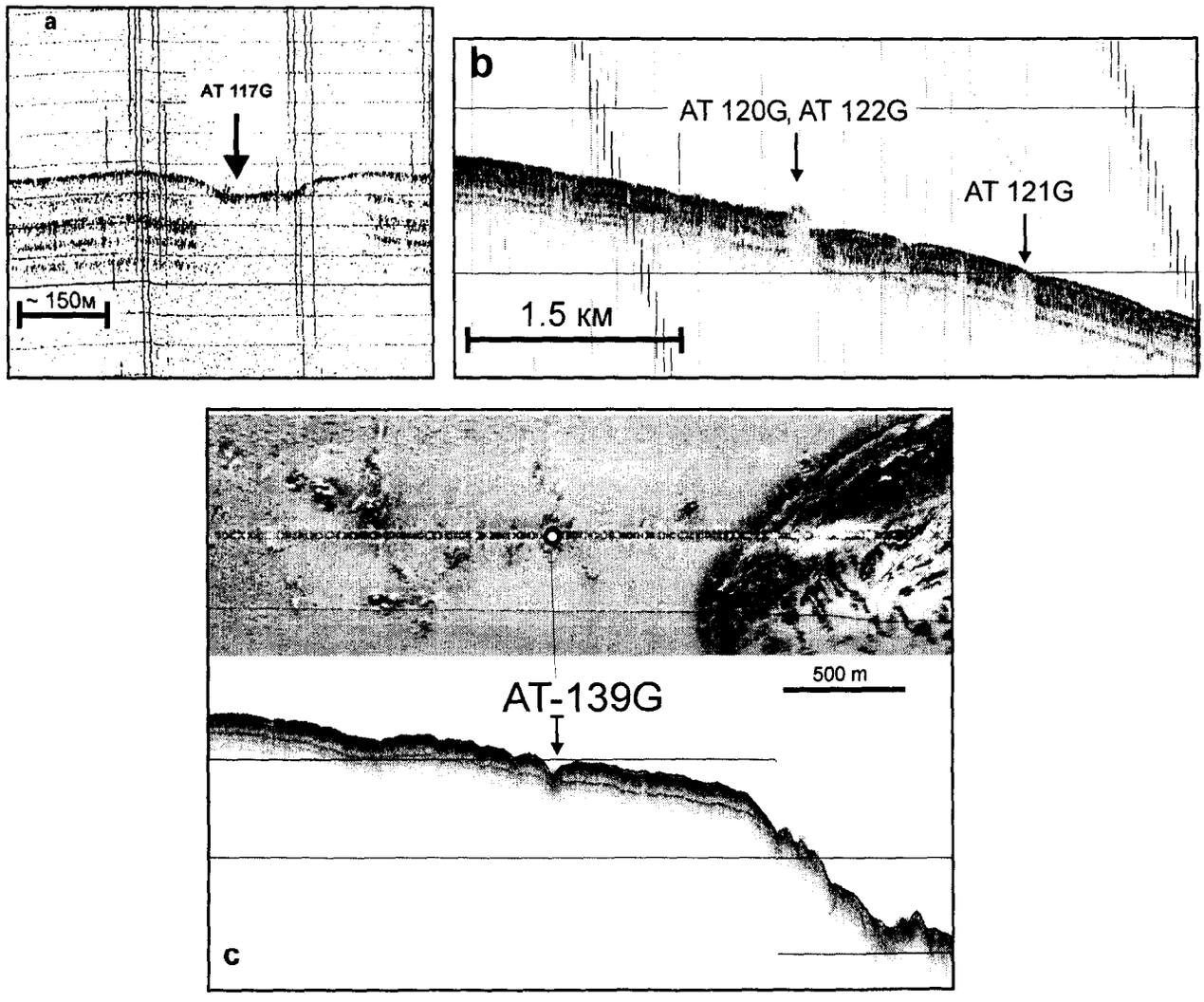


Fig. 59. Sampled pockmarks (a, c) and diapirs (b) on 3.5 and 5 kHz subbottom profiler records and OREtech sonograph.

*Pockmarks area*

In the north-western part of the studied area the high backscatter patches, seen both on the TOBI and OKEAN side-scan sonars, often correspond to circular, flat bottomed depressions having a diameter of 200 m and a maximum depth of 7-8 m. Seismic lines and subbottom profiles show that subsurface reflectors are laterally interrupted in correspondence with these features, indicating the presence of gas in the sediments, and are interpreted as pockmarks (Fig.59a). Four cores (AT 116G, AT 117G, AT 118G and AT119G) were taken from two of these features. Other, similar, high backscatter patches do not seem to have a morphological expression but correspond to zones of acoustic turbidity on seismic records. One gravity core (AT137G) and two box cores (AT142B and AT143B) were taken from these areas, looking for evidence that the acoustic turbidity was generated by the presence of gas in the sediment.

Core AT 116G (Fig. 60)

This core consists mainly of dark grey silty clay, intensely bioturbated with burrows frequently filled with hydrotroilite. This core is very similar to those taken far from gas seepage/mud expulsion features and is interpreted as deposited by contour currents. The occurrence of this type of sediment in the pockmark is discussed below.

Core AT 117G (Fig. 61)

The dark grey silty clay in this core is intensely bioturbated and smells strongly of $H_2S$. Burrows are frequently filled with dark pelitic material and with hydrotroilite. Several carbonate nodules form a discrete layer at a depth of about 4.5 m in the core.

Core AT 118G (Fig. 62)

The dark grey silty clay in this core is intensely bioturbated and smells strongly of $H_2S$. Burrows are frequently filled with dark pelitic material and with hydrotroilite. Several carbonate nodules form a discrete layer at a depth of about 5.5 m in the core.

Core AT 119G (Fig. 63)

This core consists mainly of dark grey silty clay, intensely bioturbated, with burrows frequently filled with hydrotroilite. This core is very similar to those taken far from gas seepage/mud expulsion features and is interpreted as deposited by contour currents. The occurrence of this type of sediments in the pockmark is discussed below.

Core AT 137G (Fig. 64)

This core consists mainly of dark grey silty clay. All the sediment is bioturbated from a depth of about 80 cm. Bioturbation is expressed as mottling and burrows that are frequently filled with hydrotroilite. This core is very similar to those taken far from gas seepage/mud expulsion features and interpreted as deposited by contour currents.

Core AT 142B

This box core contains dark grey silty clay, the first two centimetres of which are oxidised.

Core AT 143B

This box core contains dark grey silty clay, the first two centimetres of which are oxidised. The sediment is bioturbated.

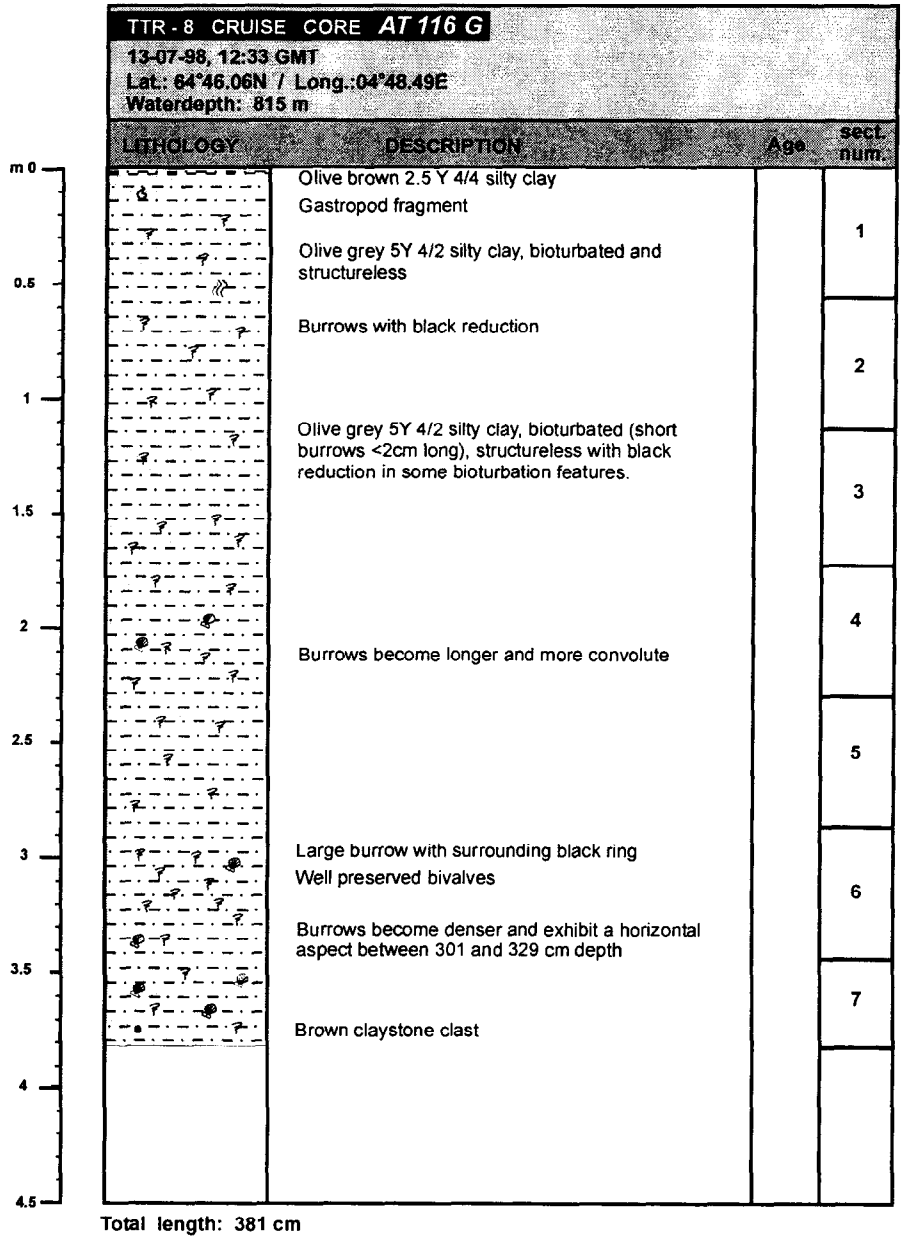


Fig. 60. Core log AT-116G.

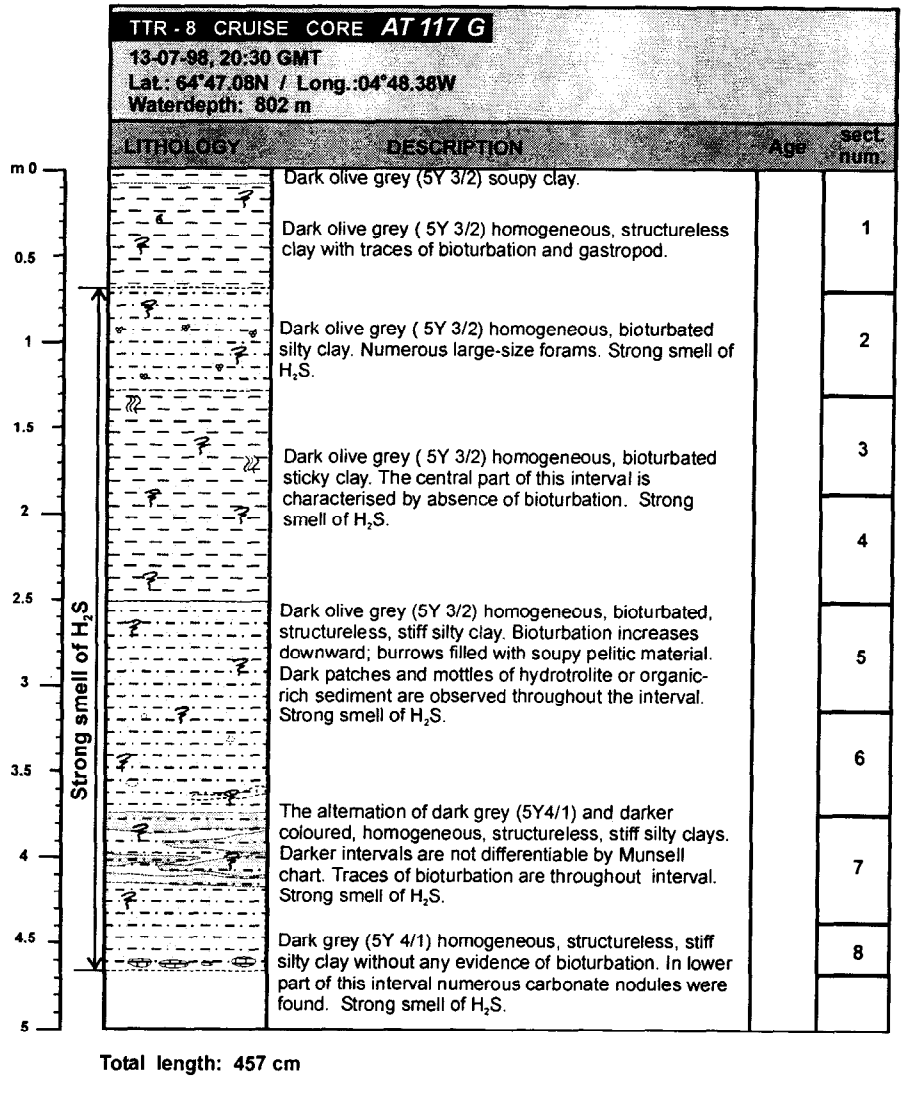


Fig. 61. Core log AT-117G.

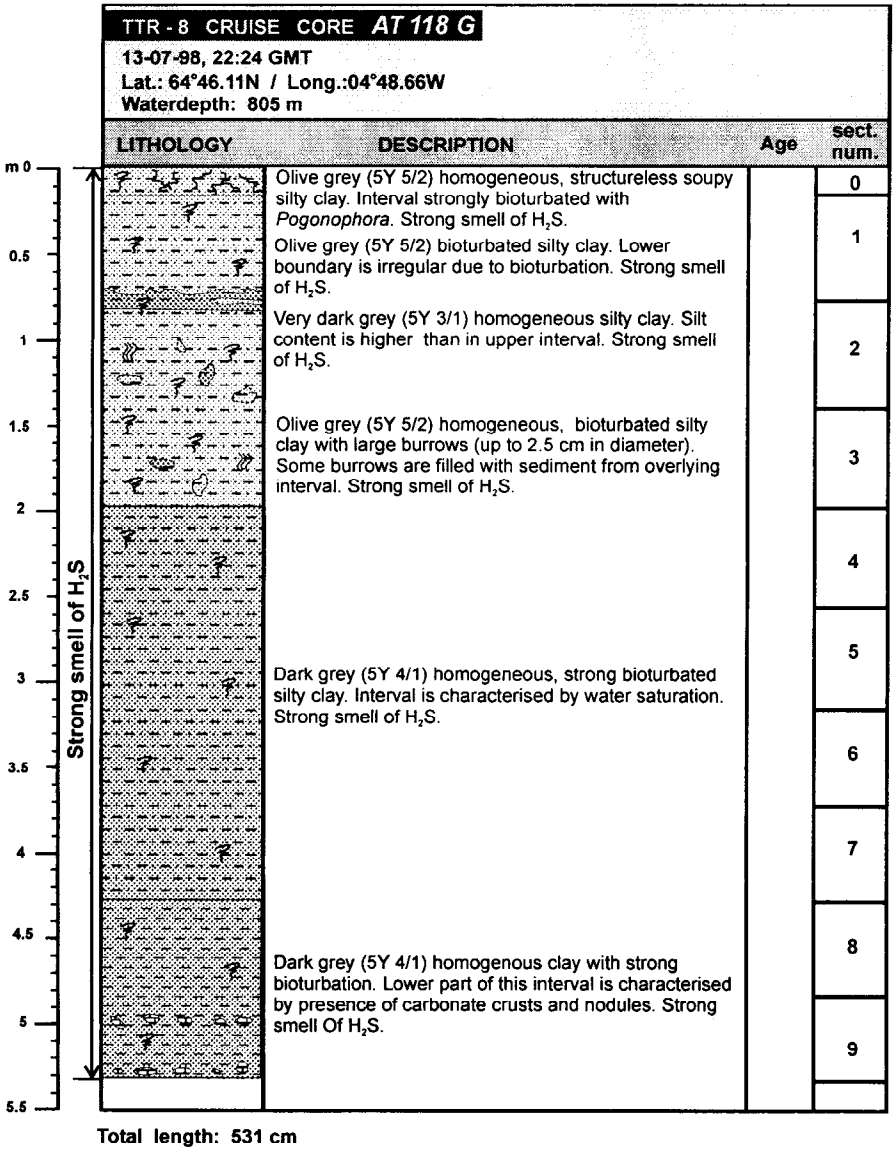


Fig. 62. Core log AT-118G.

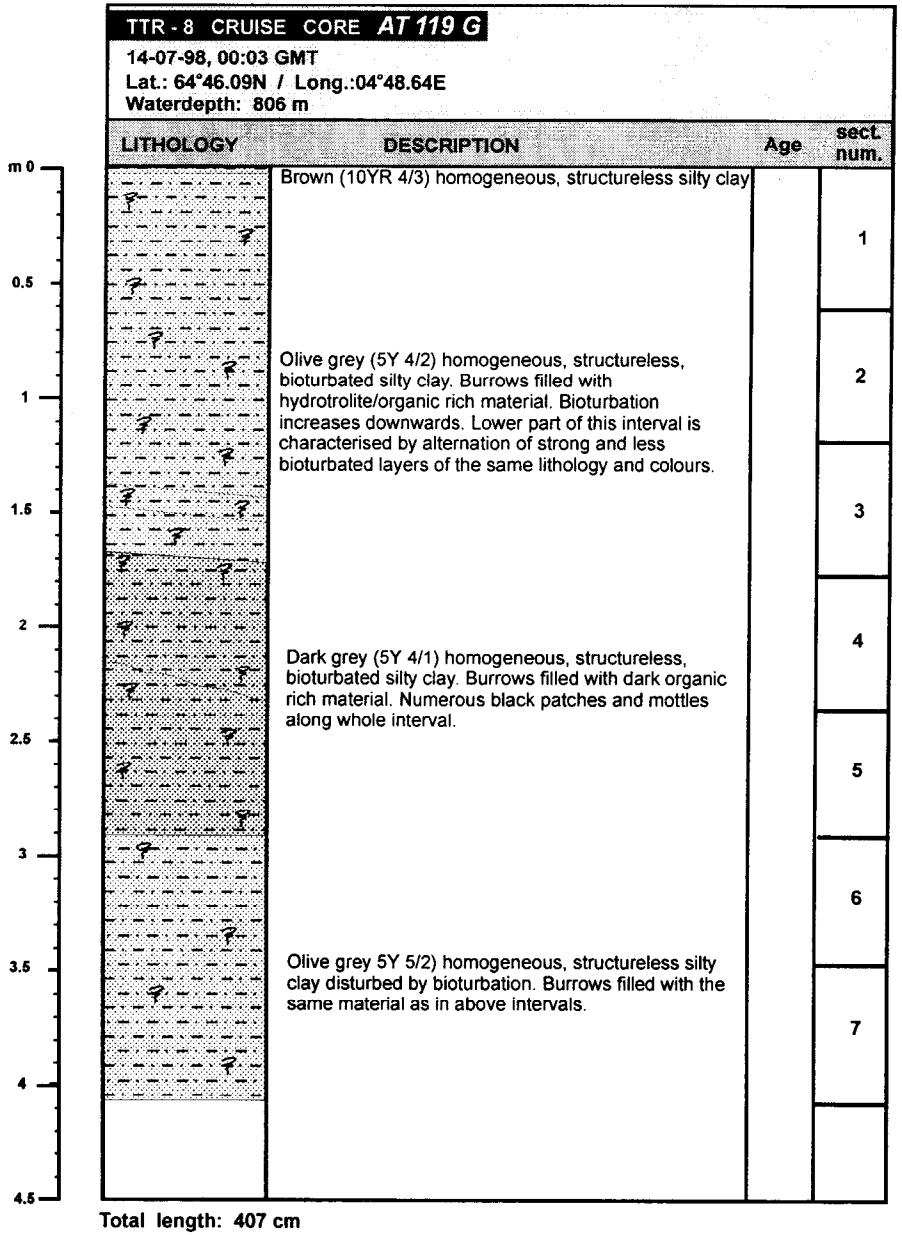


Fig. 63. Core log AT-119G.

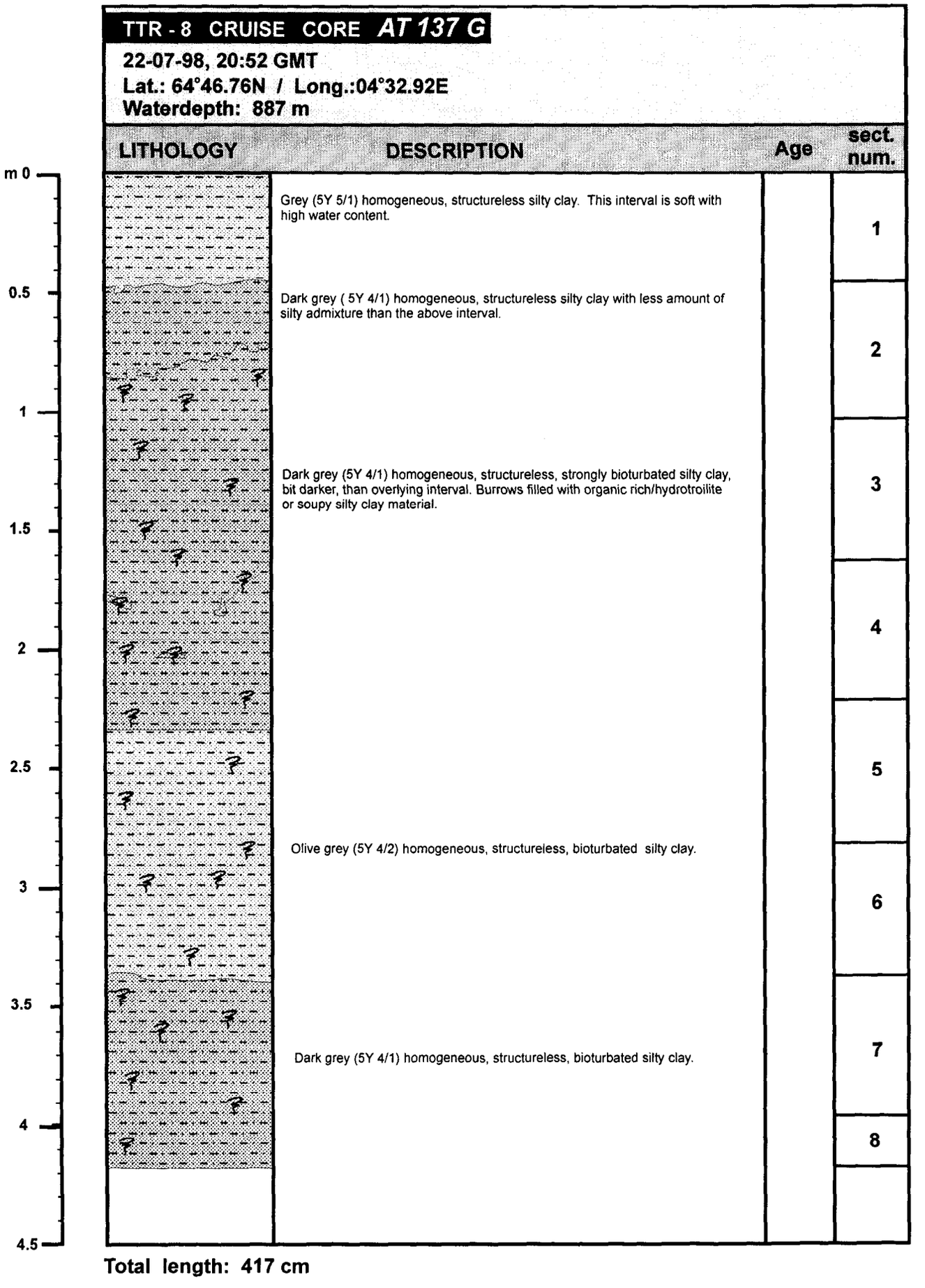


Fig. 64. Core log AT-137G

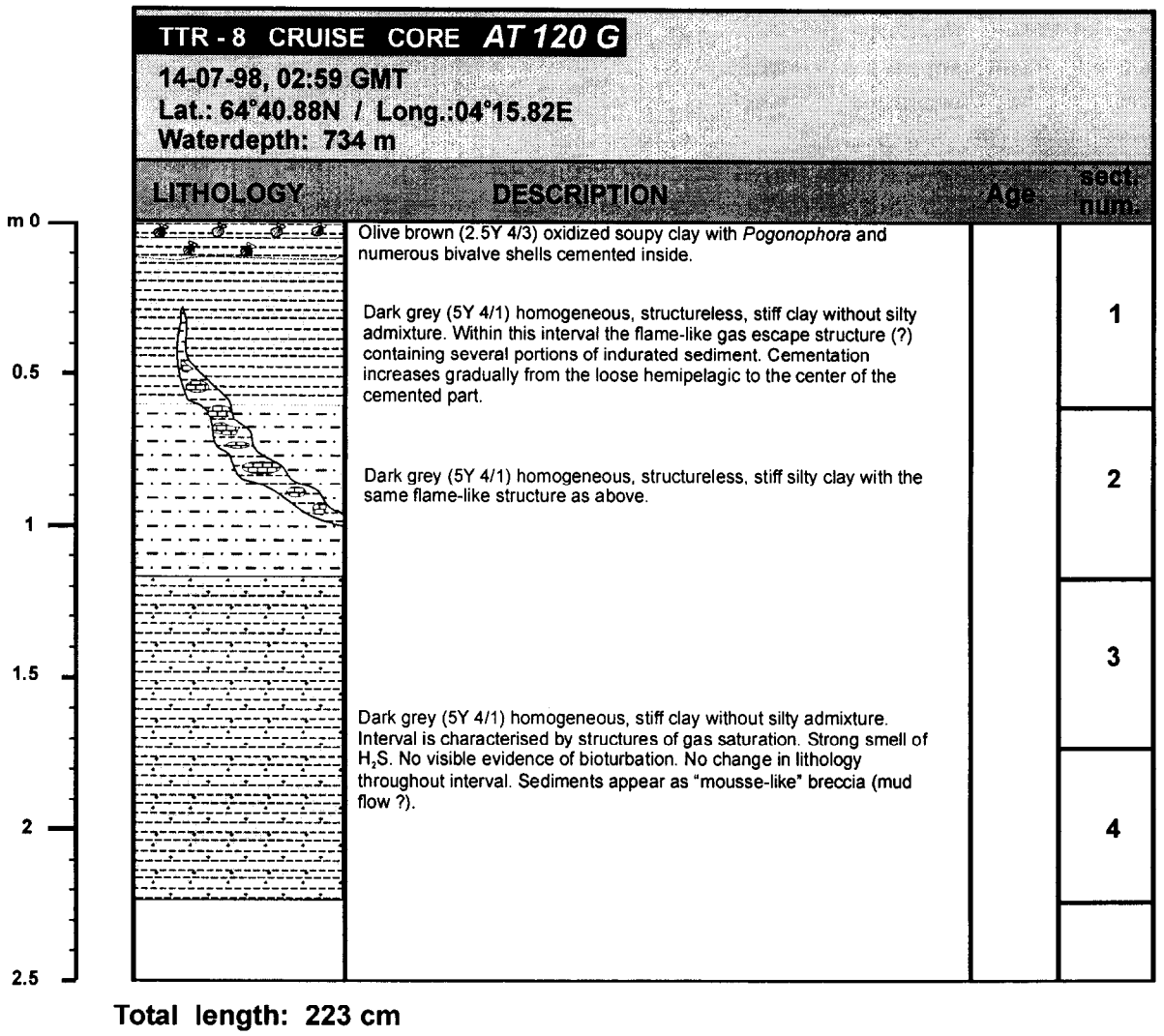


Fig. 65. Core log AT-120G

*Mud diapirs area*

The high reflectivity circular patches seen on the TOBI record in the eastern part of the investigated area were thought to be mud volcanoes or mud diapirs. Additional geophysical survey was planned before using coring to check this hypothesis. On the OKEAN record these features did not appear clearly, but the high resolution seismic lines and the subbottom profiler records showed that they correspond to positive morphologies having a diameter of less than 200 meters and height of 10 meters. Furthermore, subsurface reflectors are laterally interrupted corresponding to these features, indicating the suspected presence of gas in the sediments. Two features of this kind were investigated with a total of three cores (AT 120G, AT 121G, AT 122G, Fig. 59b). Clear evidence of mud diapirism was found on one of the mounds and the same process is though to be responsible for the formation of the other mound. Two gravity cores (AT 138G and AT 140G) where taken from circular high reflectivity patches which did not correspond to a morphological anomaly on the subbottom profiler but were associated with acoustic turbidity zones; these are probably linked to the presence of gas in the sediments (Fig. 59b). Core AT 139G was taken from a depression that

overlies a zone of acoustic turbidity seen on the high-resolution seismic record (Fig. 59c). The occurrence of this depression in the vicinity of the main scarp of the Storegga Slide is discussed below. Box core AT 141B was taken in an attempt to sample benthic fauna and carbonate crusts seen on a TV profile.

Core AT 120G (Fig. 65)

The lower part of this core consists of homogeneous, dark grey, stiff clay characterised by a strong $H_2S$ smell and with structures indicating gas saturation. This interval lacks bioturbation and is interpreted as being deposited by a mudflow. The overlying interval of hemipelagic stiff clay is traversed by flame-like gas escape structures, 60 cm in length, bearing light grey silty clay sediment and calcareous concretions. In the topmost, oxic, part of the hemipelagic clay, several *Pogonophora* and aggregates of cemented bivalves were found.

Core AT 121G (Fig. 66)

The silty clay in this core shows evidence of being gas saturated in the upper metre where gas expansion pockets and cracks are common. Several gas escape structures are filled with light grey silty clay and with calcareous concretions. The central portion of the core is disturbed by faulting, which occasionally interrupts and displaces hydrotroilite filled burrows. The inferior part of the core is heavily bioturbated and is black due to the widespread presence of hydrotroilite.

Core AT 122G (Fig. 67)

The lower part of this core consists of homogeneous, dark grey, stiff clay characterised by a strong $H_2S$ smell. This interval lacks bioturbation and is interpreted as being deposited by a mudflow. The overlying interval of hemipelagic clay has irregular patches of light grey silty clay sediment containing calcareous concretions. In the topmost, oxic, part of the hemipelagic clay several aggregates of cemented bivalves were found.

Core AT 138G (Fig. 68)

This core consists mainly of dark grey silty clay. Bioturbation is common and expressed as mottling and burrows that are frequently filled with hydrotroilite. This core is very similar to those taken far from gas seepage/mud expulsion features and interpreted as deposited by contour currents.

Core AT 139G (Fig. 69)

The dark grey silty clay in this core is disturbed by mottling and contains several sediment filled cracks interpreted as gas escape structures. Strong $H_2S$ smell confirms the high gas content of the sediment. Centimetric sized portions of sediment are light grey in colour and are semi-indurated. Small scale faulting also disturbs the upper part of the core.

Core AT 140G (Fig. 70)

The dark grey silty clay in this core is disturbed by bioturbation that gives it a patchy aspect. Several burrows are filled with hydrotroilite. Several sediment filled cracks are interpreted as gas escape structures. A strong $H_2S$ smell confirms the high gas content of the sediment. Small scale faulting also disturbs the upper part of the core.

Core AT 141B

This box core contains dark grey silty clay, the first two centimetres of which are oxidised.

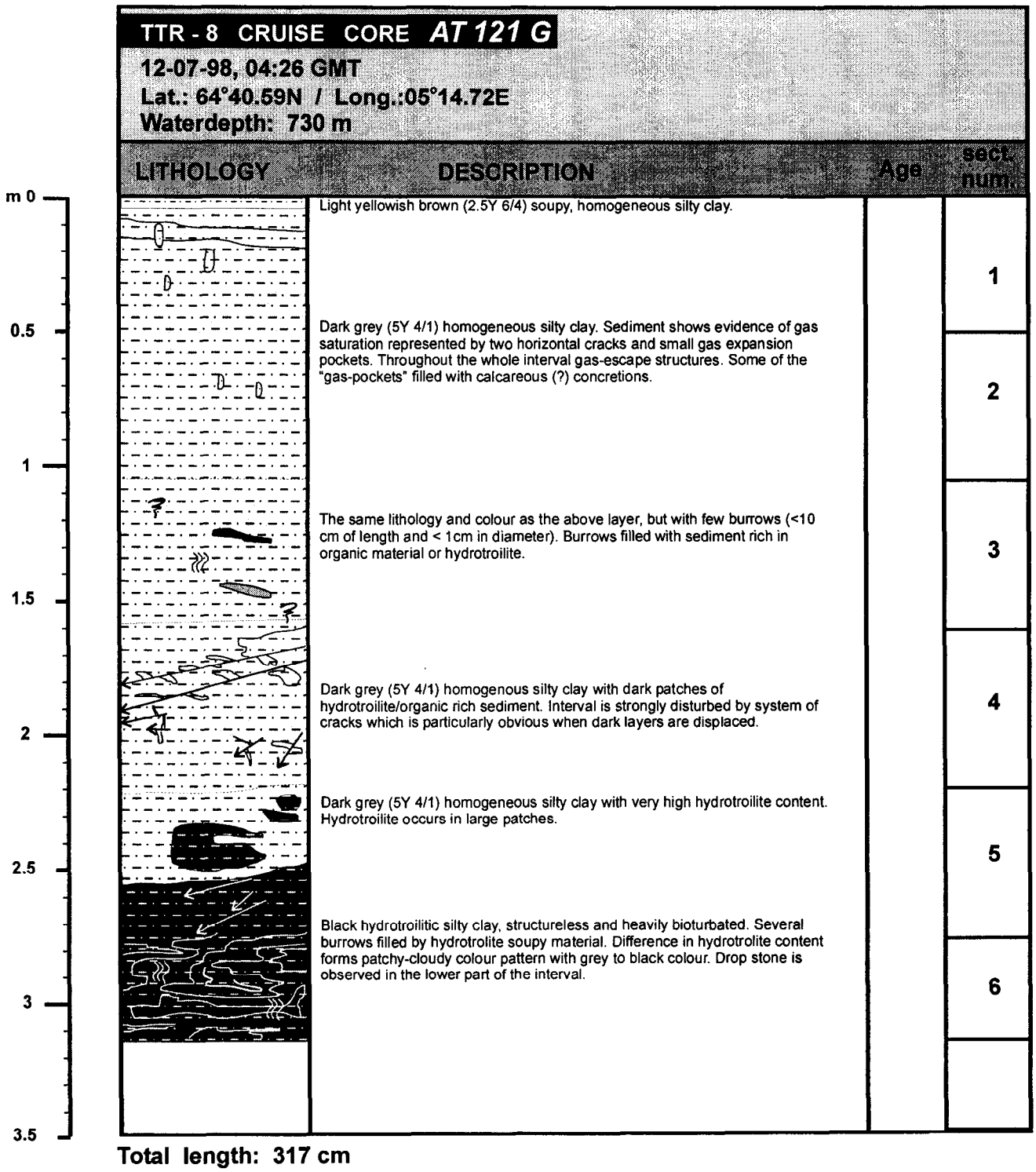


Fig. 66. Core log AT-121G

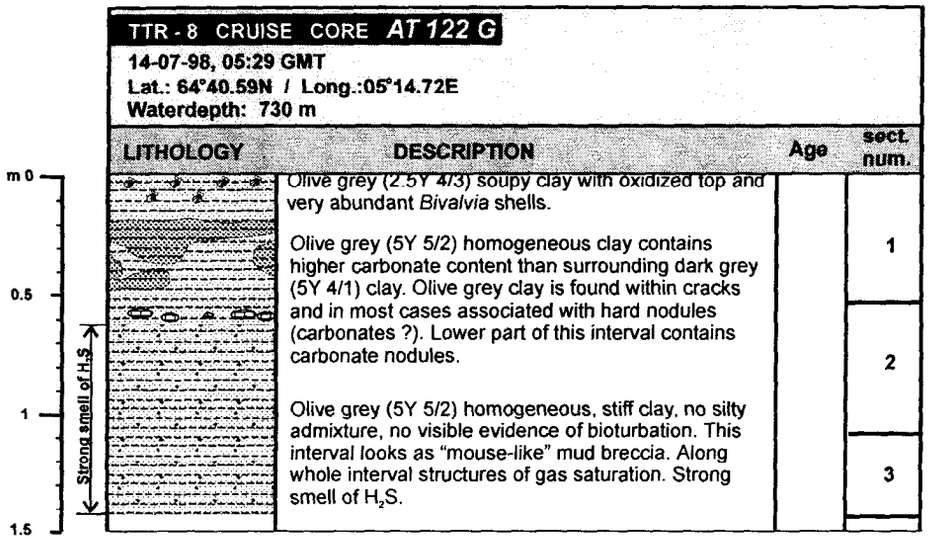


Fig. 67. Core log AT-122G.

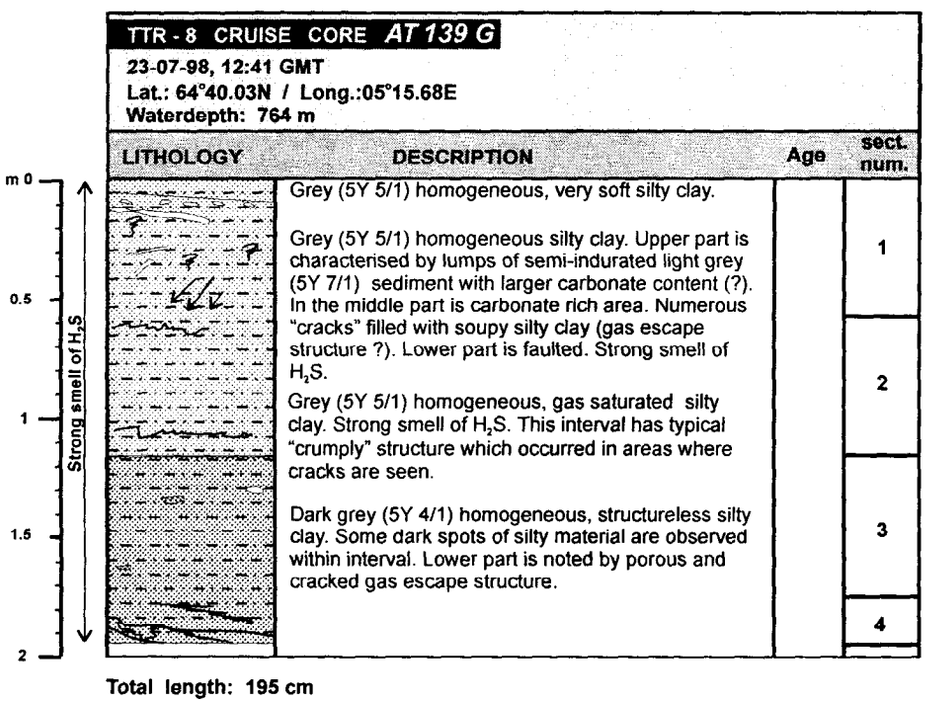


Fig. 69. Core log AT-139G.

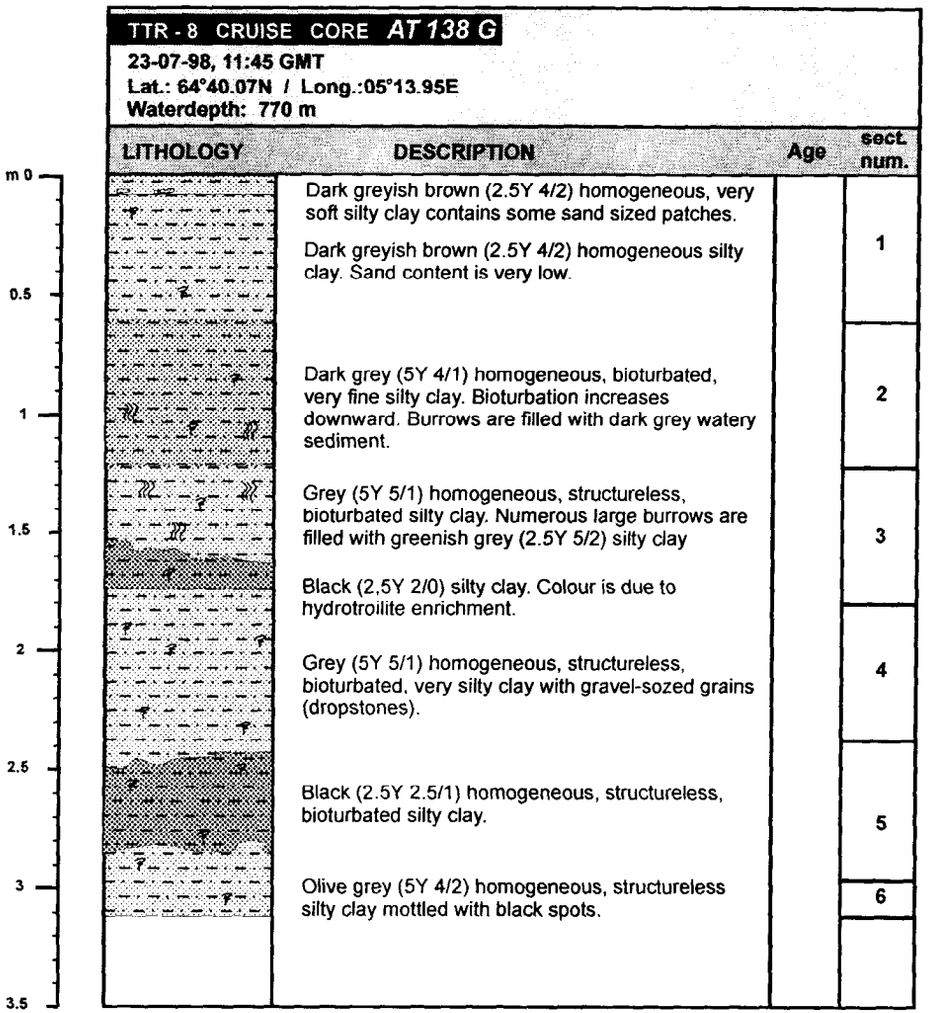


Fig. 68. Core log AT-138G.

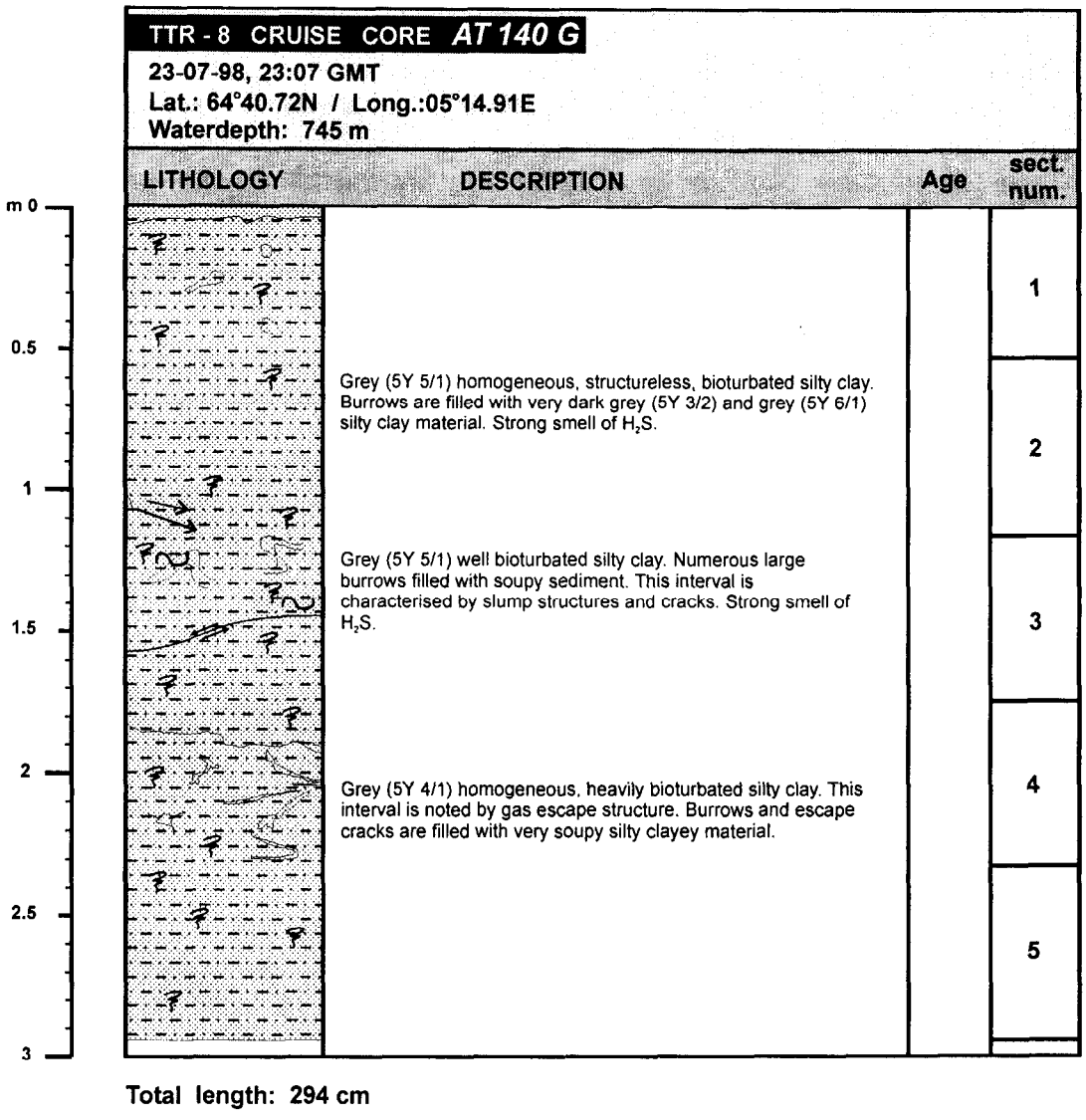


Fig. 70. Core log AT-140G

*Discussion*

A clear distinction can be made between cores recovered from gas seepage/mud expulsion structures and those recovered from the surrounding areas that register the background sedimentation. Core AT 111G is a good example of the background hemipelagic sedimentation which consists mainly of bioturbated grey to dark grey silty clay interpreted as being deposited by contour currents. The oxic topmost part of the section is generally less than 10 centimetres thick and is olive brown in colour. A widespread bioturbation and presence of dropstones at various depths are also characteristic of this sedimentation. Two cores (AT 116G and AT 119G) containing the above described sediment have been recovered from one of the two investigated pockmarks. The accuracy of ship positioning and the relatively large dimensions of the seafloor targets indicate that they are correctly located. Gas seepage in a pockmark may involve discrete portions of the sediment, leaving the surrounding areas relatively undisturbed. Cores AT 116G and AT 119G are interpreted as coming from these undisturbed, non gas-bearing, parts of the pockmark.

Two of the gravity cores (AT137G and AT138G) and two box cores (AT142B and AT143B)

aimed at recovering gas bearing sediments but did not show evidence for presence of gas. It is possible that the sea bottom targets were missed because of their small dimension (less than 100 meters in diameter). Box core AT 141G also recovered the topmost part of the hemipelagic section but failed to recover the carbonate crusts and benthic organisms seen on the TV records. The patchy distribution of both benthic organisms and crusts on the seafloor is responsible for the missing of the target.

The other seven cores recovered from this area all show evidence of gas seepage and /or mud expulsion processes. The different type of evidence will be briefly discussed:

*Presence of gas in the sediment*

Six of the seven cores contain sediment that gives off a strong $H_2S$ smell. The strong $H_2S$ smell was only noted in cores taken from seabed features connected to fluid seepage/mud expulsion processes and is not present in cores taken from adjacent areas. Additional evidence for high gas content is provided by cracks in the sediment of cores AT121G, AT139G and AT140G that are probably due to gas expansion. Hydrogen sulphide is a product of biologically mediated sulphate reduction. The two most common reactions involve organic matter or methane as reducing agents:

Organic matter oxidation

$$2CH_2O + SO_4^{2-} \rightarrow H_2S + 2HCO_3^-$$

Methane oxidation

$$CH_4 + SO_4 \rightarrow HCO_3^- + HS^- + H_2O$$

The first reaction defines the sulphate reduction zone of the sediments, which lies under the aerobic respiration zone and overlies the zone of methane generation. In the Vøring Plateau-Storegga Slide area, the boundary between the aerobic respiration zone and the sulphate reduction zone lies at a depth of about 2 to 12 centimetres and is evidenced by a colour change (from olive brown to olive grey). Although this process is responsible for the production of a certain amount of $H_2S$, it cannot account for the great difference in $H_2S$ concentration from core to core. The high $H_2S$ content found in the six cores is probably

produced when rising methane is oxidised by the dissolved sulphate (reaction 2, above).

The three cores containing mud volcanic or associated sediments (AT120G, AT121G and AT122G) are characterised by the presence of flame-like gas escape structures that indicate gas movement in the sediment. The presence of authigenic carbonates in the flame-like structures will be discussed below

The presence of gas-related structures in core AT139G is probably a consequence of its vicinity to the main scarp of the Storegga Slide. Seismic lines show that the depression from which it was taken lies 700 m from the main scarp and it overlies gas-saturated sediments. It is possible that the upward movement of gas was initiated by the formation of a new scarp, located in correspondence with the cored depression. Alternatively, gas escape in the slope area behind the main scarp may have initiated slope failure.

*Methane-related diagenesis*

Authigenic carbonates occur both in sediment from the pockmarks and from those in mud volcanoes. In pockmarks a discrete level of subrounded centimetric carbonate nodules was found at a depth of 4.5m and 5.5m (cores AT117G and AT118G respectively). Since the OKEAN side-scan sonar has a maximum sub bottom penetration depth of more than six meters, the carbonate nodules could be responsible for the high backscatter associated with the pockmarks.

The light grey flame-like structures in the hemipelagic sediments overlying mud flows (cores AT 120G, AT 121G and AT 122G) contain numerous soft to semi-indurated calcareous nodules. Similar structures are also present in core AT 139G. The colour of the flame-like structures and of the nodules varies from light grey to whitish, indicating a higher carbonate content than the surrounding grey coloured hemipelagics. The tops of these three cores also contain aggregates of cemented bivalves.

The occurrence of these three types of authigenic carbonates is probably linked to the migration and oxidation of methane (reaction 2, above). When methane is oxidised the alkalinity of the pore waters is increased and eventually precipitation of carbonates is induced.

## IV.3. EASTERN VØRING PLATEAU

### IV.3.1. Seismic Profiling Data

*A. Akhmetzhanov and E. Yakovlev*

Seven single-channel seismic lines were shot in the area of the Vema Dome known for its diapir fields (Hjelstuen et al., 1997). Four lines were run downslope and one was transverse to them in order to obtain a better correlation (Fig. 71). The most important lines are described as follows.

Line PSAT-74

The line runs from SE to NE and penetration is about 800 m. From 21:00 to 23:10 several seismic units can be clearly identified. The upper unit is 100 ms thick and comprises a package of numerous high-amplitude parallel reflectors. The reflectors are continuous and can be traced over the entire line. Between 21:20 and 21:40 several acoustically semitransparent lens-like bodies are observed in the lower part of the package. Their length is about 4 km and they are 20-30 ms thick. Downslope the uppermost package downlaps on the underlying sequence, and it thins in the upperslope part where two small notches are observed.

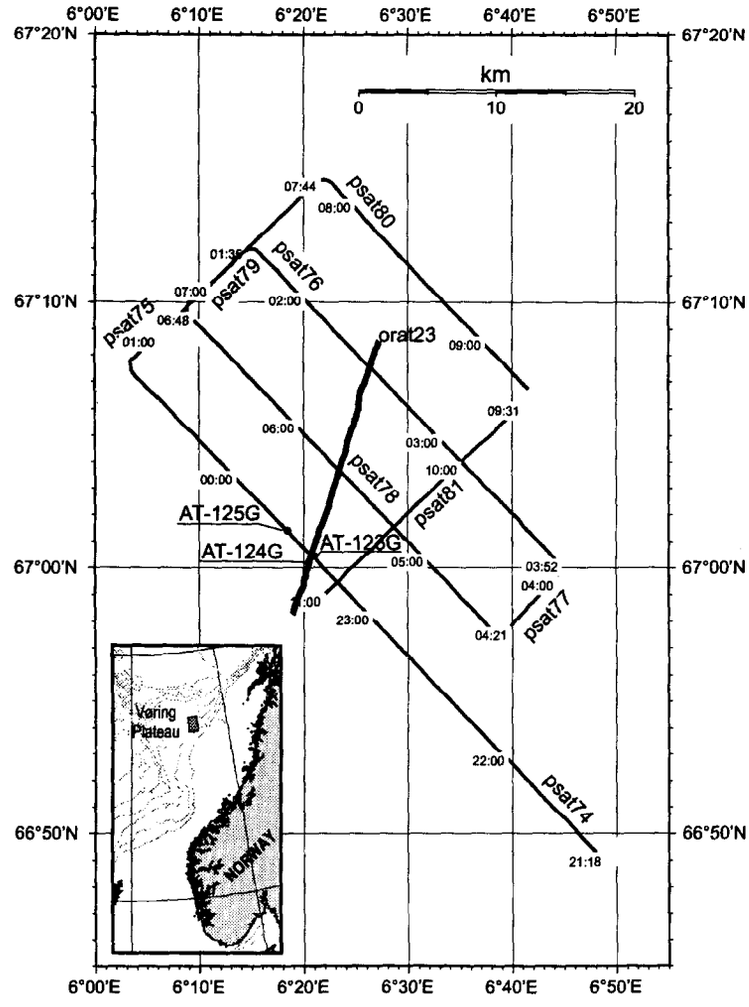


Fig. 71. Location map of the northeastern Vøring Plateau

The underlying sequence is represented by a set of acoustically transparent units separated from each other by prominent high-amplitude events. The upper one is lens-shaped and pinches out at approximately 22:40. Most of the units have a near constant thickness of about 150 ms. Only the third unit has a different geometry, being about 75 ms thick, becoming much thinner at 22:10 and getting thicker again downslope and finally pinching out at 23:20. From 23:20 to 0:40 the seismic pattern changes significantly. The uppermost well-stratified package is disturbed by the presence of seabed mounds which are about 100 ms high and 2-4 km long. They have a complex morphology at their upper surface which probably has multiple tops. In some cases they are covered by the uppermost package but in others it is not so evident due to the rough character of the upper surface. The mounds have a chaotic internal structure which probably is a reason for the strong scattering of the acoustic energy within them. It results in significant loss of acoustic penetration underneath the mounds. At only one place (0:30) is it seen that the mound does not extend downward below the second transparent unit. Between mounds the uppermost package is found and it is likely that the transparent units are also present although high-amplitude reflectors are imaged very poorly. Between 23:20 and 0:20, at the depth of 2.3-2.4 s, there are several discontinuous high-amplitude reflectors whose geometry suggests the presence of a broad dome-like structure. Only the top of the structure is recorded.

Line PSAT-78

The sedimentary sequence consists of the same seismic units, including the uppermost well-stratified package and 6 transparent units underneath. The upper package is thicker in the southeast where it infills a gentle basin formed by the undulating surface of the upper transparent unit. At the lower part of the uppermost package there are several lens-like acoustically transparent bodies. From 5:00 to 6:20 an upper surface of the Vema Dome is seen on the record. The top of the dome is found at a depth of 1.5 sec. The dome protrudes through the sequence of transparent units, pushing them up. As a result the seabed is also upraised above the dome although the presence of an elevation has been partially masked by the uppermost package. The upper surface of the dome has a broken outline suggesting some faulting. The internal structure cannot be resolved and only a chaotic pattern of rare weak seismic reflectors is observed.

Above the dome several mounded features are encountered on the seabed. The largest one is found at about 5:15 where its height is about 75 m. The internal chaotic structure of the mound is similar to those observed on PSAT-74. In spite of poor penetration below the mounds, the presence of the second and third transparent units is seen. Besides the large mounds with chaotic internal pattern there are several smaller mounds, which are found mainly within the uppermost package, and which are acoustically transparent. They have almost no expression on the seabed relief. To the northwest there are four other mounds, three of which are 50–75 m high and have chaotic internal structure, and one at 6:18 is an acoustically transparent feature.

Line PSAT-76

This line is comparable to the others, having a similar set of seismic units with the well-defined Vema Dome seen between 3:20 and 1:40. Above the dome, two large, complex-shaped mounded features appear on the seabed (Fig. 72). Their lengths vary from 3 to 4 km. They seems to be 250 ms thick lens-like bodies with chaotic internal structure, although their lower boundaries are poorly seen. The upper surface of the mounds is usually complicated with several small acoustically transparent bodies or mounds which creates a rough topography on the seafloor. Similar features are seen between the large mounds where they are present within the uppermost well-stratified package. To the southeast, the dome-like structure abuts on at least five transparent units, including the first one which wedges out at 3:20. At the contact zone (at 2:50) the presence of an overthrust is suggested, although it is not clear whether it is a part of the dome or it is formed by one or several transparent units. At 3:00 and 3:30 the line reveals two fragments with chaotic character which occur within the second transparent unit. This may be caused by the presence of buried mounds.

Line PSAT-80

The line shows all the previously described units. The top of the dome lies deeper and is found at a depth of 2.5 s. As for other lines, a mounded complex is found above the dome. It has the same appearance but the mound bases are resolved better and their concave shapes are observed. The other mound is seen at 9:10 and it is located aside from the dome. The lack of penetration below the mound makes it difficult to establish its relationship with host sediments. At least four transparent units are observed.

Line PSAT-81

The line runs parallel to the slope and is transverse to the rest of the lines. All the main

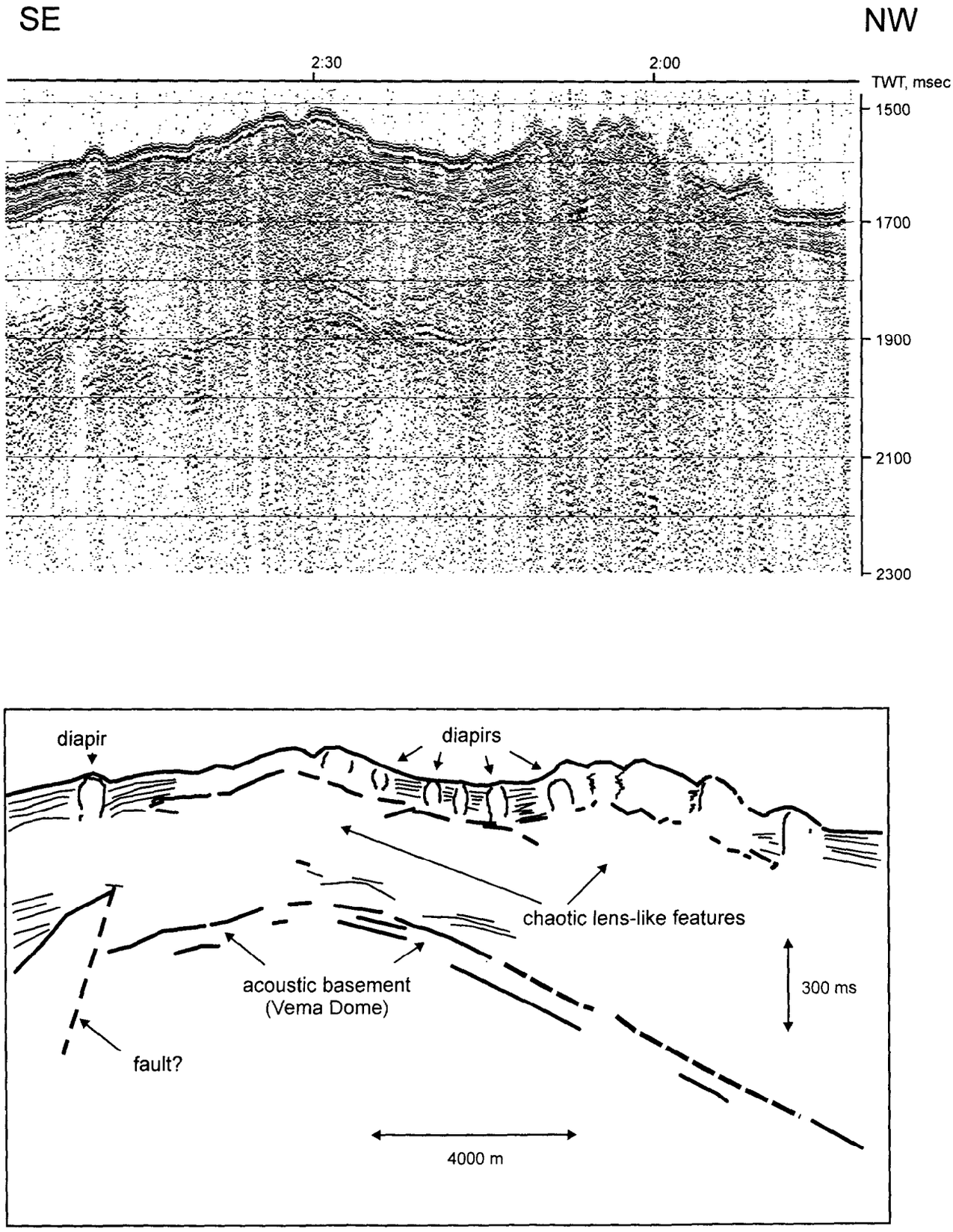


Fig. 72. Fragment of seismic line PSAT-76 and its interpretation (lower panel) showing numerous diapir-like structures above Vema Dome.

previously described units are identified. Vema Dome is seen between 9:50 and 11:00 and its top is found at the depth of 2.2 s. The seafloor above the structure is mounded and one of the mounds (at 10:30) is particularly massive, being about 90 m high and 3.5 km long. It has a relatively flat top and steep slopes, which results in a characteristic box-like shape. The concave base of the mound is resolved by the line. Two smaller mounds are found on both sides of the large one. To the northeast of the dome-like feature at least four transparent units are seen and they probably correspond to the transparent units 2, 4, 5 and 6 described on PSAT-74. At 9:30, between the second and fourth units, the seismic record shows a 100 ms lens-like, acoustically transparent body which can be interpreted as the buried mound also imaged on PSAT-80.

*Discussion*

The sedimentary sequence studied by the seismic profiling reveal some features typical for glaciated margins. Acoustically transparent units are thought to be debris flow packages which were reaching this area during glacial periods (Henriksen and Vorren, 1996). High amplitude reflectors between the transparent units probably correspond to interglacial time when low-energy hemipelagic sedimentation prevailed. The uppermost package is also a result of significant change in depositional mode, probably with dominant turbidites or contourites, although some influence of debris flow activity has been observed in the lower part. Seismic records showed that some mounds or diapirs are arranged into large lens-like features with complex surface morphology mainly found above Vema Dome.

### IV.3.2. Side-Scan Sonar Data

*A. Akhmetzhanov, M. Ivanov, E. Yakovlev.*

Approximately 750 km$^2$ of the seafloor were mapped with OKEAN long-range side-scan sonar. The obtained image doesn't show much and most of features are seen because of their relief expression. A number of mounds were imaged (Fig. 73). Some of them are seen when crossed by the ship track and appear as isometric high backscatter patches, 3-4 km in diameter. The others are elongate and are found mainly at the northwestern part of the surveyed area. They can be 4-5 km long and are NW-SE oriented, although some have a W-E orientation. Apart from the mound at the southeastern edge of the area several linear high backscatter features are imaged. They are interpreted as downslope running channels probably filled with coarse sediments.

The OREtech line 23 was run oblique to the seismic and OKEAN lines and was intended to cross several mounds seen on the seismic data. The backscatter level is generally medium along the line. Observed backscatter variations in most cases are caused by topography. Between 19:00 and 20:30 the sonograph shows a pattern of moderate to low backscattering features indicating the presence of small-scale roughness of the elevated part of the seafloor corresponding to one of the mounds observed on the seismic data. This roughness is also seen on the subbottom profiler record. From 20:30 to 21:30 the sonograph reveals smooth seafloor and then from 21:30 to 23:30 another mound is crossed and the seafloor again has rough topography. The southern edge of the mound is relatively upraised forming an upstanding block with steep slopes and flat top.

At some places (e.g. 22:30) there is evidence of local slope instability as small slides are observed on the sonograph. From 23:30 to 0:00 the line crosses another intermound area with smooth seafloor. From 0:00 to 2:00 the topography becomes rougher again and a mound rises above the seafloor for about 100 m. On the sonograph it appear to be a ridge-like feature with multiple tops seen also on the subbottom profiler record (Fig. 74). The ridge has a complex

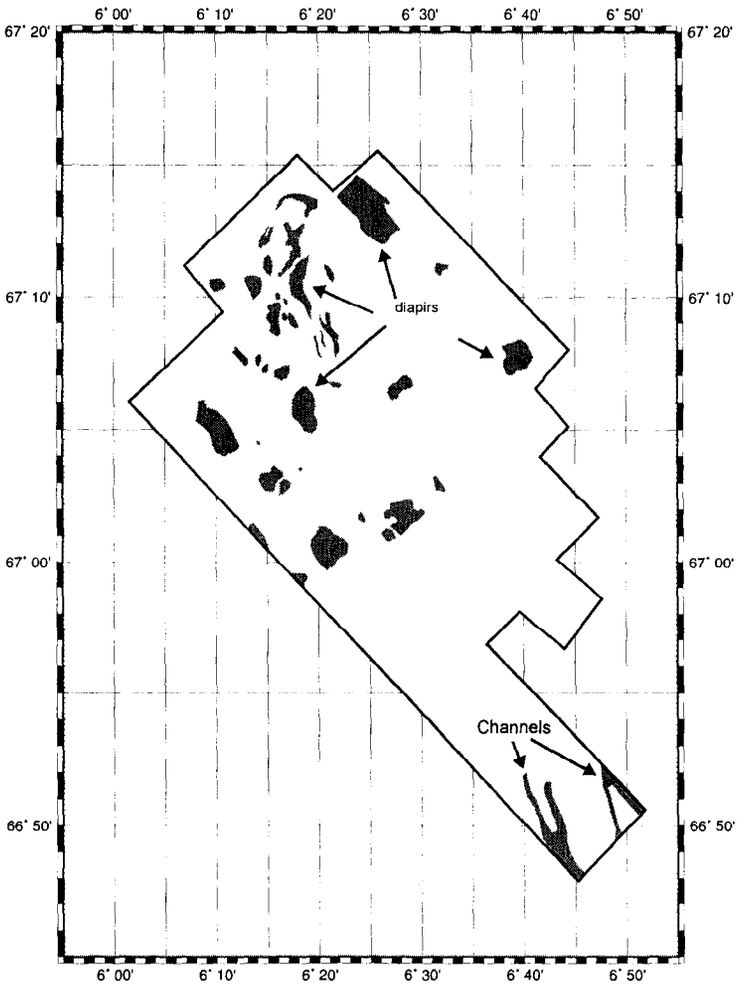


Fig. 73. Interpretation of OKEAN mosaic showing distribution of diapiric structures in Vema Dome area.

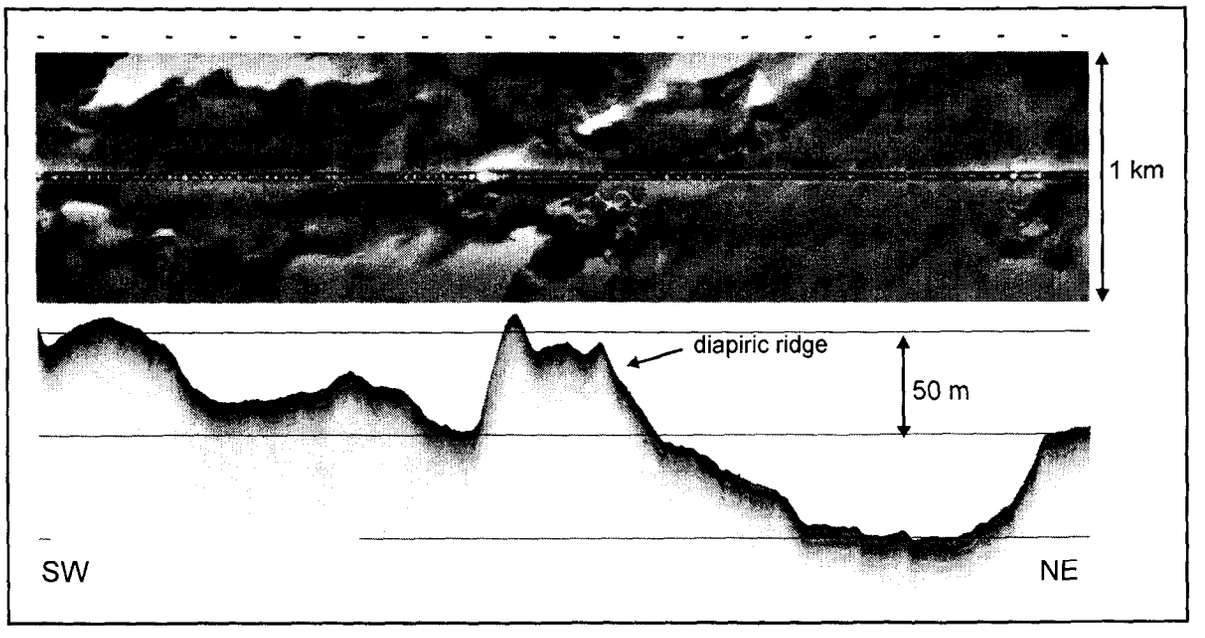


Fig. 74. Fragment of ORAT-23 sonograph and subbottom profiler record showing a diapiric ridge above Vema Dome.

morphology and is composed of several smaller parallel ridges arranged into an en echelon pattern. On some of the slopes evidence of sediment failure is observed.

The subbottom profiler revealed that the mounds are covered with an approximately 10 m thick veneer of well stratified sediments, which is a good explanation for the low backscatter level and smoothed outlines of the seabed features.

### IV.3.3. Bottom Sampling

*G. Akhmanov, A. Stadnitskaya, E. Kozlova, A. Wheeler, A. Akhmetjanov,*
*G. Aloisi, B. De Mol, A. Sautkin, I. Belenkaya, S. Lubentsova, M. Kozachenko, I. Mardanyan*

The aim of the sediment sampling program in this area was basically to obtain material from the diapiric bodies. Two long gravity cores were recovered: one from the top of an assumed diapir; the second from its slope (Fig. 75). A third core was taken as a reference core from a flat area not far away from the mound.

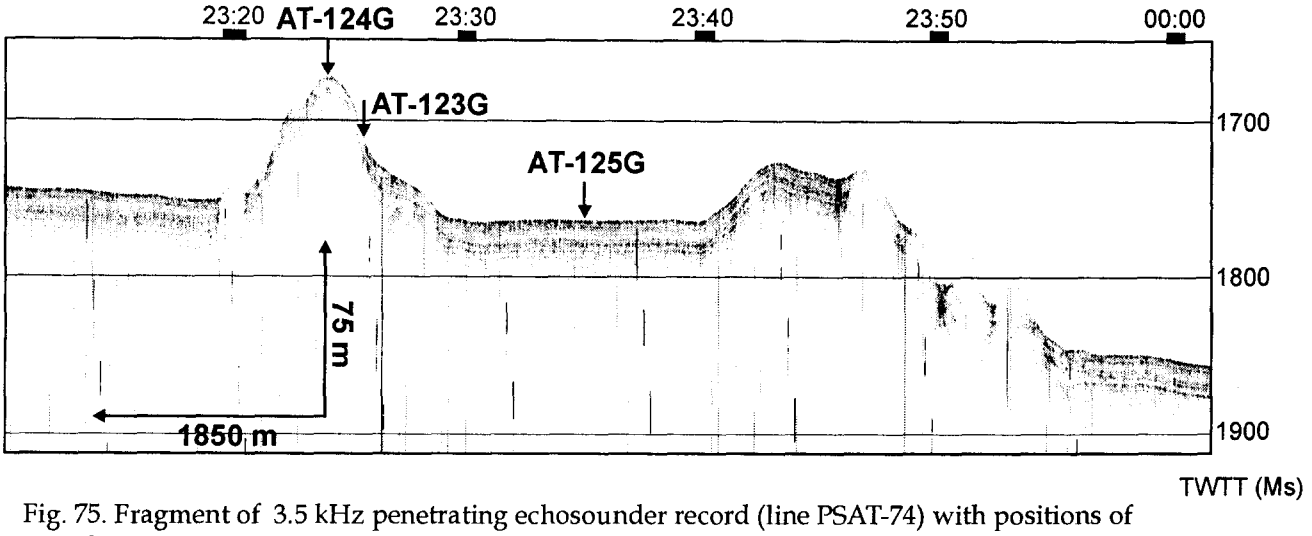


Fig. 75. Fragment of 3.5 kHz penetrating echosounder record (line PSAT-74) with positions of sampling stations.

| Station No | Date | Time (GMT) | Latitude | Longitude | Depth, m | Recovery, Cm |
|---|---|---|---|---|---|---|
| TTR8-AT-123G | 15.07.98 | 12:34 | 67°00.451N | 6°21.012E | 1198 | 342 |
| TTR8-AT-124G | 15.07.98 | 13:47 | 67°00.202N | 6°20.465E | 1173 | 320 |
| TTR8-AT-125G | 15.07.98 | 15:08 | 67°01.394N | 6°18.442E | 1262 | 308 |

**Table 9.** General information on the sampling stations

Sampling site locations in the area were chosen from subbottom profiles, side-scan sonographs, and seismic lines collected during the present cruise. Basic information on sampling sites were summarised in tables 9, 10.

| Station No. | Geographical Setting | Sedimentary Summary | Instrumentation | Acoustic characteristics |
|---|---|---|---|---|
| TTR8-AT-123G | Steep slope of the mound on the northern part of the Vøring Plateau | Hemipelagic structureless grey silty clay, bioturbated, with hydrotroilite-rich lenses, with a few dropstones. Upper interval is oxidized | Seismic, OKEAN side-scan sonar and onboard profiler line PSAT-74, 23:25,5, OREtech profile ORAT-23 | Moderate backscatter on the OKEAN and OREtech images, no penetration on the onboard profiler |
| TTR8-AT-124G | Top of the mound on the northern part of the Vøring Plateau | Hemipelagic structureless grey silty clay, bioturbated, with hydrotroilite-rich lenses, with a few dropstones. Upper interval is oxidized | Seismic, OKEAN side-scan sonar and onboard profiler line PSAT-74, 23:24,5, OREtech profile ORAT-23 | Moderate backscatter on the OKEAN and OREtech images, no penetration on the onboard profiler |
| TTR8-AT-125G | Flat surface between two mounds on the northern part of the Vøring Plateau | Hemipelagic structureless grey silty clay, bioturbated, with hydrotroilite-rich lenses, with a few dropstones. Upper interval is oxidized | Seismic, OKEAN side-scan sonar and onboard profiler line PSAT-74, 23:36, OREtech profile ORAT-23 | Moderate backscatter on the OKEAN and OREtech images, parallel well-layered sequence on the onboard profiler |

**Table 10**. Sedimentological, acoustic and geological characteristic of sampling stations..

Core TTR8-AT-123G (Fig. 76)

A 342 cm long core was recovered, presenting an hemipelagic Holocene-Upper Pleistocene succession composed mainly of homogeneous grey silty clay, occasionally bioturbated throughout the whole core and with darker mottles of sediments enriched in hydrotroilite. The uppermost interval is brown in colour due to surficial oxidization. The presence of dropstones randomly distributed throughout the core suggests a supply of ice-rafted material affecting sedimentation in this area during the Upper Pleistocene. Although the core was taken on the slope, no evident slumping structure was described.

Core TTR8-AT-124G (Fig. 77)

The 318 cm of sediment recovered mainly showed the same hemipelagic sedimentary pattern as observed in the core from the slope (AT-123G). The succession is represented mainly by structureless grey silty clay, bioturbated throughout the whole core, with darker mottles and lenses enriched in hydrotroilite, reflecting prevalent hemipelagic sedimentation in the area. Several dropstones were found to be randomly distributed, implying a contribution of ice-rafted material to the Upper Pleistocene sedimentation. The uppermost interval was oxidized.

Core TTR8-AT-125G (Fig. 78)

The recovery of 308 cm consisted of structureless silty clays, affected by bioturbation, with mottles, lenses and layers enriched in hydrotroilite. The uppermost part of the core was brown in colour due to surficial oxidization. A few dropstones found in the core suggest an influence of ice-rafted material on the sedimentation. The succession recovered in this core did not show any significant difference from the sedimentary pattern of the cores taken from the mound.

It can be concluded from the coring result that the main mound body is probably blanketed with an at least 4 m thick veneer of the Holocene-Upper Pleistocene hemipelagic sediments, implying a relatively recent burial.

The sedimentary record in the core taken from the mound slope did not show any evident slope process activity. Such slope stability suggests the absence of significant tectonic movements in the area.

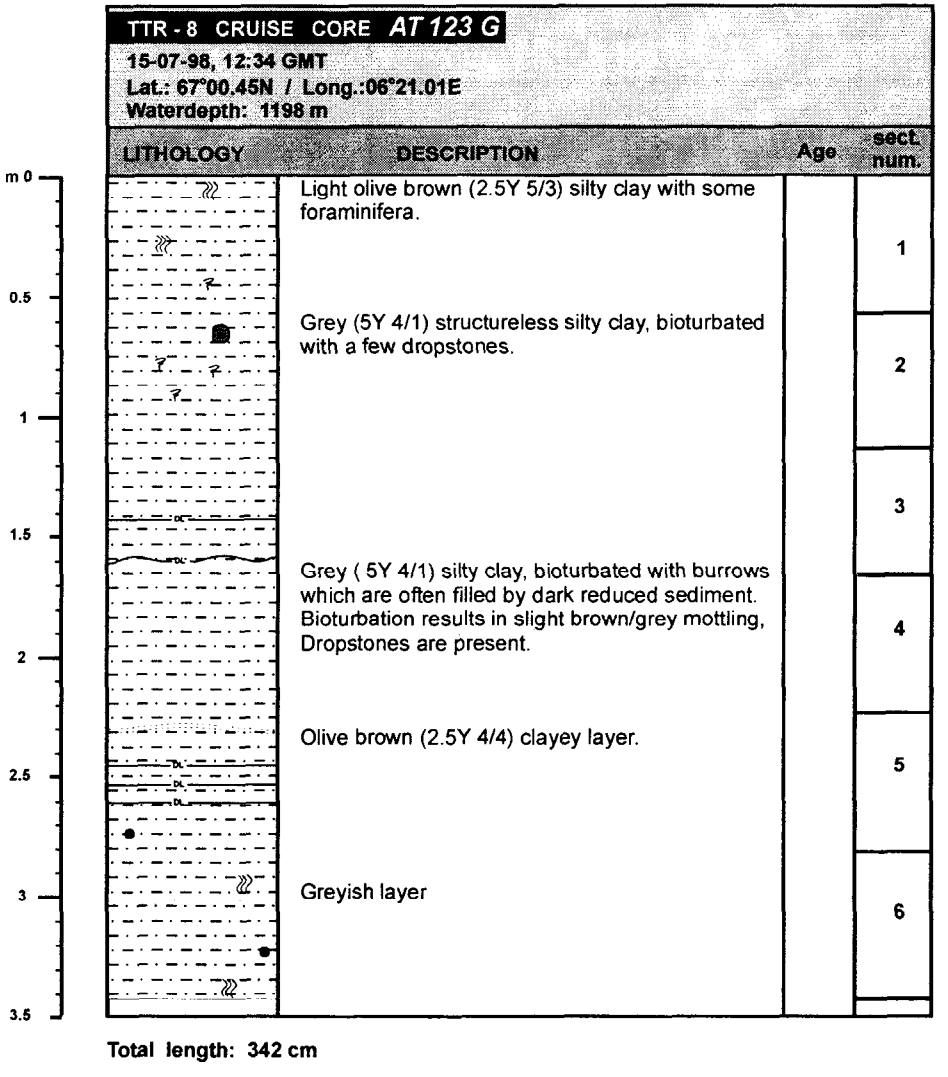


Fig. 76. Core log AT-123G.

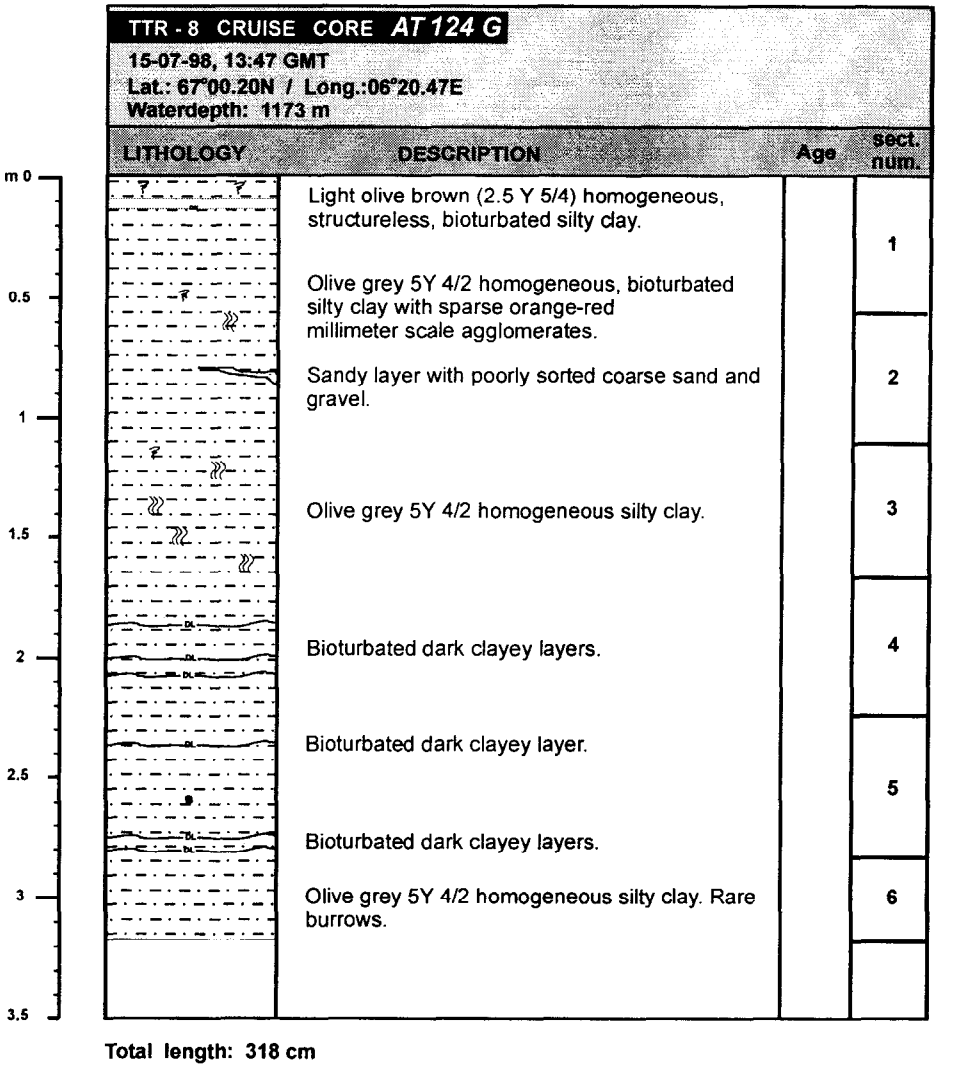


Fig. 77. Core log AT-124G.

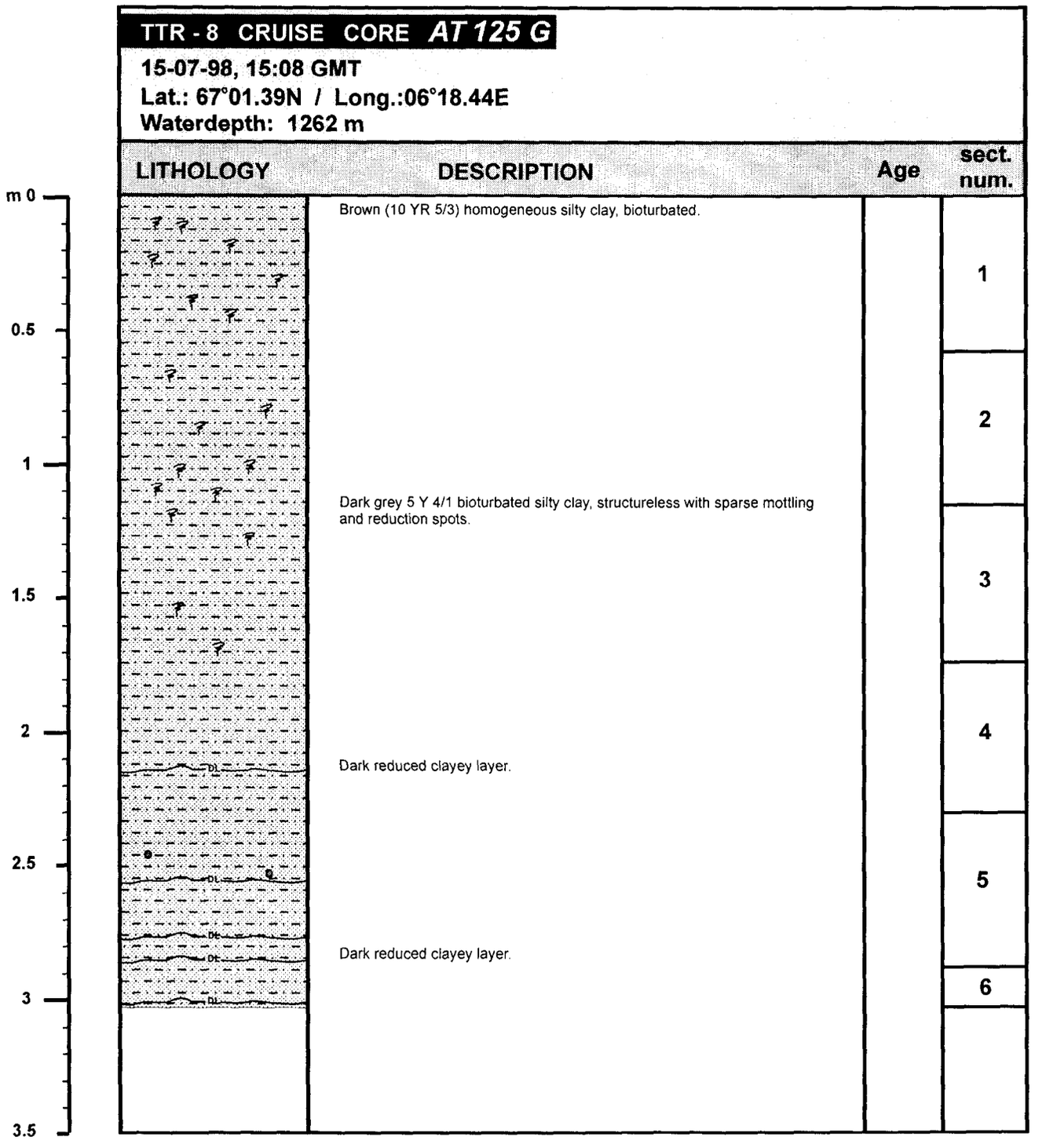


**Total length: 308 cm**

Fig. 78. Core log AT-125G

# IV.4. BEAR ISLAND AREA

## IV.4.1. Seismic Profiling Data

*R. Pevzner, B. De Mol, and S. Bouriak*

Seismic profiling was carried out in the Haakon Mosby mud volcano area near Bear Island. Twelve profiles (PSAT82-PSAT93) were collected and their total length is about 395 km (Fig. 79). The longest lines have a NE-SW orientation (PSAT82, 84, 86, 88, 90, 92), perpendicular to the SW dipping slope. Generally, penetration reaches 0.6 s with a best resolution of about 20-25 ms.

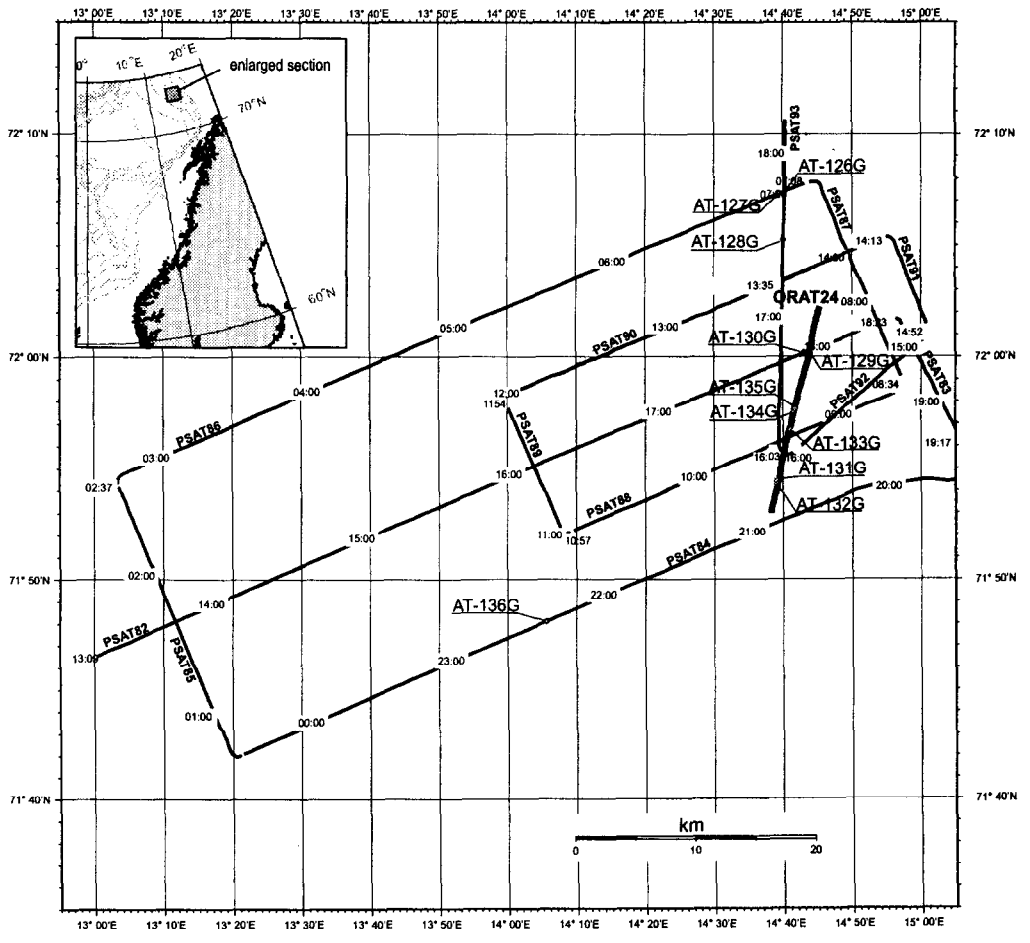


Fig. 79. Location map of Bear Island Trough Mouth area

The seafloor morphology is generally smooth, gently dipping to the south-west from 1450 to 2550 ms TWT. The bottom reflector is generally of high amplitude and is disturbed only where mud diapirs and the Haakon Mosby mud volcano are encountered. A scarp is recognized in the seafloor topography on the northern-most part of the survey area, which is also seen on the OKEAN mosaic. In fact, almost the whole area is located within a large slide, oriented in a SW direction (Saettem et al., 1992).

The seismic section was divided into 4 main acoustic units (Fig. 80).

The lower boundary of the first unit is the acoustic basement. This is a rather weak flat (undisturbed) reflector, which can be traced on most of the longer lines. Thickness of the

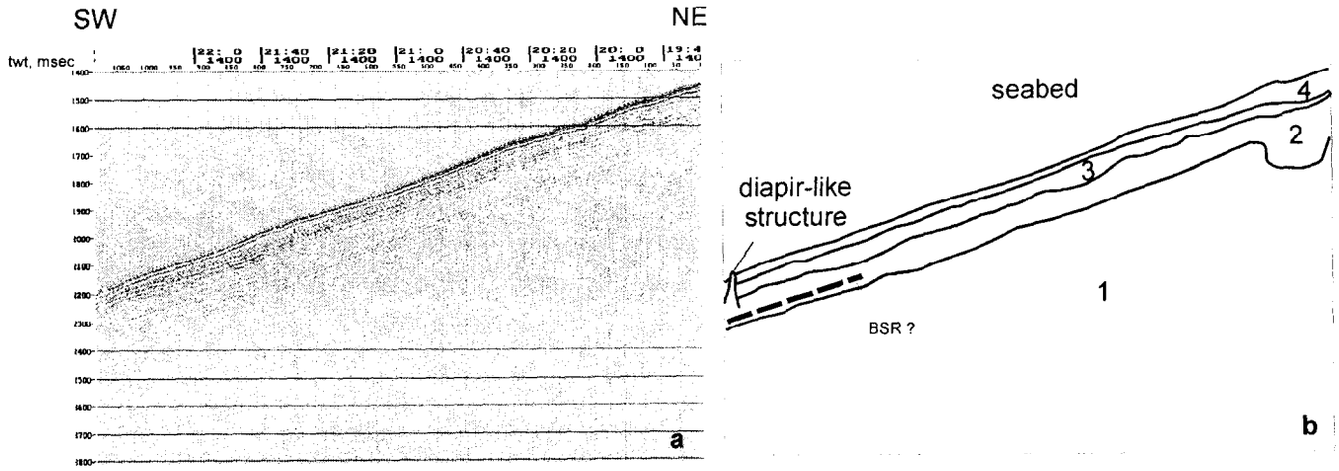


Fig. 80. Fragment (a) and interpretation (b) of seismic line PSAT-44 showing main seismic units in the area.

unit 1 tends to increase to the north and reaches 300-350 ms TWT. The unit shows a chaotic pattern with some weak reflectors.

Unit 2 is separated from unit 1 by a strong continuous reflector, usually parallel to the sea floor and rather flat. Its thickness varies from 100 up to 250 ms and increases to the south and to the west with minimum values on the uppermost part of the slope. Some weak parallel reflectors could be observed inside the unit. Also there is one internal, high amplitude reflector, which can be traced on profiles PSAT84, 86, 90, 89 and 82. The behaviour of the reflector is similar to that of a Bottom Simulating Reflector (BSR).

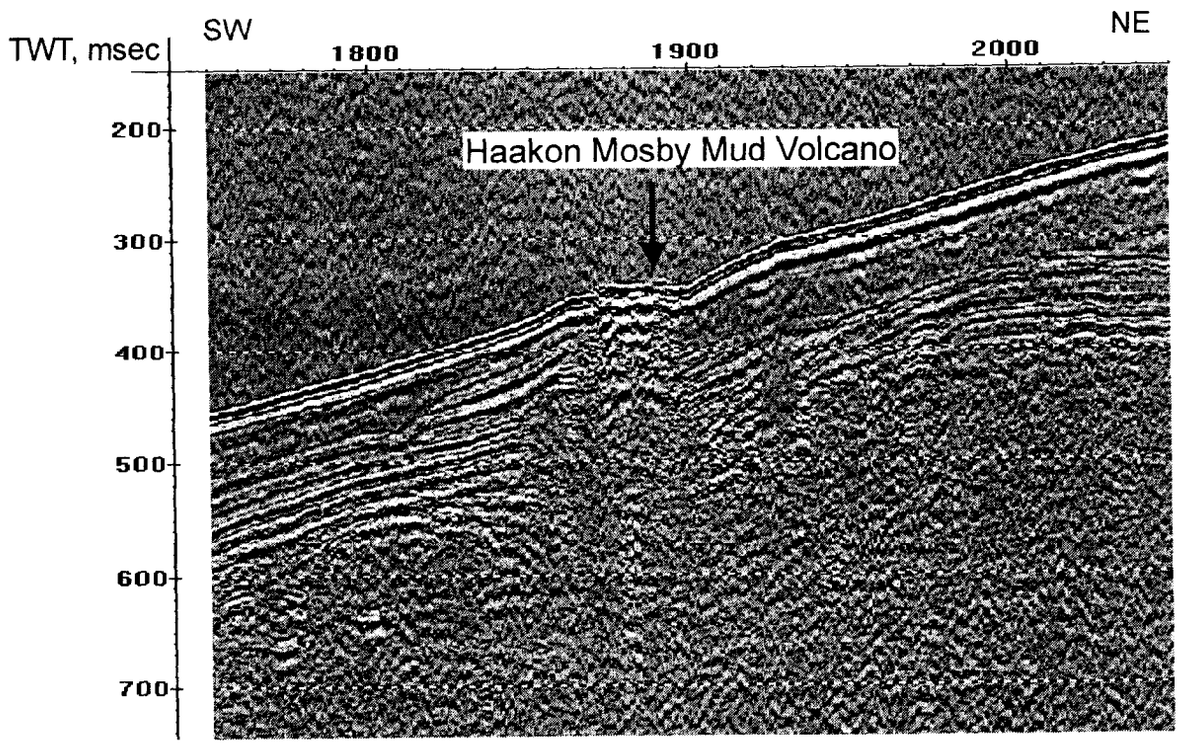


Fig. 81. Fragment of seismic line PSAT 82 across Haakon Mosby mud volcano

The thickness of Unit 3 varies from 0 up to 100 ms TWT and its internal structure is characterised by a pattern of parallel continuous reflectors.

Unit 4 has a chaotic internal structure. Its thickness varies from 0 to 150 ms (in a valley like structure in the uppermost part of the area).

Seismic line PSAT82 crosses the Haakon Mosby mud volcano at about 17:50 (Fig. 81). It appears as a flat topped elevation, expressed on the seafloor. The crater is about 1 km in diameter. Below the surface a number of low frequency strong reflectors can be recognized. Below them, an acoustically transparent zone presumed to mark the feeder channel of the mud volcano is presented. Two faults are seen on the profile (at 13:17 and 16:45). One of them seems to be associated with Haakon Mosby mud volcano (17:50) and another with a diapir-like feature (13:35). The trend of the faults is NW-SE and they dip to the SW.

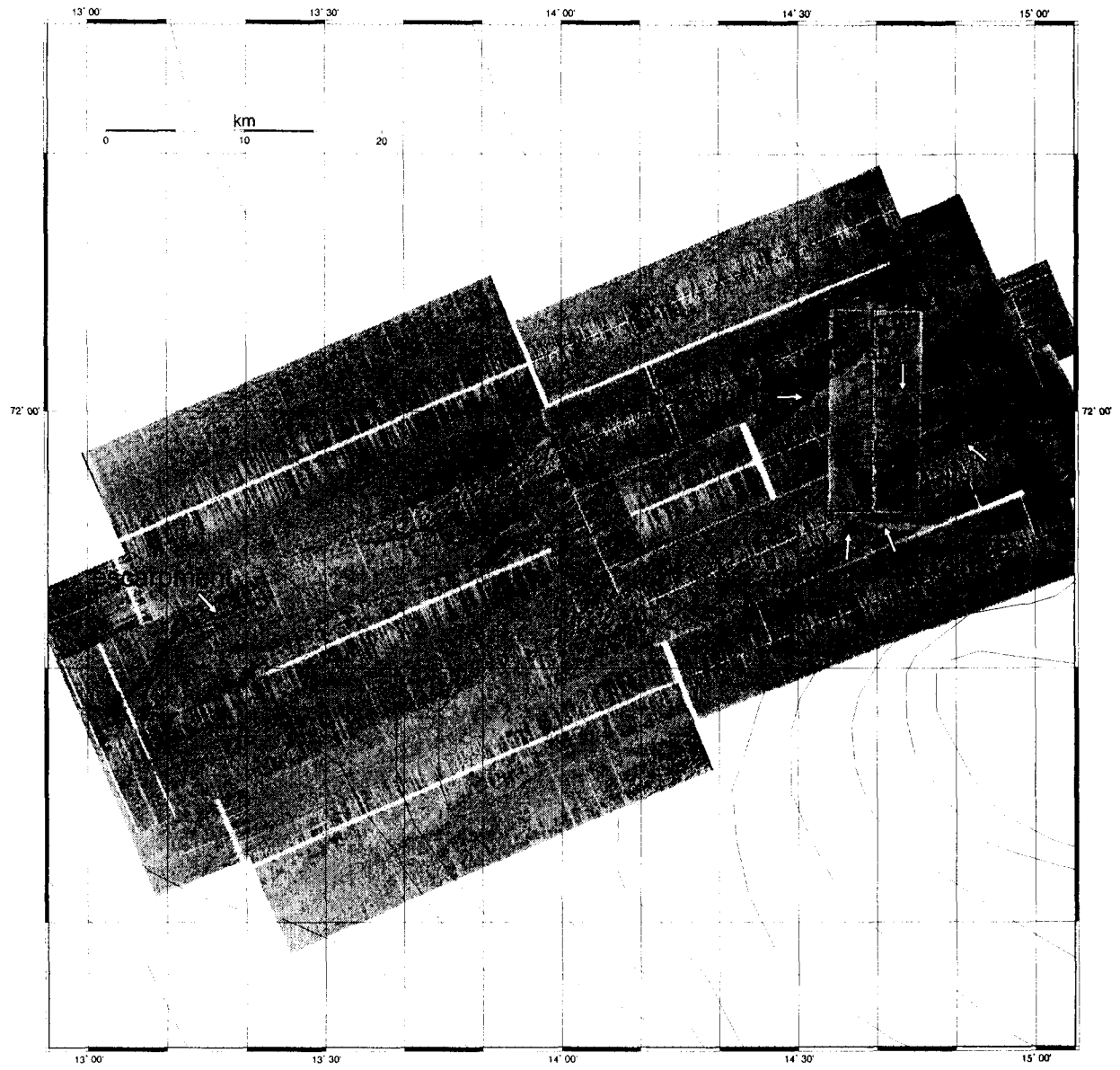


Fig. 82. OKEAN mosaic of the study area on the margin south of Bear Island.

There are several diapir-like features observed on the seismic lines. Usually they have acoustically transparent cores and show pull-ups of the internal reflectors of hosting sediments. Although the diapirs are distributed quite randomly, a certain trend along the contours of the upper part of the slope can be inferred.

### IV.4.2. Side-Scan Sonar Data

#### Description of OKEAN mosaic from the Bear Island area

*A. Wheeler*

The OKEAN long-range side-scan sonar mosaic from the Bear Island area images is shown in Fig. 82. The survey was completed in order to build up an understanding of the seabed morphology in the area surrounding the Haakon Mosby mud volcano and with a view to discovering further gas-escape features.

The Haakon Mosby is represented by a ring of low backscatter with a moderately high backscattering core. No other similar features are apparent on the mosaic.

The OKEAN is imaging the Bear Island slide described by Laberg and Vorren (1995). Numerous large-scale lineations are seen on this image and consistently trend SW-NE. These lineations are gently curved or scallop shaped. Three areas of lineation are defined. The first occurs in a band on the northwestern side of the mosaic and may represent one continuous feature with associated shorter sub-parallel lineations. This lineation is consistently seen as a line of high backscatter in the same relationship to the fishtrack and is interpreted as a scarp with its down-thrown side to the south. The second area of lineations is parallel to the first area and occupies the south-eastern area of the mosaic. Associated shorter sub-parallel lineations are also present. Backscatter interpretations inferred that this is also a scarp except that its down-thrown side is to the north. Also associated with this third area of lineations are two sets of paired lineations running perpendicular to the general trend. Both of these sets define an area of low backscatter bounded by the two high backscatter lineations. The sharpness of these lineations is more diffuse suggesting a lower amplitude topographic feature. These may represent the terminations of mud flows. The third area of lineations occurs between the other two areas but is only present in the eastern side of the mosaic in the same area as the Haakon Mosby mud volcano.

Numerous spots of high backscatter are also visible on the mosaic and are usually concentrated in the vicinity of the lineations. It is not possible to say whether these are poorly imaged continuations of the lineations or whether these are pockmarks or mud diapirs. In the eastern part of the image, south of the Haakon Mosby mud volcano, a group of large dark spots are clearly imaged and they appear to be shallow ovate mounds.

#### High resolution OREtech line Orat 24

*R. Pevzner and A. Akhmetzhanov*

Orat 24 OREtech side-scan sonar line runs from north to south across the Haakon Mosby mud volcano.

The northern part of the line has low backscatter. The Haakon Mosby mud volcano is the only contrasting feature and appears as an isometric, or slightly elongate in SN direction, circular structure (6:20 to 6:30) (Fig. 83)

In the centre of the mud volcano there is an irregularly shaped area of very strong backscatter. To the west of the centre the image is a rather complicated pattern of several angular clusters of low backscatter separated from each other by narrow dark stripes.

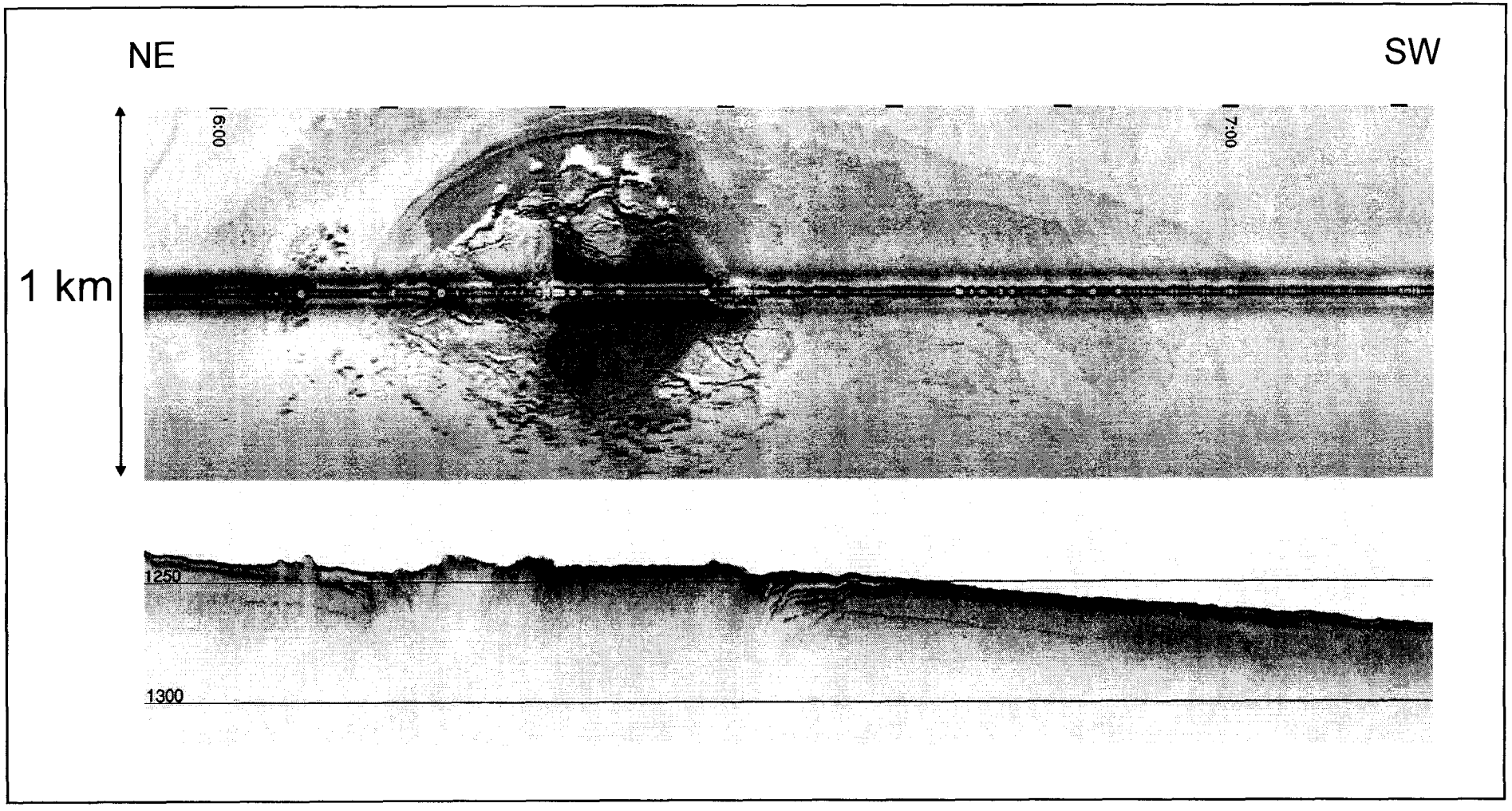


Fig. 83. Fragment of ORAT-24 sonograph and subbottom profiler record showing Haakon Mosby mud volcano.

This pattern is caused by the presence of large displaced blocks of sedimentary cover on the seafloor. They seem to be larger on the eastern part of the volcano (6:20 to 6:30). In the vicinity of the crater there are several curvilinear features which are interpreted as cracks.

Irregular elongate tongue-like features of relatively high backscatter observed to the south are likely to be mud flows spreading out of the crater of the mud volcano.

The subbottom profiler record shows that the sea floor along this part of the line is covered by a 2-3 m thick acoustically transparent layer of presumably hemipelagic sediments. Close to the mud volcano the sedimentary section is a well-bedded package, up to 25 m thick, which probably represents a sequence of mud flows interbedded with hemipelagic layers.

The middle part of ORAT 24 line has a contrasting, moderate to high backscatter pattern caused by irregular topography. There are some isometric mounds approximately 50-100 m in diameter surrounded by flat areas of high backscatter.

The subbottom profiler record along this part of the line shows a well-stratified sequence, up to 15 m thick, which is underlain by an acoustically transparent section. The mounds seem to be rooted in this section. At some places they penetrate through the stratified part of the sequence and form diapir-like features (8:10, 9:00). Some mounds are surrounded by depressions filled with finely layered sediments (8:50-9:00).

The middle and northern parts of the line are separated by a wide channel (9:40-9:55) seen on the sonograph as a band of low-moderate backscatter. Its depth is about 10 m and width is 200-500 m. The structure is elongate in a WE direction. The edges of the channel are marked by bands of higher backscatter up to 50-70 m wide. All layers observed on the northern side of the channel disappear on the southern side of it.

The southern part of the ORAT-24 sonograph is characterised by a low-moderate backscatter level. Some small (10 m in diameter) dark spots of irregular shape can be seen. Also there is one rather big patch (at 10:30) of moderate to high backscatter consisting of two groups of small isometric clusters. Each group contains 5-6 of them.

The subbottom profiler shows flat sea floor in this part of the area. There is only one irregular boundary, indicating the presence of an unconformity. The latter separates an eroded layer characterised by a strong acoustic return, from an overlying acoustically transparent veneer. Where the lower layer crops out at the surface the dark spots and patches described above are seen on the sonograph.

### IV.4.3. Bottom Sampling

*G. Akhmanov, A. Stadnitskaya, E. Kozlova, A. Wheeler, A. Akhmetjanov,*
*G. Aloisi, B. De Mol, A. Sautkin, I. Belenkaya, S. Lubentsova, M. Kozachenko, I. Mardanyan*

The area lying to south-west of the Bear Island has been an object of intensive marine investigations in recent years and is known for the discovery of the mud volcanic structure named Haakon Mosby (Vogt et al., 1997). The survey with seismic and OKEAN side-scan sonar systems performed during the present cruise detected several dome-like structures, well-expressed on seafloor morphology and with acoustic and seismic characteristics which allow us to assume a mud diapiric genesis. These assumed mud diapirs were the target for 5 sediment samples in this area. Two other cores were recovered from the Haakon Mosby mud volcano in order to obtain gas-saturated mud volcanic deposits for a comparison with diapiric material and to collect gas hydrates and authigenic carbonates connected to gas expulsion. Four additional cores were taken to characterize different acoustic facies on the OREtech profile ORAT-24.

Sampling site locations in the area were chosen on the basis of subbottom profiles, side-scan sonographs, and seismic lines collected during the present cruise. Basic information on sampling sites is summarised in Tables 11, 12.

| Station No | Date | Time (GMT) | Latitude | Longitude | Depth, m | Recovery, cm |
|---|---|---|---|---|---|---|
| TTR8-AT-126G | 18.07.98 | 20:30 | 72°07.491N | 14°40.358E | 1154 | 165 |
| TTR8-AT-127G | 18.07.98 | 21:29 | 72°07.356N | 14°39.420E | 1201 | 253 |
| TTR8-AT-128G | 18.07.98 | 23:12 | 72°05.243N | 14°40.079E | 1187 | 39 |
| TTR8-AT-129G | 19.07.98 | 00:47 | 72°00.249N | 14°43.933E | 1291 | 316 |
| TTR8-AT-130G | 19.07.98 | 01:47 | 72°00.202N | 14°43.091E | 1287 | 73 |
| TTR8-AT-131G | 19.07.98 | 14:11 | 71°54.323N | 14°39.060E | 1333 | 153 |
| TTR8-AT-132G | 19.07.98 | 15:11 | 71°54.445N | 14°39.070E | 1337 | 346 |
| TTR8-AT-133G | 19.07.98 | 16:26 | 71°56.753N | 14°40.975E | 1325 | 323 |
| TTR8-AT-134G | 19.07.98 | 17:23 | 71°57.539N | 14°41.562E | 1326 | 286 |
| TTR8-AT-135G | 19.07.98 | 18:17 | 71°57.653N | 14°41.795E | 1326 | 259 |
| TTR8-AT-136G | 19.07.98 | 20:56 | 71°48.101N | 14°05.620E | 1618 | 43 |

**Table 11.** General information on the sampling stations on the southern Bear Island margin

Core TTR8-AT-126G (Figs. 84, 85)

The 165 cm thick sequence recovered was composed of olive grey structureless, occasionally bioturbated silty clay, of Holocene - Upper Pleistocene age and of hemipelagic origin, interbedded with three intervals of a different lithology. The latter have a very dark grey, very stiff clay, structureless and poorly sorted, with gravel sized subangular fragments of consolidated clay. All of these intervals showed an oxidized upper part and irregular, sharp boundaries, and their thickness varied from 25 to 40 cm. They contained rare nannofossils suggesting an Eocene age for the material and were preliminarily interpreted as mud flows redepositing diapiric material downslope.

Core TTR8-AT-127G (Fig. 86)

The core recovered 253 cm of Holocene - Upper Pleistocene sediment and was mainly composed of olive grey silty clay with a sandy admixture and a few dropstones, reflecting hemipelagic sedimentation affected by bioturbation and ice-rafted material. The hemipelagic sequence was interbedded with an 80 cm thick very dark grey, stiff, silty clay, which is poorly sorted with fragments of consolidated clay and an abundant sandy admixture. The upper part of the interval was oxidized. The interval is mainly of a similar lithology and with structural peculiarities comparable with the mud flow deposits described in the core AT-126G. This suggests the same origin and the same source of the material. A convolute lamination observed in the upper part of the interval may also imply slumping as a mechanism of redeposition for diapiric material. This interval was overlain by a 15 cm thick debrite composed of fragments of hemipelagic silty clay in a clayey matrix, indicating down slope flow processes for that period. No evidence of gas presence was found.

Core TTR8-AT-128G (Figs. 87, 88)

The recovery was 39 cm of very stiff, very consolidated, structureless, silty clay with numerous dropstones and other rock fragments. The uppermost 32 cm were olive brown in colour due to surficial oxidation. The rest of the core was very dark grey. Very high consolidation of the diapiric material exposed on the seafloor caused poor penetration. Lack of a hemipelagic veneer suggests that the diapir is still growing.

Core TTR8-AT-129G (Figs. 89, 90)

The core contained 316 cm of homogeneous, structureless, strongly gas saturated clay with millimetre scale gas hydrates widespread throughout all of the sediments, which gave off a strong odour of hydrogen sulphide. The gas hydrates occur in the entire core as small clusters

of crystals up to 0.5 cm in diameter (Table 13, type 2) and three-dimensional irregular veins (0.5-2 cm) (Table 13, type 1). Occasional dropstones were also found.

| Station No. | Geographical Setting | Sedimentary Summary | Instrumentation | Acoustic characteristics |
|---|---|---|---|---|
| TTR8-AT-126G | Upper slope of the diapir structure in the northwestern part of the Bear Island Area | Hemipelagic succession of grey silty clay interbedded with three intervals of redeposited diapiric material | Seismic, OKEAN side-scan sonar and onboard profiler line PSAT-86, 06:59 | High backscatter on the OKEAN image, transparent layer on the onboard profiler |
| TTR8-AT-127G | Steep slope of the diapir structure on the northwestern part of the Bear Island Area | Hemipelagic succession of grey silty clay interbedded with the interval of redeposited diapiric material | Seismic, OKEAN side-scan sonar and onboard profiler line PSAT-86, 06:57 | High backscatter on the OKEAN image, transparent layer on the onboard profiler |
| TTR8-AT-128G | Top of the diapir structure on the northwestern part of the Bear Island Area | Very stiff, consolidated dark grey silty clay, oxidised at the top. Diapiric material | Seismic, OKEAN side-scan sonar and onboard profiler line PSAT-93, 17:28 | High backscatter on the OKEAN image, transparent layer on the onboard profiler |
| TTR8-AT-129G | Central part of the Haakon Mosby mud volcano | Homogeneous clay, very gas-saturated, with a few dropstones and abundant millimetric gas hydrate crystals | Seismic, OKEAN side-scan sonar and onboard profiler line PSAT-82 | High backscatter on the OKEAN image |
| TTR8-AT-130G | Southern levee of the Haakon Mosby mud volcano | Structureless, gas-saturated, grey clay with millimetric gas hydrate crystals underlain by *Pogonophora* mat interval and clayey layer very enriched in gas hydrates | Seismic, OKEAN side-scan sonar and onboard profiler line PSAT-82, 17:50 | High backscatter on the OKEAN image |
| TTR8-AT-131G | Flat surface to the south of the Haakon Mosby mud volcano | Stiff, structureless, poorly sorted clay of diapiric origin interbedded with debris flow deposit composed of mixture of hemupelagic sediments and diapiric material | OREtech profile ORAT-24, 10:33 | High backscatter on the OREtech image, |
| TTR8-AT-132G | Flat surface to the south of the Haakon Mosby mud volcano, close to AT-131G | Grey structureless silty clay, in lower part heavily bioturbated and with dropstones, is underlain by dark grey very stiff clay of diapiric origin | OREtech profile ORAT-24, 10:30 | Low backscatter on the OREtech image, no layered sequence |
| TTR8-AT-133G | Flat surface to the south of the Haakon Mosby mud volcano | Thick series of intercalated grey structureless silty clay and thin graded layers of fine-grained sand and silt of turbiditic origine | OREtech profile ORAT-24, 08:52 | Low backscatter on the OREtech image, well-layered sequence on the onboard profiler |
| TTR8-AT-134G | Flat surface to the south of the Haakon Mosby mud volcano | Hemipelagic grey silty clay interbedded with debris flow deposits and three layers of redeposited diapiric material composed of dark stiff poorly sorted clay | OREtech profile ORAT-24, 08:19 | High backscatter on the OREtech image, parallel well-layered sequence on the onboard profiler |
| TTR8-AT-135G | Top of the diapir to the south of the Haakon Mosby mud volcano | Hemipelagic grey silty clay interbedded with debris flow deposits and two layers of redeposited diapiric material | OREtech profile ORAT-24, 08:14 | High backscatter on the OREtech image |
| TTR8-AT-136G | Top of the diapir structure | Very stiff, consolidated dark grey silty clay, oxidised at the top. Diapiric material | Seismic, OKEAN side-scan sonar and onboard profiler line PSAT-84, 22:27 | High backscatter on the OKEAN image, no penetration on the onboard profiler |

**Table 12.** Sedimentological, acoustic and geological characteristic of the sampling stations on the southern Bear Island margin

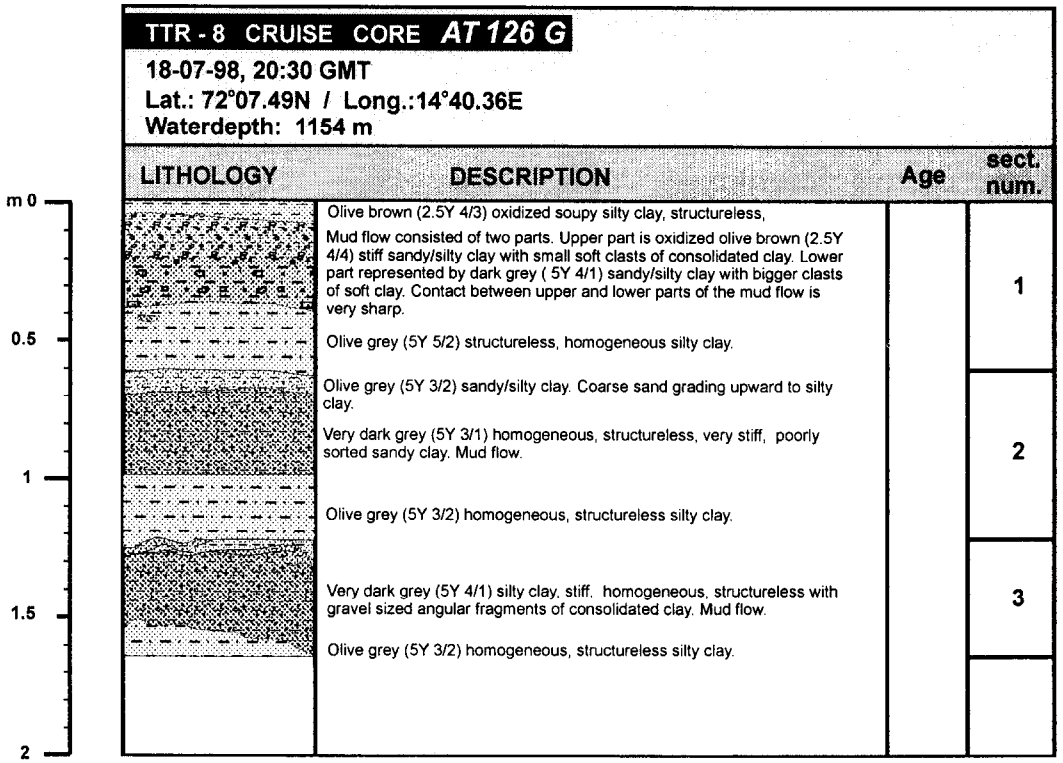


Fig. 84. Core log AT-126G

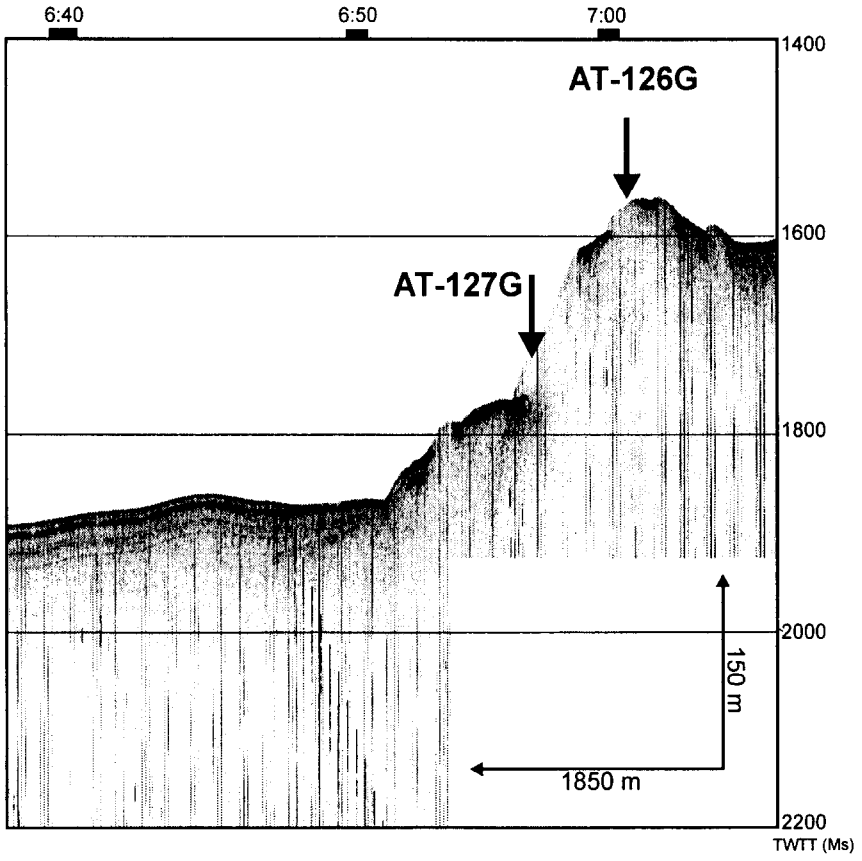


Fig. 85. Fragment of 3.5 kHz subbottom profiler record (Line PSAT-86) with sampling stations indicated.

Core TTR8-AT-130G (Figs. 90, 91)

The recovered sequence was 73 cm long and contained a layer of homogeneous, structureless, heavily gas saturated clay in the upper 37 cm. This interval was full of small (up to 2 mm) crystals of gas hydrates. The underlying layer consisted of a *Pogonophora* mat in a clayey matrix. The lower part of the core is represented by homogeneous, structureless clay with large (up to 4 cm in diameter) gas hydrate crystals. The whole core is characterised by a strong smell of $H_2S$.

Two zones of gas hydrate occurrence are recognised in core AT-130G. These zones are separated by a black clayey layer, which mainly consists of a fine black mat of *Pogonophora* worms. *Pogonophora* lives on endosymbiotic methane-oxidising bacteria and are described by Southward et al. (1981), Flügel & Langhof (1983), Schmaljohann & Flügel (1987), and have recently been reported from small methane seeps (Flügel & Callsen-Cencic, 1992). They are mainly exposed at the surface in seeping areas, which makes this observation important. These *Pogonophora* worms are the only animals currently known to derive most of their nutrition from methane. This is an indication that the gas hydrates probably consists of methane, which creates the most stable and common gas hydrate structure. It is not clear if the 17cm thick layer presented an active or dead *Pogonophora* community.

In the uppermost section (0-37cm) of core AT-130G, the gas hydrates recovered showed a

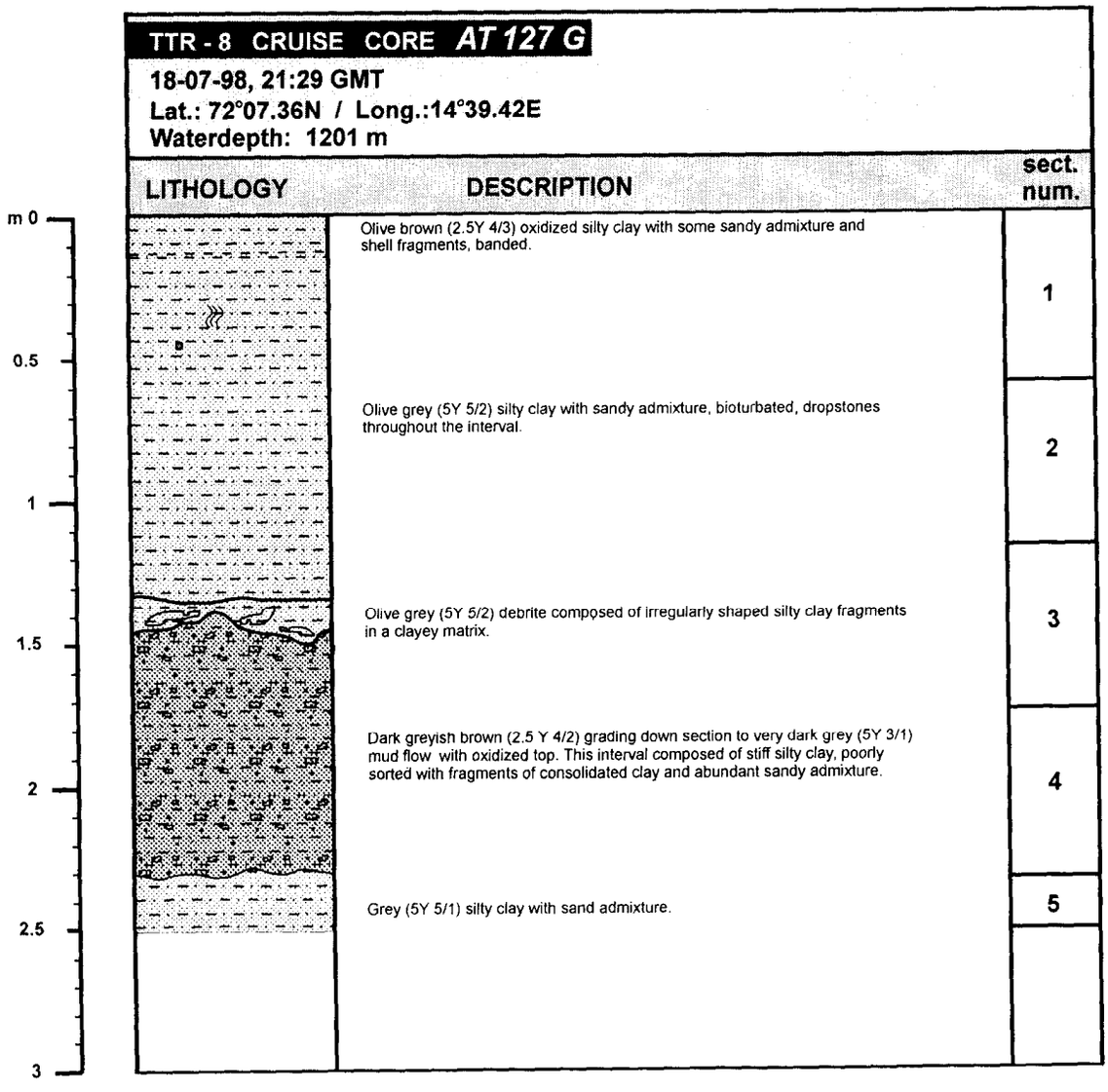


Fig. 86. Core log AT-127G.

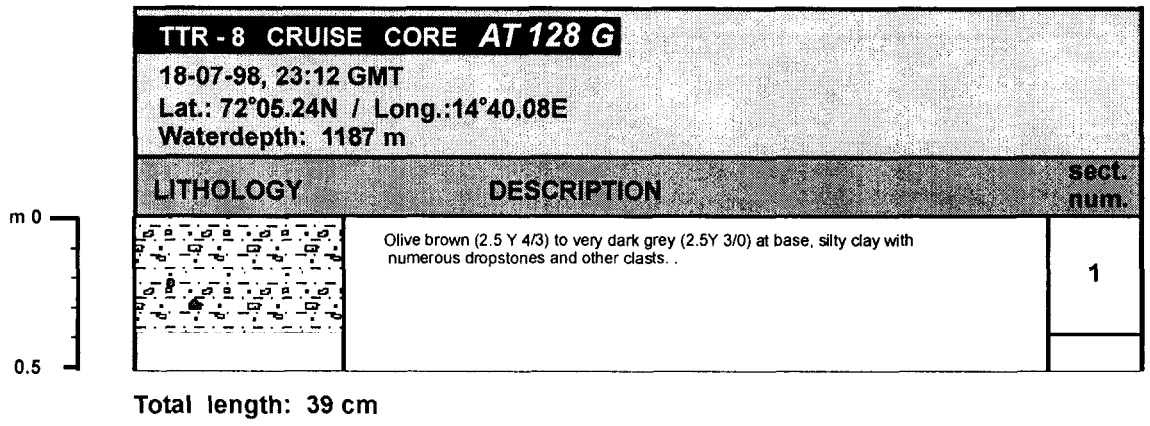


Fig. 87. Core log AT-128G.

similar morphology as in core AT-129G (Table 13, type 1). The lowermost part (54-73cm) of the core consists of large gas hydrate clasts (up to 4cm in diameter). These clasts were divided into four main types according to their morphology as shown in Table 13.

Due to the destabilisation of the gas hydrates some of them released a strong $H_2S$ smell and were non-flammable. Others were more inflammable and were odourless. These observations, including the occurrence of *Pogonophora,* allow us to assume that at least two compositional types of gas hydrates were present in the sediment recovered: methane and hydrogen sulphide hydrates.

The cores from AT-131G to AT-135G were taken to the south of the Haakon Mosby mud volcano. Their position was choosen on the basis of the OREtech side-scan sonar profile ORAT-24 data. The main purpose for sampling was to give a lithological characteristic to different acoustic facies on the profile.

Core TTR8-AT-131G (Figs. 92, 93)

The 153 cm long recovery from an area of high backscatter consisted of four main intervals, different in composition and genesis. The uppermost 6 cm were represented by an olive brown, rather poorly sorted, silty layer, soupy and enriched in clayey matrix, with a few dropstones up to 3 cm in diameter. The lower boundary of the interval was sharp and very oblique, probably reflecting an infill of an irregular surface by ice-rafted material. This interval was underlain by stiff, very poorly sorted, structureless clay with abundant sandy and silty admixture and with gravel sized fragments of consolidated clay. The lithology implied a deep source for the material. The interval was entirely oxidized and had a very sharp, erosional lower boundary, suggesting redeposition of oxidized diapiric material as

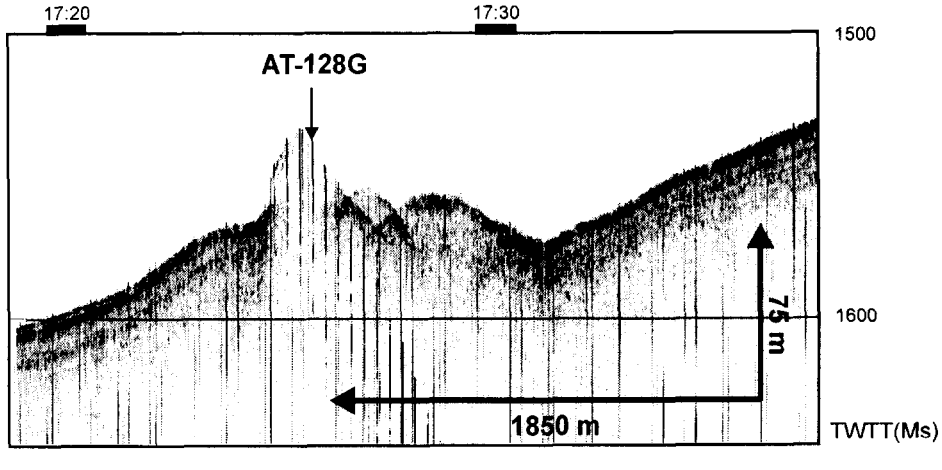


Fig. 88. Fragment of 3.5 kHz subbottom profiler record (Line PSAT-93) with sampling stations indicated.

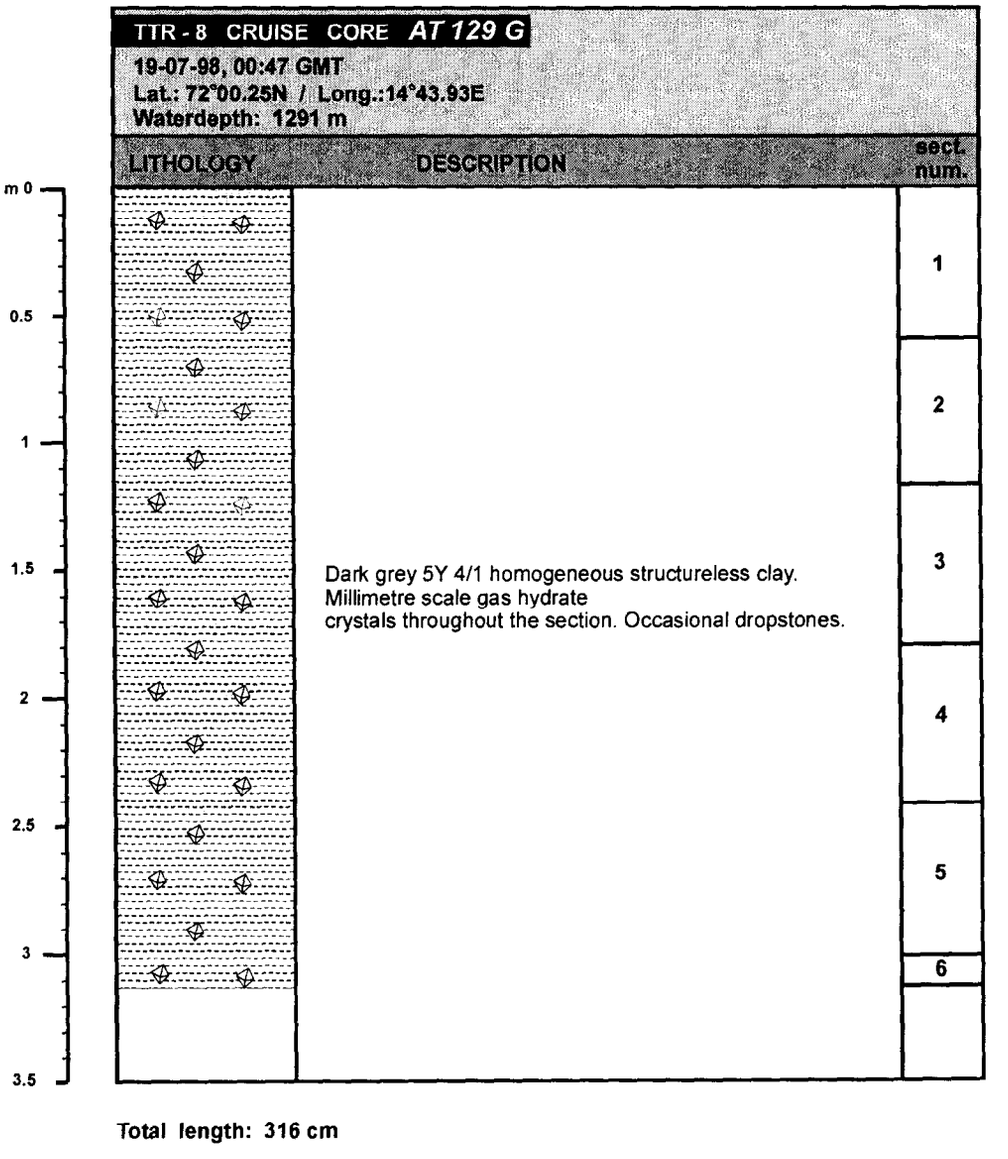


Fig. 89. Core log AT-129G

a high density mud flow moving very slowly downslope.

The described interval overlies a light grey, rather unconsolidated, structureless clay which also has very poor sorting, abundant silty and sandy admixture and millimetric angular fragments of claystone. It has a compositional similarity to the diapiric clay, but looked more like a hemipelagic succession, being soupy rather then stiff. It is represented by a mixture of hemipelagic material and material which was supplied from depth by diapir growth. Mixing with hemipelagic material can occur during rapid downslope redeposition of diapiric clay by debris flows or high concentration turbidity currents. The idea of mixing of material of two sources was partially supported by a micropaleontological investigation of the samples from this interval. The interval contained recent nannofossil species as well as reworked Eocene-Oligocene species.

The lower interval of the core consisted of very dark, very stiff, poorly sorted, structureless clay of diapiric origin, similar to the mud flow intervals observed in the cores AT-126G and AT-127G.

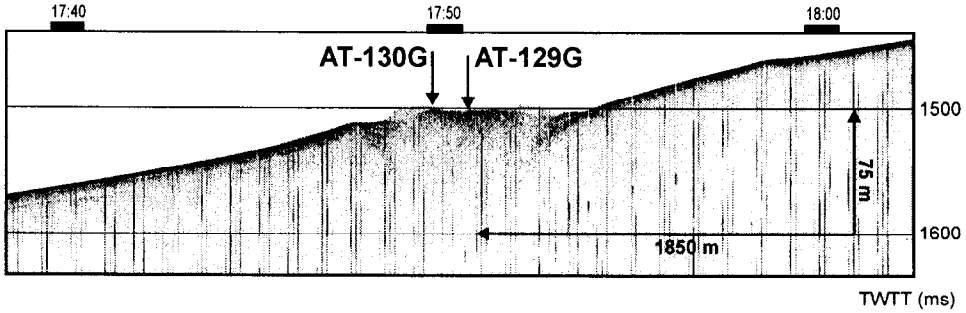


Fig. 90. Fragment of 3.5 kHz subbottom profiler record (Line PSAT-82) across Haakon Mosby mud volcano with sampling stations indicated.

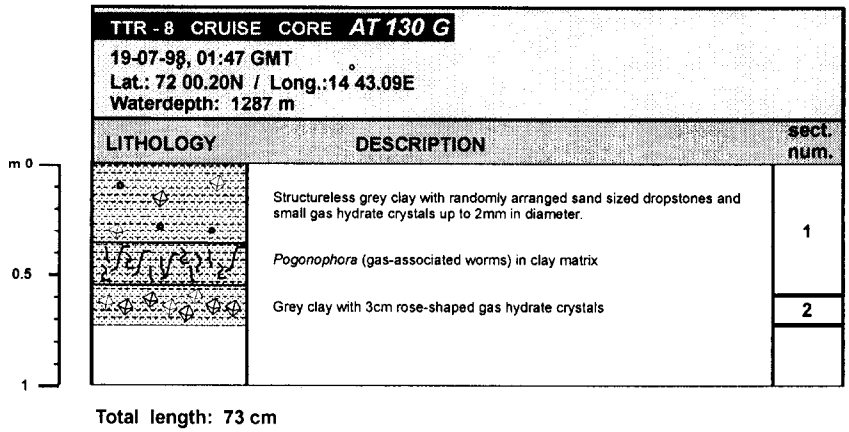


Fig. 91. Core log AT-130G

The sedimentary patterns in the described core show the presence of a diapir-like structure nearby and the high backscatter of the area can be explained by the abundance of the more consolidated diapiric material in the sedimentary succession. No evidence of gas in the sediment was observed.

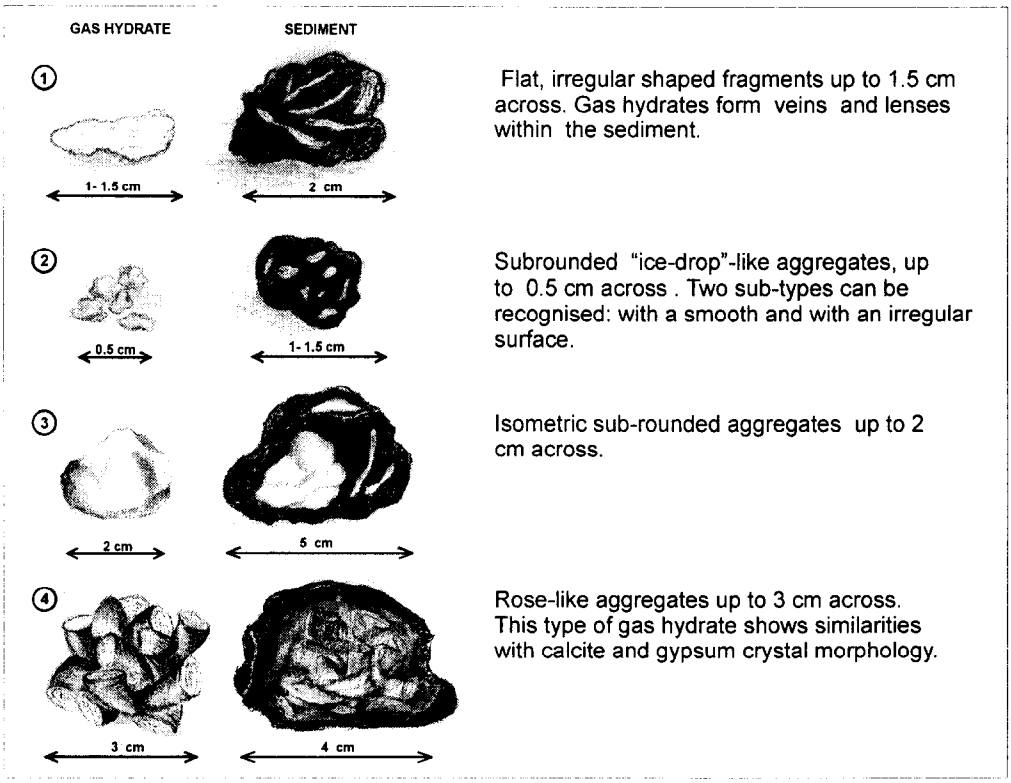


Table 13. Morphology of the gas hydrate aggregates

Core TTR8-AT-132G (Fig. 94)

A 346 cm thick, rather monotonous Holocene-Upper Pleistocene succession was recovered, consisting of three main intervals with slight lithological differences. The uppermost brown oxidized, hemipelagic silty clay, with occasional bioturbation was underlain by a 1.3 m thick structureless, grey silty clay, with several layers enriched in sandy admixture. No visible structure of bioturbation was found in this interval which probably resulted from Holocene-Upper Pleistocene bottom current activity and/or recorded distal mass-wasting from the west, showing relatively high sedimentation rates at this time. The interval was underlain by a gradational boundary above a 1.5 m thick sequence composed of similar grey, structureless silty clay. No significant change in composition was noted from the visual description, apart from abundant bioturbation and the presence of several dropstones which allowed this to be described as a separate interval. In our opinion, the deposition of this succession was less affected by bottom current and turbidite activity, reflecting mainly hemipelagic sedimentation in the area.

The lower interval was represented by the familiar very dark grey and stiff, structureless clay with abundant silty and sandy admixture and with angular fragments of claystone. This interval may represent a mud flow deposit from the diapiric structure cored by AT-131G, although the presence of another diapir blanketed with recent sediments is possible.

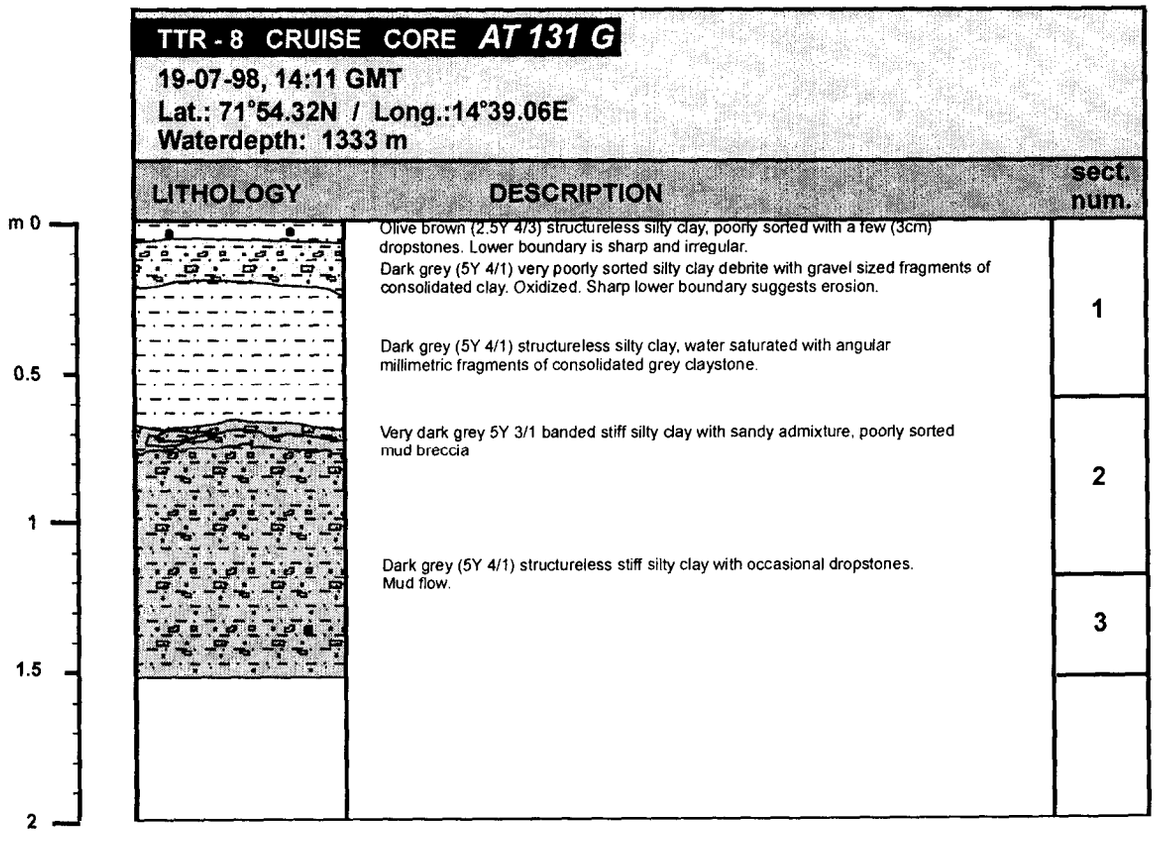


Fig. 92. Core log AT-131G.

Core TTR8-AT133G (Fig. 95)

A 323 cm thick recovery was composed of an uppermost interval of oxidized silty clay and a thick series of intercalated, grey structureless silty clay and thin graded layers of fine-grained sand and silt. The succession records Holocene-Upper Pleistocene hemipelagic

sedimentation and the periodical activity of turbidity currents, which supply the coarser material. The absence of coarser grained layers in the middle part of the succession was noted from the visual description. The initial interpretation of a relationship with the latest interglacial high sea level stand was then confirmed by micropaleontological study of the samples.

Core TTR8-AT134G (Fig. 96)

The recovered sequence was 286 cm long and showed a very complex sedimentary succession. From the top to the bottom it has a 35 cm thick interval of grey silty clay, brownish on the top due to surficial ozidization and bioturbated throughout the whole interval. It reflects prevalent hemipelagic sedimentation, with a thin sandy layer of possible

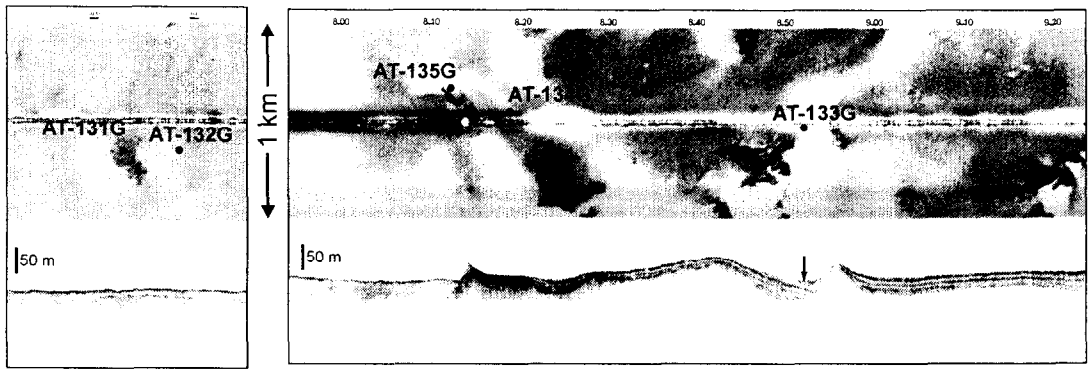


Fig. 93. Fragments of ORAT-24 sonograph and subbottom profiler record with sampling stations.

turbiditic origin in the middle part. This interval is underlain by a thick layer of structureless grey, poorly sorted silty clay with abundant sandy admixture and angular gravel-sized fragments of claystone. Nannofossil study determined the presence of reworked Eocene species. The lithology implies a diapiric material as a source. Relative water saturation of this interval might suggest that the material has been redeposited from the flank of a growing diapir by debris flow.

This layer is underlain by very dark clay of similar lithology, suggesting the same source. The difference is that this interval is very stiff and its structural peculiarities imply a redeposition of diapiric material as a high density mud flow moving very slowly downslope.

An interval of folded bedding of a different lithology is seen below the mud flow deposits. Different layers and lenses of silty clay vary significantly in colour and in sandy admixture content. The structural peculiarities of this interval imply deposition from a debris flow reworking hemipelagic material.

The lower interval of the core is a hemipelagic succession mainly composed of grey silty clay, occasionally bioturbated, with dark laminae, lenses, and mottles enriched in hydrotroilite, and with a few dropstones randomly distributed throughout the core. Close to the bottom the hemipelagic deposit is interbedded with a thin layer of very dark stiff clay, poorly sorted. This layer shows sharp and oblique boundaries and, probably, has been formed by a high density mud flow slowly moving diapiric material downslope.

Core TTR8-AT135G (Fig. 97)

A 259 cm thick Holocene-Upper Pleistocene sequence was recovered and showed a succession very similar to the core AT-134G. Starting from the top, it consisted of 75 cm thick hemipelagic greyish brown silty clay, bioturbated and structureless, interbedded with a thin layer of fine grained sand of turbiditic origin. It is followed downcore by an interval of diapiric material: very dark stiff structureless clay, poorly sorted, with abundant sandy admixture and angular claystone fragments. This interval was underlain by a folded and

faulted succession of different lithologies with a structure implying deposition from a debris flow. Lower part of the core consists mainly of hemipelagic silty clay, bioturbated, and with a few dropstones. The hemipelagic succession is interbedded in the middle part with a thin layer of dark grey, stiff, poorly sorted clay, which was interpreted as a mud flow deposit from a diapiric structure.

Core TTR8-AT136G (Figs. 98, 99)

Only 43 cm of very stiff, indurated, poorly sorted clay was recovered. It is material from the body of the diapir. The hard-ground at the top and a 39 cm thick oxidized upper part imply a relatively long period of exposure of the diapir body at the surface. The lack of hemipelagic sediment at the top might suggest recent diapir growth.

*Discussion*

The area under investigation is characterised by a very complex sedimentary pattern resulting from a combination of various processes recently ongoing to the south-west of the Bear Island. These include hemipelagic settling through the water column, bottom current activity, resedimentation processes, mud diapirism and mud volcanism.

I. Hemipelagic sediments are present in most cores taken in this area. They are mainly grey silty structureless clay, usually strongly affected by bioturbation. The presence of dropstones in many of the hemipelagic sequences implies a large supply of ice-rafted material to this area in the Upper Pleistocene time. Subordinate biogenic components in the sediments reflect prevalent cold water conditions with relatively low biogenic productivity.

II. Inferred bottom current deposits are described in the core AT-132G. They consist of grey silty clay and are rather similar in composition to hemipelagic sediments. Differences are a lack of bioturbation structures and an absence of coarse-grained ice-rafted material in these deposits. These peculiarities of fabric and structure, together with the presence of several interbedded layers enriched in a sandy admixture, allowed the interpretation of these deposits as contourites and the supposition of recent bottom current activity in the area.

III. Mud volcanic deposits are recovered in two cores taken from the Haakon Mosby mud volcano - AT-129G and AT-130G. They were seen as a homogeneous, structureless clay. Gas saturation and abundant gas-hydrates imply a relatively recent activity of this mud volcano.

IV. Most core recoveries showed evidence for active mud diapirism in the area and for various resedimentation processes caused by diapir growth. Two cores (AT-128G and AT-136G) succeeded in sampling the diapir bodies and recovered very stiff, consolidated, structureless silty clays, poorly sorted, with abundant sandy admixture and millimetric angular claystone fragments. Nannofossil study showed the presence of Eocene-Oligocene species, thus buried Paleogene rocks are a source for the diapiric material. Both cores taken from diapirs were characterised by a relatively deeply developed oxidisation front (32 and 39 cm) and the lack of a sediment veneer at the top, implying recent continuous growing of the diapirs.

The mud dome growth leads to instability of the slopes and resedimentation of diapiric material by slumping and debris flows. Debrites, composed of clay of diapiric origin, were described in the cores AT-126G, AT-134G and AT-135G. In contrast to the mud flow discussed above they are less stiff and with a characteristic structure. Slumped diapiric material was found in the core AT-127G. At the base of the mud domes the slope instantly results in formation of debrites composed of recent hemipelagic sediment and diapiric material mixed during rapid resedimentation. An interval of such deposits was observed in the core AT-131G.

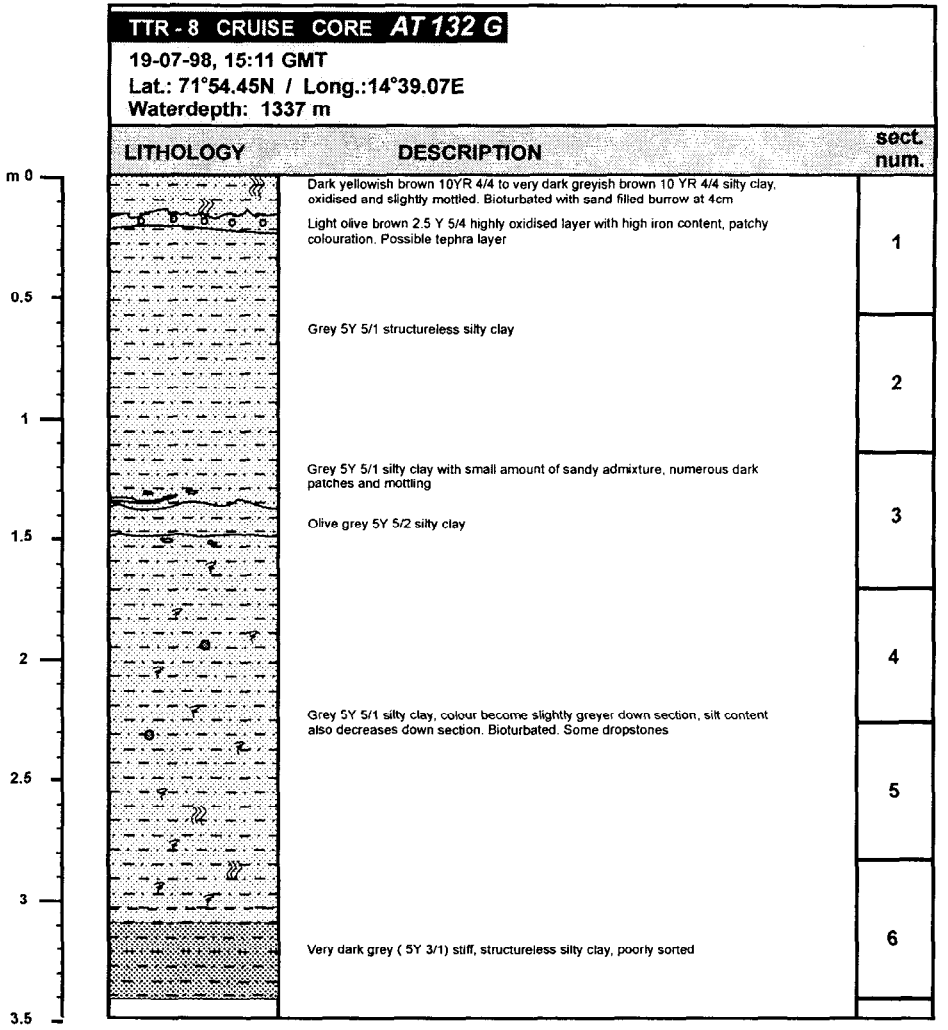


Fig. 94. Core log AT-132G.

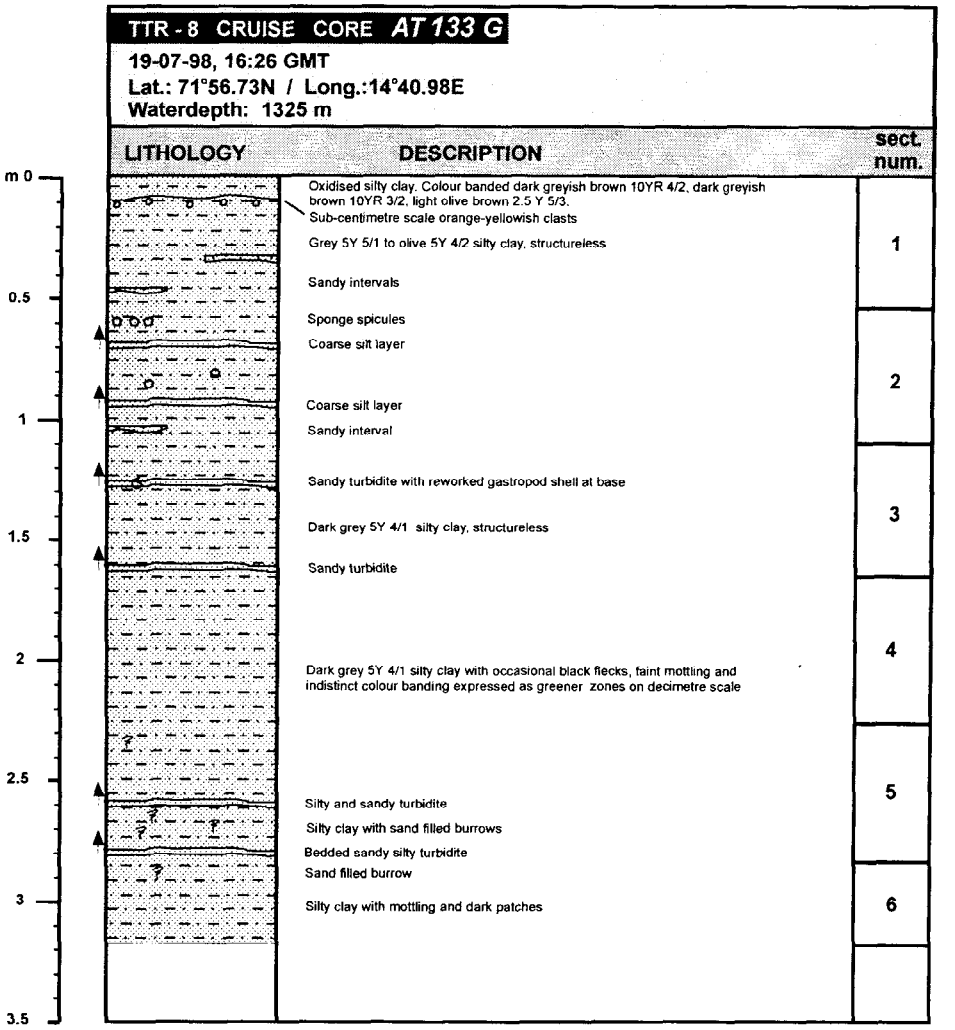


Fig. 95. Core log AT-133G.

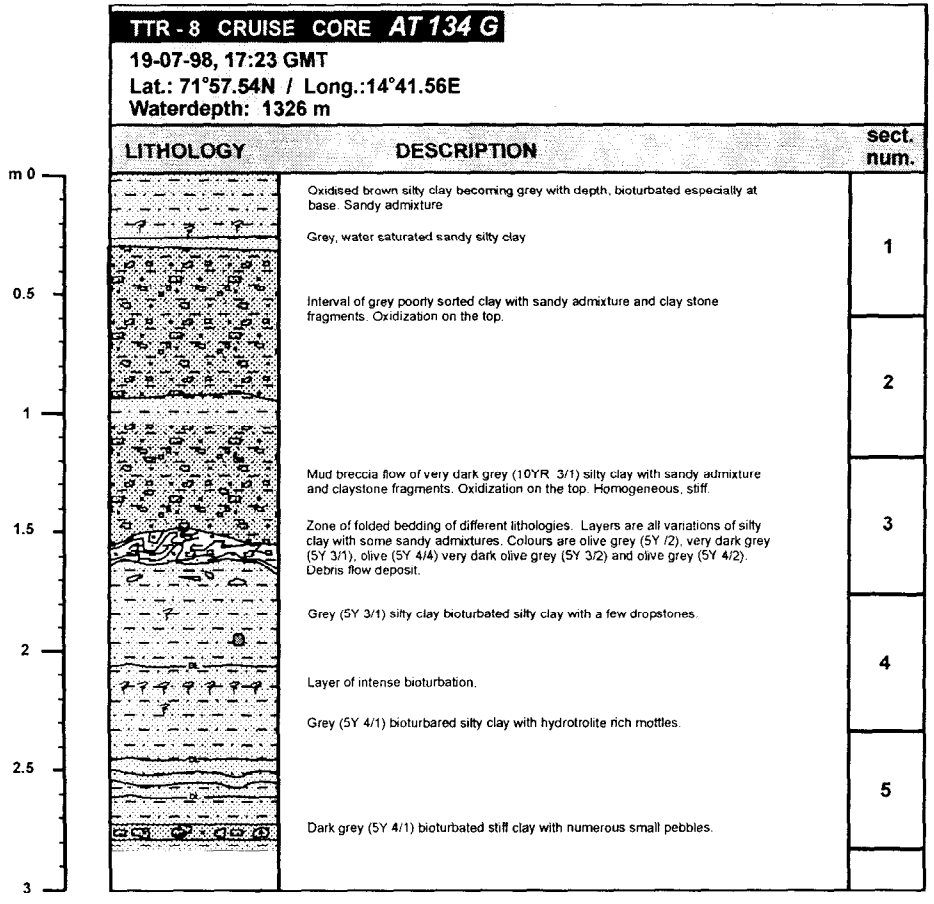


Fig. 96. Core log AT-134G.

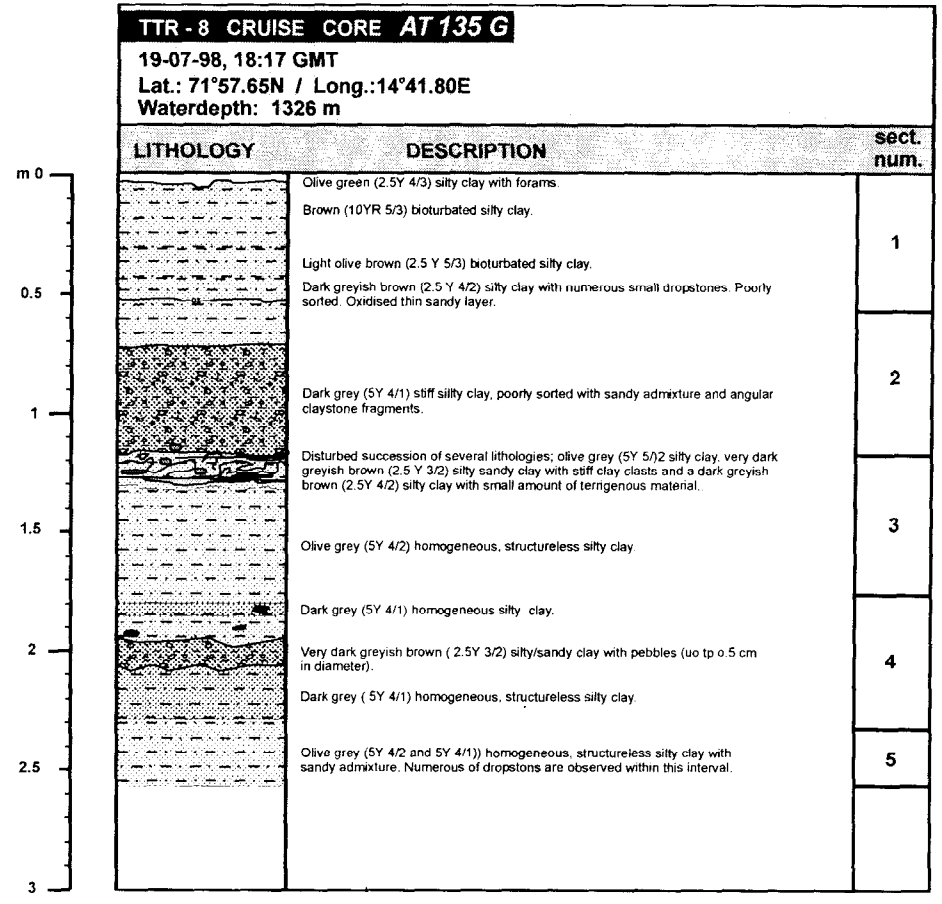


Fig. 97. Core log AT-135G.

V. Hemipelagic material resedimented as debris flow deposits are described in the cores AT-127G, AT-134G and AT-135G. These layers have the characteristic debrite structure and do not contain material from diapirs. However they all were found overlying or underlying layers of redeposited diapiric material. Such an association might suggest that these debris flows were also caused by active diapir growth.

VI. Clear evidence of Upper Pleistocene periodical activity of turbidity currents was found only in the core AT-133G, taken in a small elongate depression. The turbidites are represented there by thin graded layers of fine-grained sand and silt. These deposits may be widespread in the region.

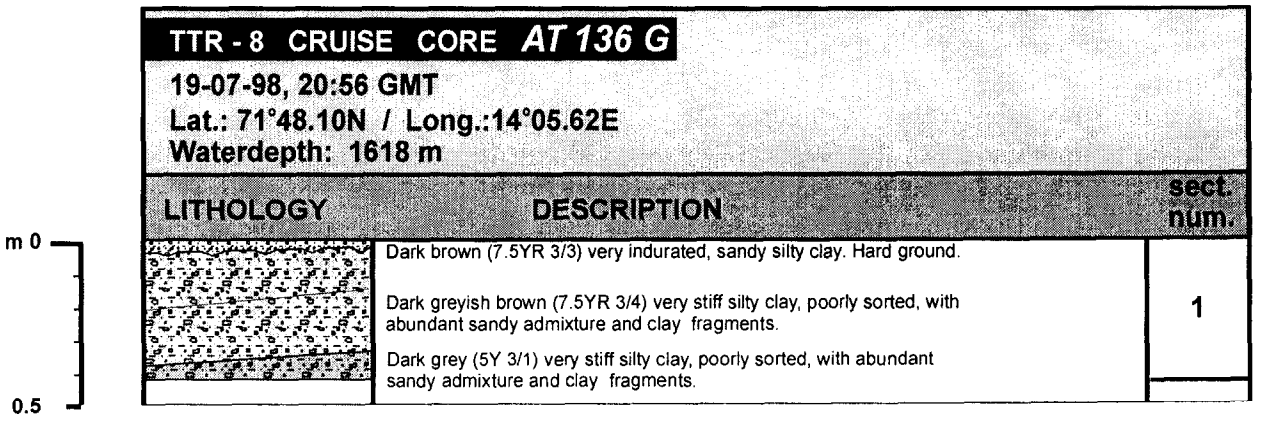


Fig. 98. Core log AT-136G.

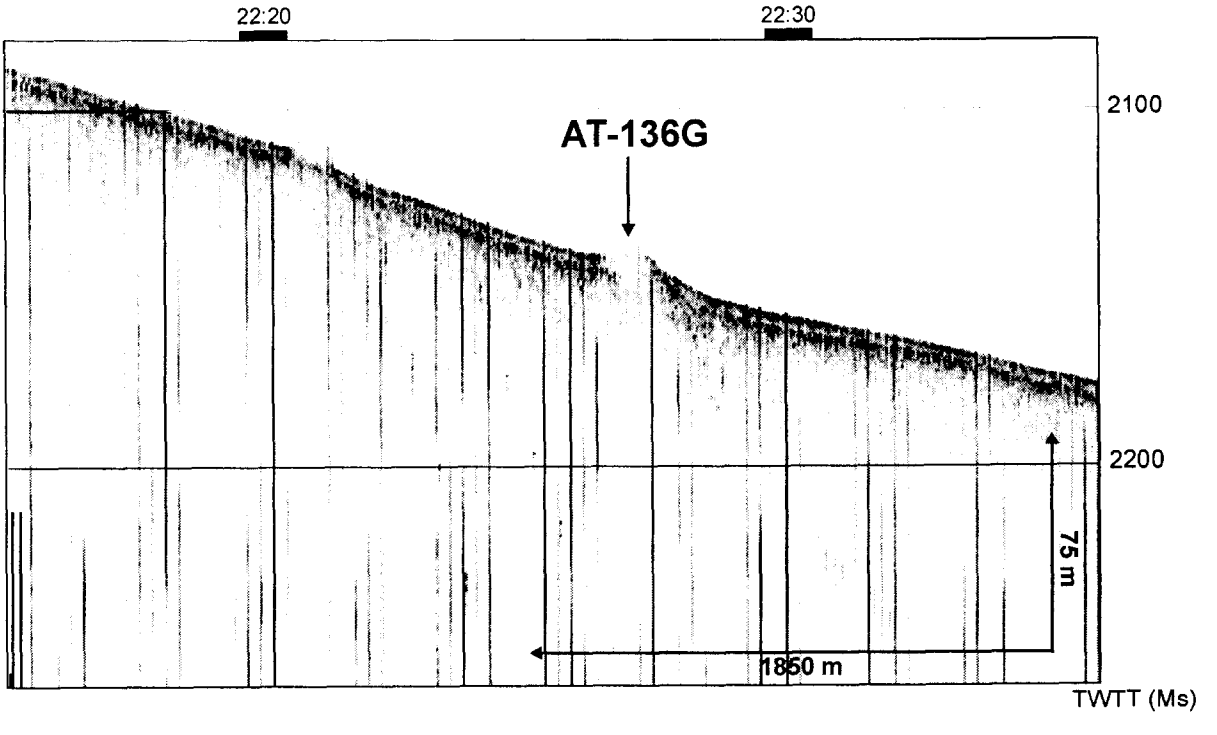


Fig. 99. Fragment of 3.5 kHz subbottom profiler record (Line PSAT-84) with sampling station indicated.

## IV.5. Conclusions

*M. Ivanov, A. Wheeler, A. Akhmetzhanov*

More data on the numerous fluid escape structures and evidence of possible gas hydrates presence were collected during the investigations of the southeastern part of the Vøring Plateau adjacent to the Storegga Slide. A bottom simulating reflector (BSR) was observed and in several places it was pierced by diapiric structures disturbing the sedimentary cover and sometimes even exposed on the seafloor. Several pockmarks recognised on the sonographs were carefully studied with high-resolution acoustic tools and a bottom TV survey was carried out. The latter reveals the presence of a bottom biota possibly associated with gas seepages as well as direct observations of escaping fluids. Many samples taken from the pockmarks contained gas-charged sediments, and concretions of carbonate minerals whose formation is very likely due to methane oxidation.

The complex morphology of the seabed mounds located in the northwestern part of the Vøring plateau are observed on the OREtech sonograph. At the present time they are covered by a veneer of hemipelagic sediments suggesting a cessation of active growth.

The unique nature of the Haakon Mosby mud volcano located to the southwest from the Bear Island is confirmed by extensive seismic and OKEAN survey. No other mud volcanoes were found in the study area although several mud diapiric structures were recognised and sampled.

# REFERENCES

Boldreel, L.O. and Andersen, M.S., 1993. **Late Paleocene to Miocene compression in the Faeroe-Rockall area.** In: Parker, J.R. (ed). *Petroleum Geology of Northwest Europe: Proceedings of the 4th Conference.* The Geological Society, London, 1025-1034.

Boldreel, L.O. and Andersen, M.S., 1994. **Tertiary development of the Faroe-Rockall Plateau based on reflection seismic data.** *Bulletin of the Geological Society of Denmark,* 41, 162-180.

Bolli, H.M., Saunders, J.B. and Perch-Nielson, K., 1985. **Plankton Stratigraphy.** Cambridge University Press.

Bugge, T, Befring, S., Belderson, R.H., Eidvin, T., Jansen, E., Kenyon, N.H., Holtedahl, H., and Sejrup., H.P., 1987. **A giant three-stage submarine slide off Norway.** *Geo-Marine Letters,* 7, 191-198.

Burton, K.W., Ling, H-F., and O'nions, R.K., 1997. **Closure of the Central American Isthmus and its effect on deep-water formation in the North Atlantic.** *Nature,* 386(6623), 382-385.

Carta Geológica de Portugal, 5th Edition, 1:500000, 1992. IGM, Departamento de Geologia.

Cita, M.B., Camerlenghi, A., and Rimoldi, B., 1996. **Deep-sea tsunami deposits in the eastern Mediterranean: new evidence and depositional models.** *Sedimentary Geology,* 104, 155-173.

R/V Belgica Cruise Report, 1997. Shipboard Scientific Party. Gent, RCMG. *Unpublished.*

R/V Belgica Cruise Report, 1998. Shipboard Scientific Party. Gent, RCMG. *Unpublished.*

Damuth, J.E. and Olson, H.C., 1993. **Preliminary observations of Neogene-Quaternary depositional processes in the Faeroe-Shetland Channel revealed by high resolution seismic facies analysis.** In: Parker, J.R. (ed.). *Petroleum Geology of Northwest Europe: Proceedings of the 4th Conference.* The Geological Society, London, 1035-1045.

Dawson, A., Long, D. and Smith, D.E., 1988. **The Storegga Slides: evidence from eastern Scotland for a possible tsunami.** *Marine Geology,* 82, 271-276.

Dickson, R.R., and McCave, N., 1986. **Nepheloid layers on the continental slope west of Porcupine Bank.** *Deep Sea Research,* 33A, 791-818.

Dowdeswell, J.A.,1996. Cruise Report. **MV Siren - 20 July to 8 August 1996. Long-range side-scan sonar investigations of the North Sea Fan and North Faroes Margin, North Atlantic.** Aberystwyth, The University of Wales, Centre for Glaciology. Report 96-3.

Ellett, D.G., Edwards, A. and Bowers, R., 1986. **The hydrography of the Rockall Channel - an overview.** *Proceedings of the Royal Society of Edinburgh (B),* 88B, 61-81.

Evans, D., King, E.L., Kenyon, N.H., Brett, C. and Wallis, D., 1996. **Evidence for long-term instability in the Storegga Slide region off western Norway.** *Marine Geology,* 130(3/4), 281-292.

Flügel, H.J. and Langhof, I., 1983. **A new hermaphroditic pogonophore from Skagerrak.** *Sarsia,* 67, 211-212.

Flügel, H.J. and Callsen-Cencic, P., 1992. **New observations on the biology of Siboglinum posendom Flügel & Langhof (Pogonophora) from Skagerrak.** *Sarsia,* 77, 287-290.

Frederiksen, R., Jensen, A., and Westerberg, H., 1992. **The distribution of the Scleractinian coral *Lophelia pertusa* around the Faroe Islands and the relation to internal tidal mixing.** *Sarsia,* 77, 157-171.

Gardner, J.V. and Kidd, R.B., 1987. **Sedimentary processes on the northwestern Iberian continental margin viewed by long-range side-scan sonar and seismic data.** *Journal of Sedimentary Petrology,* 57(3), 397-407.

Gartner, S., 1977. **Calcareous nannofossil biostratigraphy and revised zonation of the Paleocene.** *Marine Micropaleontology,* 2, 1-25.

Hargreaves, P.M., 1984. **The distribution of Decapoda (Crustacea) in the open ocean and near-bottom over an adjacent slope in the northern northeast Atlantic Ocean during autumn 1979**. *Journal of the Marine Biological Association of the United Kingdom*, 64, 829-857.

Harvey, G., 1982. **Relationships and water masses in the eastern North Atlantic.** *Deep Sea Research*, 29A, 1021-1033.

Hedebol Nielsen, P., Waagstein, R., Rasmussen, J. and Larsen, B., 1979. **Marine seismic investigation of the shelf around the Faroe Islands**. *Fródskaparrit (Annal. Societ. Scient. Faeroensis)*, 27. Bók. Tórshavn, 102-113.

Henriet, J.P., De Mol, B., Pillen, S., Vanneste, M., Van Rooij. D., Versteeg, W., Crocker, P.F., Shannon, P.M., Unnithan, V., Bouriak, S. and Chachkine, P., 1998. **Gas hydrate crystals may help build reefs**. *Nature*, 391, 647-649.

Henriksen, S. and Vorren, T.O., 1996. **Late Cenozoic sedimentation and uplift history on the mid-Norway continental shelf**. In: Solheim, A. et al. (eds). *Impact of Glaciations on basin evolution: data and models from the Norwegian margin and adjacent areas*. Special Volume of Global and Planetary Changes, 12, 179-199.

Hjelstuen, B.O., Eldholm, O. and Skogseid, J., 1997. **Voring Plateau diapir fields and their structural and depositional settings**. *Marine Geology*, 144(1/3), 33-57.

Hovland, M., Croker, P.F. and Martin, M., 1994. **Fault-associated seabed mounds (carbonate knolls?) off western Ireland and north-west Australia.** *Marine and Petroleum Geology*, 11, 232-246.

Hovland, M., Nygaard, E. and Thorbjornsen, S., 1998. **Piercement shale diapirism in the deep-water Vema Dome area, Voring basin, offshore Norway**. *Marine and Petroleum Geology*, 15, 191-201.

Ivanov, M.K., Limonov, A.F. and van Weering, Tj.C.E., 1996. **Comparative characteristics of the Black Sea and Mediterranean Ridge mud volcanoes**. *Marine Geology*, 132, 253-271.

Kastens, K.A. and Cita M.B., 1981. **Tsunami induced sediment transport in the Abyssal Mediterranean Sea.** *Geol. Soc. Am. Bull.*, 89, 591-604.

Kellogg, T.B., 1980. **Paleoclimatology and paleo-oceanography of the Norwegian and Greenland Seas: glacial-interglacial contrasts**. *Boreas*, 9, 115-137.

Kenyon N.H., Ivanov M.K. and Akhmetzhanov A.M. (eds), 1998. **Cold water carbonate mounds and sediment transport on the Northeast Atlantic margin. Preliminary results of geological and geophysical investigations during the TTR-7 cruise of R/V Professor Logachev in co-operation with the CORSAIRES and ENAM 2 programmes**. *Intergovernmental Oceanographic Commission Reports, Technical series*, 52, 178 pp.

Kenyon, N.H., Belderson, R.H. and Stride, A.H., 1978. **Channels, canyons and slump folds on the continental slope between south-west Ireland and Spain**. *Oceanologica Acta*, 1, 369-380.

Krawczyk, C.M., Reston, T.J., Beslier, M.-O., and Boillot, G., 1996. **Evidence for detachment tectonics on the Iberia Abyssal Plain rifted margin**. In: Whitmarsh, R.B., Sawyer, D.S., Klaus, A. and Masson D.G. (eds), *Proceedings of the Ocean Drilling Program, Scientific Results*, 149: College Station, TX (Ocean Drilling Program), 603-616.

Kuijpers, A. and Shipboard Scientific Party, 1997. **Deep-tow side-scan sonar study of Norwegian Sea overflow pathways off the Faeroe Islands**. R/V Dana Cruise No 97/9. *Unpublished.*

Kuijpers, A., Andersen, M.S., Kenyon, N.H. and van Weering, T.C.E., 1998. **Quaternary sedimentation and Norwegian Sea overflow pathways around Bill Bailey Bank, NE Atlantic**. *Marine Geology*, 152, 101-128.

Kuijpers, A., Troelstra, S.R., Wisse, M., Heier Nielsen, S. and van Weering, T.C.E., 1998. **Norwegian Sea overflow variability and NE Atlantic surface hydrography during the past 150,000 years**. *Marine Geology*, 152, 58-74.

Laberg, J.S. and Vorren, T.O., 1995. **Late Weichselian submarine debris flow deposits on the Bear Island Trough Mouth Fan.** *Marine Geology*, 127: 45-72.

Lee, A. and Ellett, D., 1965. **On the contribution of overflow water from the Norwegian Sea to the hydrographic structure of the North Atlantic Ocean**. *Deep Sea Research*, 12, 129-142.

Limonov A.F., Woodside J.M, and Ivanov M.K. (eds), 1994. **Mud volcanism in the Mediterranean and Black Seas and shallow structure of the Eratosthenes Seamount. Initial results of geological and geophysical investigations during the Third UNESCO-ESF "Training-through-Research" Cruise of R/V Gelendzhik (June-July 1993).** - *UNESCO Reports in Marine Science*, 64, 173 pp.

Limonov, A.F., Kenyon, N.H, Ivanov, M.K. and Woodside, J.M., 1995. **Deep-sea depositional systems of the western Mediterranean and mud volcanism on the Mediterranean Ridge: initial results of geological and geophysical investigations during the fourth UNESCO-ESF 'Training-through-Research' cruise of R/V "Gelendzhik".** *UNESCO Reports in Marine Science*, 67, 171 pp.

Limonov, A.F., van Weering, Tj.C.E., Kenyon, N.H., Ivanov, M.K. and Meisner, L.B., 1997. **Seabed morphology and gas venting in the Black Sea mudvolcano area: Observations with MAK-1 deep-tow sidescan sonar and bottom profiler.** *Marine Geology*, 137, 121-136.

McQuillin, R., Bacon, M. and Barclay, W., 1984. **An Introduction to seismic interpretation.** Graham and Trotman, London.

Mienert, J., Posewang, J. and Baumann, M., 1998. **Gas hydrates along the northeastern Atlantic margin: possible hydrate-bound margin instabilities and possible release of methane.** In: Henriet, J.-P., and Mienert, J. (eds) *Gas Hydrates: Relevance to World Margin Stability and Climate Change*. Geological Society, London, Special Publications, 137, 275-291.

Nielsen, T. and van Weering, T.C.E., 1998. **Seismic stratigraphy and sedimentary processes at the Norwegian Sea Margin northeast of the Faeroe Islands**. *Marine Geology*, 152, 141-157.

Nielsen, T., van Weering, T.C.E. and Andersen, M.S., 1998. **Cenozoic changes in the sedimentary regime on the northeastern Faeroes margin.** In: Stoker, M., Evans, D., and Cramp, R (eds). *Geological Processes on Continental Margins: Sedimentation, Mass-Wasting and Stability*. Geological Society Special Publications 129, 167-172.

Pingree, R.D. and LeCann, B., 1989. **The Celtic and Armorican slope and shelf residual currents.** *Progress in Oceanography Series*, 23, 303-338.

Pingree, R.D. and LeCann, B., 1990. **Structure, strength and seasonality of the slope currents in the Bay of Biscay region**. *Journal of the Marine Biological Association of the United Kingdom*, 70, 857-885.

Rasmussen, T.L., Thomsen, E. and van Weering, T.C.E., 1998. **Cyclic changes in sedimentation on the Faeroe Drift 53-10 kyr BP related to climate variations.** In: Stoker, M., Evans, D., and Cramp, R. (eds). *Geological Processes on Continental Margins: Sedimentation, Mass-Wasting and Stability*. Geological Society Special Publications 129, 255-267.

Rasmussen, T.L., Thomsen, E., Labeyrie, L. and van Weering, T.C.E., 1996b: **Circulation changes in the Faeroe-Shetland Channel correlating with cold events during the last glacial period (58-10 ka).** *Geology*, 24, 937-940.

Rasmussen, T.L., Thomsen, E., van Weering, T.C.E. and Labeyrie, L., 1996c: **Rapid changes in surface and deep water conditions at the Faeroe Margin during the last 58,000 years.** *Palaeoceanography,* 11, 757-771.

Rasmussen, T.L., van Weering, T.C.E. and Labeyrie, L., 1996a: **High resolution stratigraphy of the Faeroe-Shetland Channel and its relation to North Atlantic paleoceanography: the last 87 ka.** *Marine Geology,* 131, 75-88.

Rice, A.L., Billett, D.S.M., Thurston, M.H., and Lampitt, R.S., 1991. **The Institute of Oceanographic Sciences biology program in the Porcupine Seabight: background and general introduction.** *Journal of the Marine Biological Association of the United Kingdom,* 71, 281-310.

Rothwell, G. and Weaver, P.P.E., 1994. **Clayey nanofossil ooze turbidites and hemipelagites at Sites 834 and 835 (Lau Basin, SW Pacific).** In: Hawkins, J. Parsons, L. et al. (eds). *Proceedings of the Ocean Drilling Program,* 135, 101-130.

Saettem, J., Poole, D.A.R., Ellingsen, L. and Sejrup, H.P., 1992. **Glacial geology of outer Bjørnøyrenna, southweastern Barents Sea.** *Marine Geology,* 103, 15-51.

Sawyer, D.S., Whitmarsh, R.B., Klaus, A., et al., 1993. **Ocean Drilling Program Leg 149 preliminary report.** Texas A & M University Ocean Drilling Program, Preliminary Report No. 49, 719 pp.

Schmaljohann, R. and Flügel, H.J., 1987. **Methane oxidising bacteria in Pogonophora.** *Sarsia,* 72, 91-98.

Southward, A.J., Southward, E.C., Dando, P.R., Rau, G.H., Feldbeck, H. and Flügel, H. (1981). **Bacterial symbionts and low 13C/12C ratios in tissues of Pogonophora indicate unusual nutrition and metabolism.** *Nature,* 293, 616-620.

Stoker, M.S., 1995. **The influence of glacigenic sedimentation on slope-apron development on the continental margin off northwest Britain.** In: Scrutton R. A., Stoker, M.S., Shimmield, G.B., and Tudhope, A.W. (eds). *The Tectonics, Sedimentation and Palaeoceanography of the North Atlantic region.* Geological Society, London, Special Publications, 90, 159-177.

Talwani, M., Udintsev, G., Bjørklund, K., Caston, V.N.D., Faas, R.W., Kharin, G.N., Morris, D.A., Müller, G., Nilsen, T.H., van Hinte, J., Warnke, D.A. and White, S.M., 1976. **Initial reports of the Deep Sea Drilling Project,** Vol.38. Washington DC: US Government Printing Office, 1256.

Taylor, J., Dowdeswell, J.A., Kenyon, N.H., Whittington, R.J., van Weering, Tj.C.E., and Mienert, J., submitted. **Morphology and Late Quaternary sedimentation of the North Faeroes slope and abyssal plain, North Atlantic.** *Marine Geology.*

The GEBCO Digital Atlas, 1997. The British Oceanographic Data Centre on behalf of IOC and IHO.

van Weering, Tj. C. E., Nielsen, T., Kenyon, N.H., Akentieva, K. and Kuijpers, A.H., 1998. **Large submarine slides on the NE Faeroe continental margin.** *In* Stoker, M.S., Evans, D. & Cramp, A. (eds) *Geological Processes on Continental Margins: Sedimentation, Mass-Wasting and Stability.* Geological Society, London, Special Publications, 129, 5-17.

Vangriesheim, A., 1985. **Hydrologie et circulation profonde.** In: Laubier, L. and Monniot, C. (eds). *Peuplements profonds du golfe du Gascogne.* Brest, IFREMER. 43-70.

Vogt P.R., et al., 1997. **Haakon Mosby mud volcano provides unusual example of venting.** *Eos, Transactions, American Geophysical Union,* 78, 48, 556-557.

Waagstein, R. 1988. **Structure, composition and age of the Faeroe basalt plateau.** *In*: Parsons, L. and Morton, A.C. (eds). *Early Tertiary Volcanism and the Opening of the NE Atlantic.* Geological Society, London, Special Publications , 39, 225-238.

Waagstein, R. and Rasmussen, J., 1975. **Glacial erratics from the sea floor southeast of the Faeroe Islands and the limit of glaciation.** *Fródskaparrit (Annal. Societ. Scient. Faeroensis)*, 23, Bók. Tórshavn, 111-116.

Wiltshire, K.H., Blackburn, J. and Paterson D.M., 1997. **The cryolander: a new method for in situ sampling of intertidal surface sediments minimising distortion of sediment structure.** *Journal of Sedimentary Research*, 67, 981-997.

Woodside J.M., Ivanov M.K. and Limonov A.F. (eds), 1997. **Neotectonics and fluids flow through sea-floor sediments in the eastern Mediterranean and Black seas. Preliminary results of geological and geophysical investigations during the ANAXIPROBE/TTR-6 cruise of R/V Gelendzhik (July-August 1996). Volumes 1,2 -** *Intergovernmental Oceanographic Commission Reports, Technical Series*, 48, UNESCO, 226 pp.

# ANNEX 1. LIST OF TTR-RELATED REPORTS

Limonov, A.F., Woodside, J.M. and Ivanov, M.K. (eds.)., 1992. **Geological and geophysical investigations in the Mediterranean and Black Seas. Initial results of the "Training through Research" Cruise of R/V Gelendzhik in the Eastern Mediterranean and the Black Sea (June-July 1991).** *UNESCO Reports in Marine Science*, 56, 208 pp.

Limonov, A.F., Woodside, J.M. and Ivanov, M.K. (eds.), 1993. **Geological and geophysical investigations of the deep-sea fans of the Western Mediterranean Sea. Preliminary report of the 2rd cruise of the R/V Gelendzhik in the Western Mediterranean Sea, June-July, 1992.** *UNESCO Reports in Marine Science*, 62. 148 pp.

**"Training-Through-Research" Opportunities Through the UNESCO/TREDMAR Programme. Report of the first post-cruise meeting of TREDMAR students. Moscow State University, 22-30 January, 1993.** *MARINF*, 91, UNESCO, 1993.

Limonov, A.F., Woodside, J.M. and Ivanov, M.K. (eds.), 1994. **Mud volcanism in the Mediterranean and Black Seas and shallow Ssructure of the Eratosthenes Seamount. Initial results of the geological and geophysical investigations during the Third UNESCO-ESF 'Training-through-Research" Cruise of RV Gelendzhik (June-July 1993).** *UNESCO Reports in Marine Science*, 64, 173 pp.

**Recent Marine Geological Research in the Mediterranean and Black Seas through the UNESCO/TREDMAR programme and its 'Floating University project, Free University, Amsterdam, 31 January-4 February 1994. Abstracts.** *MARINF*, 94, UNESCO, 1994.

Limonov, A.F., Kenyon, N.H., Ivanov, M.K. and Woodside J.M. (eds.), 1995. **Deep sea depositional systems of the Western Mediterranean and mud volcanism on the Mediterranean Ridge. Initial results of geological and geophysical investigations during the Forth UNESCO-ESF 'Training through Research" Cruise of R/V Gelendzhik (June-July 1994).** *UNESCO Reports in Marine Science*, 67, 171 pp.

**Deep-sea depositional systems and mud volcanism in the Mediterranean and Black Seas. 3rd post-cruise meeting, Cardiff, 30 January - 3 February 1995. Abstracts.** *MARINF*, 99, UNESCO, 1995.

Ivanov, M.K., Limonov, A.F. and Cronin, B.T. (eds.), 1996. **Mud volcanism and fluid venting in the eastern part of the Mediterranean Ridge. Initial results of geological, geophysical and geochemical investigations during the 5th Training-through-Research Cruise of R/V Professor Logachev (July-September 1995).** *UNESCO Reports in Marine Science*, 68, 127pp.

**Sedimentary Basins of the Mediterranean and Black Seas. 4th Post-Cruise Meeting, Training-through-Research Programme. Moscow and Zvenigorod, Russia, 29 January-3 February. Abstracts.** *MARINF*, 100, UNESCO, 1996.

Woodside, J.M., Ivanov, M.K. and Limonov, A.F. (eds.), 1997. **Neotectonics and Fluid Flow through Seafloor Sediments in the Eastern Mediterranean and Black Seas. Preliminary results of geological and geophysical investigations during the ANAXIPROBe/TTR-6 cruise of R/V Gelendzhik, July-August 1996.** Vols. 1, 2. *IOC Technical Series*, 48, UNESCO, 226 pp.

**Gas and Fluids in Marine Sediments: Gas Hydrates, Mud Volcanoes, Tectonics, Sedimentology and Geochemistry in Mediterranean and Black Seas. Fifth Post-cruise Meeting of the Training-through-Research Programme and International Congress, Amsterdam, The Netherlands, 27-29 January 1997.** *IOC Workshop Report*, 129, UNESCO, 1997.

**Geosphere-biosphere coupling: Carbonate Mud Mounds and Cold Water Reefs. International Conference and Sixth Post-Cruise Meeting of the Training-through-Research Programme, Gent, Belgium, 7-11 February 1998.** *IOC Workshop Report*, 143, UNESCO, 1998.

Kenyon, N.H., Ivanov, M.K. and Akhmetzhanov, A.M. (eds.), 1998. **Cold water carbonate mounds and sediment transport on the Northeast Atlantic Margin.** *IOC, Technical Series*, 52, UNESCO, 178 pp.